INHIBITION OF DISCOIDIN DOMAIN RECEPTOR 1 REDUCES COLLAGEN-MEDIATED TUMORIGENICITY IN PANCREATIC DUCTAL ADENOCARCINOMA

APPROVED BY SUPERVISORY COMMITTEE

Rolf A. Brekken, Ph.D. (Mentor)

Gray Pearson, Ph.D. (Chair)

John Minna, M.D.

Lance Terada, M.D.

For my family.

INHIBITION OF DISCOIDIN DOMAIN RECEPTOR 1 REDUCES COLLAGEN-MEDIATED TUMORIGENICITY IN PANCREATIC DUCTAL ADENOCARCINOMA

by

KRISTINA YOLANDA AGUILERA

DISSERTATION

Presented to the Faculty of the Graduate School of Biomedical Sciences

The University of Texas Southwestern Medical Center at Dallas

In Partial Fulfillment of the Requirements

For the Degree of

DOCTOR OF PHILOSOPHY

The University of Texas Southwestern Medical Center at Dallas

Dallas, Texas

August, 2015

ACKNOWLEDGEMENTS

I would like to gratefully acknowledge the following people for which the following work in this dissertation could not have been accomplished otherwise. I would first like to express my gratitude to my mentor, Dr. Rolf A. Brekken for his guidance that allowed me to mature as a scientist and as an individual. Thank you for taking me under your wing for the past four years and bestowing your enthusiasm and excitement for science. I admire your ability do great science and have fun in the process. I would also like to acknowledge the former and current members of the Brekken lab for their guidance and support: Mary Topalovski, Victoria Burton, and Dr. Miao Wang for which their encouragement, WISMAC meetings, and friendship has been fundamental. Additionally, Drs. Michael Dellinger and James Kim for their editorial critiques and help in writing manuscripts, and Drs. Moriah Hagopian, Hoon Hur, Li Li for their technical assistance with animal experiments. I would also like to acknowledge my collaborators Zhen Wang and Dr. Ke Ding (State Key Laboratory of Respiratory Diseases, Guangzhou Institutes of Biomedicine and Health, China), Dr. Diego H. Castrillon (UT Southwestern), Dr. Tae Hyun Hwang (UT Southwestern), Dr. Jason B. Fleming (M.D. Anderson), Oz Ocal and Dr. Thomas Wilkie (UT Southwestern), Dr. Amy Bradshaw (Gazes Cardiac Research Institute, Charleston, SC), Dr. Changhua Zhang (Gastric Cancer Center of Sun Yat-sen University,

China), and Dr. Hoon Hur (Ajou University, Seoul) for their valued support and teamwork; specifically, a large portion of my dissertation would not have been as successful without my collaboration with Dr. Ke Ding and his DDR1-specific small molecule inhibitors (i.e. 7rh). Thank you all.

I would also like to thank my committee members Drs. Gray Pearson, John Minna, and Lance Terada for their guidance and critical advice. I have been extremely fortunate to have the support of Dr. John Minna's laboratory, specifically Dr. Michael Peyton, for technical advice as well as collaboration. I would also like to thank the Department of Pharmacology at UT Southwestern for funding my work through the Mechanisms of Drug Action and Disposition-Pharmacology Training Grant (T32-GM007062-38), as well as the National Institutes of Health for funding my work through the Ruth L. Kirschstein National Research Service Award Individual Predoctoral Fellowship to Promote Diversity in Health-Related Research (F31 CA168350-01).

Finally, I would like to express my gratitude and appreciation for my friends and family for their support and encouragement. Specifically, I would like to thank my dear partners in crime Kacey Rajkovich, John Ochoa, Daniel Epstein, Benjamin Arellano, Louise Owens, and the Windmill for the good times, their love, and their unfaltering support. I would also like to thank my family throughout the world for their encouragement, especially Yolanda, Elizabeth, Renato, Susanne, Florian, and Horst.

Lastly, I would like to express my wholehearted appreciation and thank my best friends and life companions Stefan Hinz and Pepper, for whom their unconditional love, warmth, and patience is beyond words.

FUNDING

This work was supported in part by the NIH (R01-CA118240; T32-GM007062-38, F31-CA168350), and the Effie Marie Cain Scholarship for Angiogenesis Research.

INHIBITION OF DISCOIDIN DOMAIN RECEPTOR 1 REDUCES COLLAGEN-MEDIATED TUMORIGENICITY IN PANCREATIC DUCTAL ADENOCARCINOMA

Kristina Yolanda Aguilera, Ph.D.

The University of Texas Southwestern Medical Center at Dallas, 2015

Supervising Professor: Rolf A. Brekken, Ph.D.

An extracellular matrix (ECM) rich in fibrillar collagens is a principal component of pancreatic ductal adenocarcinoma (PDA). The ECM provides structural support for the tumor and facilitates tumor cell survival and chemoresistance by activating cell surface receptors on tumor cells. Fibrillar collagens bind the collagen-specific receptor tyrosine kinase discoidin domain receptor 1 (DDR1), implicated in regulating cell proliferation, migration,

adhesion, ECM remodeling, and response to growth factors. Additionally, collagen has been shown to promote chemoresistance in pancreatic tumor cells. I hypothesize that the regulation of collagen-mediated DDR1 signaling promotes chemoresistance. Collagen expression and deposition is a complex process that is orchestrated in part by the matricellular protein SPARC. SPARC expression in human PDA patients correlates with improved chemoresponse; however, the mechanism underlying this is unclear. I proposed that SPARC reduces collagen binding to collagen receptors. Structural studies identified that SPARC and DDR1 share the same collagen-binding site. I demonstrated that SPARC inhibited collagen binding to DDR1 via *in vitro* binding assays and cell-based activity assays. To determine the functional relevance of Sparc expression and collagen-mediated Ddr1 activation in PDA, *Sparc-null* (*Sparc*$^{-/-}$) mice were crossed with a GEMM of PDA, *KIC (LSL Kras*$^{G12D/+}$*; Ink4aArf*$^{lox/lox}$*; p48*$^{Cre/+}$*)*. Survival was reduced and tumors were more aggressive in *Sparc*$^{-/-}$*; KIC* mice. Tumors from these animals also displayed elevated Ddr1-mediated signaling. Human PDA, and primary PDA cell lines isolated from *Sparc*$^{+/+}$*; KIC* and *Sparc*$^{-/-}$*; KIC* animals, were used to probe collagen signaling and collagen activation of DDR1 stimulated downstream intermediates including protein tyrosine kinase 2 (PYK2) and pseudopodium-enriched atypical kinase 1 (PEAK1). Furthermore, utilization of a novel DDR1 small molecule inhibitor (7rh) abrogated collagen-induced DDR1 signaling and blunted tumor cell colony formation, migration, and

enhanced sensitivity to gemcitabine. Additionally, 7rh inhibited Ddr1 signaling in syngeneic, genetic, and human xenograft pancreatic tumors and was well tolerated. Therapy studies combining standard chemotherapy (gemcitabine plus nab-paclitaxel) with 7rh *in vivo* dramatically improved survival of mice compared to standard therapy alone. These data confirm that inhibition of collagen signaling in PDA is an attractive therapeutic strategy and demonstrate that DDR1 is a target that can be inhibited pharmacologically.

TABLE OF CONTENTS

PRIOR PUBLICATIONS

1. K. Y. Aguilera, M. M. Hagopian, L. Li, Z. Wang, S. Hinz, T. H. Hwang, J. B. Fleming, D. H. Castrillon, K. Ding, and R. A. Brekken. Inhibition of discoidin domain receptor 1 reduces collagen-mediated tumorigenicity in pancreatic ductal adenocarcinoma. Oncotarget. (Under review)

2. H. Hur, I. Ham, D. Lee, H. Jin, K. Y. Aguilera, H. Oh, J. Kwon, Y. Kim, K. Ding, R. Brekken. Discoidin domain receptor 1 activity drives an aggressive phenotype in gastric cancer. Clinical cancer research. (Under review)

3. Y. Zhang, K. Y. Aguilera, R. A. Brekken, A. D. Bradshaw. SPARC and Discoidin Domain Receptor (DDR) 2 Compete for Binding to Collagen I: Implications for Fibroblast Function. (Under review)

4. F. Mateo, Ó. Meca, T. Celià-Terrassa, Y. Fernández, I. Abasolo, L. Sánchez-Cid, R. Bermudo, V. Cánovas, M. Marín-Aguilera, L. Mengual, A. Alcaraz, S. Schwartz Jr., B. Mellado, K. Y. Aguilera, R. Brekken, P. L. Fernández, R. Paciucci, T. M. Thomson. SPARC mediates metastatic cooperation between CSC and non-CSC prostate cancer cell

subpopulations. Molecular Cancer. DOI: 10.1002/jcb.24649. 2014 Jan; 115 (1): 17-26.

5. K. Y. Aguilera, R. A. Brekken. Hypoxia Studies with Pimonidazole *in vivo*. Bio-protocol, http://www.bio-protocol.org/e1254. 2014 Oct 6. 4(19): e1254.

6. K. Y. Aguilera, L. B. Rivera, J. G. Carbon, J. E. Toombs, C. D. Goldstein, M. Dellinger, D. Castrillon, R. A. Brekken. Collagen signaling enhances tumor progression after anti-VEGF therapy in a murine model of PDA. Cancer Research. DOI: 10.1158/0008-5472 CAN-13-2800. 2014 Feb 15; 74 (4):1032-44.

7. K. Y. Aguilera, R. A. Brekken. Recruitment and Retention: Factors that Affect Pericyte Migration. Cell and Molecular Life Sciences. DOI: 10.1007/s00018-013-1432-z. 2014 Jan; 71 (2):299-309.

8. M. Yichoy, T.T. Duarte, A. De Chatterjee, T.L. Mendez, K.Y. Aguilera, D. Roy, S. Roychowdhury, S.B. Aley, S. Das. Lipid metabolism in Giardia: a post-genomic perspective. Parasitology. DOI: 10.1017/S0031182010001277.2011 Mar; 138 (3): 267-78.

LIST OF FIGURES

Chapter 1

Chapter 3

Chapter 4

Chapter 5

LIST OF TABLES

Chapter 1

Chapter 2

LIST OF APPENDICES

LIST OF ABBREVIATIONS

3M — 3 month old

5-Aza — 5-Aza-2’deoxycytidine

5-FU — 5-fluorouracil

5M — 5 month old

7rh — 3-(2-(Pyrazolo[1,5-a]pyrimidin-6-yl)-ethynyl)

ABX — Abraxane

AICART — Aminoimidazole carboxamide ribonucleotide transformylase

AKT — Protein kinase B

ALB — Albumin

ALT — Alanine aminotransferase

AML — Acute myelogenous leukemia

ARB — Angiotensin receptor blocker

AST — Aspartate aminotransferase

AT1 — Angiotensin-II-receptor-1

ATCC — American Type Culture Collection

Bcr-Abl — Breakpoint Cluster Region-Abelson kinase

BM-40 — Basement membrane protein 40

BSA — Bovine serum albumin

BUN — Blood urea nitrogen

CAF — Cancer associated fibroblast

cDNA — Complementary deoxyribonucleic acid

Chemo — Chemotherapy

CI — Confidence interval

CO2 — Carbon dioxide

CO-IP — Co-immunoprecipitation

Col — Collagen

Combo — Combination

CREA — Creatine

CSK — C-terminal Src kinase

CT — Computerized axial tomography

DACH — Diaminocyclohexane

DAPI — 4’, 6-diamidino-2-phenylindole

DDR — Discoidin domain receptor

DDR1 — Discoidin domain receptor 1

DDR2 — Discoidin domain receptor 2

DMEM — Dulbecco’s modified eagles medium

Dmso — Dimethyl sulfoxide

DNA — Deoxyribonucleic acid

Dnmt1 — DNA methyltransferase 1

DPD — Dihydropyrimidine dehydrogenase

DCE — Dynamic contrast enhanced

ECM — Extracellular matrix

EGF — Epithelial growth factor

EGFR — Epithelial growth factor receptor

ELISA — Enzyme-linked immunosorbent assay

EMT — Epithelial to mesenchymal transition

ER — Endoplasmic reticulum

FACIT — Fibril associated collagens with interrupted triple helices

FAK — Focal adhesion kinase

FBS — Fetal bovine serum

FC — Fragment crystallizable region

FDA — Food and Drug Administration

FN — Fibronectin

GAG — Glycosaminoglycan

GART — Glycinamide ribonucleotide transformylase

GDP — Guanosine diphosphate

Gem — Gemcitabine

GEMM — Genetically engineered mouse models

Gemzar— Gemcitabine

GLU — Glucose

Gp60 — Glycoprotein 60

GTP — Guanosine-5'-triphosphate

H&E — Hemotoxylin and eosin

HRP — Horseradish peroxidase

HSP — Heat shock protein

HSP47 — Heat shock protein 47

IACUC — Institutional Animal Care and Use Committees

IC_{50} — Inhibitory concentration that kills 50% of cells

ICC — Immunocytochemistry

IDE — Immunodepleted

IHC — Immunohistochemistry

IP — Immunoprecipitation

IP — Intraperitoneal

ITGα1 — Integrin α1

ITGα2 — Integrin α2

ITGαV — Integrin αV

ITGβ1 — Integrin β1

JM — Juxtamembrane

Kb — Kilobases

KC — LSL-Kras$^{G12D/+}$; p48$^{Cre/+}$

kDa — Kilodalton

KIC — LSL-Kras$^{G12D/+}$; Ink4aArf $^{lox/lox}$; p48$^{Cre/+}$

KO — *Sparc*$^{-/-}$

KPC — LSL-Kras$^{G12D/+}$*; LSL-Trp53*$^{R172H/+}$*; p48*$^{Cre/+}$

KPS — Karnofsky performance score

KRAS — V-Ki-ras2 Kirsten rat sarcoma viral oncogene homolog

LSL — Lox-stop-lox

mAb293 — SPARC monoclonal antibody 293

MAPK — Mitogen-activated protein kinase

MAPK2 — Mitogen-activated protein kinase kinase

mcr84 — Mouse chimeric r84

MDM2 — Mouse double minute 2 homologue

Mets — Metastases

mg — Milligram

mg/day — Milligrams per day

mg/kg — Milligram/kilogram

MMP — Matrix metalloprotease

mOS — Median overall survival

mRNA — Messenger RNA

MTS — (3-(4, 5-dimethylthiazol-2-yl)-5-(3-carboxymethoxyphenyl)-2-(4-sulfophenyl)-2H-tetrazolium)

MUC1 — Mucin1

MVD — Microvessel density

Nab — Nanoparticle albumin-bound

Nab-pac — Nab-paclitaxel

NCI — National Cancer Institute

NCK2 — Non-catalytic region of tyrosine kinase adaptor protein 2

ng — Nanogram

NOD/SCID — Non-obese diabetic/severe combined immunodeficiency

NSCLC — Non-small cell lung cancer

NSQ NSCLC — Non-squamous non-small cell lung cancer

O — Hydroxyproline

O_2 — Oxygen

OPRT — Orotate phosphoribosyltransferase

OS — Overall survival

PanIN — Pancreatic intraepithelial lesion

PATX — Patient-derived tumor xenograft

PBS — Phosphate buffered saline

PCNA — Proliferating cell nuclear antigen

PCR — Polymerase chain reaction

PDA — Pancreatic ductal adenocarcinoma

PEAK1 — Pseudopodium-enriched atypical kinase 1

PEGPH20 — PEGylated recombinant human hyaluronidase

PFS — Patient free survival

PI-3— Phosphatidylinositol

PI3K — Phosphoinositide 3-kinase

PIK3C2A — Phosphatidylinositol-4- phosphate 3-kinase

PLCL2 — Phospholipase C-like 2

PVDF — Polyvinylidene fluoride

PYK2 — Protein tyrosine kinase 2

qPCR — Quantitative polymerase chain reaction

RAF — Rapidly accelerated fibrosarcoma

RB — Retinoblastoma protein

rDDR1 — Recombinant DDR1/Fc

RIPA — Radioimmunoprecipitation

RNA — Ribonucleic acid

RPMI — Roswell Park Memorial Institute medium

rSPARC — Recombinant SPARC/His

RTK — Receptor tyrosine kinase

RUNX2 — Runt-related transcription factor 2

S Phase— Synthesis phase

Sac — Sacrifice

SC — Soluble collagen I

SCLC — Small cell lung cancer

SDS — Sodium dodecyl sulfate

SDS-PAGE — SDS-polyacrylamide gel electrophoresis

SH2 — Src homology 2

SHC — Src-homology 2 domain containing transforming protein

SHH — Sonic hedgehog

SHP-1 — SH2–containing tyrosine phosphatase-1

shRNA — Short hairpin ribonucleic acid

siRNA — Small interfering ribonucleic acid

SMO — Smoothened

SPARC — Secreted protein acidic and rich in cysteine

SQ NSCLC — Squamous non-small cell lung cancer

STAT — Signal Transducers and Activators of Transcription

TB — Tumor bearing

TBIL — Total bilirubin

TCBN — Triciribine

TCI — Tumor cell injection

Tgf-β — mouse transforming growth factor-β

Tgf-βr2 — mouse transforming growth factor β receptor 2

TKI — Tyrosine kinase inhibitor

TMA — Tissue microarray

TME — Tumor microenvironment

TP — Total protein

TS— Thymidylate synthase

TSP-1 — Thrombospondin-1

TTP — Time to progression

TX — Therapy

VEGF — Vascular endothelial growth factor

VEGF-A — Vascular endothelial cell growth factor-A

VEGFR — Vascular endothelial growth factor receptor

VEGFR1 — Vascular endothelial cell growth factor receptor 1

VEGFR2 — Vascular endothelial cell growth factor receptor 2

WT — *Sparc*$^{+/+}$

α — alpha

αDDR1 — DDR1 monoclonal antibody

µg — Microgram

µl — Microliter

µm — Micrometer

CHAPTER ONE

Review of the Literature

CHAPTER ONE

Review of the Literature

1.1 Problem Statement

The extracellular matrix (ECM), which is rich in fibrillar collagens, is a principal component of pancreatic ductal adenocarcinoma (PDA). The dysregulation of ECM-driven signaling programs is associated with an alteration of normal physiology. This dysregulation contributed to tumor progression and metastasis in different cancer types (Mahadevan & Von Hoff, 2007; Valiathan, Marco, Leitinger, Kleer, & Fridman, 2012). Moreover, this fibrotic network also contributed to resistance to chemotherapy (H. Liu et al., 2012). However, the ECM-mediated signaling pathways that drive these programs are unclear. A clearer understanding of collagen-mediated signaling in the tumor microenvironment will provide novel strategies for the therapy of PDA.

Recent reports (Chauhan et al., 2013; Chauhan, Stylianopoulos, Boucher, & Jain, 2011; Jacobetz et al., 2013; X. Li et al., 2012) highlighted that the desmoplasia present in PDA reduced drug delivery to pancreatic tumor cells and suggested that depletion of ECM components may improve response to chemotherapy. Present strategies for targeting ECM components in PDA have revealed promising effects (Provenzano et al., 2012). For example, delivery of hyaluronidase to target hyaluronan, an abundant ECM protein in PDA, improved

response to gemcitabine *in vivo* (Provenzano et al., 2012). This approach is currently in phase II clinical testing to assess PEGPH20 (PEGylated recombinant human hyaluronidase) combined with gemcitabine plus nab-paclitaxel in subjects with Stage IV previously untreated pancreatic cancer (WIRB HALO-109-202). Moreover, targeting specific inducers and pathways involved in desmoplasia might be combined with chemotherapeutic compounds for effective therapy. I chose to study a signaling cascade driven by collagen activation of DDR1 in PDA in an effort to understand its contribution to PDA progression.

Dysregulated and aberrant DDR1 expression has been associated with an unfavorable outcome for patients, and DDR1 signaling likely contributes to tumorigenesis. DDR1 has been implicated in regulating processes such as cell proliferation, migration, adhesion, ECM remodeling, and response to growth factors. DDR1 has promoted resistance to chemotherapy and mediated pro-survival signals in several cancer models (Cader et al., 2013; Ongusaha et al., 2003). DDR1 is expressed highly in fibrotic diseases and has been shown to contribute to the initiation and progression of fibrosis. Fibrosis and collagen signaling are associated with chemoresistance in PDA cell lines (Erkan et al., 2008; Ghaneh, Costello, & Neoptolemos, 2007; Mahadevan & Von Hoff, 2007). Collagen expression and deposition is apparent in a multitude of tumor types, and is a complex process that is orchestrated in part by the matricellular protein known as secreted protein acidic and rich in cysteine (SPARC). SPARC

expression correlates with enhanced chemoresponse in PDA patients (D. D. Von Hoff et al., 2011). Moreover, previous structural studies (Carafoli & Hohenester, 2012) identified that SPARC and DDR1 share the same collagen-binding site. In my doctoral work I proposed that SPARC reduced collagen-mediated signaling via DDR1. SPARC inhibition of collagen signaling is a plausible explanation for the correlation of SPARC expression and chemoresponse (Grzesiak, Ho, Moossa, & Bouvet, 2007; Van Cutsem et al., 2009). Further, the studies described herein highlight the therapeutic potential of pharmacological inhibition of DDR1 as an attractive strategy to increase the efficacy of standard chemotherapeutic regimens for PDA.

1.2 Historical review

1.2.1 Pancreatic ductal adenocarcinoma

Pancreatic cancer is a significant health problem with known risk factors such as chronic and hereditary pancreatitis, familial cancer syndromes, cigarette smoking, and late onset diabetes mellitus (Wong & Lemoine, 2009). 95% of pancreatic cancers are classified as exocrine tumors including pancreatic ductal adenocarcinoma (PDA), while the other 5% account for neuroendocrine tumors (Bardeesy & DePinho, 2002). Pancreatic cancer only accounts for 3% of all cancers, though this risk is expected to increase (Rahib et al., 2014). According to

a study conducted by Rahib and colleagues (Rahib et al., 2014), there were approximately 43,000 new cases and 36,000 deaths of pancreatic cancer in the United States in 2010, and this number is projected to increase to 88,000 new cases and 63,000 deaths in the year 2030. Moreover, pancreatic cancer is projected to become the second leading cause of cancer-related death in the United States by the year 2030 (Rahib et al., 2014).

This disease is one of the most difficult conditions to treat with a 5-year survival rate of approximately 5%, which has remained largely unchanged over the past 25 years (Jemal et al., 2008). The majority of PDA patients typically present with locally advanced or metastatic disease, with a median survival of 6-10 months and 3-6 months, respectively (Pancreatric Section et al., 2005). Although 10-15% of patients have potentially resectable tumors, many experience recurrence of disease following surgery (Wong & Lemoine, 2009). Gemcitabine, which will be discussed more fully in this chapter, is the standard chemotherapeutic drug for patients with advanced pancreatic cancer after a phase III trial in 1997 demonstrated a modest survival advantage (median survival 5.6 months), and a reduction of disease-related symptoms (Burris et al., 1997). However, the severity of this disease alongside the lack of effective treatment modalities has highlighted the pressing need for improved diagnostic and treatment strategies. Fortunately, in the past decade, resources have focused on

the development of novel therapies to target the molecular aberrations of this disease (Wong & Lemoine, 2009).

1.2.2 Frequent mutations in pancreatic ductal adenocarcinoma

As shown in Figure 1.1, Figure 1.2, and Table 1 critical effectors and mutations have been previously described as oncogenic drivers of PDA development and progression. These include the activation of oncogenic KRAS and the inactivation of several tumor suppressors (p16INK4a/p19Arf, and p53) (Hruban, Iacobuzio-Donahue, Wilentz, Goggins, & Kern, 2001). In the general oncogenic sequence of mutational events pancreatic intraepithelial neoplastic (PanIN) lesions, which are non-invasive neoplastic precursors to PDA (Hruban, Adsay, et al., 2001; Hruban et al., 1999), typically harbor KRAS mutations as early events. This is followed by loss of p16INK4a/p19Arf as an intermediate event and loss of p53 as a subsequent events (Edlund, 1999; Leach, 2004; Maitra et al., 2003; van Heek et al., 2002; Yeo et al., 2002). These common mutations are further described in the following section.

1.2.2.1 KRAS

Kirsten rat sarcoma viral oncogene homolog (KRAS) is a member of the Ras gene family, which encodes membrane-bound GTP-binding proteins. When GDP is released by activated Ras proteins in exchange for GTP, this leads to the

conversion of the Ras protein to the ‘on’ state and the activation of downstream signaling events (Wong & Lemoine, 2009). The downstream events of activated Ras have generally included factors such as the Raf, MAP2K, MAPK and the PI3K-Akt cascades (Wong & Lemoine, 2009). These signaling events are typically brief due to the intrinsic GTPase activity of Ras proteins, which switches these proteins’ effects ‘off ’(Wong & Lemoine, 2009).

Mutations of KRAS, mostly at codon 12 and less commonly at codons 13 and 61, are exceptionally frequent in PDA patients (Almoguera et al., 1988). More than 90% of pancreatic tumors contain mutations in the KRAS oncogene, which results in a dominant active form of the KRAS GTPase (Jones et al., 2008). Mutations in KRAS result in impaired GTPase function, which causes KRAS to be locked in the GTP-bound ‘on’ state. KRAS is required for the initiation and is also necessary for the maintenance of PDA (Collins et al., 2012). Mutations in KRAS occur early in the development of PDA, as evidenced by their identification in early PanIN precursor lesions (Klimstra & Longnecker, 1994). These mutations trigger a variety of cellular events, which include transcription, translation, cell-cycle progression, enhanced cell survival and motility.

1.2.2.2 INK4A/ARF

The *Ink4a* (inhibitor of cyclin-dependent kinase type 4) and *Arf* (alternate reading frame protein) tumor suppressors and their respective protein products

p16INK4A and p19ARF are encoded by the 9q21 locus (Sherr, 2001). Loss of INK4A function occurs in 80%-95% of spontaneous PDA (Hustinx et al., 2005; Rozenblum et al., 1997) and INK4A loss is typically observed in moderately dysplastic PDA lesions. INK4A inhibits CDK4/6-mediated phosphorylation of retinoblastoma protein (RB), which blocks entry into the synthesis phase (S phase) of the cell cycle; ARF stabilizes p53 through inhibition of mouse double minute 2 homologue (MDM2)-dependent proteolysis (Hezel, Kimmelman, Stanger, Bardeesy, & Depinho, 2006). Given the frequent homozygous deletion of 9p21 in PDA tumors, many PDAs sustain loss of *Ink4a* and *Arf* tumor suppression pathways (Hezel et al., 2006). Recent mouse model studies have shed light on the specific functions of *Ink4a* and *Arf* tumor suppression pathways in this disease (Hezel et al., 2006). These studies have reinforced the relevance of *Ink4a* in the pathogenesis of PDA as *Ink4a* mutations cooperate with *Kras* in the development of PDA and accelerate tumor progression in the setting of concurrent mutations in *p53* (Bardeesy et al., 2006).

1.2.2.3 P53

The *p53* tumor suppressor gene is mutated, generally by missense alterations of the DNA-binding domain, in >50% of PDA cases (Rozenblum et al., 1997). *p53* mutations appear in later-stage PanIN lesions that have acquired significant features of dysplasia (Boschman, Stryker, Reddy, & Rao, 1994; Maitra

et al., 2003). In human PDA, *p53* mutations and *Arf* deletions coexist in approximately 40% of cases (Heinmoller et al., 2000; Hustinx et al., 2005; Maitra et al., 2003). Previous studies have suggested that *Arf* possesses *p53*-independent functions, which include the inhibition of ribosomal RNA processing (Paliwal et al., 2006; Qi et al., 2004; Rocha, Campbell, & Perkins, 2003; Sugimoto, Kuo, Roussel, & Sherr, 2003). In addition, ARF does not neutralize the DNA damage checkpoint that would be activated upon genetic damage which highlights the necessity of *p53* loss as this intensifies PDA progression (Greenberg et al., 1999).

1.3 Animal models of PDA

Through exploitation of the commonly mutated genes in PDA, an important milestone in the field of PDA biology and research was the development of genetically engineered mouse models (GEMM) of this disease (Hruban et al., 2006). Mice have been engineered to express oncogenes, lose the expression of tumor suppressor genes, or express dominant negative tumor suppressor genes through the use of knock-out or knock-in technologies (Neesse et al., 2011). To control the knock-out or knock-in mutations of these PDA genes in a spatiotemporal manner site-specific recombinases, such as Cre, have been used via Lox-stop-lox (LSL) technology (Capecchi, 1989). Distinct GEMMs of PDA have been generated and mimic the pathophysiological development and progression of the human disease and are summarized here.

1.3.1 *KC* and *KIC* models

The *KC* model was generated to harbor a mutation of a constitutively active endogenous *Kras* gene specifically in pancreatic progenitor cells. This was achieved through the cross of mice with a conditionally activated *Kras* allele (*LSL-Kras*^{G12D}) with transgenic strains that express Cre recombinase in pancreatic lineages (*Pdx-Cre* or *p48*^{Cre}) to yield *Kras*$^{G12D/+}$; *Pdx-Cre*$^{/+}$ or *Kras*$^{G12D/+}$; *p48*$^{Cre/+}$ mice (Neesse et al., 2011). *KC* mice develop PanIN lesions with 100% penetrance, but only a small subset of these animals progress to PDA. This highlighted the involvement of additional genetic alterations necessary for tumor formation and progression (Hingorani et al., 2003; Neesse et al., 2011). While spontaneous invasion and metastases were observed at a low frequency with post-activation of oncogenic *Kras* in the mouse pancreas, a subsequent report from Ronald DePinho and colleagues demonstrated that accelerated PanIN formation, rapid tumor progression, and metastatic disease occurred through *Pdx1-Cre*-activated *Kras*^{G12D} activation combined with the pancreas-specific *Ink4a/Arf* deficiency which yielded *Kras*$^{G12D/+}$; *Ink4a/Arf*$^{flox/flox}$; *Pdx1-Cre* mice (Aguirre et al., 2003). This study highlighted that mice which expressed *Pdx1-Cre*-activated *Kras*$^{G12D/+}$ formed PanIN lesions and progressive pancreatic fibrosis, but no evidence of invasive cancer as assessed up to 30 weeks of age. However, when these genetic alterations were combined with *Cre*-mediated excision of loxP-flanked *Ink4a/Arf* alleles, all mice (*KIC*) developed invasive and metastatic PDA

within 11 weeks (Aguirre et al., 2003; Leach, 2004). *Pdx1-Cre; Ink4a/Arf* $^{lox/lox}$ mice which lacked the Cre-activated *Kras*$^{G12D/+}$ transgene failed to develop pancreatic tumors, which further demonstrated the critical function of oncogenic *Kras* in tumor initiation and the involvement of *Ink4a/Arf* in tumor progression (Aguirre et al., 2003).

1.3.2 *KPC* model

The *KPC* GEMM of PDA was generated to harbor a constitutively active oncogenic *Kras* gene combined with the pancreas-specific *p53* deficiency through the cross of *Pdx1-Cre* mutant mice. This cross generated conditional mutations analogous to the genetic alterations in human PDA to yield *Kras*$^{G12D/+}$; *p53*$^{R172H/+}$; *Pdx1-Cre*. *KPC* mice develop advanced PDA with 100% penetrance at approximately 2-3 months of age, and recapitulate human PDA through histopathological similarities in neoplastic cells, desmoplasia, the occurrence and site of metastases, and comorbidities such as cachexia, activation of biochemical pathways and evidence of genomic instability (Hingorani et al., 2005).

Thus the use of GEMM models, in contrast to subcutaneous, orthotopic or xenograft models of PDA, are histopathologically more relevant to elucidate the interactions in the tumor microenvironment (TME) in disease initiation and progression of PDA. Moreover, GEMMs of PDA have been crucial in preclinical

studies to examine the effects of PDA-targeted agents on the TME (Neesse et al., 2011).

1.4 Current treatment modalities for PDA

PDA is clinically classified to three stages: resectable, unresectable with locally advanced disease, and metastatic. Resectable disease corresponds mostly to Stages I and II and in some cases, to Stage III. Unresectable with locally advanced disease corresponds to Stage III, and metastatic disease corresponds to Stage IV (Furuse, Nagashima et al, 2008). As treatment strategies differ by the clinical stage, the stage determination of PDA patients is crucial in the determination of the most appropriate treatment method.

In recent decades, significant efforts have focused on the enhancement of the current standard of care chemotherapy, gemcitabine (Gemzar® by Eli Lilly), through analysis of the combination of this chemotherapy with cytotoxic drugs (Desai, Zalupski et al, 2008). Randomized trials have been performed to evaluate the potential benefit of 5-FU (Berlin et al., 2002), erlotinib (Moore et al., 2007; Okusaka et al., 2011), irinotecan (Rocha Lima et al., 2004; Rocha Lima et al., 2002; Stathopoulos et al., 2006), oxaliplatin (Alberts et al., 2003; Louvet et al., 2002; Louvet et al., 2005; Poplin et al., 2009), and albumin-bound paclitaxel (D. D. Von Hoff et al., 2011), but there have not been significant enhancements of overall survival benefit with the majority of these regimens.

1.4.1 Gemcitabine (Gemzar®)

Gemcitabine (Gemzar®) was the first chemotherapeutic drug effective in the enhancement of overall patient survival. In a randomized trial (Burris et al., 1997), 126 patients with advanced PDA were randomized to receive gemcitabine 1000 mg/m^2 weekly for 7 weeks followed by 1 week off, then on days 1, 8, and 15 of a 28-day cycle. Through analysis of clinical benefit, defined by a pain score, Karnofsky performance score (KPS), and body weight, patients that received gemcitabine displayed a better clinical benefit (23.8% versus 4.2%; p=0.0022), and gemcitabine-treated patients had a statistically better median overall survival (OS; 5.65 versus 4.41 months; p=0.0025) and overall one year survival rate (18% versus 2%; p=0.0025). The Food and Drug Administration (FDA) approved gemcitabine monotherapy as the primary treatment for advanced PDA.

In past couple decades since this phase III study, gemcitabine has been widely used as the standard chemotherapy for unresectable PDA (Burris et al., 1997). Unfortunately, the anticancer activity of gemcitabine monotherapy is only modest, which emphasizes the critical need for the development of more effective treatment strategies for PDA patients.

1.4.2 5-fluorouracil (5-FU)

5-fluorouracil (5-FU) based chemotherapy was the primary treatment for PDA since the 1950s, despite a modest median of survival of less than 6 months

(Moertel, 1978). Attempts to combine 5-FU with other chemotherapeutics such as doxorubicin and cisplatin increased overall toxicities, and none of these combinations were shown to enhance the median of survival (Cullinan et al., 1985; Moertel, 1978).

1.4.3 Albumin-bound paclitaxel (Nab-paclitaxel, Abraxane®)

Nab-paclitaxel (Abraxane®) is a solvent-free, water-soluble formulation composed of paclitaxel and human albumin with an average particle size of 130 nm (D. D. Von Hoff et al., 2011). Nab-paclitaxel delivery is mediated by active transport of albumin into the interstitial space via gp60-mediated transcytosis (S. M. Vogel, Minshall, Pilipovic, Tiruppathi, & Malik, 2001). Additionally albumin is theorized to deliver paclitaxel to the stromal-rich tumors and thereby increase local intratumoral concentration of monotherapy or along with another chemotherapeutic agent (D. D. Von Hoff et al., 2011). Consistently, work with a xenograft model of PDA has shown that the combination treatment with nab-paclitaxel and gemcitabine exhibited synergistic antitumor activity and improved drug delivery (D. D. Von Hoff et al., 2011). This was noted alongside a noticeable stromal depletion after 28 days of treatment (D. D. Von Hoff et al., 2011). Additionally, the combination of nab-paclitaxel with gemcitabine increased intratumoral gemcitabine concentrations by reducing cytidine deaminase levels which enhanced antitumor activity (Alvarez et al., 2013; Frese

et al., 2012; Hamada, Masamune, & Shimosegawa, 2013). The effect of nab-paclitaxel on the depletion of tumor stroma was also confirmed in the *KPC* PDA mouse model (Neesse et al., 2014).

In a phase I/II study of the combination of nab-paclitaxel with gemcitabine, the response rate was 48% and the median overall survival was 12.2 months in patients with metastatic PDA (D. D. Von Hoff et al., 2011). In the recent multinational phase III trial (Ma & Hidalgo, 2013; D. Von Hoff et al., 2012), metastatic pancreatic cancer patients who received nab-paclitaxel–gemcitabine had a median survival of 8.5 months versus 6.7 months (HR, 0.72; P =0.000015), 1-year survival 35% versus 22% and a 2-year survival 9% versus 4%. This new regimen also improved the overall survival and progression-free survival of patients with metastatic pancreatic cancer (Heinemann et al., 2014).

1.4.4 Erlotinib

Erlotinib is an epidermal growth factor receptor (EGFR) tyrosine-kinase inhibitor and is used in the treatment of various solid tumor types, including lung cancer. A study which combined erlotinib with gemcitabine in PDA patients reduced the risk of death by 18% compared to gemcitabine monotherapy (hazard ratio 0.82; 95% confidence interval (CI), 0.69-0.99; P=0.038), with a median overall survival (OS) of 6.24 versus 5.91 months, respectively (Moore et al., 2007). A phase II study of 107 Japanese PDA patients treated with the

combination of gemcitabine and erlotinib demonstrated that the median OS and median patient-free-survival (PFS) were 9.23 and 3.48 months, respectively (Okusaka et al., 2011). The most common adverse events that were noted included skin rash and anorexia, while interstitial lung disease-like events were also reported in nine patients (8.5%) (Okusaka et al., 2011). Due to these findings, the combination therapy of gemcitabine with erlotinib has been recognized as one of the standard treatments for unresectable PDA.

1.4.5 Irinotecan (Camptosar®)

Irinotecan (Camptosar®) is a chemotherapeutic agent that targets topoisomerase I. Treatment with irinotecan monotherapy has demonstrated a response rate of 9% in advanced PDA (Wagener et al., 1995). In a phase II study in which irinotecan was combined with gemcitabine, the combination led to a response rate of 20% and 1-year survival of 27% (Rocha Lima et al., 2002). The time to progression and overall survival were modest at 2.8 and 5.7 months, respectively (Rocha Lima et al., 2002). When compared to gemcitabine alone in a randomized study, the combination did not significantly improve the overall survival (6.3 months versus 6.6 months, P=0.789) (Rocha Lima et al., 2004), although the combination had a significantly better response rate (16.1% versus 4.4%, P=0.001). The most common toxicity observed in both studies was grade 3–4 neutropenia as well as grade 3-4 diarrhoea.

1.4.6 Oxaliplatin (Eloxatin®)

Oxaliplatin (Eloxatin®) is a diaminocyclohexane (DACH)-platinum compound that is active in several solid tumor types, which include cisplatin and carboplatin resistant cancers (Louvet et al., 2002). Oxaliplatin monotherapy has demonstrated minimal antitumor activity in PDA and is usually used in combination with other chemotherapeutic agents. Oxaliplatin is generally well-tolerated by patients, and the main toxicities are laryngeal dysaesthesia during administration, as well as peripheral sensory neuropathy which tends to occur with cumulative exposure to the drug (Alberts et al., 2002). Importantly, a phase I dose escalation study of gemcitabine and oxaliplatin noted neutropenia to be the dose-limiting toxicity (Alberts et al., 2002). A phase II study reported a response rate of the combination of 11% and overall survival of 6.2 months (Alberts et al., 2003), whereas another study in which gemcitabine was administered with a fixed dose rate in combination with oxaliplatin reported that 40% of patients had a clinical benefit from treatment with a response rate of 30.6% and overall survival of 9.2 months. (Louvet et al., 2002). Unfortunately, a recent randomized phase III study reported that the combination did not significantly improve overall survival (8.8 months versus 6.9 months, P=0.15), although progression-free survival was significantly improved in patients treated with the combination (5.8 months versus 3.7 months, P=0.04), as was the response rate (26.8% versus 17.3%, P=0.04) and clinical benefit (38.2% versus 26.9%, P=0.03) (Ducreux et al., 2004).

1.4.7 FOLFIRINOX

FOLFIRINOX is a treatment regimen which is composed of oxaliplatin, leucovorin, irinotecan, and 5-fluorouracil (5-FU), and has been investigated for its use as a treatment modality in advanced PDA. In a phase III study that compared FOLFIRINOX with gemcitabine monotherapy, FOLFIRINOX therapy significantly enhanced the overall survival benefit compared to gemcitabine in patients with metastatic PDA (11.1 months versus 6.8 months, $P<0.001$) (Conroy et al., 2011). Several toxicities were reported in patients treated with FOLFIRINOX, which included febrile neutropenia (5.4% patients). Based on these results, FOLFIRINOX is considered as a first-line standard of care option for metastatic PDA. It is important to note that the appropriate selection of candidates is crucial for the use of this treatment regime. Patients enrolled for FOLFIRINOX therapy should present a suitable performance status, be younger aged and have no risk of cholangitis (Furuse & Nagashima, 2013). A small phase II study of FOLFIRINOX is currently under investigation in Japan to assess the modification of the use of 180 mg/m^2 irinotecan versus the standard 150 mg/m^2. Moreover, this treatment strategy has exhibited its potential utility for the treatment of PDA patients and is presently approved for various types of cancers in Japan (Furuse, Nagashima et al, 2008).

1.5 Desmoplasia as a regulator of tumorigenesis and chemoresistance.

As previously described, due to the severity of PDA alongside the lack of effective treatment modalities and the significant chemoresistance of the majority of these malignancies, resources have focused on the development of novel therapies to target the molecular aberrations of this disease (Wong & Lemoine, 2009). A hallmark in PDA is an aberrant stromal response, or desmoplasia, which is defined by an altered histological landscape and the aberrant accumulation of fibrotic tissue with an altered ECM (Mahadevan & Von Hoff, 2007). This has been associated as conducive to tumor growth and metastasis (Mahadevan & Von Hoff, 2007). Thus, the prospect of targeting desmoplastic-signaling networks merit exploration as a strategy to enhance the efficacy of chemotherapy.

1.5.1 Review of collagen types

The 28 types of vertebrate collagens are the most physiologically abundant proteins in the body (~30% of total protein mass) (Ricard-Blum, 2011) (Table 2). Collagens have structural functions in the extracellular matrix (ECM), mediate cellular interactions, interact with other ECM molecules and components, and delineate the physiological structure and characteristics of tissues (Leitinger, 2014). All collagen types are generally characterized by a triple-helical structure, in which three polypeptide chains (α-chains) form coiled structures, which form right-handed triple helixes (Leitinger, 2014). A characteristic of collagen α-chains

is the repetition of glycine-X-X' amino acid sequences, in which the X and X' are typically proline and 4-hydroxyproline (O), respectively (Leitinger, 2014). 4-hydroxyproline is a critical amino acid component essential for the formation of the triple-helical structure and stability (Kotch, Guzei, & Raines, 2008). Collagens are differentially organized into α-chain combinations composed of three identical α-chains (homotrimeric collagens), or composed of two or three distinct α-chains (heterotrimeric collagens) (Leitinger, 2014). Physiologically, collagens make up supramolecular structures in which the individual collagen triple helices form higher order complexes such as fibers or sheet-like configurations (Leitinger, 2014). The most common collagen families are the fibrillar collagens (collagen types I-III) and the collagens that form networks (e.g. the basement membrane collagen type IV) (Leitinger, 2014). The other collagen families are the FACIT collagen (IX, XII, XIV), short chain (Type VIII, X) and others (Type VI, VII, XIII).

1.5.2 Collagens in normal physiology

As noted in Table 2, adapted from a thorough review by Kadler and colleagues (Kadler, Baldock, Bella, & Boot-Handford, 2007), the 28 types of collagens are differentially expressed and localized amongst tissue types and display diverse functions. The more prominent types of collagen, and those of which the dissertation is focused on, are collagens that form fibrils (i.e. collagens

I, II, III, IV, and XI). These are generally expressed in various connective tissues as well as skin (Kadler et al., 2007). The collagen fibril is a critical physiological component that provides strength and flexibility and provides structural integrity for tissue (Wess, 2005). Collagen fibrils are substantial components of a variety of tissue types (i.e. skin, tendon, bone, ligament, cornea, and cartilage) where the fundamental properties of the fibril aid in biomechanical and structural roles (Kadler et al., 2007; Wess, 2005). Throughout normal physiological conditions, the collagen network supports cell–matrix interactions, as well as cell polarity, differentiation, and survival via specific cell surface receptors that incorporate cues from the ECM and trigger signaling networks that mediate cellular function (Valiathan et al., 2012).

1.5.3 Collagens in tumorigenesis

In pathological conditions, such as cancer, the dysregulation of ECM-driven signaling programs has been shown to alter normal physiology and contribute to tumor development and progression (Valiathan et al., 2012). As previously mentioned, a substantial characteristic of PDA is the formation of a dense desmoplastic reaction. This is typically characterized by an abnormal accumulation of fibrotic tissue (Mahadevan & Von Hoff, 2007) thought to facilitate tumor growth and metastasis (Mahadevan & Von Hoff, 2007). In PDA the desmoplastic landscape consists of a heterogeneous cell population that

includes fibroblasts, pancreatic stellate cells, vascular endothelial cells, and immune cells, which in conjunction with the fibrotic network and matricellular components, leads to the formation of a complex TME that promotes PDA development, invasion, metastasis and resistance to chemotherapy (H. Liu et al., 2012). The ECM is formed and regulated through the cooperation of various cytokines and matricellular proteins, which include TGF-β and matricellular proteins such as SPARC (Lane, Iruela-Arispe, & Sage, 1992; H. Liu et al., 2012; Rentz, Poobalarahi, Bornstein, Sage, & Bradshaw, 2007; Tremble, Lane, Sage, & Werb, 1993).

The tumor matrix has been attributed as a drug delivery barrier as it indirectly limits the delivery of chemotherapeutic or other targeted agents through vascular compression (Chauhan et al., 2013). Drug delivery to tumors is dependent on the structural propensity of perfused vessels (Chauhan et al., 2011; Jain, 2013; Tsai, Johnson, & Intaglietta, 2003). Pathophysiological pressure has been demonstrated to accumulate in tumors as cancer and stromal cell populations flourish aggressively in a limited interstitial space (Chauhan et al., 2013; Helmlinger, Netti, Lichtenbeld, Melder, & Jain, 1997; Stylianopoulos et al., 2012; Stylianopoulos et al., 2013). The dense formation of ECM has been shown to collapse blood vessels and reduce the microvessel density to limit perfusion (Griffon-Etienne, Boucher, Brekken, Suit, & Jain, 1999; Padera et al., 2004). Unfortunately, cancer patients that present with low tumor perfusion respond

poorly to chemotherapy and have a reduced survival compared to patients with high perfusion (Park et al., 2009; Sorensen et al., 2012).

1.6 SPARC

Secreted protein acidic and rich in cysteine (SPARC), also known as osteonectin (Termine et al., 1981) and BM-40 (Mann, Deutzmann, Paulsson, & Timpl, 1987), is a 303 amino acid (human) or 302 amino acid (mouse) glycoprotein approximately 35 kDa in size (Sage, Johnson, & Bornstein, 1984) with a protein sequence homology between mice and humans of 95% (Appendix A). It is a matricellular protein that is secreted into the ECM where it regulates angiogenesis, cell adhesion, cell migration, cell proliferation, and cell survival (Bornstein & Sage, 2002; Brekken & Sage, 2001), and tissue remodeling during wound healing (Bornstein & Sage, 2002; Brekken & Sage, 2001).

SPARC interacts with, or indirectly regulates, a variety of growth factors including fibroblast growth factor (FGF), vascular endothelial growth factor (VEGF), platelet-derived growth factor (PDGF), and transforming growth factor-β (TGF-β) (Francki et al., 2004; Hasselaar & Sage, 1992; Kupprion, Motamed, & Sage, 1998; Raines, Lane, Iruela-Arispe, Ross, & Sage, 1992). Expression of SPARC during mammalian development and tissue differentiation is robust but declines in the majority of organs after maturation (Bradshaw & Sage, 2001). Ultimately, the expression of SPARC is limited post-development to

tissues with high ECM turnover, such as bone and gut epithelia (Bradshaw & Sage, 2001). However, SPARC is induced during wound-healing, at sites of angiogenesis, and during tumorigenesis (Bornstein & Sage, 2002; Mendis, Ivy, & Brown, 1998; Pen, Moreno, Martin, & Stanimirovic, 2007; Reed et al., 1993).

1.6.1 SPARC as a regulator of collagen deposition and ECM remodeling

SPARC functions as a mediator of tissue remodeling. SPARC binds directly to fibrillar collagens I, III and V, and to basement membrane collagen IV (Sage, Vernon, Funk, Everitt, & Angello, 1989; Sasaki, Hohenester, Gohring, & Timpl, 1998; Sasaki, Miosge, & Timpl, 1999). The Brekken lab, and others, have previously demonstrated that tumors grown in *Sparc*$^{-/-}$ animals are more aggressive and exhibited a diminished deposition of ECM compared with those grown in wild-type (*Sparc*$^{+/+}$) counterparts (Brekken et al., 2003; Puolakkainen, Brekken, Muneer, & Sage, 2004). Additionally, in an orthotopic model of PDA in *Sparc*$^{+/+}$ and *Sparc*$^{-/-}$ mice tumors grown in the absence of host-derived SPARC showed a marked reduction in the deposition of fibrillar collagens I and III, basement membrane collagen IV and the collagen-associated proteoglycan decorin (Arnold et al., 2010).

1.6.2 SPARC as a regulator of cancer progression

As shown in Table 3 and Table 4, two major categories amongst a variety of cancer and tumor types have been described: the settings in which tumor cells are SPARC expressing (positive) and in which tumor cells are SPARC non-expressing (negative) (Thomas & Rempel, 2011). Although there are discrepancies throughout the literature, it has been largely accepted that SPARC overexpression is associated with oncogenesis in breast cancer, prostate cancer, melanoma, meningioma, gastric carcinoma, head and neck cancer, and glioma (Thomas & Rempel, 2011). Conversely, SPARC expression has been associated as a tumor suppressor in a variety of tumors including pancreatic, lung, renal, esophageal, hepatocellular, uterine, colorectal, ovarian, neuroblastoma, and acute myelogenous leukemia (AML) (Thomas & Rempel, 2011).

Furthermore, SPARC has been considered a biomarker for cancers. In fact, SPARC is considered a therapeutic target for tumor cells that overexpress it, but a therapeutic agent for tumor cells that underexpress it (Thomas & Rempel, 2011). The underexpression or loss of SPARC throughout many cancer types has been examined through analysis of the regulation of SPARC expression. For instance, the SPARC promoter is commonly hypermethylated in PDA cell lines and xenograft tumors (Sato et al., 2003), lung adenocarcinomas and cell lines (Suzuki et al., 2005), ovarian cancer cell lines (Socha et al., 2009), primary colorectal cancer specimens and cell lines (Cheetham et al., 2008), and multiple

myeloma patient samples and cell lines (Heller et al., 2008). SPARC is a critical tumor-secreted permeability factor and a novel paracrine mediator of endothelium permeability during melanoma metastatic dissemination to lungs (Tichet et al., 2015). Additionally, among endometrioid ovarian carcinomas, frequent epigenetic inactivation of SPARC was noted in the development of non-serous ovarian carcinomas of Lynch and sporadic origin (Niskakoski et al., 2014).

The Brekken lab, and others, have previously demonstrated that in an orthotopic model of PDA *Sparc*$^{-/-}$ mice exhibited a significant increase in metastasis compared with *Sparc*$^{+/+}$ controls (Arnold et al., 2010). These findings indicated that SPARC is critical to the host response to tumorigenesis and the loss of SPARC expression accelerates tumor progression. Interestingly, a recent study by Von Hoff (D. D. Von Hoff et al., 2011) and colleagues demonstrated the function of SPARC in the modulation of patient response to therapy. Patients were treated with the maximum-tolerated dose (MTD) of gemcitabine (1,000 mg/m^2) plus nab-paclitaxel (125 mg/m^2) weekly for 3 weeks, repeated every 4 weeks. Overall survival was 12.2 months with a 1-year survival of 48%. These findings were amongst the highest reported for a phase II study in patients with PDA. Along with this, high stromal SPARC expression was correlated with a significant increase in patient survival. Altogether these observations indicated that stromal SPARC expression may be an important biomarker for the efficacy of gemcitabine plus nab-paclitaxel combination regimens in PDA.

A retrospective study with tumor samples from 16 patients with head and neck cancer suggested a correlation of tumor response to nab-paclitaxel with a higher expression of SPARC in the tumors (Desai, Trieu, Damascelli, & Soon-Shiong, 2009). In breast cancer, a retrospective analysis of 667 tumor specimens from the German GeparTrio trial found that a high expression of SPARC in tumor cells was significantly correlated with an increased pathological complete response rate to neoadjuvant chemotherapy with docetaxel and doxorubicin (Untch, M et al. 2012). Furthermore, the efficacy of therapy associated with SPARC expression is not clear.

A unifying, biochemical, mechanistic understanding of the function of SPARC in the TME is lacking. Interestingly, structural studies indicate that SPARC and a family of collagen-specific receptor tyrosine kinases (discoidin domain receptors, DDRs) bind to the same epitope (GVMGFO) on fibrillar collagens (Carafoli et al., 2009; Carafoli et al., 2012; Konitsiotis et al., 2008; Roskoski, 2007; Xu et al., 2011) (Figure 1.3). DDRs have been implicated in driving chemoresistance and thus I propose that: 1) SPARC inhibits collagen from binding and activating DDRs; and 2) that this is the underlying mechanism of how SPARC affects chemoresponse in tumors.

1.7 Discoidin domain receptor-collagen signaling

1.7.1 Discoidin domain receptors (DDRs)

Discoidin domain receptor (DDR) sequences were discovered and isolated in the 1990s based on their homology to other receptor tyrosine kinases (Alves, 2001; Di Marco, Cutuli, Guerra, Cancedda, & De Luca, 1993; Johnson, Edman, & Rutter, 1993; Karn et al., 1993; Lai & Lemke, 1994; Laval et al., 1994; Perez et al., 1994; Zerlin, Julius, & Goldfarb, 1993). The discoidin domain is termed as such based on its homology to lectin discoidin I, a protein secreted by the slime mold *dictyostelium discoideum* (Reitherman, Rosen, Frasier, & Barondes, 1975). The DDR family includes two closely related collagen-specific receptor tyrosine kinases (RTKs), DDR1 and DDR2, both of which recognize and bind several different types of collagens (Kadler et al., 2007; Shrivastava et al., 1997; W. Vogel, Gish, Alves, & Pawson, 1997). Like other RTKs, the DDRs regulate key cellular processes, which include cell migration, cell proliferation, cell differentiation, and cell survival (Leitinger, 2014).

DDR1 and DDR2 share 94% and 97% protein sequence, respectively, homology between mice and human (Appendix A). The DDRs are widely and differentially expressed amongst tissue types throughout physiological development. DDR1 is expressed at high levels in the pancreas, brain, lung, kidney, spleen, and placenta (Di Marco et al., 1993; Johnson et al., 1993; Laval et

al., 1994; Perez et al., 1994). DDR2 is expressed highly in tissues such as skeletal and heart muscle, kidney and lung (Karn et al., 1993; Lai & Lemke, 1994). Both DDRs are expressed throughout the development of the nervous system (Lai & Lemke, 1994; Zerlin et al., 1993). Additionally, the DDRs are differentially expressed throughout cellular populations: DDR1 expression is predominant in epithelial cells, while DDR2 is found in cells of connective tissues (Alves, 2001; Alves et al., 1995). While the DDRs are important for physiological development, their tissue-specific functions are not fully understood (Leitinger, 2014).

The DDRs only bind to native triple-helical collagens and not to denatured collagens (Leitinger, 2003; Shrivastava et al., 1997; W. Vogel et al., 1997). The DDRs display variable ligand specificity and are bound to and activated by various collagen types. Fibrillar collagens are ligands for DDRs (Shrivastava et al., 1997; W. Vogel et al., 1997) while non-fibrillar collagens are recognized distinctively. DDR1, but not DDR2, binds the basement membrane collagen type IV (Shrivastava et al., 1997; W. Vogel et al., 1997), while DDR2 preferentially binds collagen type II (Leitinger, 2003) and type X (Leitinger & Kwan, 2006). Through the utility of Collagen Toolkits, derived from the collagen domains of collagens type II and type III, the DDR binding sites in fibrillar collagen sequences have been previously mapped and specific amino acid sequences have been identified (Farndale et al., 2008). These studies identified a six amino acid sequence, GVMGFO, as a high-affinity binding motif for both DDRs (Konitsiotis

et al., 2008; Xu et al., 2011) (Figure 1.3). GVMGFO is present in fibrillar collagens I-III but not in collagen IV, which is indicative that DDR1 binds a different type of motif in non-fibrillar collagens (Valiathan et al., 2012).

Typical ligand binding to receptor tyrosine kinases induces the phosphorylation of distinct cytoplasmic tyrosine residues, which serve as docking sites for the assembly of downstream signaling molecules (Lemmon & Schlessinger, 2010). DDR1 has 15 tyrosine residues in its cytosolic domain, while DDR2 has 14 (Leitinger, 2014). All of these tyrosine residues could function as potential ligand-induced phosphotyrosine docking sites for signaling adaptors; however, it is still unclear which tyrosine residues become phosphorylated upon DDR binding to collagen (Leitinger, 2014). However, several phosphosites in the juxtamembrane region of DDR1 have been identified (Tyr484, Tyr513 and Tyr520) (Lemeer et al., 2012), as well as two phosphorylation sites in the kinase domain of DDR2 (Tyr684 and Tyr813) (Iwai, Chang, & Huang, 2013), and one in the juxtamembrane (JM) domain (Tyr481) (Ikeda et al., 2002).

Additionally several adaptor molecules have been identified that are recruited to phosphorylated sites on the DDR cytosolic regions, though specific cell regulatory functions remain undefined (Leitinger, 2014). Signaling intermediates that bind to DDR1 include SRC (Dejmek, Dib, Jonsson, & Andersson, 2003; Lu, Trcka, & Bendeck, 2011), PYK2 (protein tyrosine kinase 2) (Shintani et al., 2008), P130CAS (Shintani et al., 2008), SHC (W. Vogel et al.,

1997), SH2 (Src homology 2 domain-containing protein) (Koo et al., 2006), protein tyrosine phosphatases SHP-1 (Abbonante et al., 2013) and SHP-2 (Koo et al., 2006; C. Z. Wang, Su, Hsu, Shen, & Tang, 2006), and members of the STAT (Signal Transducers and Activators of Transcription) family (Faraci-Orf, McFadden, & Vogel, 2006; C. Z. Wang et al., 2006). Additionally, I have described the interactions between collagen-mediated DDR1 activation and downstream signaling of a novel non-receptor tyrosine kinase known as PEAK1 (pseudopodium-enriched atypical kinase 1) (Aguilera et al., 2014) which was described as a tumorigenic effector in colon and pancreatic cancers (Kelber & Klemke, 2010; Kelber et al., 2012). DDR2 intracellular signaling partners are undefined (Leitinger, 2014). There are several potential downstream effectors of DDR2 signaling, including SHP-2, NCK1, the SRC family kinase LYN, PLCL2 (phospholipase C-like 2), and PIK3C2A (phosphatidylinositol-4- phosphate 3-kinase), which have been identified through phosphoproteomic analysis (Iwai et al., 2013). However, additional validation is needed to verify these candidate effectors (Leitinger, 2014).

1.7.2 DDR-Specific functions in development

As shown in Figure 1.4 DDR1 and DDR2 are functionally important in normal as well as pathological development. In normal conditions DDR1 is important in organogenesis and DDR2 in bone growth (Valiathan et al., 2012).

1.7.2.1 Discoidin domain receptor 1

Ddr1 knockout mice are phenotypically characterized by small stature and gender-specific phenotypes. The females display multiple reproductive defects including impaired blastocyst implantation, therefore a large percentage of *Ddr1*$^{-/-}$ females are infertile (W. F. Vogel, Aszodi, Alves, & Pawson, 2001). As *Ddr1* is expressed throughout all stages of mammary development the most significant *Ddr1*$^{-/-}$ defect is abnormal branch formation of the mammary gland which results in failed milk secretion and the inability to nourish pups (Barker et al., 1995; Valiathan et al., 2012). The mammary glands in pregnant *Ddr1*$^{-/-}$ mice present an altered alveolar structure, with the fat pad filled with ducts (W. F. Vogel et al., 2001). Throughout development in *Ddr1*$^{-/-}$ female mice, ductal development in the mammary glands is delayed in puberty, which results in an altered formation of the terminal end bunds and secondary branching (W. F. Vogel et al., 2001). *Ddr1*$^{-/-}$ mice also display progressive morphological alterations and severely decreased auditory function due to defective inner ear development; moreover, *Ddr1* is a crucial regulator of inner ear development and structure (Meyer zum Gottesberge, Gross, Becker-Lendzian, Massing, & Vogel, 2008).

DDR1 is up-regulated in fibrotic diseases and contributes to the initiation and progression of fibrosis. In a model of bleomycin-induced lung fibrosis, which is a widely used mouse model for human idiopathic pulmonary fibrosis, *Ddr1*$^{-/-}$ mice were largely protected from bleomycin-induced lung injury (Avivi-Green,

Singal, & Vogel, 2006). A pro-fibrotic and pro-inflammatory role for DDR1 was also demonstrated in mouse models of kidney injury (Borza & Pozzi, 2014). DDR1 expression is elevated in patients with fibrotic diseases, lupus nephritis and Goodpasture's syndrome, as well as in a mouse model of crescentic glomerulonephritis (Kerroch et al., 2012). Moreover, Alport mice, a model of chronic kidney fibrosis, crossed with the *Ddr1*$^{-/-}$ mice have reduced renal fibrosis and inflammation (Gross et al., 2010). All together, the fibrotic actions reported for DDR1 make it an attractive therapeutic target for fibrotic diseases.

1.7.2.2 Discoidin domain receptor 2

Ddr2 knockout mice exhibit a characteristic phenotype of dwarfism with short long-bones and a short snout, due to reduced chondrocyte proliferation (Labrador et al., 2001). These mice, termed slie or smallie, are sterile in addition to their dwarfism: slie females are anovulatory and slie males lack spermatogenesis (Kano et al., 2008). Ddr2 is a key regulator throughout bone growth as it participates in endochondrial ossification through the regulation of chondrocyte maturation (Y. Zhang et al., 2011). Ddr2 also regulates intramembranous ossification through the regulation of osteoblast differentiation via phosphorylation of Runx2 (runt-related transcription factor 2), a master transcription factor in skeletal development (Lin et al., 2010; Y. Zhang et al., 2011). In osteoblasts, Ddr2-collagen interactions mediate the secretion of lysyl

oxidase (Khosravi, Sodek, Faibish, & Trackman, 2014), an enzyme that catalyzes cross-linking of collagen fibers essential for bone strength.

1.7.3 DDRs as potential therapeutic targets in cancer

Ultimately, dysregulated and aberrant DDR expression has been associated with an unfavorable outcome for patients, and altered functions of DDR1 and DDR2 likely contribute to tumorigenesis.

1.7.3.1 Discoidin domain receptor 1

DDR1-mediated cell adhesion to collagen is essential for tissue and cellular functions in normal and pathological processes. In pancreatic tumor tissues, DDR1 was identified as one of the 72 genes that were significantly upregulated in malignant versus benign pancreatic tumors (Couvelard et al., 2006). High levels of *DDR1* were found in hepatocellular carcinomas, which significantly correlated with advanced tumor stage (Shen et al., 2010). A study on non-small cell lung cancer (NSCLC) indicated that DDR1 expression increases and contributes to progression of this disease (Miao et al., 2013), and a study evaluating a cohort of 83 patients with NSCLC found that tumors with high DDR1 was associated with poor survival (Valencia et al., 2012). Ford and colleagues (Ford et al., 2007) demonstrated that 146 primary NSCLC and an independent set of 23 matched tumor and normal lung tissue samples showed that

DDR1 was upregulated in tumor vs. normal tissue. Another study evaluating 171 NSCLC samples showed that *DDR1* expression was associated with lymph node metastasis and poor overall survival (Yang et al., 2010). *DDR1* was also highly expressed in high-grade pediatric (Weiner, Rothman, Miller, & Ziff, 1996) and adult brain tumors (Weiner et al., 2000). *DDR1* was also elevated in gliomas compared to normal brain tissue (Ram et al., 2006) and significantly correlated with poor clinical outcome (Yamanaka et al., 2006). Moreover, DDR1 has been associated with resistance to chemotherapy and can mediate pro-survival signals in breast cancer and lymphoma cell lines (Cader et al., 2013; Ongusaha et al., 2003) and may be involved in the recurrence of certain types of cancer (Jian et al., 2012). Likewise, downregulation of DDR1 expression significantly enhanced the chemosensitivity of breast cancer cells to genotoxic drugs (Das et al., 2006).

1.7.3.1 Discoidin domain receptor 2

DDR2 was recently shown to be a key regulator of metastasis and invasion of breast cancer cells (K. Zhang et al., 2013). Zhang and colleagues (K. Zhang et al., 2013) have reported that DDR2 is expressed in 71% of invasive ductal breast cancer and that 5% of the invasive breast tumors had an amplified DDR2 copy number, associated with worse survival rate. DDR2 enhanced invasion, migration, and metastasis of breast cancer cells as it regulated and stabilized Snail1 protein levels and activity through SRC-dependent stimulation of ERK1 activity (K.

Zhang et al., 2013; K. Zhang et al., 2012). DDR2 expression in human breast epithelial cells has been associated with an induction of EMT (Taube et al., 2010). Moreover, DDR2 has been identified as a potential RTK target for the treatment of breast cancer metastasis (K. Zhang et al., 2013). Microarray analyses in aneuploid papillary thyroid carcinomas revealed that DDR2 was one of the few genes that was highly expressed in patients with metastatic disease at time of diagnosis (Rodrigues et al., 2007). Moreover, in the same study, analysis of tumors from patients that had died from this disease revealed that DDR2 was one of the most overexpressed genes in this group as well (Rodrigues et al., 2007). In addition, genetic alterations of DDR2 have been linked to different forms of diseases such as NSCLC and squamous cell lung carcinoma (SQCLC) (Davies et al., 2005; Drilon, Rekhtman, Ladanyi, & Paik, 2012; Hammerman et al., 2011).

Consistent with a pro-tumorigenic action of DDR2, *Ddr2*$^{-/-}$ mice display reduced primary tumor-associated angiogenesis and reduced lung colonization following tail vein injection (S. Zhang et al., 2014). In another study tumor growth and vascularization was assessed in *Ddr2*$^{-/-}$ mice (S. Zhang et al., 2014). Wild-type and *Ddr2*$^{-/-}$ mutant mice were implanted subcutaneously with three types of syngeneic tumor cells, including B16-F10 melanoma, H22 hepatic carcinoma and S180 sarcoma (S. Zhang et al., 2014). Tumor growth in *Ddr2*$^{-/-}$ mice was slow compared with that in control mice, which led to an approximately

five-fold difference in tumor volume at the end of the study (S. Zhang et al., 2014).

1.7.4 DDR inhibitors

Efforts have focused on methods to target DDRs for drug discovery. Approaches to target the tyrosine kinase activity of DDR1 and DDR2 have included the utility of small molecule inhibitors designed to disrupt the intracellular kinase activity. Small molecule tyrosine kinase inhibitors (TKIs) are generally ATP-competitive inhibitors, which bind to either the active (type I inhibitors) or inactive (type II and type III inhibitors) conformation of the kinase thereby interfering with the transfer of the terminal phosphate of ATP to proteins which contain a tyrosine residue (Gschwind, Fischer, & Ullrich, 2004; J. Zhang, Yang, & Gray, 2009). Type IV inhibitors are likewise useful for kinase modulation because they allosterically impair kinase activity by binding at sites outside of the ATP binding cleft (Fang, Grutter, & Rauh, 2013; Schneider et al., 2012). However, type II and especially type III inhibitors, or those that stabilize catalytically inactive states, are particularly useful in drug development initiatives (Over et al., 2013).

Several small molecule inhibitors that were originally developed to target the activity of the Breakpoint Cluster Region-Abelson kinase (Bcr-Abl) for the use in myelogenous leukemia, namely imatinib (also known as STI-571 or

Gleevec), dasatinib, nilotinib, and bafetinib (also known as INNO-406) also potently inhibit DDR activity (Day et al., 2008; Rix et al., 2007) (Figure 1.5, Table 1). Imatinib and nilotinib are type II inhibitors that bind to and stabilize an inactive kinase form that is characterized by 'DFG-out' conformation (Kothiwale, Borza, Lowe, Pozzi, & Meiler, 2014). The 'DFG-out' motif opens an additional cavity, a hydrophobic allosteric site that, in addition to the ATP binding pocket, is targeted by type II inhibitors (Kothiwale et al., 2014). Other type II Bcr-Abl inhibitors such as bafetinib have also displayed strong DDR inhibition (Bantscheff et al., 2007). Dasatinib is a type I inhibitor that targets kinase domains in the active form and is characterized by an open conformation of the activation loop (Kothiwale et al., 2014). Dasatinib in particular has demonstrated promising therapeutic efficacy in lung cancer cells harboring gain-of-function mutations of DDR2 (Ding et al., 2008), as well as two squamous cell carcinoma (SCC) patients with a $DDR2^{S768R}$ mutation were shown to have significant shrinkage of their tumors after dasatinib treatment (Pitini, Arrigo, Di Mirto, Mondello, & Altavilla, 2013).

Only recently, Gao et al. (M. Gao et al., 2013) reported a pyrazolopyrimidine alkyne derivative of the previously described DDR1 inhibitors which displayed a potently specific IC_{50} for DDR1 over DDR2. This is therapeutically attractive as a DDR1-specific inhibitor was not previously available. On the basis of the sequence similarity of DDR1, DDR2, and Bcr-Abl

in the kinase domain, Gao et al. (M. Gao et al., 2013) conducted a focused screening against an internal library containing approximately 2000 kinase inhibitors and identified 3-(2-(Pyrazolo[1,5-a]pyrimidin-6-yl)-ethynyl) 7rh benzamide (7rh) as a new potent DDR1 inhibitor. The compound potently inhibits DDR1 with an IC_{50} value of 6.8 nM and is significantly less active against DDR2 and Bcr-Abl, with IC_{50} values of 101.4 nM and 355 nM, respectively (M. Gao et al., 2013). The detailed interaction of the 7rh compound with DDR1 remains unclear, though it is predicted that the compound binds to the receptor with a type II binding mode (Y. Li, Lu, Ren, & Ding, 2015). Cell-based investigation has demonstrated that 7rh inhibited the activation of DDR1 and downstream signaling in a concentration-dependent manner and potently suppressed the proliferation, invasion, adhesion, and tumorigenicity of cancer cells (M. Gao et al., 2013). Ultimately, Gao et. al (M. Gao et al., 2013) has suggested that this compound is therapeutically attractive as preliminary pharmacokinetic studies in rats have demonstrated that the compound possesses promising PK profiles, with an oral bioavailability of 67.4% and $T_{1/2}$ of 15.5 hours when dosed at 25 mg/kg by oral gavage.

The role of DDR2 in tumor progression has indicated the need for the identification of potent DDR2 inhibitors. There is only limited understanding of its pharmacological interactions of DDR2 inhibition (Richters et al., 2014). Recently, Richters and colleagues (Richters et al., 2014) discovered novel DDR2-

specific type II and type III small molecule inhibitors. The IC_{50} for two compounds in cell-free kinase assays reported for DDR2 versus DDR1 were 18 nM and 75 nM compared to 39 nM and 235 nM, respectively. The discovery of novel DDR2 inhibitors is crucial as previous DDR2-specific inhibitors have not existed. Furthermore these compounds may be therapeutically attractive in targeting DDR2 in breast cancer patients or in SCC patients with the $DDR2^{S768R}$ mutation, as suggested by dasatinib treatment.

1.8 Figures

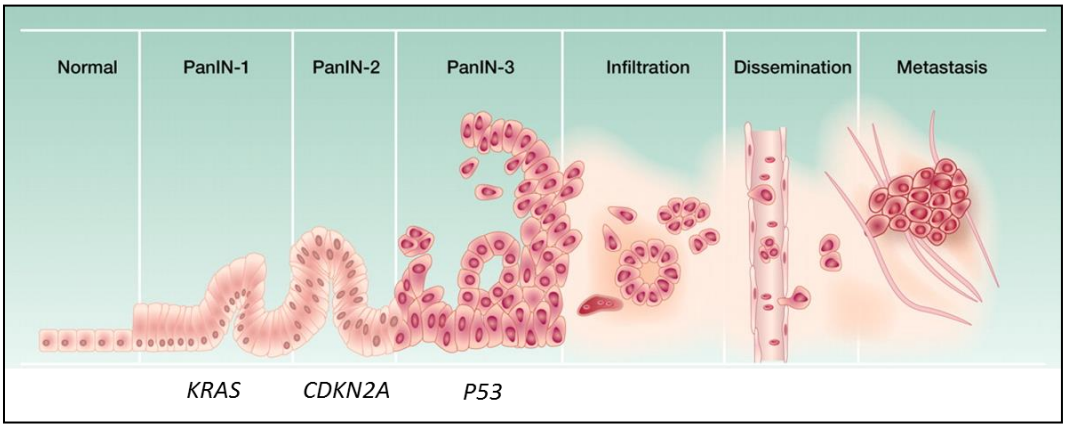

Figure 1.1: PDA progression.

Model of the progression from a normal cell to metastatic pancreatic cancer. Common mutations are described at the stage of PDA development (*KRAS, CDKN2A, and P53*). Adapted from (Iacobuzio-Donahue, Velculescu, Wolfgang, & Hruban, 2012).

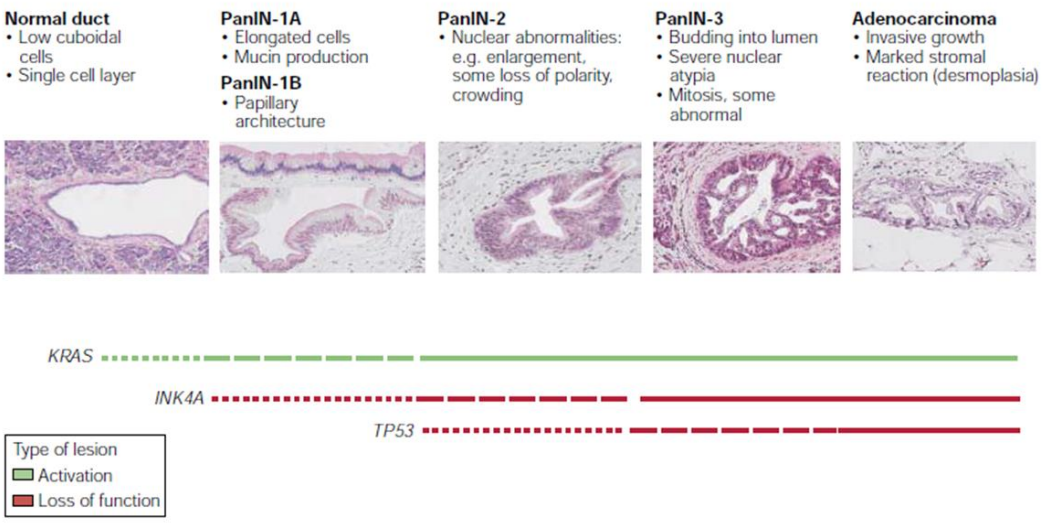

Figure 1.2: Mutations throughout PDA progression.

The genetic alterations documented in adenocarcinomas occur in a temporal sequence. The stage of onset of these lesions is depicted. The thickness of the line corresponds to the frequency of a lesion. Adapted from (Bardeesy & DePinho, 2002). (http://pathology.jhu.adu/pancreas/panin)

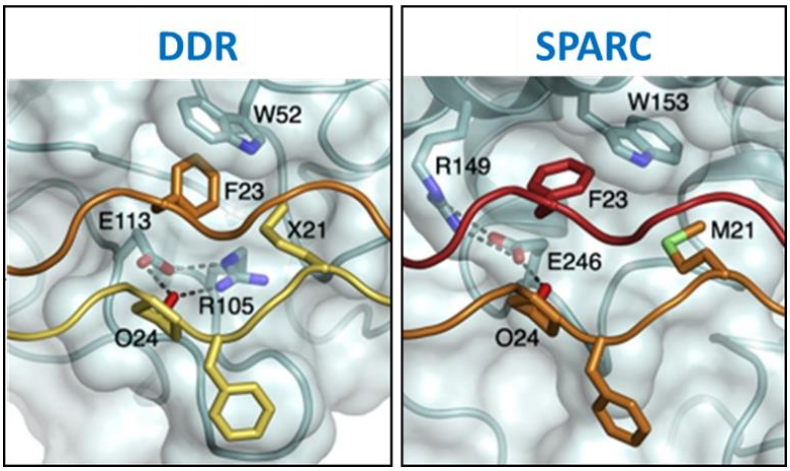

Figure 1.3: DDR and SPARC interactions with GVMGFO collagen sequence.

DDR1 and SPARC are in cyan and shown as cartoons with semitransparent surfaces. The leading, middle, and trailing chains of the collagen peptides are in yellow, orange, and red, respectively. Selected residues are shown as sticks. X denotes norleucine. Dashed lines indicate hydrogen bonds. Adapted from (Carafoli et al., 2009; Carafoli & Hohenester, 2012).

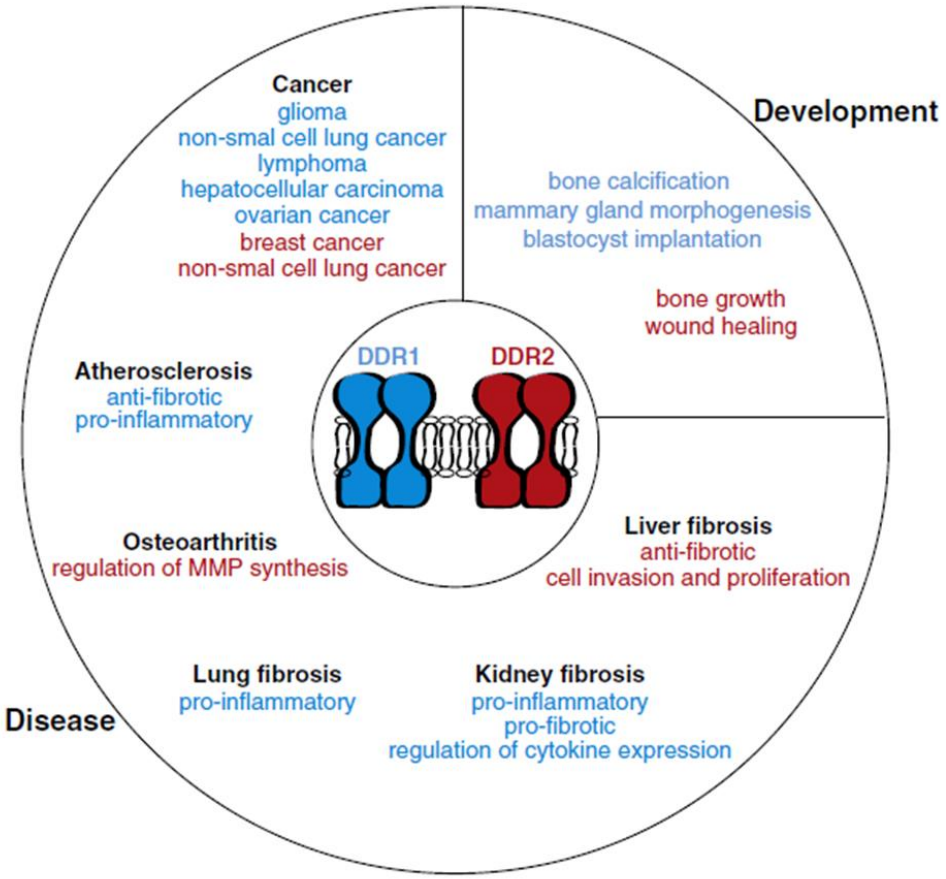

Figure 1.4: Physiological and pathological functions of DDRs.

Schematic of DDR1 (blue) and DDR2 (red) context-dependent roles. DDR expression and/or activation plays a role in both physiological and pathological conditions by controlling key cellular processes, including protease production, cytokine secretion, cell migration, immune cell recruitment, and matrix production. Taken from (Borza & Pozzi, 2014).

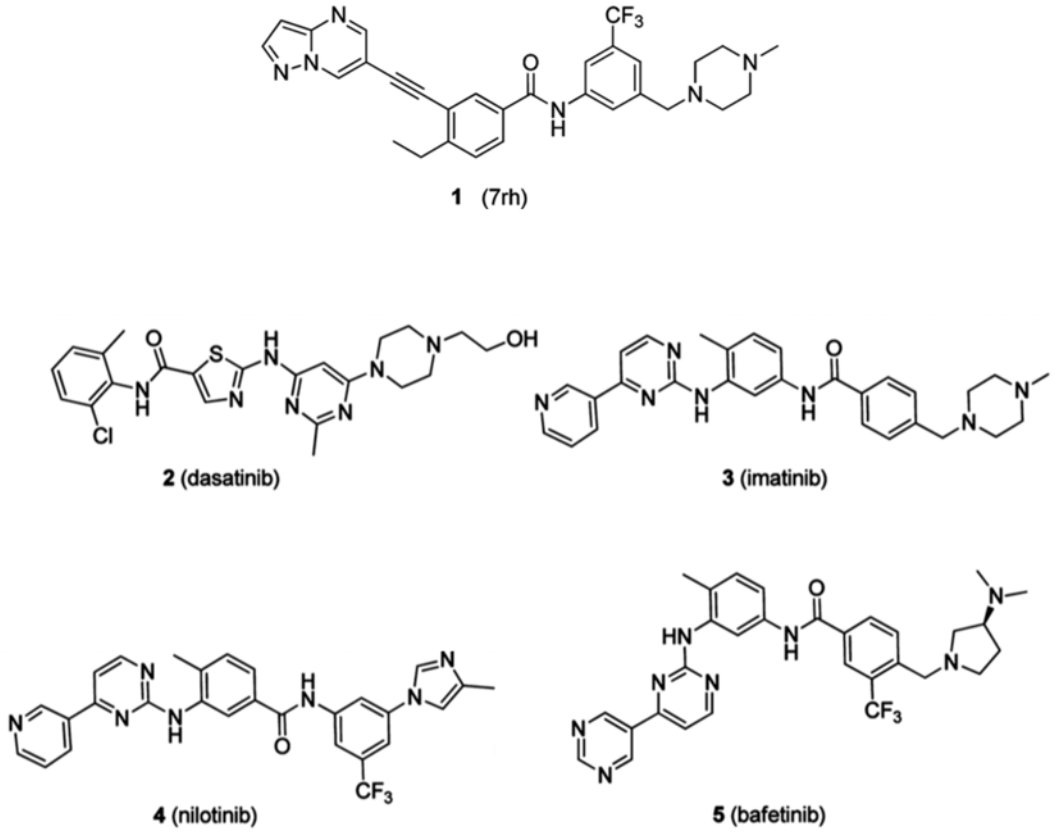

Figure 1.5: Structures of DDR inhibitors.

Comparison of previously defined DDR inhibitors: 7rh, dasatinib, imatinib, nilotinib, and bafetinib. Figure adopted from (Y. Li et al., 2015).

1.9 Tables

Gene	Chromosome	Cancers with a mutation (%)
KRAS	12p	95
P16/CDKN2A	9p	>90
TP53	17p	75

Table 1: Common somatic mutations in PDA.

Adapted from (Iacobuzio-Donahue et al., 2012)

Type	Classification	Localization/Function
I	Fibril-forming	Non-cartilaginous connective tissues (e.g. tendon, ligament, cornea, bone, annulus fibrosis, skin)
II	Fibril-forming	Cartilage, vitreous humour and nucleus pulposus
III	Fibril-forming	Co-distributes with collagen I, especially in embryonic skin and hollow organs
IV	Network-forming	Basement membranes
V	Fibril-forming	Co-distributes with collagen I, especially in embryonic tissues and in cornea
VI	Beaded filament-forming	Widespread, especially muscle
VII	Anchoring fibrils	Dermal-epidermal junction
VIII	Network-forming	Descement's membrane
IX	FACIT	Co-distributes with collagen II, especially in cartilage and vitreous humour
X	Network-forming	Hypertrophic cartilage
XI	Fibril-forming	Co-distributes with collagen II
XII	FACIT	Found with collagen I
XIII	Transmembrane	Neuromuscular junctions, skin
XIV	FACIT	Found with collagen I
XV	Endostatins	Located between collagen fibrils that are close to basement membranes; found in the eye, muscle and microvessels; a close structural homologue of collagen XVIII
XVI	FACIT	Integrated into collagen fibrils and fibrillin-1 microfibrils
XVII	Transmembrane	Also known as the bullous pemphigoid antigen 2/BP180; localized to epithelia; an epithelial adhesion molecule; ectodomain cleaved by ADAM proteinases
XVIII	Endostatins	Associated with basement membranes; endostatin is proteolytically released from the C-terminus of collagen XVIII; important for retinal vasculogenesis
XIX	FACIT	Rare; localized to basement membrane zones; contributes to muscle physiology and differentiation
XX	FACIT	Widespread distribution, most prevalent in corneal epithelium
XXI	FACIT	Widespread distribution
XXII	FACIT	Localized at tissue junctions (e.g. myotendinous junction, cartilagesynovial fluid, hair follicle-dermis)
XXIII	Transmembrane	Limited tissue distribution; exists as a transmembrane and shed form
XXIV	Fibril-forming	Shares sequence homology with the fibril-forming collagens; has minor interruptions in the triple helix; selective expression in developing cornea and bone
XXV	Transmembrane	CLAC-P – precursor protein for CLAC (collagenous Alzheimer amyloid plaque component)
XXVI	Beaded filament-forming	Also known as EMI domain-containing protein 2, protein Emu2, Emilin and multimerin domain-containing protein 2
XXVII	Fibril-forming	Shares sequence homology with the fibril-forming collagens; has minor interruptions in the triple helix; found in embryonic

		cartilage, developing dermis, cornea, inner limiting membrane of the retina and major arteries of the heart; restricted to cartilage in adults; found in fibrillar-like assemblies
XXVII	Beaded filament-forming	A component of the basement membrane around Schwann cells; a von Willebrand factor A domain-containing protein with numerous interruptions in the triple helical domain

Table 2: List of collagen types, classifications, locations, and functions.

Modified from: (Kadler et al., 2007).

Cancer		Human biopsies			Mouse models or cell culture	
Site	**Classification**	**Detection**	**Expression[a]**	**References**	**Description**	**References**
Bladder	Carcinoma	RT-PCR; IHC	Increased stromal SPARC; Positive Correlation	(Nimphius et al. 2007; Yamanaka et al. 2001)		
Blood	Leukemia	Microarray	Increased SPARC expression	(Hedvat et al. 2003; Martinez et al. 2003)		
Bone	Osteosarcoma	Microarray; RT-PCR; IHC	Positive Correlation	(Dalla-Torre et al. 2006; Fanburg-Smith et al. 1999; Schulz et al. 1998)		
Brain	Glioblastoma, Astrocytoma & Meningioma	Northern Blot; IHC; Microarray; RT-PCR	Positive Correlation; SPARC expression increased in invasive benign and malignant tumors	(Huang et al. 2000; Pen et al. 2007; Rempel et al. 1998, 1999; Rich et al. 2005)	SPARC increased invasion and survival; Endogenous SPARC increased adhesion and migration but decreased proliferation	(Golembieski et al. 1999, 2008; Kunigal et al. 2006; McClung et al. 2007; Rempel et al. 2001; Rich et al. 2003, 2005; Schultz et al. 2002; Seno et al. 2009; Shi et al. 2004, 2007)
Breast	Invasive Ductal Carcinoma	Microarray; IHC; RT-PCR; SAGE; ISH	High stromal SPARC; Positive Correlation	(Amatschek et al. 2004; Barth et al. 2005; Bellahcene and Castronovo 1995; Bergamaschi et al. 2008; Helleman et al. 2008;	Exogenous SPARC increased cancer cell invasion; Tumor growth reduced in SPARC deficient mice; SPARC	(Briggs et al. 2002; Campo McKnight et al. 2006; Gilles et al. 1998; Jacob et al. 1999; Minn et al. 2005; Sangaletti et al. 2003, 2008;

Cancer		Human biopsies			Mouse models or cell culture	
Site	**Classification**	**Detection**	**Expression[a]**	**References**	**Description**	**References**
				Iacobuzio-Donahue et al. 2002; Jones et al. 2004; Lien et al. 2007; Parker et al. 2004; Porter et al. 2003, 1995; Sarrio et al. 2008; Watkins et al. 2005; Woelfle et al. 2003)	expression increased in metastasis	Zajchowski et al. 2001)
Colon	Colorectal Adenocarcinoma	Microarray; Western Blot; Northern Blot; ISH; IHC; RT-PCR	SPARC expression increased in tumor, tumor stroma and at metastatic sites	(Kaiser et al. 2007; Lussier et al. 2001; Madoz-Gurpide et al. 2006; Porte et al. 1995; Porter et al. 1995; St Croix et al. 2000; Wewer et al. 1988; Wiese et al. 2007)	Increased SPARC expression associated with increased invasive capacity; Reduced tumor development in SPARC deficient mice	(Sansom et al. 2007; Volmer et al. 2004)
Esophagus	Squamous Cell Carcinoma (ESCC) & Adenocarcinoma (EA)	Western Blot; Microarray; IHC; Northern Blot; RT-PCR	Positive Correlation	(Brabender et al. 2005; Che et al. 2006; Luo et al. 2004; Mitas et al. 2005; Porte et al. 1998; Wong et al. 2009; Xue et al. 2006; Yamashita et al. 2003)		
Head & Neck	Squamous Cell Carcinoma (HNSCC)	IHC; Microarray	Positive Correlation	(Chin et al. 2005; Choi et al. 2008; Kato		

Cancer		Human biopsies			Mouse models or cell culture	
Site	**Classification**	**Detection**	**Expression[a]**	**References**	**Description**	**References**
				et al. 2005)		
Kidney	Sarcomatoid & Clear-cell renal cell carcinoma	Microarray; IHC; Northern Blot	SPARC expression increased in tumors	(Amatschek et al. 2004; Gieseg et al. 2002; Sakai et al. 2001)	SPARC increased cancer cell invasion	(Kato et al. 1998)
Liver	Hepatocellular Carcinoma (HCC)	RT-PCR; IHC; ISH; Western Blot; Microarray	Positive Correlation	(Goldenberg et al. 2002; Lau et al. 2006; Le Bail et al. 1999)		
Lung	NSCLC, Squamous Cell Carcinoma, Adenocarcinoma	IHC; Microarray	High stromal SPARC; Positive Correlation	(Amatschek et al. 2004; Koukourakis et al. 2003; Siddiq et al. 2004)	SPARC expression increased during transformation and increased colony formation; Coculture of NSCLC lines & fibroblasts induced SPARC	(Fromigue et al. 2003; Siddiq et al. 2004)
Ovary	Carcinoma	IHC; ISH	High stromal SPARC; Positive Correlation	(Brown et al. 1999; Paley et al. 2000; Porter et al. 1995)		
Pancreas	Ampullary Carcinoma	Microarray; IHC	Positive Correlation	(Bloomston et al. 2007)		
Pancreas	Ductal Adenocarcinoma (PDA)	SAGE; Microarray; IHC; RT-PCR; ELISA	High stromal SPARC; Positive Correlation	(Guweidhi et al. 2005; Infante et al. 2007; Mantoni et al. 2008; Prenzel et al. 2006; Ryu	Exogenous SPARC increased cancer cell invasion	(Guweidhi et al. 2005; Mantoni et al. 2008)

Cancer		Human biopsies			Mouse models or cell culture	
Site	**Classification**	**Detection**	**Expression[a]**	**References**	**Description**	**References**
				et al. 2001; Sato et al. 2003)		
Prostate	Carcinoma	Microarray; IHC; ISH; RT-PCR	Increased SPARC expression at the metastatic site; Positive Correlation	(Best et al. 2005; Lapointe et al. 2004; Thomas et al. 2000)	Exogenous SPARC increased cancer cell invasion and bone metastasis	(Chen et al. 2007; De et al. 2003; Jacob et al. 1999)
Skin	Melanoma	IHC; Western Blot; ELISA	Positive Correlation; Serum SPARC levels useful as a diagnostic indicator	(Alonso et al. 2007; Ikuta et al. 2005; Ledda et al. 1997a; Massi et al. 1999)	SPARC knock-down inhibited tumor formation; Increased SPARC expression by metastatic cell lines; SPARC expression correlated with EMT	(Alvarez et al. 2005; Kato et al. 2000; Kuphal et al. 2005; Ledda et al. 1997b; Prada et al. 2007; Robert et al. 2006; Rumpler et al. 2003; Smit et al. 2007; Sosa et al. 2007; Sturm et al. 2002)
Skin	Squamous Cell Carcinoma				SPARC deficient mice refractory to UV induced carcinogenesis	(Aycock et al. 2004)
Stomach	Gastric Cancer	Northern Blot; ISH; IHC; RT-PCR; Microarray	High stromal SPARC; Positive Correlation	(Inoue et al. 2002; Maeng et al. 2002b; Takeno et al. 2008; Wang et al. 2004; Wewer et al. 1988)	SPARC expression increased during transformation	(Maeng et al. 2002a)

Cancer		Human biopsies			Mouse models or cell culture	
Site	**Classification**	**Detection**	**Expression[a]**	**References**	**Description**	**References**
Thyroid	Anaplastic Carcinoma	RT-PCR	High stromal SPARC expression in poorly differentiated tumors	(Takano et al. 2002)		
Uterus	Cervical & Endometrial Carcinoma	RT-PCR; IHC; ISH; Western Blot	High stromal SPARC	(Chen et al. 2003; Rodriguez-Jimenez et al. 2007)		

Table 3. SPARC as a tumor promoter.

Adapted from (Arnold & Brekken, 2009). Please address the comprehensive review by (Arnold & Brekken, 2009) for the respective references within the Table.

[a]:Positive Correlation refers to one of the following: 1) Tumors had increased SPARC expression compared to normal tissue 2) Increased SPARC expression correlated with increased tumor stage, grade or metastasis 3) Increased SPARC expression correlated with decreased survival or a negative prognosis 4) Decreased SPARC expression correlated with increased survival or a positive prognosis. This table combines, updates and expands the data presented in several previous reviews (Clark and Sage 2008; Framson and Sage 2004; Podhajcer et al. 2008)

Cancer		Human biopsies				Mouse models or cell culture	
Site	**Classification**	**Detection**	**Expression[a]**	**References**	**Methylation**	**Description**	**References**
Bladder	Carcinoma	Genetic mapping	Locus deletion associated with neoplasia	(Kram et al. 2001)			
Blood	Acute Myeloid Leukemia (AML) with MLL Translocation	Microarray; RT-PCR; Western Blot	SPARC expression decreased	(Bullinger et al. 2004; DiMartino et al. 2006; Ross et al. 2004)		Exogenous SPARC inhibited proliferation; SPARC silencing associated with promoter methylation	(DiMartino et al. 2006)
Brain	Neuroblastoma	IHC	Inverse Correlation	(Chlenski et al. 2002)		SPARC inhibited migration and angiogenesis but activated apoptosis	(Chlenski et al. 2002, 2004)
Breast	Carcinoma	Microarray	Inverse Correlation; Increased stromal SPARC	(Beck et al. 2008; Bergamaschi et al. 2008)		SPARC overexpression inhibited proliferation; Endogenous SPARC expression reduced metastasis	(Dhanesuan et al. 2002; Koblinski et al. 2005)
Colon	Colorectal Adenocarcinoma	IHC; methylation specific PCR; Microarray; RT-PCR	Inverse Correlation	(Cheetham et al. 2008; Tai et al. 2005; Yang et al. 2007)	80-100%	SPARC expression decreased in chemoresistant cancer cells; SPARC treatment restored	(Cheetham et al. 2008; Taghizadeh et al. 2007; Tai et al. 2005; Yang et al. 2007)

Cancer		Human biopsies				Mouse models or cell culture	
Site	**Classification**	**Detection**	**Expression[a]**	**References**	**Methylation**	**Description**	**References**
						sensitivity to chemotherapy; SPARC methylated in 70% cell lines	
Kidney	Transformed Cells					Endogenous SPARC inhibited tumor growth	(Chlenski et al. 2006, 2007)
Liver	Hepatocellular Carcinoma (HCC)					SPARC overexpression reduced tumor growth and angiogenesis	(Lau et al. 2006)
Lung	NSCLC & SCLC	RT-PCR; IHC	Inverse Correlation	(Suzuki et al. 2005)	69%	SPARC methylated in cancer cell lines; SPARC promoter demethylation inhibited invasion; Increased tumor growth in SPARC deficient mice	(Brekken et al. 2003; Pan et al. 2008; Suzuki et al. 2005)
Nose & Pharynx	Nasopharyngeal Carcinoma					Endogenous SPARC inhibited proliferation	(Huang et al. 2008)
Ovary	Carcinoma	IHC; Western Blot; RT-PCR	Inverse Correlation	(Socha et al. 2009; Yiu et al. 2001)	68%	Reduced SPARC expression and secretion in cancer cells; SPARC	(Bull Phelps et al. 2009; Mok et al. 1996; Said and Motamed

Cancer		Human biopsies				Mouse models or cell culture	
Site	**Classification**	**Detection**	**Expression[a]**	**References**	**Methylation**	**Description**	**References**
						inhibited tumor growth; Exogenous SPARC inhibited cancer cell proliferation, adhesion and invasion; enhanced apoptosis; Tumor growth and carcinomatosis augmented in SPARC deficient mice	2005; Said et al. 2007a, b; Socha et al. 2009; Yiu et al. 2001)
Pancreas	Ductal Adenocarcinoma (PDA)	SAGE; Microarray; IHC; RT-PCR	SPARC methylation; Inverse Correlation	(Brune et al. 2008; Hong et al. 2008; Sato et al. 2003)	88-92%	SPARC methylated in cancer cell lines; SPARC inhibited cancer cell proliferation; Increased tumor growth in SPARC deficient mice	(Arnold et al. 2008; Guweidhi et al. 2005; Puolakkainen et al. 2004; Sato et al. 2003)
Prostate	Carcinoma					SPARC hypermethylated in cancer cell lines compared to normal cells	(Wang et al. 2005)
Skin	Melanoma					Endogenous SPARC inhibited migration and spheroid tumor cell growth;	(Prada et al. 2007)

Cancer		Human biopsies				Mouse models or cell culture	
Site	**Classification**	**Detection**	**Expression[a]**	**References**	**Methylation**	**Description**	**References**
						SPARC knock-down enhanced spheroid formation	
Uterus	Cervical & Endometrial Carcinoma	Microarray; RT-PCR	Iinverse Correlation	(Kahn et al. 2008; Rodriguez-Jimenez et al. 2007; Sova et al. 2006)	66-86%		

Table 4. SPARC as a tumor suppressor.

Adapted from (Arnold & Brekken, 2009). Please address the comprehensive review by (Arnold & Brekken, 2009) for the respective references within the Table.

[a]:Inverse Correlation refers to one of the following: 1) Tumors had decreased SPARC expression compared to normal tissue 2) Decreased SPARC expression correlated with increased tumor stage, grade or metastasis 3) Decreased SPARC expression correlated with decreased survival or a negative prognosis 4) Increased SPARC expression correlated with increased survival or a positive prognosis. This table combines, updates and expands the data presented in several previous reviews (Clark and Sage 2008; Framson and Sage 2004; Podhajcer et al. 2008)

	Dasatinib	Imatinib	Nilotinib	Bafetinib	7rh
DDR1 IC_{50}	0.5 nM	337 nM	43 nM	337 nM	6.8 nM
DDR2 IC_{50}	1.4 nM	675 nM	44 nM	220 nM	101.4 nM

Table 5: Specificities of DDR inhibitors.

Comparison of previously defined DDR inhibitors: dasatinib, imatinib, nilotinib, bafetinib, and 7rh. Based on previous findings from (Day et al., 2008; M. Gao et al., 2013; Rix et al., 2010).

CHAPTER TWO

Materials and methods

CHAPTER TWO

Materials and methods

2.1 Antibodies and reagents

Assays were performed with antibodies against: phospho-DDR1 (Tyr792, Cell Signaling #11994), DDR1 (D1G6, Cell Signaling #5583), phospho-SRC (Tyr416, Cell Signaling #2101), phospho-PYK2 (Tyr402, Cell Signaling #3291), phospho-P130CAS (Tyr165, Cell Signaling #4015), α-Amylase (D55H10, Cell Signaling #3796), VIMENTIN (Millipore AB5733), E-CADHERIN (ab15148, Abcam), ZEB1 (D80D3, Cell Signaling #3396) phospho-FAK (Abcam #4803), activated β1 INTEGRIN (Millipore #2079Z), PEAK1 (Millipore 09-274) phospho-PEAK1 (Tyr665, Millipore #ABT52), YH2AX (p Ser139, Novus #NB100-384), ENDOMUCIN clone V.5C7 (Millipore mAB2624), and CLEAVED CASPASE-3 (Asp175, Cell Signaling #9661). DDR1 polyclonal Ab H-126 (blocking antibody) was obtained from Santa Cruz Biotechnology, Inc. (Santa Cruz, CA). Recombinant Human DDR1/Fc, CF (2396-DR-050), Recombinant Human SPARC/His, CF (941-SP-050) and Recombinant Mouse SPARC/His, CF (942-SP-050) were obtained from R&D Systems. Collagen I (rat tail) was obtained from BD Biosciences. Human Collagen Type IV was obtained from Millipore. Fibronectin from bovine plasma solution (F1141) was obtained from Sigma Aldrich.

2.2 Cellular assays

2.2.1 Cell lines

Isogenic cell lines were derived from 5-week old PDA transgenic *Kras$^{G12D/+}$; Ink4a$^{lox/lox}$; p48$^{Cre/+}$ (Sparc$^{+/+}$; KIC) or Sparc$^{-/-}$; Kras$^{G12D/+}$; Ink4a$^{lox/lox}$; p48$^{Cre/+}$ (Sparc$^{-/-}$; KIC)* mice. Mouse pancreata from 5-wk-old *Sparc$^{+/+}$; KIC* and *Sparc$^{-/-}$; KIC* mice were minced and then subjected to digestion with 1% collagenase type 1, DME, 10 mM Hepes, 1% fetal bovine serum, and PBS at 37°C until a single-cell suspension was obtained. Cell suspensions were centrifuged at low speed to pellet large debris, resuspended in wash buffer, and passed through a 70-µm-cell strainer. The final cell suspension was plated at low density to isolate tumor cell populations. These cell lines were expanded and stained for tumor cell markers for validation of the tumor cell populations. Cell lines were confirmed to be pathogen-free. Human pancreatic cancer cell lines (AsPC-1 and PANC-1) were purchased from the American Type Culture Collection (ATCC; Manassas, VA) and were confirmed to be pathogen-free and fingerprinted for validation of authenticity. Mouse and human cells were cultured in DMEM (Invitrogen) or RPMI (Invitrogen) containing 5% fetal bovine serum (FBS) and maintained at 37^{o}C in a humidified incubator with 5% CO_2 and 95% air.

2.2.2 Immunocytochemistry

Cell lines were cultured in 4-well chamber slides in respective treatment conditions. For stimulation or inhibitory studies, 10 µg/ml collagen I and/or inhibitors were added to cells for 24 hours after ~80% confluency. Cells were then fixed with methanol, washed with TBS-T, permeabilized with PBS+0.1% TX-100, and then blocked with PBS+20% AquaBlock™ (EastCoast Bio). Antibodies diluted PBS+5% bovine serum albumin (BSA) were added and allowed to incubate overnight at 4°C. Cells were then washed with TBS-T and incubated overnight with the appropriate secondary antibodies diluted PBS+5% BSA. After another round of washes with TBS-T, coverslips were mounted with ProLong® Gold (Life technologies) with DAPI.

2.2.3 Liquid colony formation assay

Cells were cultured in 6-well tissue culture plates at low density (250 cells per well) in 2 ml of media with 5% FBS +/- 10 µg/ml collagen I and/or inhibitors for approximately 1.5-2 weeks, or until significant colony formation. 7rh was added in 4, 4-fold dilutions, to respective wells, a DMSO control was added to respective wells to demonstrate the vehicle-independent effect. Cells were then fixed with 10% formalin and stained with crystal violet. Images were analyzed with Image J or NIS Elements 3.1 (Nikon Instruments).

2.2.4 Western blot analysis

For stimulation or inhibitory studies, 10 µg/ml collagen I and/or inhibitors were added to cells for 24 hours after ~80% confluency. Sub-confluent monolayers of cells were lysed, supernatants were recovered by centrifugation at 13,000 rpm, protein concentrations were measured, and equal amounts of total protein were separated by SDS-PAGE. Proteins were transferred to polyvinylidene fluoride (PVDF) membranes (Bio-Rad, Hercules, CA) followed by blockade for 1 hour in 5% milk in TBS-T. The membranes were incubated overnight at 4°C with primary antibody. The membranes were then incubated with the corresponding HRP-conjugated secondary antibody (Pierce Biotechnologies, Santa Cruz, CA) for 1 to 2 hours. Specific bands were detected with the enhanced chemiluminescence reagent (ECL, Perkin Elmer Life Sciences, Boston, MA) on autoradiographic film.

2.2.5 *In vitro* cytotoxicity and drug response assay

MTS assays were conducted in 96-well plates; cells were plated on day 0 and drug was added on day 1 in 4-fold dilutions. Drugs were evaluated as single agents for gemcitabine and 7rh. For combination studies 7rh was added with a fixed concentration of 250 nM or 500 nM with a 4-fold dilution of gemcitabine. To measure cell viability the MTS system by Promega was used. Shortly, MTS

powder was dissolved in 21 ml of PBS. Then 1.05 ml of PMS (Promega Corporation) was added to the MTS solution. 20 µl of this solution was transferred into every well and incubated for 1-3 h at 37° C, 20% O_2 and 5% CO_2 in a humidified atmosphere. MTS penetrates the cells and can be reduced on the cell membrane or cytoplasm if the cell is vital. Reduction of MTS leads to the formation of a soluble formazan product. This reaction leads to a change of the absorbance maximum from λ=570 nm (MTS) to λ=490 nm (formazan). After 3-6 hours the OD490 values of the 96-well plates were measured using the FLUOstar OPTIMA plate reader (BMG LABTECH GMBH). Each plate contained eight replicates for each concentration and the whole experiment was repeated at least twice. Drug sensitivity curves and IC_{50}s were calculated with in-house software (Dineen et al., 2010).

2.2.6 Wound healing (scratch) assay

Cells were cultured in 6-well tissue culture plates at high density (~90% confluence) in 2 ml of media with 5% FBS. Uniform scratches were made down the center of each well with a p20 pipette tip, cells were gently washed with PBS to remove the loose cell debris, and drug was added in media containing 5% FBS. Cells were plated on respective culture conditions and images from the center of each well were taken at different times. The wound width (µm) was measured

using NIS Elements 3.1 software (Nikon Instruments). The initial wound width was used to verify consistency in scratches.

2.2.7 Immunoprecipitation

Cell lines were lysed in modified radioimmunoprecipitation (RIPA) assay buffer (0.5% deoxycholate, 0.5% SDS, 1% Triton X-100, 10 mM sodium phosphate, pH 7.2, 150 mM sodium chloride, and protease inhibitor (Complete Mini)). Lysis was performed on serum-starved adherent cells after being washed with chilled PBS. Lysates were allowed to rotate at 4°C on a nutator for 1 hour and then vortexed several times before centrifugation at 13,000 rpm for 10 min to pellet any insoluble material. Lysates were then pre-cleared with protein A/G beads (Thermo Fisher Scientific). 200 µg cellular protein in 1 ml lysis buffer was used per immunoprecipitation reaction. 1 µg of the appropriate IgG was added with 50 µl protein A/G bead slurry to each sample; each sample was then allowed to rotate overnight at 4°C on a nutator. Immunoprecipitated complexes were washed twice in lysis buffer and then boiled in sample buffer and subjected to SDS-PAGE and western blot analysis.

2.2.8 Sircol collagen assay

Cell lines were prepared as indicated by the Sircol manual (Sircol Collagen Assay Kit, Oubis Ltd). Sircol dye reagent was used to saturate the

collagen in the supernatant. The colorimetric principle of the Sircol collagen assay is the binding of a dye to collagen. A collagen-dye complex formed and precipitated out, is recovered by centrifugation, eluted with alkali, and measured with a spectrophotometer at 555 nm. The intensity of color measurement was proportional to the collagen concentration in the sample.

2.2.9 RNA isolation/purification and RT-PCR

RNA was isolated from cell line pellets with TRIzol® (Invitrogen) reagent according to the manufacturer's protocol. The samples were then eluted in RNAse/DNAse free water and utilized for subsequent cDNA synthesis. Purified RNA was reverse transcribed into cDNA with the iScript™ cDNA synthesis kit (Bio-Rad, Hercules, CA). The following human primer sets were used for RT-PCR:

DDR1-FWD: CCTCTTTGCAGGTCCTTGGTT,

DDR1-REV: AGCTCCAAGCTGCTGAAGTTG.

ColI α1-FWD: GACGCCATCAAGGTCTACTG,

ColI α1-REV: ACGGGAATCCATCGGTCA.

ColI α2-FWD: GGAGGGAACGGTCCACGAT,

ColI α2-REV: GAGTCCGCGGTATCCACAA.

SPARC-FWD: GTGACCTGGACAATGACAAGTA,

SPARC-REV: GCCAAGACCCTGAAATGAAATG.

Itg α1-FWD: TGGGTGCTTATTGGTTCTCC,

Itg α1-REV: CCTCCTTTCTTGCTGTGTCTAT.

Itg β1-FWD: GAAGCTCAAGCCAGAGGATATT,

Itg β1-REV: CTGGACAAGGTGAGCAATAGAA.

PEAK1-FWD: GTTGGAGTAGCCTCCCATTATC,

PEAK1-REV: GACGCTTAGTAGGACCCAAAG.

RPS6-FWD: GAGCGTTCTCAACTTGGTTATTG,

RPS6-REV: GTGCTTTGGTCCTAGGTTTCT.

2.2.10 Hypoxia studies with hypoxic chamber *in vitro*

Cell lines were grown in 4-well chamber slides in a humidified atmosphere containing 5% CO_2 and 1% O_2 (hypoxic conditions) in a modular incubator chamber (Billups-Rothenberger) for 48 hours for immunocytochemical analysis. Immunocytochemical analysis was conducted for the validation of Hif1α induction. For liquid colony formation cell lines were placed in the respective

conditions for approximately 1.5-2 weeks, or until robust colony formation. For control conditions cells were cultivated in an incubator with a humidified atmosphere containing 5% CO_2 and 20% O_2 (normoxic conditions).

2.3 siRNA mediated knockdown of DDR1

Cell lines were plated 18-24 hours before transfection ($1x10^5$ cell/well in 6 well dish) at an initial confluence of 60-80%. TransIT-siQUEST reagent and siRNA complexes were prepared and added according to manufacturer instructions (Mirus Bio LLC). siRNA complexes were added to the cells at a final siRNA complex concentration of 1 μM. Protein was then harvested 72 hours post-transfection for western blot analysis. siRNA duplexes were purchased from Integrated DNA Technologies. DDR1 duplexes used were (NM_001954 duplexes 1-3):

siDDR1 Duplex #1: 5'-GUCUUGUAGCUAGAACUUCUCUAAG-3',
3'-GUCAGAACAUCGAUCUUGAAGAGAUUC-5'.

siDDR1 Duplex #2: 5'-GCACUAGGCAGGUAAUAAUAAAGGT-3',
3' GACGUGAUCCGUCCAUUAUUAUUUCCA-5'.

siDDR1 Duplex #3: 5'-ACACUAAUAUAUGGACCUAGAUUGA-3',
3'-AAUGUGAUUAUAUACCUGGAUCGAACU-5'.

2.4 Recombinant protein binding assays

96-well ELISA plates were coated with 10 µg/ml rat tail collagen I, 10 µg/ml fibronectin (BD Biosciences), or 2% Casein Acid Hydrolysate (Sigma) in PBS (Casein-PBS) for 1 Hour at 37^{o}C. Plates are blocked with 2% Casein for 1 Hour at 37^{o}C. For competitive binding assays, human recombinant DDR1/Fc (R&D Systems), human recombinant SPARC/His (R&D Systems), or monoclonal antibody 293 (mAb293) (Sweetwyne et al., 2004) were added to the wells at respective concentrations in triplicate in ELISA Binding Buffer and incubated overnight at 4^{o}C. Binding of DDR1/Fc or SPARC/His was detected with primary and secondary antibodies for human DDR1 (R&D Systems) or human SPARC (R&D Systems) in 2% Casein-PBS. 50 µl TMB One Component HRP-Microwell Substrate (TMB) (SurModics-BioFx) was added per well to detect bound protein, along with addition of 50 µl 10% hydrochloric acid (HCl) to quench the TMB reaction.

2.5 Animal Studies and Human Sample Analysis

2.5.1 Animal Studies

All animals were housed in pathogen-free facility with access to food and water *ad libitum*. Experiments were approved and performed in accordance with the Institutional Animal Care and Use Committee (IACUC) at the University of

Texas Southwestern Medical Center. *C57BL*/6, *Sparc*$^{-/-}$, and NOD-SCID (non-obese diabetic/severe combined immunodeficiency) mice were purchased from an on-campus supplier. *Kras*$^{G12D/+}$*; LSL-Trp53*$^{R172H/+}$*; p48*$^{Cre/+}$ (*KPC*) mice (Hingorani et al., 2005) and *LSL-Kras*$^{G12D/+}$*; Cdkn2a*$^{lox/lox}$*; p48*$^{Cre/+}$ (*KIC*) mice (Dineen et al., 2010; Ostapoff et al., 2013) were generated as previously described. Mice were randomized to receive treatment as indicated in Table 6. For endpoint studies experiments were stopped after the designated time post-tumor cell injection (TCI). For survival studies, therapy was maintained until mice were moribund. Moribund status was designated at a loss of 15% of initial body weight, or after visible characteristics such as jaundice, malaise, or ascites. At the time of sacrifice all mice were subjected to careful necropsy where visible metastases were noted, and organs and plasma harvested for further analysis. Liver micrometastases were assessed by hematoxylin and eosin (H&E) on the anterior lobes of the liver.

2.5.2 Hypoxia studies

Hypoxia studies with pimonidazole. Three mice per group were injected intravenously with 60 mg/kg of pimonidazole (30 mg/mL in 0.9% saline, Hypoxyprobe Plus; HPI Inc.) that was allowed to circulate for 90 minutes before the sacrifice of the animals. Designated organs were harvested and snap frozen for further analysis. Frozen tissue sections were interrogated with FITC-conjugated

anti-pimonidazole primary antibody (Chemicon) and endothelial cell markers (CD31, Dianova; Meca-32, DSHB; or Endomucin, Santa Cruz Biotechnology). Eight images per tissue area were obtained and analyzed with NIS Elements 3.1 (Nikon Instruments).

2.5.3 Histology

Tissues were fixed in 4% formalin, embedded in paraffin, sectioned, and stained with routine hematoxylin and eosin (H&E) or used for immunohistochemistry. After routine deparaffinization, tissue sections were incubated in primary antibody overnight at 4^{o}C. Detection with appropriate antibodies was as described previously.

2.5.4 TMA sample analysis

Formalin-fixed tissues were embedded in paraffin, sectioned and stained as respectively indicated. Human (44) and matched patient-derived tumor xenograft (PATX) (150) TMA samples were scored on a scale of 0 (no stain) to 4 (very high stain) independently by two researchers, the data was collected and averaged accordingly.

2.5.5 Gene expression data analysis

RNA-sequencing data from The Cancer Genome Atlas (TCGA) PDA cBioPortal was collected (Cerami et al., 2012; J. Gao et al., 2013) using CGDS MATLAB toolbox with RNA Seq V2 RSEM option. RNA-seq data were z-transformed. For Kaplan–Meier (KM) survival analysis of individual genes, the survival of patients was compared with high expression (greater than median) versus low expression (lower than median) of each gene. Statistical analysis was performed with a log-rank tested implemented in R using the survival package.

2.6 Statistical analysis

Quantification of immunohistochemistry was conducted with NIS Elements 3.1 software (Nikon Instruments). All data were analyzed with GraphPad Prism 5.0 software (GraphPad Software Inc.). Datasets were analyzed by Student t-test or ANOVA followed by Dunn post-test or Tukey's MCT and results were considered as significant at $p < 0.05$. Results are shown as mean ± SEM.

2.7 Tables

Endpoint: 7rh titration	Experiment start	10 days post tumor cell injection
	Experiment length	12 hours
	Animals	*C57BL*/6, (n=3/group)
	Treatment groups	Vehicle: 1 dose 7rh: 0.1 mg/kg, 1 dose 7rh: 1 mg/kg 1 dose 7rh: 10 mg/kg, 1 dose
	Associated figure	Figure 4.6
Endpoint: 7rh titration	Experiment start	10 days post tumor cell injection
	Experiment length	21 days post tumor cell injection
	Animals	*C57BL*/6, (n=5/group)
	Treatment groups	Vehicle: 3x/week 7rh: 3.3 mg/kg, 3x/week 7rh: 10 mg/kg, 3x/week 7rh: 30 mg/kg, 3x/week
	Associated figures	Figures 4.7-4.8
Survival: 7rh	Experiment start	19 days post tumor cell injection
	Experiment length	40 days post tumor cell injection
	Animals	*C57BL/6*, (n=16/group)
	Treatment groups	Vehicle: 3x/week 7rh: 25 mg/kg, 3x/week
	Associated figure	Figure 4.9

Survival: 7rh +/- chemotherapy	Experiment start	27 days post tumor cell injection
	Experiment length	Until moribund
	Animals	Nod Scid, (n=12/group) Vehicle: 3x/week 7rh: 25 mg/kg, 3x/week
	Treatment groups	Chemotherapy: Gem (15 mg/kg, 2x/week), Nab-pac (5 mg/kg, 2x/week) Combination: 7rh plus chemotherapy
	Associated figures	Figures 4.10-4.14
Survival: 7rh +/- chemotherapy	Age of experiment start	16 weeks old
	Experiment length	Until moribund
	Animals	*KPC (LSL-Kras$^{G12D/+}$; LSL-Trp53$^{R172H/+}$; P48$^{Cre/+}$),* (n=12/group)
	Treatment groups	Vehicle: 3x/week 7rh: 25 mg/kg, 3x/week Chemotherapy: Gem (15 mg/kg, 2x/week), Nab-pac (5 mg/kg, 2x/week) Combination: 7rh plus chemotherapy
	Associated figures	Figures 4.15-4.19

Table 6 Description of animal experiments where mice were treated with 7rh (M. Gao et al., 2013), gemcitabine, or nab-paclitaxel.
Abbreviation: Gem, gemcitabine; Nab-pac, nab-paclitaxel.

	Gemcitabine	Nab-paclitaxel
Human	1000 mg/m^2/week	125 mg/m^2/week
	27 mg/kg/week	3.4 mg/kg/week

	Gemcitabine	Nab-paclitaxel
Mouse	90 mg/m^2/week	30 mg/m^2/week
	30 mg/kg/week	10 mg/kg/week

Table 7 Description of human and mouse chemotherapy dosages.

The chemotherapy (gemcitabine plus nab-paclitaxel) dosing regimen used for the xenograft PDA and *KPC* models is shown below. The translation of these dosages to that established in the clinic was compared. The calculation of human to mouse and vice versa utilized the K_m factor for human ($K_m = 37$) and mouse ($K_m = 3$), based on (Reagan-Shaw, Nihal, & Ahmad, 2008). The mouse dosage of mg/kg/week was multiplied by 3 to achieve the mg/m^2/week concentration.

CHAPTER THREE

Collagen Signaling Drives Pancreatic Ductal Adenocarcinoma

Note: The following chapter is in part made up of a research article written by Kristina Y Aguilera under the guidance of Rolf A. Brekken (Aguilera et al., 2014).

CHAPTER THREE

Collagen Signaling Drives Pancreatic Ductal Adenocarcinoma

3.1 Introduction

Collagen signaling drives malignant changes in tumor cell phenotype and can promote tumor cell survival and chemoresistance. As described previously, this is particularly relevant to pancreatic adenocarcinoma (PDA), which is a desmoplastic disease (Grzesiak et al., 2007; Shields, Dangi-Garimella, Redig, & Munshi, 2012). Each cell in the PDA microenvironment interacts with fibrillar collagen, which has the potential to impact cell signaling events via crosstalk of its receptors with other signaling cascades (Shields et al., 2012). Collagen receptors are expressed broadly and have been linked to cellular processes that are prominent in PDA, including the epithelial to mesenchymal transition (EMT) and chemoresistance (Grzesiak et al., 2007; Shintani et al., 2008). For example, Shintani et al. (Shintani et al., 2008) demonstrated that collagen I induced N-cadherin expression (a marker of mesenchymal cells) in human pancreatic cancer cells through signaling pathways that required activation of DDR1. Coincident with collagen expression is the production of a matricellular protein known as secreted protein acidic and rich in cysteine (SPARC).

SPARC participates in the orchestration of collagen deposition but a unifying principal of SPARC function in the tumor microenvironment is lacking

(Arnold & Brekken, 2009). I proposed that a major function of SPARC was to reduce collagen binding to its receptors, in particular DDR1. This was supported by the following observations: a) The GVMGFO amino acid sequence that comprised the SPARC binding region on fibrillar collagens is the same sequence recognized by DDR1 (Carafoli et al., 2009; Keunen et al., 2011); b) Collagen was associated preferentially with cell surfaces instead of being deposited into the ECM in the absence of SPARC (Harris et al., 2011); c) Tgf-β-induced EMT required collagen interaction with the cell surface (Shintani et al., 2008); d) Loss of SPARC expression by tumor cells was correlated with the switch of TGF-β from a suppressor to a promoter of PDA (Gao et al., 2010; Sato et al., 2003); and e) Pancreatic tumor cells were more aggressive in preclinical PDA models in the absence of SPARC (Arnold et al., 2012; Arnold et al., 2010).

I proposed that a previously undescribed function of SPARC was to reduce the binding of newly secreted collagen to the cell membrane. This was consistent with the ability of SPARC to bind collagen and promote collagen deposition into the ECM (Brune et al., 2008; Sato et al., 2003). Furthermore, the fact that SPARC and DDR1 share the same binding site on collagen (Carafoli et al., 2009; Konitsiotis et al., 2008) was highly suggestive of SPARC's perturbation of the collagen interaction with this receptor. However, as previously described in PDA, malignant epithelial cells often downregulate SPARC expression via gene hypermethylation (Gao et al., 2010; Sato et al., 2003). The gradual loss of SPARC

expression in pancreatic ductal epithelial cells was also seen in the progression of intraductal papillary mucinous neoplasms, precursors to invasive adenocarcinoma (Truty & Urrutia, 2007). Furthermore, the lack of SPARC expression by tumor cells in pancreatic cancers was correlated with poor response to therapy. I proposed that this was due at least in part to elevated collagen receptor signaling in tumor cells. In addition, results in colorectal carcinoma demonstrated that re-expression of SPARC or addition of recombinant SPARC to tumor cells improved response to chemotherapy (Tai & Tang, 2008) which supported the hypothesis that blockade of collagen receptor signaling would improve chemosensitivity.

Therefore this proposal was poised to make a significant impact in the understanding of how collagen signaling affected PDA progression. I proposed that targeting pathways such as DDR1 signaling would have the potential to directly affect tumor cell proliferation, migration, and viability. Furthermore I suggested that SPARC, through its inhibition of collagen receptor signaling, reduced pancreatic tumor progression. If successful this would create a new paradigm for the therapy of PDA by targeting signaling pathways initiated by a major component (e.g., collagen) of the tumor microenvironment.

3.2 Results

3.2.1 Correlations of collagen-mediated DDR1 signaling in murine and human PDA

As the studies relied on genetic as well as xenograft models of PDA, clinical correlations were established of aberrant desmoplasia through the histological analyses of tissue from the *KIC (LSL-Kras$^{G12D/+}$; Ink4aArf$^{lox/lox}$; p48$^{Cre/+}$)* and *KPC (LSL-Kras$^{G12D/+}$; LSL-Trp53$^{R172H/+}$; p48$^{Cre/+}$)* GEMMs of PDA (Figure 3.1). PDAs formed in the *KIC* model with short latency, were desmoplastic and lethal (Aguirre et al., 2003; Dineen et al., 2010; Hezel et al., 2012). Tumors were first detected at 3-4 weeks of age and death from PDA occurred by 8-10 weeks. The *KPC* mice developed advanced PDA with 100% penetrance at approximately 2-3 months of age, and also recapitulated the human PDA through histopathological similarities. Through trichrome staining, which stained fibrillar collagens in blue, the two animal models recapitulated the human pathological characteristic of the formation of a dense stroma. This desmoplastic phenotype was noted at the ages of 6- and 8-week old *KIC* mice, and 3- and 5-month old *KPC* mice (Figure 3.1).

Human PDA displays a spectrum of histologies and for this reason the expression of *COLLAGEN I α1*, *DDR1*, *PYK2*, and *PEAK1* was analyzed in human PDA patients (n=168) using an online database (TCGA via Cbiportal).

RNA-sequencing data from The Cancer Genome Atlas (TCGA) PDA cBioPortal was collected (Cerami et al., 2012; J. Gao et al., 2013) using CGDS MATLAB toolbox with RNA Seq V2 RSEM option. Relative changes (G score) were assessed by comparing RNA sequencing data between normal and cancer patients to define high and low expression. Expression of *COLLAGEN I α1*, *DDR1*, *PYK2,* and *PEAK1* was divided into high and low at the median and displayed a trend of a worse overall prognosis (Figure 3.2). The downstream effectors of DDR1-mediated signaling have been undefined since its discovery (Leitinger, 2014; Valiathan et al., 2012); however, there are factors that have been implicated downstream of this signaling cascade (Aguilera et al., 2014; Leitinger, 2014) (Figure 3.3). Moreover, the expression data in human PDA samples was consistent with tissue microarray analyses (TMA) of the activation of DDR1 and a downstream effector (PEAK1) in 44 human pancreatic tumor samples and in 150 matched patient-derived tumor xenograft (PATX) samples (Figure 3.4). TMA analysis demonstrated that phospho-DDR1 and phospho-PEAK1 were inversely correlated with SPARC expression in the human and PATX samples. Pearson coefficient analyses were used to calculate the relationships between the phospho-DDR1, phospho-PEAK1, and SPARC scored values for staining positivity. These analyses demonstrated a positive correlation between phospho-DDR1 and phospho-PEAK1 (R^2= 0.34 in human, R^2= 0.75 in PATX). The majority of the human and PATX samples for phospho-DDR1 and

phospho-PEAK1 scored between 2-3, while the score for SPARC was between 0-2. The scoring system was denoted as: low or no stain (0-1), intermediate stain (2), high stain (3), and very high stain (4). Qualitatively, this suggested the involvement of these effectors throughout the progression of PDA.

Moreover, Ddr1 activation and downstream signaling through effectors such as Pyk2 and Peak1 was present throughout tissue from the early and late stages of the *KIC* and *KPC* GEMMs of PDA (Figure 3.5). Through immunohistochemical analysis, Ddr1 activation and downstream signaling was present in early PanIN lesions shown by correlative staining in similar regions positive for a marker of early PDA lesions, Muc-1. Additionally, these effectors were present throughout the tumor epithelium at the late stages of each model, 8-week old *KIC* and 5-month old *KPC,* as depicted by the consistent staining in areas positive for the tumor cell-specific marker Sox9. Sox9 was expressed in the malignant epithelium and confined to the duct-like cells; differentiated acinar and endocrine cells did not express Sox9 (Furuyama et al., 2011; Seymour et al., 2008). Moreover, collagen deposition and signaling was noted in liver metastases from 6-month old *KPC* mouse tissue (Figure 3.6). H&E and trichrome staining depicted the dense stromal formation and collagen deposition (Figure 3.6 A-B) as well as the presence of phosphorylated Ddr1 and Peak1 at regions of metastasis compared to normal regions (Figure 3.6 C-D). These effectors were colocalized with the mesenchymal marker Vimentin and a marker of cell proliferation

(proliferating cell nuclear antigen, Pcna) (Figure 3.6 E-F), factors highly expressed by tumorigenic cells. These findings demonstrated the propensity of the presence of collagen deposition and Ddr1 signaling at metastatic sites in the liver. These findings were correlative with other reports which depicted hepatic fibrosis (Friedman, 2004; Garcia-Trevijano et al., 1999; Gressner & Weiskirchen, 2006; Pinzani & Rombouts, 2004) as well as the expression of DDR1 at metastatic sites in different cancer models (Ford et al., 2007; Valencia et al., 2012).

3.2.2 Sparc inhibited collagen-DDR1 interaction

As previously described, of particular interest was the fact that SPARC and DDR1 shared the same GVMGFO binding site on fibrillar collagens (Carafoli et al., 2009; Konitsiotis et al., 2008) (Figure 1.3) which was suggestive of SPARC's perturbation of the collagen interaction with this receptor. ELISA-type binding assays were utilized in which 96-well ELISA plates were coated with different ECM substrates (collagen I or fibronectin), recombinant protein was added in a concentration-dependent manner, and respective primary and secondary antibodies detected the amounts of protein bound to the substrate. Recombinant DDR1/Fc and SPARC/His recognized and bound collagen I, not fibronectin, in a concentration-dependent manner (Figure 3.7). The competitive nature of the interactions between DDR1/Fc, SPARC/His, and collagen I was then explored after optimization of the initial ELISA-type binding assay. SPARC/His

inhibited the amount of DDR1/Fc (2 nM) bound to collagen I in a concentration-dependent manner (Figure 3.8 B). Additionally, this competitive interaction was analogous with the ability of increasing concentrations of DDR1/Fc to inhibit the amount of SPARC/His (2 nM) bound to collagen I (Figure 3.8 C). A SPARC blocking monoclonal antibody, mAb293 (Sweetwyne, 2004) at increasing concentrations was used to block the SPARC/His-collagen I interaction (Figure 3.8 D). Moreover, the addition of the mAb293 antibody to the SPARC/His-DDR1/Fc competitive binding assay inhibited the ability of SPARC/His to inhibit the levels of DDR1/Fc (2 nM) bound to collagen I. Moreover, the addition of mAb293 restored the DDR1-collagen I interaction (Figure 3.8 E). The recombinant binding and competitive binding assays demonstrated the competitive nature of the interactions of SPARC and DDR1 for binding to collagen I, and was ultimately proof of concept of the ability of SPARC to perturb DDR1 binding to collagen I.

To assess the effect of Sparc *in vivo*, *Sparc*$^{-/-}$ mice were crossed with *KIC* mice (Figure 3.9). The absence of endogenous *Sparc* (*Sparc*$^{-/-}$*; KIC*) enhanced primary tumor size and reduced the median survival to approximately 50 days compared to approximately 70 days of the *Sparc*$^{+/+}$*; KIC* mice (Figure 3.9 A-B). Additionally, tumors in *Sparc*$^{-/-}$*; KIC* mice were less differentiated as demonstrated through Alcian blue-PAS staining (Figure 3.9 C) which depicted a more progressed PDA phenotype shown by the reduction of mucin-positive

tissue, a surrogate marker of PanIN lesions. Furthermore, through immunohistochemical analyses the activation of Ddr1 and downstream effectors (Pyk2, Src, and Peak1), as well as levels of the mesenchymal marker Vimentin, were elevated in tumors from *Sparc*$^{-/-}$*; KIC* animals compared to controls (Figure 3.10 A-F).

To investigate how Sparc interfered with collagen-stimulated Ddr1 signaling, Isogenic cell lines were derived from 5-week old PDA transgenic *Sparc*$^{+/+}$*; KIC and Sparc*$^{-/-}$*; KIC* tumors (Figure 3.11). Through expression analysis of these cell lines by PCR, these PDA cell lines differentially expressed collagen receptors (*Ddr1*, *Ddr2*, *Integrin α1 (Itgα1)*, *Integrin α2 (Itgα2)*, and *Integrin β1 (Itgβ1)*), *Sparc*, and collagen subunits (*Collagen I α1* (*ColI α1*) (Figure 3.11 A-C). When these cell lines were plated onto different ECM substrates including fibronectin or collagen I, the presence of collagen I enhanced the phosphorylation of Ddr1, Pyk2, and Peak1 as well as the levels of Vimentin. This was more pronounced in the absence of *Sparc*, which demonstrated the function of Sparc in the modulation of collagen-mediated Ddr1 activation and downstream signaling (Figure 3.11 B-C).

The absence of *Sparc* expression was assessed in the context of response to a standard chemotherapeutic agent, gemcitabine. Sensitivity to 4-fold dilutions of gemcitabine was reduced in the absence of *Sparc*, comparing two *Sparc*$^{+/+}$*; KIC* (mPLRB8 and mPLRB9) and two *Sparc*$^{-/-}$*; KIC* (mPLR6A and

mPLR6C) cell lines (Figure 3.12). The IC_{50}s of the two *Sparc*$^{+/+}$*; KIC* cell lines (mPLRB8 and mPLRB9) were 38.6 nM and 20.3 nM compared to the *Sparc*$^{-/-}$*; KIC* cell lines (mPLR6A and mPLR6C) at 754 nM and 285 nM. This shift in sensitivity according to *Sparc* expression depicted the role of *Sparc* as a biomarker for response to therapy. This data was in line with other reports that demonstrated the correlation of SPARC expression with chemoresponse in PDA patients (Grzesiak et al., 2007; Paez-Ribes et al., 2009; Van Cutsem et al., 2009).

In the assessment of effectors involved in collagen deposition, tumorigenicity of PDA cells through hypoxia-induced collagen production and stimulation of Ddr1 was assessed. Commonly the tumor microenvironment is characterized by hypoxia, due to the fast and uncontrolled neoplastic growth. Hypoxia induced growth factor production and decreased the efficacy of chemotherapy (Carmeliet, 2005; Carmeliet & Jain, 2000). Hypoxia has also been associated with tumor cell signaling and migration in multiple tumor types (J. Chen, Imanaka, & Griffin, 2010; Luo et al., 2006; Mills, Joshi, & Niles, 2009; Mitchell & Bryan, 2010). Primary murine *KIC* PDA cells were plated on collagen under normoxic (20% O_2) and hypoxic (1% O_2) conditions to evaluate the influence of hypoxia in the modulation of a malignant phenotype. Hypoxia stimulated Hif1α and an induced collagen secretion from PDA cells (Figure 3.13 A) as well as liquid colony formation (Figure 3.13 B-C). The liquid colony formation was more pronounced in the absence of *Sparc*.

3.2.3 Enhanced collagen deposition and signaling drives DDR-mediated PDA progression

The downstream effectors of DDR1-mediated signaling have been undefined since the discovery of the receptor (Leitinger, 2014; Valiathan et al., 2012). To directly investigate the interactions of the effectors downstream of DDR1, immunoprecipitation assays were performed in a human PDA cell line (AsPC-1) (Figure 3.14 A). The pull down of DDR1 immunoprecipitated the downstream effectors PYK2, P130CAS, SRC, and PEAK1 (Figure 3.14 A). The absence of integrins αv and β1 suggested that DDR1-mediated activation of these effectors was independent of integrin activation. To further define the directionality as well as involvement of these signaling effectors the use of DDR1 inhibitors, a DDR1-blocking antibody (Castro-Sanchez, Soto-Guzman, Navarro-Tito, Martinez-Orozco, & Salazar, 2010) and recombinant SPARC/His, as well as an intermediate inhibitor of the pathway (PYK2 inhibitor: PF431396 (PF)) inhibited the phosphorylation of respective downstream targets (Figure 3.14 B-C). These findings demonstrated that the activation of these proposed downstream effectors of DDR1-mediated signaling were sensitive to DDR1 blockade by an anti-DDR1 antibody, recombinant SPARC/His, or the use of a PYK2 inhibitor. These findings were recapitulated with the use of siRNA-mediated knockdown of DDR1 in a human PDA cell line (AsPC-1), which abrogated the activation of these effectors (Figure 3.14 D-E). Loss of DDR1 expression reduced the

activation of PYK2, SRC, PEAK1 and AKT1. The inhibition of AKT1 phosphorylation demonstrated a mechanism of action of 7rh in the inhibition of AKT1-mediated pro-survival and anti-apoptotic pathways [34]. Additionally, knockdown of DDR1 reduced the migratory capacity of human cells (AsPC-1), which depicted a functional consequence of DDR1 inhibition (Figure 3.14 F). This data supported that collagen-mediated activation of DDR1 induced a signaling pathway that included PYK2, SRC, PEAK1 and AKT1, which in turn were potentially responsible for collagen-induced pathways, including chemoresistance [30, 31], that promoted tumor progression.

The knockdown data of DDR1 in the context of a functional consequence was recapitulated through Ddr1 blockade with the Ddr1-blocking antibody and recombinant Sparc/His. These inhibitors reduced Peak1 activation by immunocytochemical analysis of the mPLR6C (*Sparc*$^{-/-}$; *KIC*) cell line as well as migration through wound-healing analysis (Figure 3.15 A). Functional consequences of Ddr1 blockade through the use of the Ddr1-blocking antibody and recombinant Sparc/His demonstrated a loss of liquid colony formation which was more evident in the *Sparc*$^{+/+}$:*KIC* (mPLRB8) cell line compared to the *Sparc*$^{-/-}$:*KIC* (mPLR6C) cell line (Figure 3.15 B).

3.3 Figures

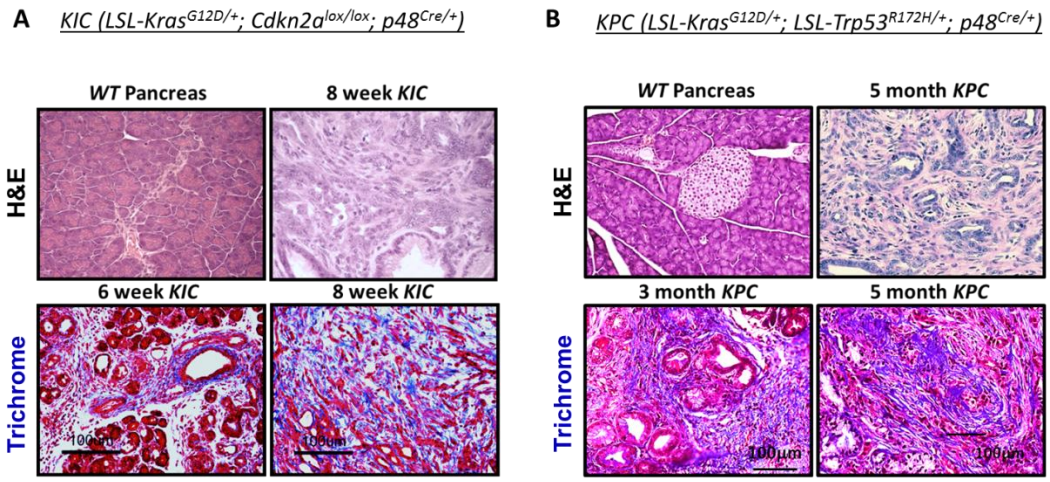

Figure 3.1: Desmoplastic phenotype throughout PDA development and progression.

PDA tumor tissue from two GEMMS of PDA: *KIC (LSL-Kras$^{G12D/+}$; Ink4aArf$^{lox/lox}$; p48$^{Cre/+}$)* and *KPC (LSL-Kras$^{G12D/+}$; LSL-Trp53$^{R172H/+}$; p48$^{Cre/+}$).* Tissue was analyzed by H&E and trichrome stain (blue). In each model, the trichrome data mimicked the desmoplastic aberration that presents in the clinic. Positive staining (blue) per high-powered field was evaluated with Nikon Elements 3.1 software (Nikon Instruments). *KPC* figure adopted from the submitted manuscript M. Wang, M. Topalovski, et al. 2015.

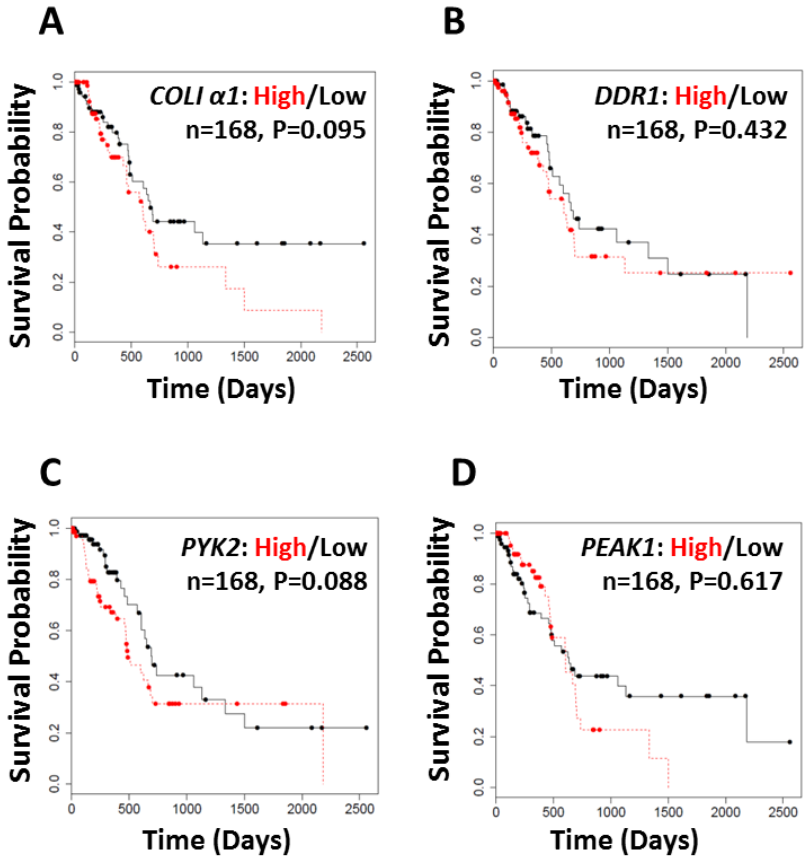

Figure 3.2: Kaplan-Meier analysis of collagen signaling in PDA patients.

(A) 168 human patient samples were assessed for expression of *COLLAGEN I α1* (*COLI α1*), *DDR1*, *PYK2*, and *PEAK1*. RNA-sequencing data from The Cancer Genome Atlas (TCGA) PDA cBioPortal was collected (Cerami et al., 2012; J. Gao et al., 2013) Relative changes (G score) were assessed by comparing RNA sequencing data between normal and cancer patients to define high and low expression via Cbioportal. High expression of *COLI α1*, *DDR1*, *PYK2*, and *PEAK1* led to a trend of a worse overall patient survival.

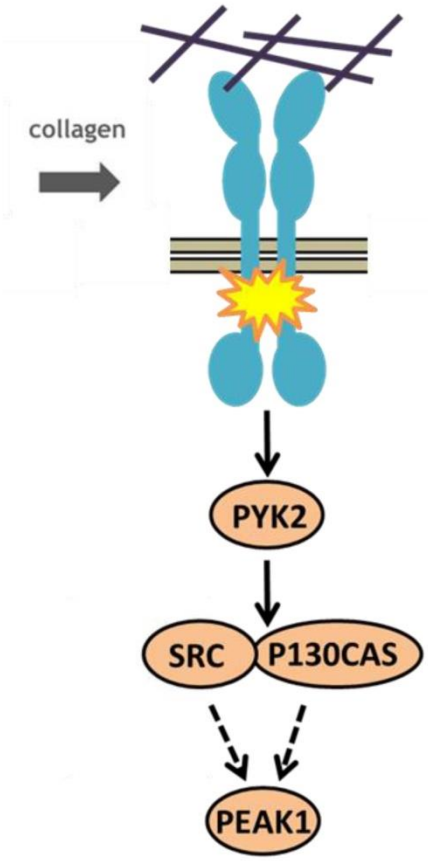

Figure 3.3: DDR1-mediated signaling.

Schematic representation of effectors downstream of DDR1-mediated signaling via collagen activation. Based on findings from (Kelber & Klemke, 2010; Lu et al., 2011; Shintani et al., 2008).

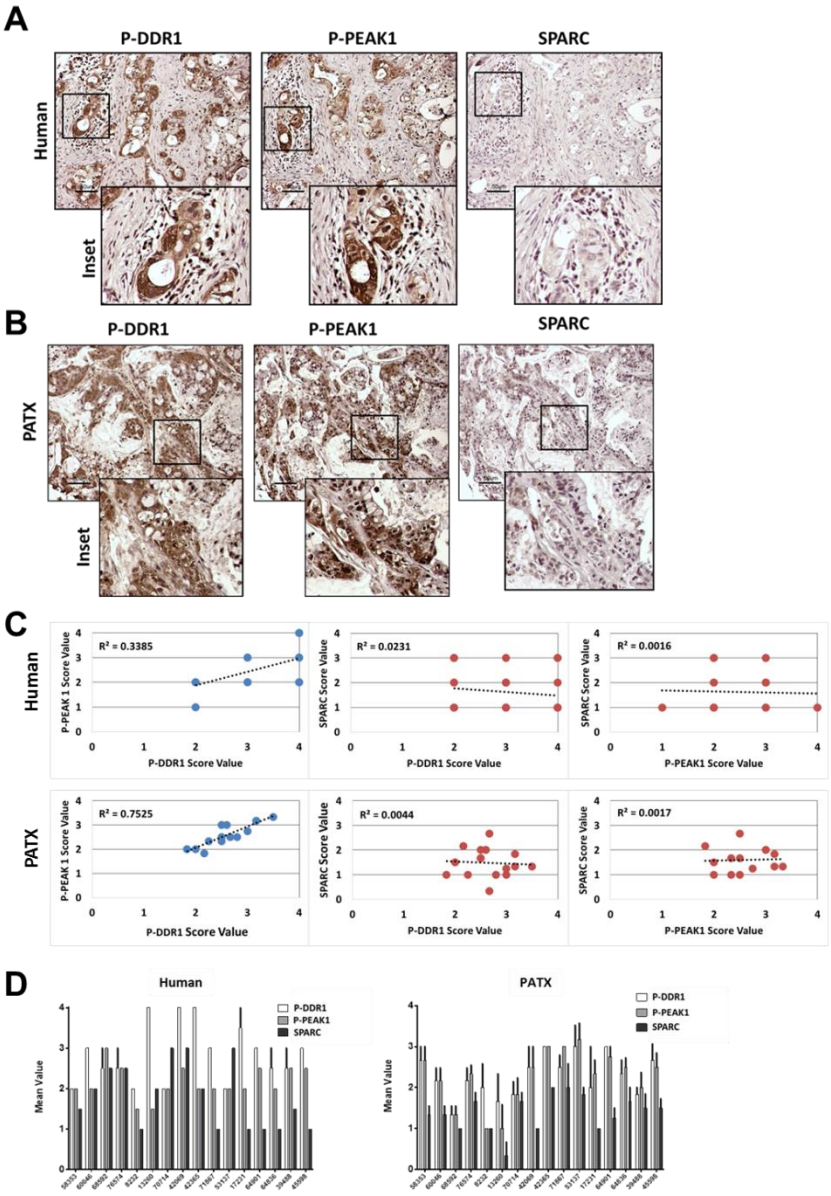

E

	Phospho-DDR1				Phospho-PEAK1				SPARC			
Score	0-1	2	3	4	0-1	2	3	4	0-1	2	3	4
Human (%)	0	31.25	37.5	31.25	3.61	43.7	38.25	14.45	56.25	22.75	21.75	0
PATX (%)	6.25	53.125	34.38	6.25	13.4	36.5	36.5	13.65	55.26	31.57	13.157	0

Figure 3.4: TMA analysis for DDR1 signaling.

Figure 3.4: TMA analysis for DDR1 signaling.

Representative images from the analyses of 44 human samples (A) and matched patient-derived tumor xenograft (PATX) (150 samples, B). TMA analysis demonstrated that phospho-DDR1 and phospho-PEAK1 were inversely correlated with SPARC expression. (C) Pearson coefficient was used to calculate the relationships between phospho-DDR1, phospho-PEAK1, and SPARC. (D) Correlative analyses of scored values for staining positivity for each effector throughout a subset of samples. (E) Overall positivity of staining for phospho-DDR1, phospho-PEAK1, and SPARC in human and PATX PDA samples. Scoring system is denoted as: low or no stain (0-1), intermediate stain (2), high stain (3), and very high stain (4).

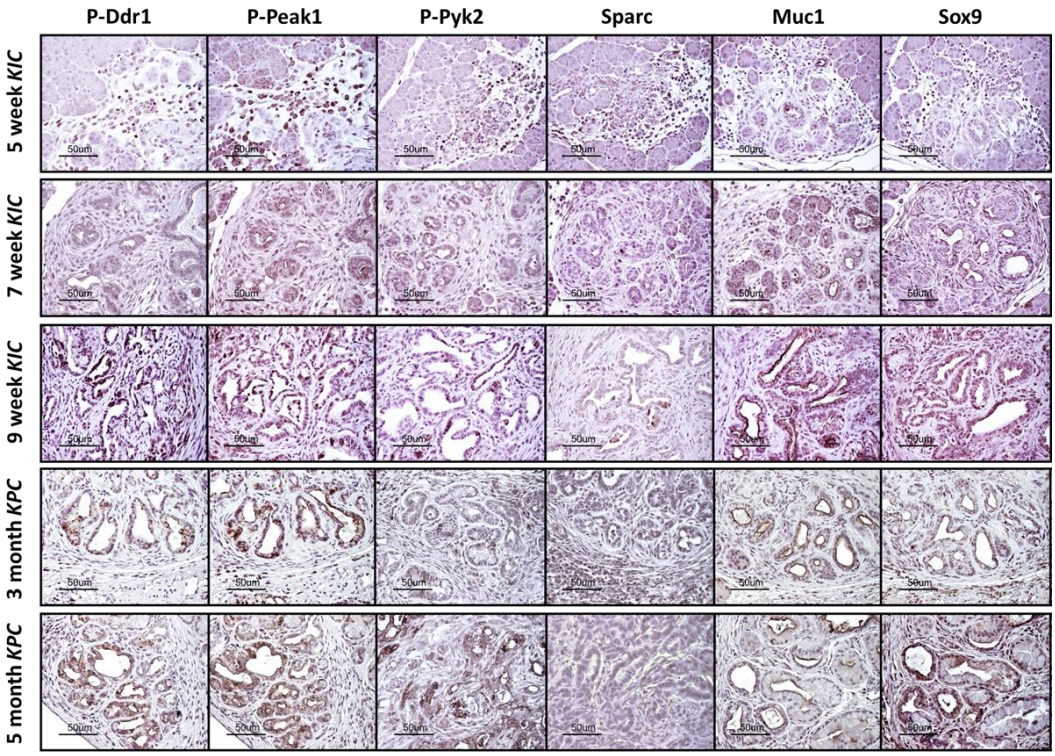

Figure 3.5: Analysis of PDA GEMM for Ddr1 signaling.

Stages of the *KIC (LSL-Kras$^{G12D/+}$; Ink4aArf$^{lox/lox}$; p48$^{Cre/+}$)* and *KPC (LSL-Kras$^{G12D/+}$; LSL-Trp53$^{R172H/+}$; p48$^{Cre/+}$)* mouse models. Ddr1 activation and downstream signaling through effectors such as Pyk2 and Peak1 was present in early PanIN lesions (Muc-1) and in advanced adenocarcinoma (Sox9) through immunohistochemical analysis.

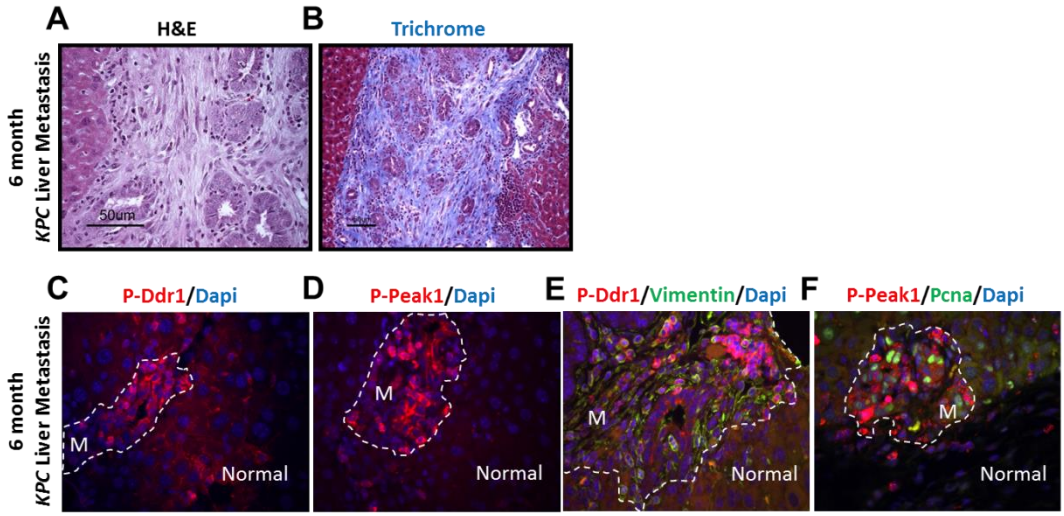

Figure 3.6: Expression of Ddr1 signaling in liver metastases.

Ddr1 activation and tumorigenicity was assessed in liver tissue from 6-month old *KPC (LSL-Kras$^{G12D/+}$; LSL-Trp53$^{R172H/+}$; p48$^{Cre/+}$)* mice. (A) Histological analysis by H&E depicted dense stromal reaction in the liver. (B) Trichrome stain (blue) depicted dense collagen staining in the site of metastasis. (C-D) Analyses demonstrated the presence of metastatic lesions (M) and the activation of Ddr1 (C) and Peak1 (D) in those regions compared to normal liver tissue. (E-F) Evidence of metastatic lesions (M) was noted through positive staining with Vimentin (E) and Pcna (F).

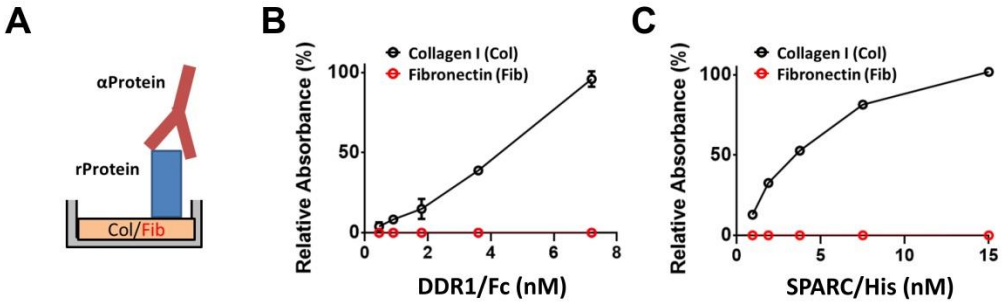

Figure 3.7: DDR1 and SPARC bind to collagen I.

(A) Schematic representation of recombinant ELISA-type binding assay. The binding of human recombinant DDR1/Fc (B) and SPARC/His (C) to collagen I was determined. 96-well plates were coated with collagen I (black) or fibronectin (red). Protein binding was detected via respective primary antibody and corresponding secondary antibody. TMB ELISA substrate (Abcam) was added to assess the protein bound to the substrate.

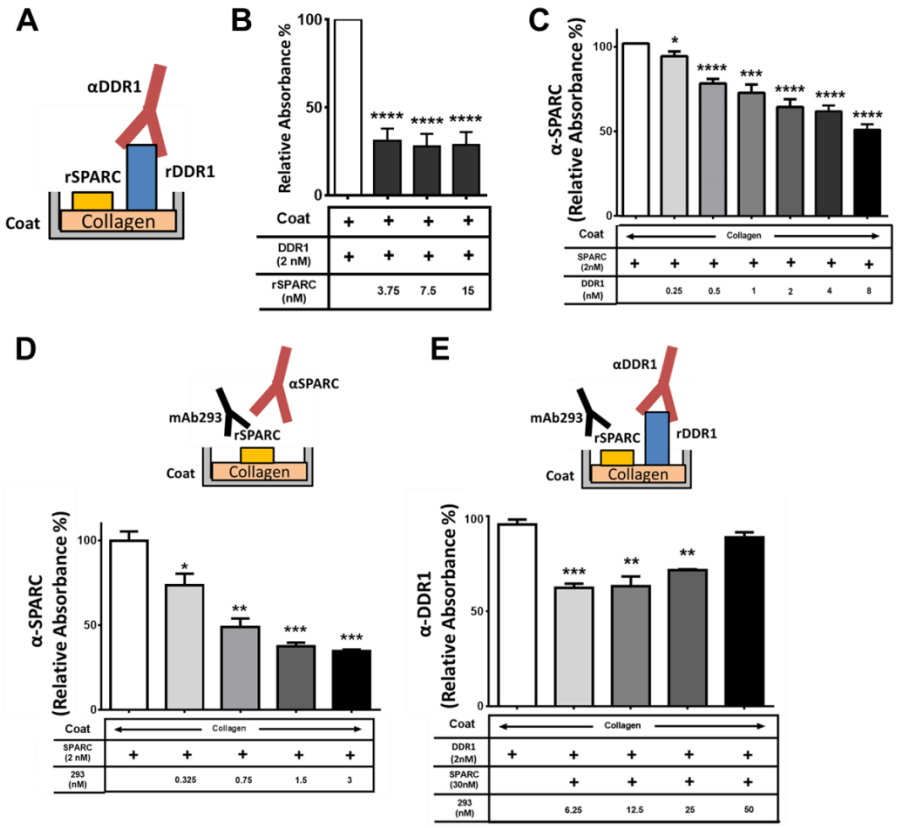

Figure 3.8: Competitive interactions of DDR1 and SPARC binding to collagen I.

(A) Schematic of competitive ELISA-type binding assay. (B) By ELISA, the binding of DDR1/Fc (2 nM) to collagen I was blocked by increasing concentrations of human recombinant SPARC/His. (C) The binding of recombinant SPARC/His (2 nM) to collagen I was blocked by increasing concentrations of recombinant DDR1/Fc. (D) The binding of recombinant SPARC/His (2 nM) to collagen I was blocked by increasing concentrations of monoclonal antibody 293 (mAb 293) (Sweetwyne, 2004). (E) The binding of DDR1/Fc (2 nM) to collagen I was restored by blocking recombinant SPARC/His (30 nM) with increasing concentrations of mAb 293. Each condition is coated with collagen I (10 µg/ml) in the solid phase. 96-well plates were coated with collagen I. Protein binding was detected via respective primary antibody and corresponding secondary antibody. TMB ELISA substrate (Abcam) was added to assess the protein bound to the substrate. Error bars: (*, $p < 0.05$; **, $p < 0.005$; ***, $p < 0.0005$; ****, $p < 0.00005$), one-way ANOVA with Tukey's MCT, all shown versus Column 1.

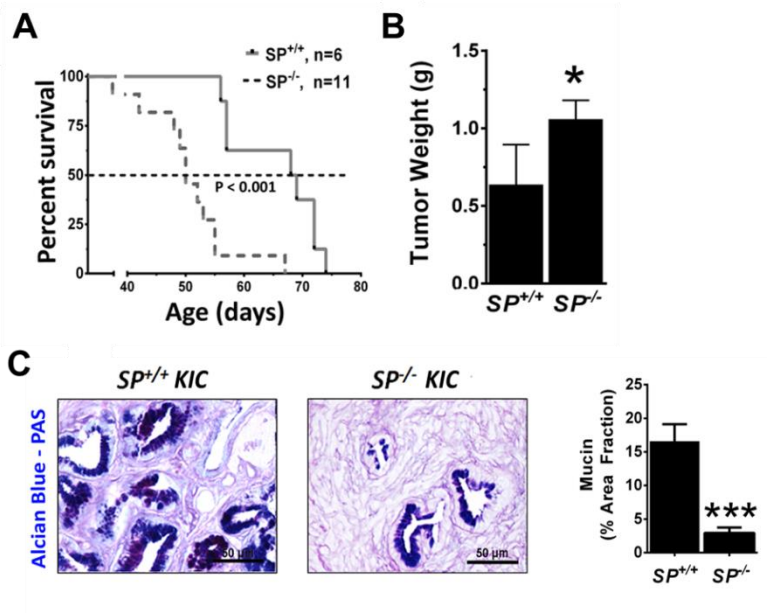

Figure 3.9: *Sparc* attenuated PDA progression.

(A) Decreased survival of *Sparc*$^{-/-}$*; KIC* mice. *Sparc*$^{-/-}$ mice were crossed with *KIC* mice to generate *Sparc*$^{+/-}$*; KIC* animals which were crossed with each other to generate *KIC* (*SP*$^{+/+}$) and *Sparc*$^{-/-}$*; KIC* (*SP*$^{-/-}$) animals. Survival of these animals is shown. (B) Mean pancreas/tumor weight in *Sparc*$^{+/+}$*; KIC* and *Sparc*$^{-/-}$*; KIC* animals. (C) Alcian blue-PAS histology of tumors from *Sparc*$^{+/+}$*; KIC* and *Sparc*$^{-/-}$*; KIC* animals. Error bars: (*, $p < 0.05$; **, $p < 0.005$; ***, $p < 0.0005$; ****, $p < 0.00005$), one-way ANOVA with Tukey's MCT.

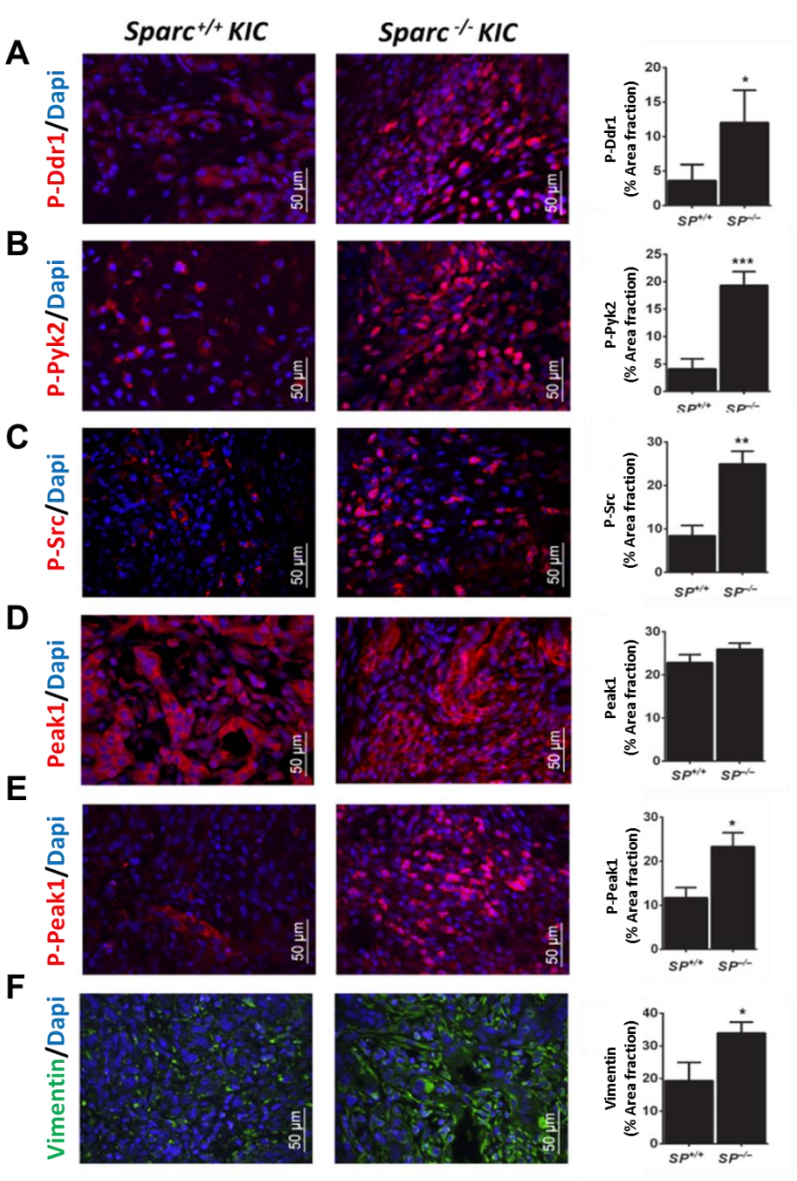

Figure 3.10: *Sparc* attenuated collagen signaling.

Tumors were harvested from moribund *KIC* and *Sparc*$^{-/-}$*; KIC* mice, sectioned and stained for phosphorylated Ddr1 (A, P-Ddr1), phosphorylated Pyk2 (B, P-Pyk2), phosphorylated Src (C, P-Src), total Peak1 (D, Peak1), phosphorylated Peak1 (E, P-Peak1), and Vimentin (F). Error bars represent SEM (*, $p < 0.05$ vs *SP*$^{+/+}$; **, $p < 0.005$ vs *SP*$^{+/+}$; ***, $p < 0.0005$ vs *SP*$^{+/+}$; ****, $p < 0.00005$ vs *SP*$^{+/+}$).

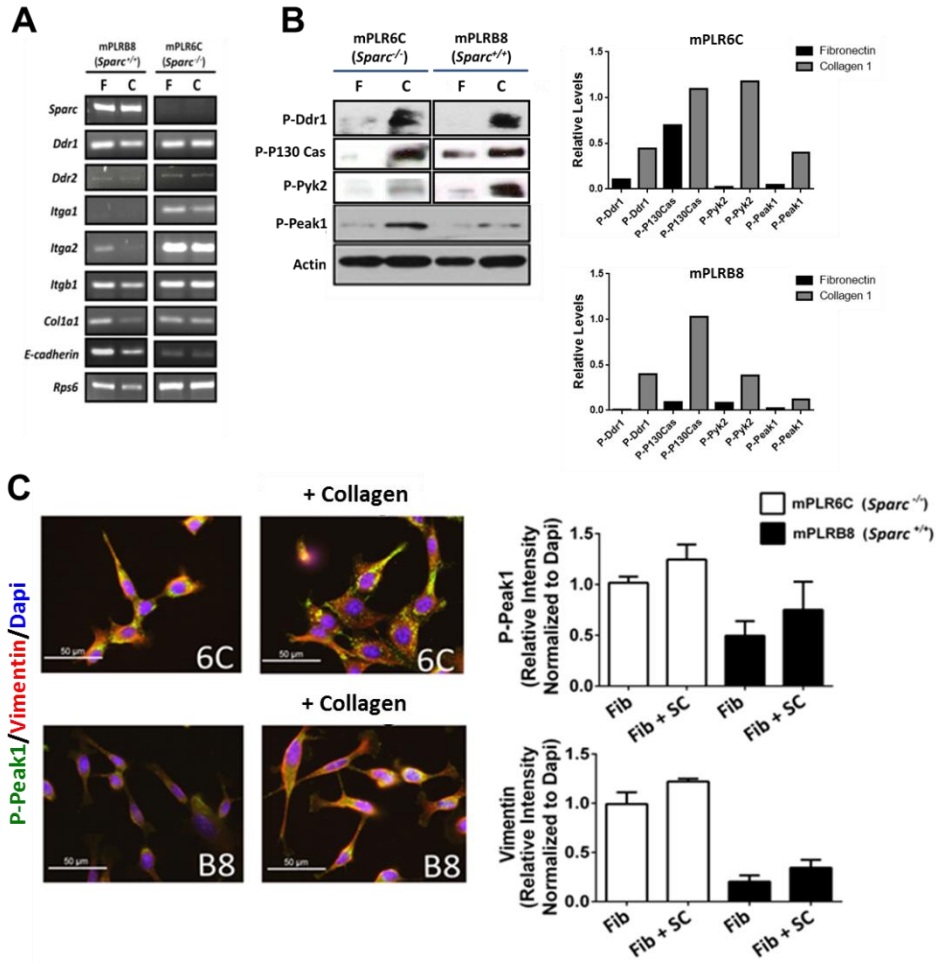

Figure 3.11: PDA cells expressed collagen receptors and *Sparc*.

(A) Collagen receptor and *Sparc* expression profile of PDA clones mPLRB8 (*Sparc*$^{+/+}$; *KIC*) and mPLR6C (*Sparc*$^{-/-}$; *KIC*) on fibronectin-coated and collagen I-coated conditions. (B) mPLRB8 cells were plated on fibronectin and stimulated with soluble collagen I (10 µg/ml) for 1 or 4 hours. Lysates were probed for the indicated targets by western blotting. (C) PDA cells differentially express *Sparc*, which mediated differential induction of Peak1 activation. mPLRB8 (*Sparc*$^{+/+}$; *KIC*) and mPLR6C (*Sparc*$^{-/-}$; *KIC*) were plated on fibronectin in the presence or absence of 10 µg/ml soluble collagen (+ collagen). The presence of soluble collagen (10 µg/ml) enhanced the phosphorylation of Peak1 and the induction of a mesenchymal marker, Vimentin. Collagen-induced Peak1 activation was elevated in cells that lack *Sparc*. Error bars: (*, $p < 0.05$; **, $p < 0.005$; ***, $p < 0.0005$; ****, $p < 0.00005$), one-way ANOVA with Tukey's MCT.

	Gemcitabine (nM) Avg IC_{50}
mPLRB8	38.6 (5)
mPLRB9	20.3 (4)
mPLR6A	754 (5)
mPLR6C	285 (5)

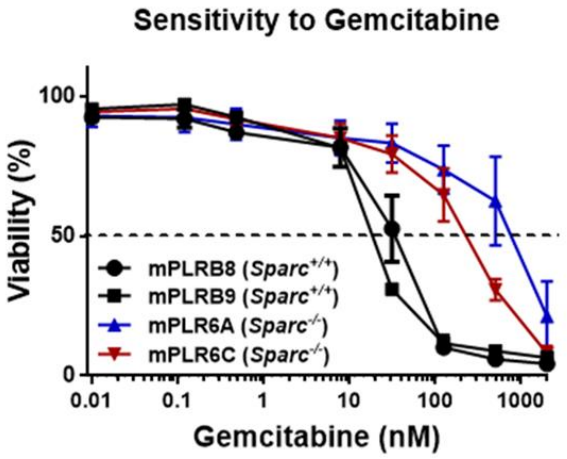

Figure 3.12: *Sparc* regulated drug response of murine PDA cell lines.

Isogenic cell lines were derived from 5-week old PDA transgenic (*Kras*$^{G12D/+}$*; Ink4a*$^{lox/lox}$*; p48*$^{Cre/+}$ *and Kras*$^{G12D/+}$*; Ink4a*$^{lox/lox}$*; p48*$^{Cre/+}$*; Sparc*$^{-/-}$*)* mice. Drug sensitivity was assessed in two *KIC* (mPLRB8 and mPLRB9) cell lines and two *Sparc*$^{-/-}$*; KIC* (mPLR6A and mPLR6C) cell lines in the presence of 4-fold dilutions of gemcitabine. Drug sensitivity curves and IC_{50}s were calculated with in-house software (Dineen et al., 2010).

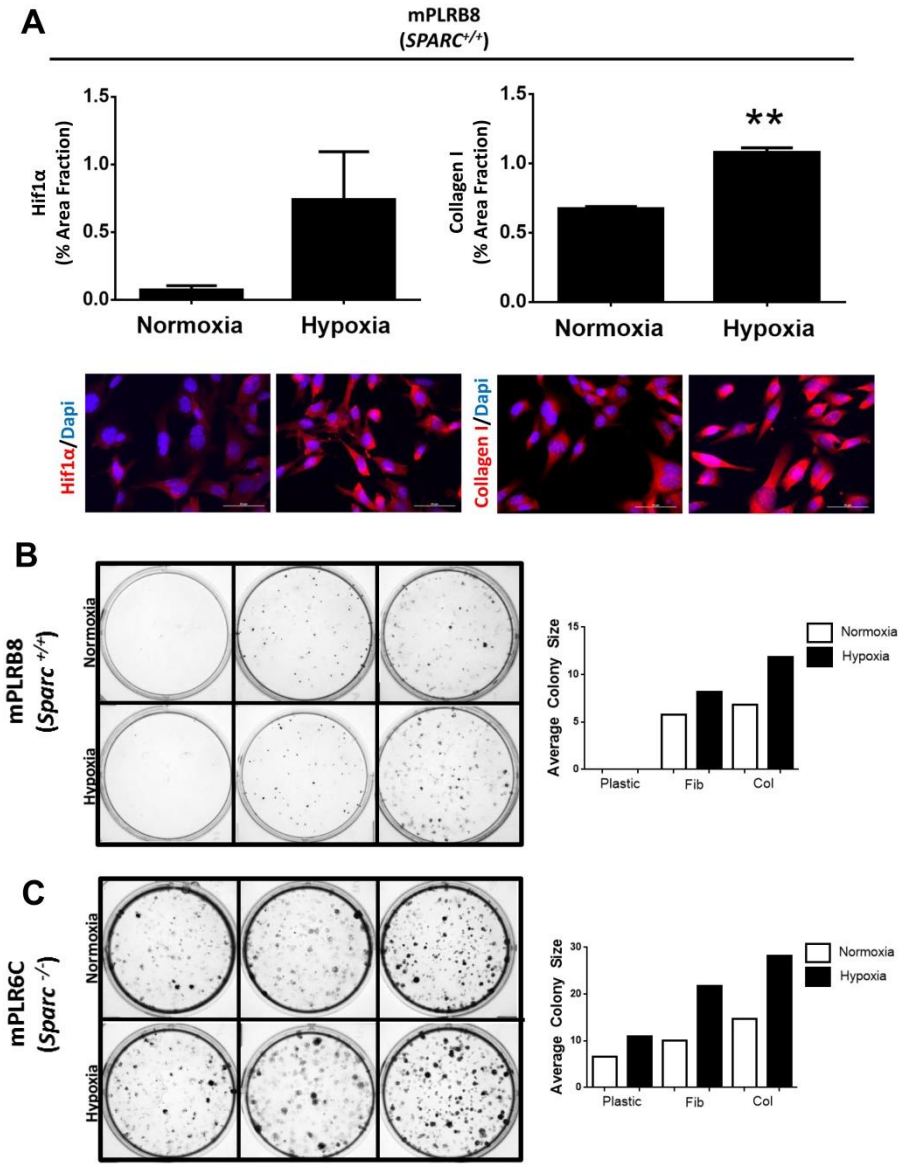

Figure 3.13: Hypoxia induced collagen production and EMT phenotype.

Primary murine *KIC* PDA cells, mPLRB8 (*Sparc*$^{+/+}$; *KIC*) and mPLR6C (*Sparc*$^{-/-}$; *KIC*), were plated on collagen I under normoxic (20% O_2) and hypoxic (1% O_2) conditions. Hypoxia stimulated Hif1α expression and an induction in collagen I secretion from PDA cells (A), as well as enhanced liquid colony formation measured in square pixels (B-C). Error bars: (*, $p < 0.05$; **, $p < 0.005$; ***, $p < 0.0005$; ****, $p < 0.00005$), one-way ANOVA with Tukey's MCT.

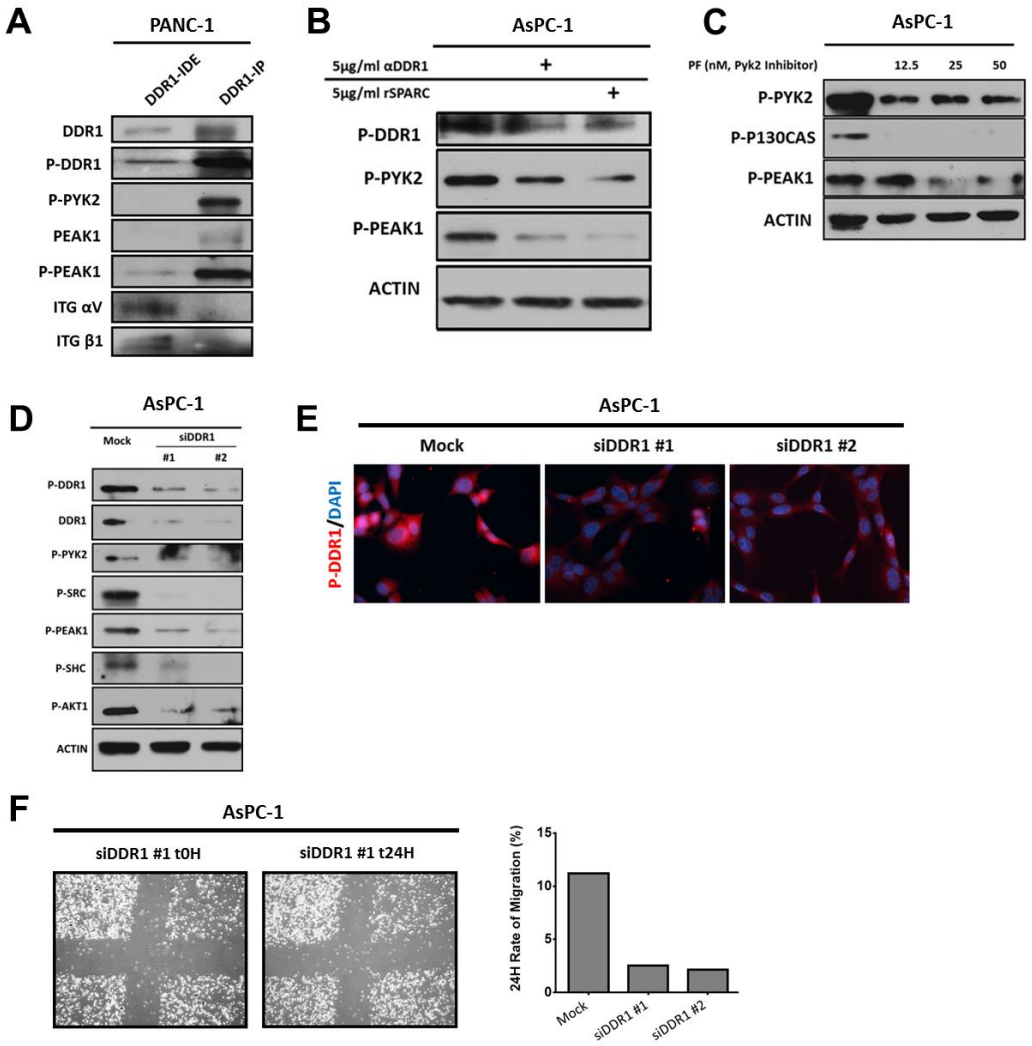

Figure 3.14: Inhibition of the DDR1 signaling pathway.

Figure 3.14: Inhibition of the DDR1 signaling pathway.

(A) Immunoprecipitation (IP) analysis of DDR1 interactions. The DDR1 IP pulled down PYK2 and PEAK1, but not integrin alpha V (ITG αV) or β1 (ITG β1) as shown in the immunodepleted (IDE) fraction. Lysates were probed for the indicated targets by western blot analysis. (B) Blockade of DDR1 reduced the activation of downstream effectors including PYK2 and PEAK1 in a human PDA cell line (AsPC-1). Cells were stimulated with no treatment, anti-DDR1 (5 μg/ml) or rSPARC (5 μg/ml). Activation was measured after 24 hours of stimulation. Lysates were probed for the indicated targets by western blot analysis. (C) Utilization of PYK2 inhibitor (PF431396) abrogated respective downstream effectors P130CAS and PEAK1. Lysates were probed for the indicated targets by western blot analysis. (D) siRNA-mediated knockdown of DDR1 compared to Mock siRNA controls reduced the activation of DDR1, PYK2, SRC, and PEAK1. Lysates were probed for the indicated targets by western blot analysis. (E) siRNA-mediated knockdown of DDR1 compared to Mock siRNA controls reduced the activation of DDR1 through immunocytochemistry. (F) siRNA-mediated knockdown of DDR1 compared to Mock siRNA control reduced the migration of human PDA cells.

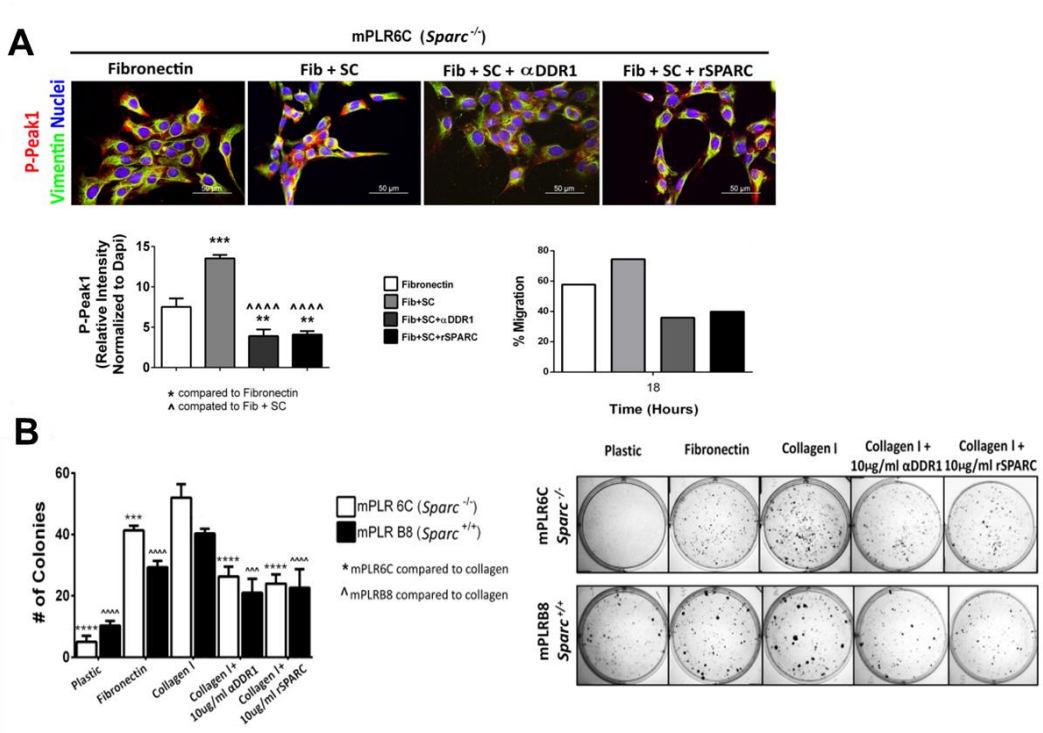

Figure 3.15: Functional consequences of Ddr1 inhibition.

(A) mPLR6C (*Sparc*$^{-/-}$; *KIC*) was plated on fibronectin-coated (Fib) chamber slides in the presence or absence of 10 μg/ml soluble collagen I (SC), a DDR1-blocking antibody (αDDR1), or recombinant SPARC/His (rSPARC). Ddr1 inhibitors reduced Peak1 activation as well as migration in a 15 hour time period via scratch migration assay. Migration was measured with a scratch (wound healing) assay. (B) Functional consequences of Ddr1 blockade. *Sparc*$^{-/-}$; *KIC* clone (mPLR6C) and *Sparc*$^{+/+}$; *KIC* clone (mPLRB8) were plated on plastic, 10 μg/ml fibronectin, or 10 μg/ml collagen I in the presence or absence of Ddr1 inhibitors (Ddr1 blocking antibody or recombinant SPARC/His) and colony formation was determined. Error bars: (*, $p < 0.05$; **, $p < 0.005$; ***, $p < 0.0005$; ****, $p < 0.00005$), one-way ANOVA with Tukey's MCT.

3.4 Discussion

The goal of this project was to determine if changes in collagen deposition and Ddr1 activation contributed to tumor response to therapy in the context of *Sparc* expression. The matricellular protein *Sparc* reduced collagen I signaling through Ddr1 (Aguilera et al., 2014). This ultimately agreed with the observations that SPARC was correlated with enhanced chemoresponse in PDA patients (Paez-Ribes et al., 2009), that collagen signaling was associated with chemoresistance in PDA cell lines (Erkan et al., 2008; Ghaneh et al., 2007; Mahadevan & Von Hoff, 2007), and that DDR1 conferred resistance to chemotherapy and mediated pro-survival signals in several cancer models (Cader et al., 2013; Ongusaha et al., 2003). Thus it was plausible that the correlation of *SPARC* expression with chemoresponse (Figure 3.12) (D. D. Von Hoff et al., 2011) was due to a reduction of collagen induced signaling, which further highlights the potential value of DDR1 inhibition in PDA and other solid tumors.

Interestingly, as a unifying function of SPARC is presently lacking, structural human studies indicated that SPARC and the DDRs bind to the same epitope (GVMGFO) on fibrillar collagens (Carafoli et al., 2009; Carafoli et al., 2012; Konitsiotis et al., 2008; Roskoski, 2007; Xu et al., 2011) (Figure 1.3). Through ELISA-type binding assays molar excess concentrations of recombinant SPARC/His inhibited recombinant DDR1/Fc binding to collagen I (Aguilera et al., 2014), and vice versa, which elucidated the competitive interactions between

these effectors for binding to collagen I. Additionally, the utility of a SPARC blocking monoclonal antibody mAb293 (Sweetwyne, 2004) restored the levels of DDR1 bound to collagen I. These were critical initial experiments that demonstrated the proof of concept of SPARC blocking DDR1 binding to collagen I.

The relevance in the assessment of SPARC's contribution to PDA progression and chemoresponse stemmed from conflicting reports that have demonstrated tissue and context-specific functions of SPARC. It was previously reported that the SPARC promoter was commonly hypermethylated in PDA cell lines and xenograft tumors (Sato et al., 2003). Ultimately PDA tumors grown in *Sparc*$^{-/-}$ mice exhibited increased collagen signaling and enhanced disease progression, and the loss of *Sparc* expression *in vitro* reduced the sensitivity of PDA cell lines to therapeutic agents. Collagen signaling through Ddr1 stimulated pro-tumorigenic downstream signaling through effectors such as protein tyrosine kinase 2 (Pyk2) and pseudopodium enriched atypical kinase 1 (Peak1) and this was more pronounced in the absence of *Sparc*. These findings supported previous findings that demonstrated that subcutaneous tumors grown in *Sparc*$^{-/-}$ animals displayed significantly augmented tumor growth compared to *Sparc*$^{+/+}$ counterparts (Brekken et al., 2003; Puolakkainen et al., 2004), as well as other data in which *Sparc*$^{-/-}$ mice exhibited a significant increase in metastasis in an orthotopic PDA model compared with *Sparc*$^{+/+}$ controls (Arnold et al., 2010).

These findings indicated that SPARC governed tumorigenesis and thereby regulated tumor progression. These findings were also in line with recent reports from Harris and colleagues (Harris et al., 2011) which demonstrated that increased amounts of collagen I were associated on the cell surface with *Sparc*$^{-/-}$ versus *Sparc*$^{+/+}$ cells, and the proportion of total collagen produced by *Sparc*$^{-/-}$ cells was higher than in *Sparc*$^{+/+}$ cells. In addition, the amount of total collagen sensitive to collagenase digestion (extracellular) was greater in *Sparc*$^{-/-}$ cells than in *Sparc*$^{+/+}$ cells, which indicated an increase in cell surface-associated collagen in the absence of *Sparc*. Moreover, the enhanced phosphorylation of Ddr1 and downstream effectors in *Sparc*$^{-/-}$*; KIC* versus *Sparc*$^{+/+}$*; KIC* was suggestive of the enhanced collagen associated with the cell surface and an increase in the associations between these effectors with collagen.

Moreover, previous results in colorectal carcinoma have demonstrated that re-expression of *SPARC* or addition of recombinant SPARC to human colon cancer cells improved response to chemotherapy (Tai, Dai, Owen, & Chen, 2005; Tai & Tang, 2008) which supported the hypothesis that blockade of collagen receptor signaling would improve chemosensitivity. Tai and colleagues (Tai et al., 2005) have previously reported that SPARC increased sensitivity to chemotherapy in colorectal cancer tumor xenograft models. There was complete tumor regression in 50% of the animals implanted with a *SPARC*-overexpressing MIP human colon cancer cells following treatment with 3 cycles of 5-FU.

Additionally, treatment with exogenous SPARC combined with 5-FU dramatically improved tumor response to therapy and significantly increased tumor regression. These results suggested a role for SPARC in the enhancement of sensitivity to tumors. Tai and colleagues (Tai et al., 2005) have suggested that *SPARC* likely promoted increased sensitivity to chemotherapy via the enhancement of tumor cell apoptosis. This was supported by their findings that there was a greater degree of cleaved caspase-3 in cells that overexpressed *SPARC* following exposure to chemotherapy *in vitro* (Tai et al., 2005). These results corroborated other studies in which the exposure of Lewis lung cancer cells to SPARC inhibited cell proliferation *in vitro* (Brekken et al., 2003), and in which glioma cells which overexpressed *SPARC* had delayed tumor growth *in vivo* (Schultz, Lemke, Ge, Golembieski, & Rempel, 2002). Additionally, Yiu and colleagues (Yiu et al., 2001) demonstrated that exposure of exogenous SPARC alone induced apoptosis in ovarian cancer cells. Moreover, studies with *Sparc*$^{-/-}$ mice demonstrated enhanced pancreatic and lung tumor growth in these animals (Brekken et al., 2003; Puolakkainen et al., 2004).

As previously discussed, aberrant *Sparc* methylation was commonly observed in colorectal cancers (Lee, Hwang, Lee, Kim, & Kang, 2004; Toyota et al., 1999), and recent studies have revealed that aberrant hypermethylation of the *Sparc* promoter was responsible for low levels of *Sparc* expression (DiMartino et al., 2006; Sato et al., 2003; Suzuki et al., 2005). A recent report has demonstrated

that exposure of colorectal cell lines to 5-Aza-2'deoxycytidine (5-Aza), a nucleoside anti-metabolite and a potent inhibitor of DNA methyltransferase 1 (Dnmt1) activity, effectively demethylated the CpG regions within the *Sparc* promoter, which led to greater *Sparc* gene and protein expression (Cheetham et al., 2008). Moreover, in this study *Sparc* promoter demethylation by 5-Aza led to higher *Sparc* levels which resulted in enhanced chemosensitivity and chemotherapeutic response (Cheetham et al., 2008). Another study corroborated these findings and demonstrated that gastric cancer patients with hypermethylated *SPARC* had a lower overall survival, and that 5-Aza inhibited the cell proliferation, invasion and migration in the gastric cell lines with methylated *SPARC* (Z. Y. Chen et al., 2014). Ultimately, these results were promising as aberrant methylation of *Sparc* was also detected at a high frequency (~90%) in pancreatic cancer, and *Sparc* expression has been shown to be inducible by 5-aza in pancreatic cancer which resulted in reduced cellular proliferation (Sato et al., 2003).

In aggregate these studies suggested that inhibition of collagen signaling through DDR1 would enhance therapeutic response in PDA.

CHAPTER FOUR

Targeting DDR1 as a Therapeutic Approach in Combination with Chemotherapy

Note: The following chapter is in part made up of a research article written by Kristina Y Aguilera under the guidance of Rolf A. Brekken (Aguilera et al. *Oncotarget*, under review).

CHAPTER FOUR

Targeting DDR1 as a Therapeutic Approach in Combination with Chemotherapy

4.1 Introduction

The extracellular matrix (ECM) is a crucial factor for tumor progression. Specifically, enhanced desmoplasia in the tumor microenvironment actively participates in enhanced tumorigenicity and chemoresistance, and correlates with poor prognosis in PDA patients (Conklin & Keely, 2012; Provenzano et al., 2008). Collagen is expressed in PDA by stromal cells, mainly fibroblasts, and tumor cells (Apte et al., 2004; Kalluri & Zeisberg, 2006). Collagen receptors such as DDR1 are expressed broadly and are linked to cellular processes that are prominent in PDA, including the epithelial to mesenchymal transition (EMT) and chemoresistance. As previously discussed, DDR1 conferred resistance to chemotherapy and mediated pro-survival signals in breast cancer and lymphoma cell lines (Cader et al., 2013; Ongusaha et al., 2003) and may be involved in the recurrence of certain types of cancer (Jian et al., 2012). Shintani et al. found that collagen I induced N-cadherin expression (a marker of mesenchymal cells) in human pancreatic cancer cells through signaling pathways that required activation of DDR1. DDR1 is a critical factor in driving the activation of tumorigenic

elements and I established that the activation of DDR1 is elevated in human PDA *in vitro* and *in vivo*, and that inhibition of this receptor is an attractive target in the reduction of tumorigenicity and the enhancement of chemoresponse to standard of care PDA regimens.

Recent reports have highlighted the complexity of therapeutically targeting DDR1 either *in vitro* or *in vivo* due to the unspecific nature of currently available inhibitors (Day et al., 2008; Rix et al., 2007) (Figure 1.5). I demonstrated the utility of a novel small molecule inhibitor with high specificity towards DDR1, known as 3-(2-(Pyrazolo[1,5-a]pyrimidin-6-yl)-ethynyl) benzamide (7rh) (M. Gao et al., 2013).

4.2 Results

4.2.1 Regulation of collagen signaling

The expression of genes involved in collagen signaling (*DDR1*, *PEAK1*, *INTEGRIN α1* (ITG α1), *INTEGRIN β1* (*ITG β1*), *COLLAGEN I α1* (*COL I α1*), and *COLLAGEN I α2* (*COL I α2*)) were endogenously similar in human PDA cell lines (AsPC-1 and PANC-1) determined by PCR (Figure 4.1 A). The amount of soluble collagen secreted by these cell lines was assessed by Sircol collagen assay and depicted that AsPC-1 produced significantly more collagen than PANC-1, which suggested that AsPC-1 cells have high endogenous activation of DDR1

potentially due to endogenous expression of collagen (Figure 4.1 B). The presence of exogenous soluble collagen I enhanced the phosphorylation of DDR1, SRC, and PEAK1 (Figure 4.1 C-D). The phosphorylation of these effectors was demonstrated regardless of the presence of exogenous soluble collagen I for AsPC-1 possibly due to autocrine collagen production of this cell line.

I evaluated the effect of a small molecule inhibitor, 7rh (M. Gao et al., 2013), on collagen-induced signaling in PANC-1 cells. 7rh has high specificity for DDR1 versus other related kinases (IC_{50}: DDR1, 6.8 nM; DDR2, 101.4 nM; Bcr-Abl, 355 nM) based on previously published cell-free kinase assays (M. Gao et al., 2013). 7rh inhibited DDR1-mediated signaling (PYK2, PEAK1, SHC, and AKT1) induced by soluble collagen I (10 µg/ml) in PANC-1 cells in a concentration-dependent manner (Figure 4.2 A). The inhibition of AKT1 phosphorylation demonstrated a mechanism of action of 7rh in the inhibition of AKT1-mediated pro-survival and anti-apoptotic pathways (Sheppard, Kinross, Solomon, Pearson, & Phillips, 2012) in addition to DDR1 blockade. However, 7rh did not affect the activation of focal adhesion kinase (FAK), an effector that has not been previously associated with DDR1-induced signaling (Shintani et al., 2008). Functionally, 7rh inhibited the migration (scratch assay) and liquid colony formation of human PDA cell lines (AsPC-1 and PANC-1) in a concentration-dependent manner. The effect of DDR1 was more apparent in PANC-1 compared

to AsPC-1 cells, consistent with the higher basal collagen production and DDR1 signaling in AsPC-1 (Figure 4.2 B-C).

Chemoresistance is a major challenge in the treatment of patients with PDA. Given the effect of 7rh on PDA cell colony formation I evaluated the effect of 7rh alone or in combination with gemcitabine, a chemotherapeutic agent commonly used for the treatment of PDA, on cell viability. I established the inhibitory concentration (IC_{50}) of 7rh and gemcitabine in both of these cell lines (Figure 4.3 A). The sensitivity for both of these cell lines was greater to the 7rh compound versus gemcitabine: 7rh IC_{50} for AsPC-1 = 490 nM, 7rh IC_{50} for PANC-1 = 380 nM; gemcitabine IC_{50} for AsPC-1 > 2 μM, gemcitabine IC_{50} for PANC-1 > 2μM). Therefore, to enhance the sensitivity of these human PDA cell lines to gemcitabine a constant concentration of either 250 nM of 7rh or the approximate IC_{50} of 7rh (500 nM) was combined with a titration of gemcitabine. The presence of 7rh enhanced the overall sensitivity of these two cell lines to the titration of gemcitabine. 7rh at 500 nM dramatically decreased the IC_{50} of gemcitabine in each cell line from > 2000 nM to < 5 nM. The IC_{50} for AsPC-1 was 2.05 nM and the IC_{50} for PANC-1 was 0.0135 nM. Moreover, when these cells were plated on collagen I the IC_{50} of each compound were shifted to the right (Figure 4.3 B). This marked response was further assessed through CompuSyn Synergistical Analysis (http://www.combosyn.com) (Chou, 2006) which demonstrated that the combination of gemcitabine with 500 nM 7rh was

synergistic for both cell lines (Figure 4.3 C). With the software, a calculated combination index (CI) of less than or equal to 0.9 is synergistic. These findings highlighted the therapeutic potential of this combination for *in vivo* assessment. The curves and IC_{50} values were calculated through the use of in-house software (Dineen et al., 2010).

In conjunction with studies from Chapter 3 the efficacy of 7rh therapy was assessed in the context of *Sparc*-mediated chemoresponse. The efficacy of 7rh-mediated inhibition of cell migration as well as liquid colony formation was enhanced in the *KIC* (mPLRB8) cell line versus the *Sparc*$^{-/-}$*; KIC* cell line (mPLR6C) (Figure 4.4 A-B). This highlighted *SPARC* as a potential biomarker for patient response to 7rh therapy. Drug sensitivity was assessed in two *KIC* (mPLRB8 and mPLRB9) cell lines and two *Sparc*$^{-/-}$*; KIC* (mPLR6A and mPLR6C) cell lines in the presence of 4-fold dilutions of gemcitabine or 7rh (Figure 4.5 A-B). Drug sensitivity to gemcitabine was reduced in the absence of *Sparc*, though sensitivities to 7rh were similar throughout (Figure 4.5 A-B, E). Drug sensitivity assays of the two *Sparc*$^{-/-}$*; KIC* (mPLR6A and mPLR6C) cell lines were evaluated with a constant concentration of 7rh (250 nM) in combination with a titration of gemcitabine. The presence of 250 nM 7rh in combination with gemcitabine enhanced the sensitivity of both *Sparc*$^{-/-}$*; KIC* cell lines to gemcitabine treatment (Figure 4.5 C-D, E). This further highlighted

SPARC as a potential biomarker for patient response to 7rh and gemcitabine therapy.

4.2.2 7rh benzamide inhibits collagen-mediated signaling *in vivo*

The *in vitro* sensitivity assays of 7rh and gemcitabine in our panel of murine and human cell lines highlighted therapeutically attractive findings for the future use of 7rh combined with chemotherapeutic agents for therapeutic treatment. In order to initially assess the therapeutic window and tolerability of 7rh treatment a syngeneic orthotopic PDA model injected with the Pan02 murine PDA cell line was assessed. Prior pharmacokinetic studies (M. Gao et al., 2013) established the *in vivo* half-life of 7rh to be approximately 12 hours in rats. Therefore in these studies, mice bearing established orthotopic Pan02 pancreatic tumors were given a single dose of 0.1, 1, or 10 mg/kg of 7rh via oral gavage. Tumor tissue was collected 12 hours post-treatment and analyzed for Ddr1 activity. 7rh at 1 mg/kg and 10 mg/kg significantly reduced the phosphorylation of Ddr1 and downstream effectors Pyk2 and Peak1 as shown by immunohistochemical analysis (Figure 4.6, Table 6).

After demonstration that 7rh could reduce Ddr1 activity in the TME a following single agent therapy experiment was performed using a titration of 7rh for 2 weeks. A syngeneic orthotopic PDA model injected with the Pan02 murine PDA cell line was evaluated. Therapy was initiated 10 days post tumor cell

injection (TCI) and animals were treated for two weeks (until experiment day 21) with a titration of 7rh therapy (3.3, 10, or 30 mg/kg, 3x/week) (Figure 4.7, Table 6). At the end of the study animals were sacrificed and major organs and plasma collected for further analysis. 7rh treatment resulted in an increase in the presence of normal acinar tissue (amylase) (Figure 4.7 C-D), which depicted that 7rh inhibited tumor development and progression. This was correlated with histological analyses of pancreata which depicted a more normal pancreatic landscape in the presence of 7rh (Figure 4.7 C). Histological and immunohistological analysis of tissues demonstrated the significant inhibition of Ddr1 and Peak1 activation (Figure 4.7 D-E), as well as a reduction in proliferation (Pcna) (Figure 4.7 F) in a concentration-dependent manner. In addition to this data weight was monitored throughout the experiment and a metabolic study was conducted, both of which demonstrated the tolerability of 7rh treatment. Metabolites for proper physiological liver and kidney functions were evalauted including: Alb (albumin), Alt (liver transaminases), Ast (aspartate transaminase), Bun (blood urea nitrogen), Crea (creatine), Glu (glucose), Tbil (total bilirubin), and Tp (plasma total protein). No significant toxicity was reported (Figure 4.8).

These findings primarily demonstrated the ability of 7rh to inhibit the targets of interest (i.e. P-Ddr1 and P-Peak1) as well as demonstrate the tolerability of this compound *in vivo*. To evaluate a therapeutically useful concentration of 7rh a syngeneic orthotopic PDA model was treated with 7rh (25 mg/kg, 3x/week)

(Figure 4.9, Table 6). Therapy of the animals was initiated 19 days post tumor cell injection, once tumors were palpable, of a Pan02 cell line and was continued until day 40 of the experiment at which point the animals were sacrificed (Figure 4.9 A). 7rh therapy significantly reduced tumor weight as evidenced by histological analysis of pancreata tissue from these animals (Figure 4.9 B). This therapeutic advantage was depicted immunohistochemically through the enhanced presence of a more normal pancreatic landscape (H&E) and a significantly enhanced amount of Amylase expression, a marker of normal acinar tissue (Figure 4.9 C-D). 7rh demonstrated a reduction of Ddr1 phosphorylation and downstream signaling (P-Peak1 and P-Pyk2) (Figure 4.9 E-G), as well as an increase in apoptosis (Cleaved Caspase-3) and a reduction of proliferation (Pcna) (Figure 4.9 H-I). Ddr1 has been previously associated with the inhibition of apoptosis (Ongusaha et al., 2003) and these findings demonstrated a therapeutic implication of 7rh monotherapy (25 mg/kg).

4.2.3 7rh benzamide in combination with chemotherapy *in vivo*

To further assess the therapeutic utility of 7rh *in vivo* and model the findings that were noted from *in vitro* sensitivity assays (Figure 4.3, Figure 4.5), 7rh therapy was combined with the pancreatic cancer standard of care chemotherapy (gemcitabine and nab-paclitaxel) (Figure 4.10, Table 6). *In vitro*, the IC_{50} of 7rh (500 nM) synergistically enhanced the IC_{50} of gemcitabine in the

human PDA cell lines (Figure 4.3) as well as the murine PDA cell lines (Figure 4.5). To model these findings *in vivo* a xenograft model of AsPC-1 in NOD-SCID animals was utilized. Therapy of these animals began 27 days post tumor cell injection, once tumors were palpable and visible via ultrasound. Animals were treated with the 7rh vehicle, 7rh monotherapy (25 mg/kg, 3x/week), the standard of care regimen (chemo) including gemcitabine (15 mg/kg, 2x/week) plus nab-paclitaxel (5 mg/kg, 2x/week), or the combination (combo) of these three therapeutic agents (Figure 4.10 B-C, Table 7). The concentration of gemcitabine and nab-paclitaxel used in the *in vivo* experiments (30 mg/kg/week, 10 mg/kg/week, respectively) model similar concentrations used in the clinic (27 mg/kg/week, 3.4 mg/kg/week, respectively) (Table 7). Animals (n=12) were sacrificed at the start of therapy to evaluate the tumor burden at that point (initial group). Therapy of each regimen was continued until the individual animals became moribund, at which point the animals were sacrificed. The combination significantly enhanced the overall median of survival to 98 days, compared to chemotherapy, 7rh, or vehicle at 73, 57, and 54.5 days respectively. After the median survival was achieved for the combination group, therapy was withdrawn at day 102 to assess the consequence of therapy removal (withdrawn group). The 7rh, chemotherapy, and combination groups significantly reduced tumor weight according to time of individual sacrifice (Figure 4.10 D-E), though tumor growth

was restored and significantly larger in the withdrawn group. These findings highlighted the ability of the combination to inhibit tumor progression.

Enhanced presence of a more normal pancreatic landscape was noted through histological analyses of the 7rh, chemotherarpy, and combination treatment groups (Figure 4.11 A). Immunohistochemically, treatment with 7rh and chemotherapy significantly reduced the phosphorylation of DDR1, PEAK1, and PYK2 as well as the levels of the mesenchymal marker VIMENTIN and the tumorigenic marker PCNA (proliferating cell nuclear antigen), and this was more efficacious when treated with the combination regimen, and significantly enhanced in the withdrawn group (Figure 4.10 G-K, 4.11 B-F). Additionally, through immunohistochemical analysis the levels of apoptosis (CLEAVED CASPASE-3) and DNA damage (YH2AX) were significantly increased in the 7rh and chemotherapy groups, this was more efficacious when treated with the combination regimen, and this inhibition was significantly reversed in the withdrawn group (Figure 4.10 L-M, 4.11 G-H). Additionally, we noted that 7rh, chemotherapy, and the combination reduced trichrome staining (Figure 4.12). This is consistent with previous findings that DDR1 inhibition or loss reduces fibrosis (Avivi-Green et al., 2006; Gross et al., 2010). In addition to this data animal weight stability as well as a metabolic study was conducted to assess the tolerability of long-term treatment with 7rh monotherapy or in combination with the chemotherapy regimen. Metabolites for proper physiological liver and kidney

functions were evalauted including: Alb (albumin), Ast (aspartate transaminase), Crea (creatine), Glu (glucose), Tbil (total bilirubin), and Tp (plasma total protein). No significant toxicity was reported (Figure 4.13, Figure 4.14).

The therapeutic utility of the combination of 7rh with gemcitabine and nab-paclitaxel was further assessed in the *KPC (LSL-Kras$^{G12D/+}$; LSL-Trp53$^{R172H/+}$; p48$^{Cre/+}$)* genetic model of PDA (Figure 4.14, Table 4). Therapy was initiated at 4 months of age after tumor ultrasound for validation of tumor development. These animals were treated with the 7rh vehicle, 7rh monotherapy (25 mg/kg, 3x/week), the standard of care regimen including gemcitabine (15 mg/kg, 2x/week) plus nab-paclitaxel (5 mg/kg, 2x/week) (chemo), and the combination (combo) (Figure 4.14, Table 7). The concentration of gemcitabine and nab-paclitaxel used in the *in vivo* experiments model similar concentrations used in the clinic Table 7. Animals (n=9) were sacrificed at the start of therapy to evaluate the tumor burden at that point (initial group). Treatment with the combination regimen enhanced the median of survival to 208 days compared to treatment with chemotherapy, 7rh, or vehicle at 180, 159, and 144 days respectively (Figure 4.14 B-C). Treatment with 7rh and chemotherapy reduced tumor burden according to day of individual sacrifice/death, and this was significantly more efficacious when treated with the combination regimen (Figure 4.14 D-E). These findings corresponded to the enhanced presence of a more normal pancreatic landscape through histological analyses of the 7rh,

chemotherapy, and combination treatment groups (Figure 4.16 A). Analysis of the inhibition of collagen-mediated Ddr1 signaling immunohistochemically demonstrated that treatment with the combination was more efficacious at reducing the Ddr1 activation and downstream signaling, as well as the levels of the mesenchymal marker Vimentin and the tumorigenic marker Pcna (Figure 4.15 F-I, 4.16 B-E). Additionally, the levels of apoptosis (Cleaved Caspase-3) and DNA damage (YH2ax) were significantly increased in the 7rh and chemotherapy groups and this was more efficacious when treated with the combination regimen (Figure 4.15 J-K, Figure 4.16 F-G). Concurrent with our previous findings in the xenograft model, we noted that 7rh, chemotherapy, and the combination reduced trichrome staining (Figure 4.17) consistent with previous findings that DDR1 inhibition of loss reduces fibrosis (Avivi-Green et al., 2006; Gross et al., 2010). In addition to this data animal weight stability and a metabolic study was conducted to assess the tolerability of long-term treatment with 7rh monotherapy or in combination with the chemotherapy regimen. Metabolites for proper physiological liver and kidney functions were evalauted including: Alb (albumin), Ast (aspartate transaminase), Crea (creatine), Glu (glucose), Tbil (total bilirubin), and Tp (plasma total protein) (Figure 4.18, Figure 4.19). The data from this *in vivo* experiment highlight the therapeutic importance of the development of a multi-pronged approach to target pancreatic cancer.

In conclusion these findings have highlighted DDR1 inhibition by a small molecule inhibitor such as 7rh as a therapeutic avenue to enhance pancreatic cancer therapy and the patient outcome in combination with other chemotherapeutic agents (Figure 4.20).

4.3 Figures

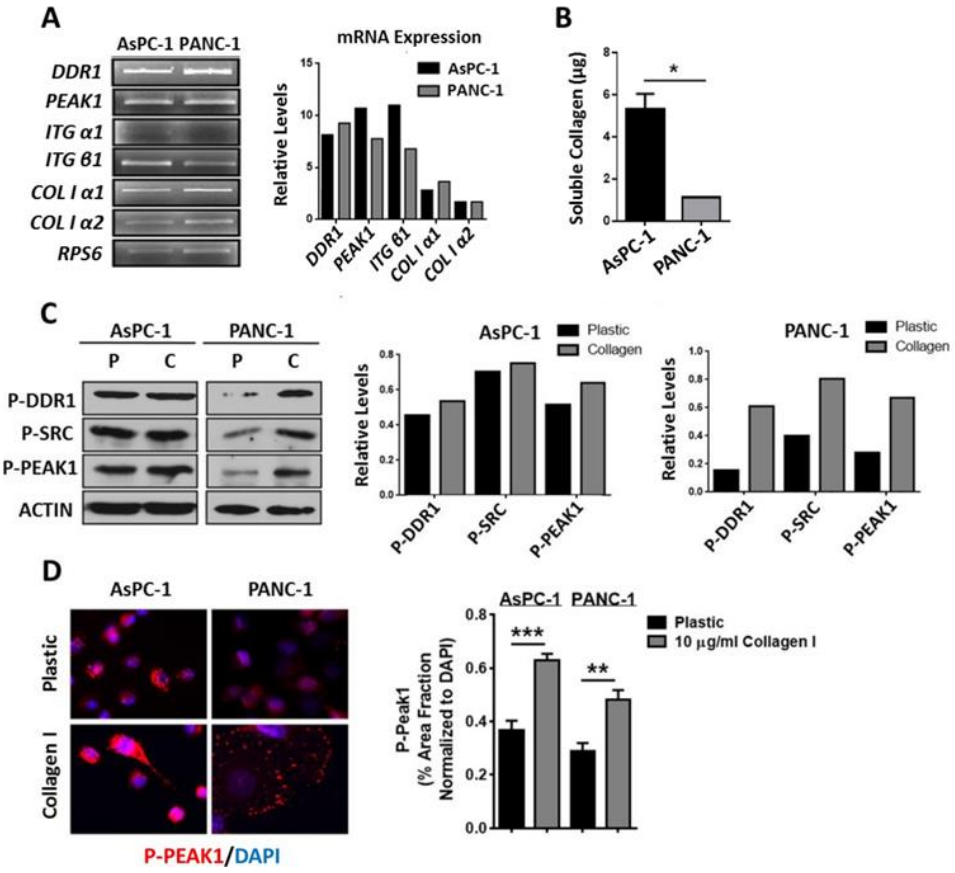

Figure 4.1: Human PDA cells expressed collagen receptors.

(A) Collagen receptor expression profile of human PDA cell lines (AsPC-1 and PANC-1). Each cell line expressed similar levels of *DDR1*, *PEAK1*, *INTEGRIN α1* (ITG α1), *INTEGRIN β1* (*ITG β1*), *COLLAGEN I α1* (*COL I α1*), and *COLLAGEN I α2* (*COL I α2*). PCR analysis was run for 30 cycles with respective primer sets. (B) Soluble collagen production assessed by Sircol^{TM} collagen assay of human PDA cell lines. (C) Human PDA cell lines were plated on plastic and stimulated with soluble collagen I (10 µg/ml) for 24 hours. Lysates were probed for the indicated targets by western blot analysis. (D) Human PDA cell lines were plated in the presence or absence of 10 µg/ml soluble collagen. The presence of soluble collagen enhanced the phosphorylation of PEAK1 via immunocytochemistry. Error bars: (*, $p < 0.05$; **, $p < 0.005$; ***, $p < 0.0005$; ****, $p < 0.00005$), one-way ANOVA with Tukey's MCT.

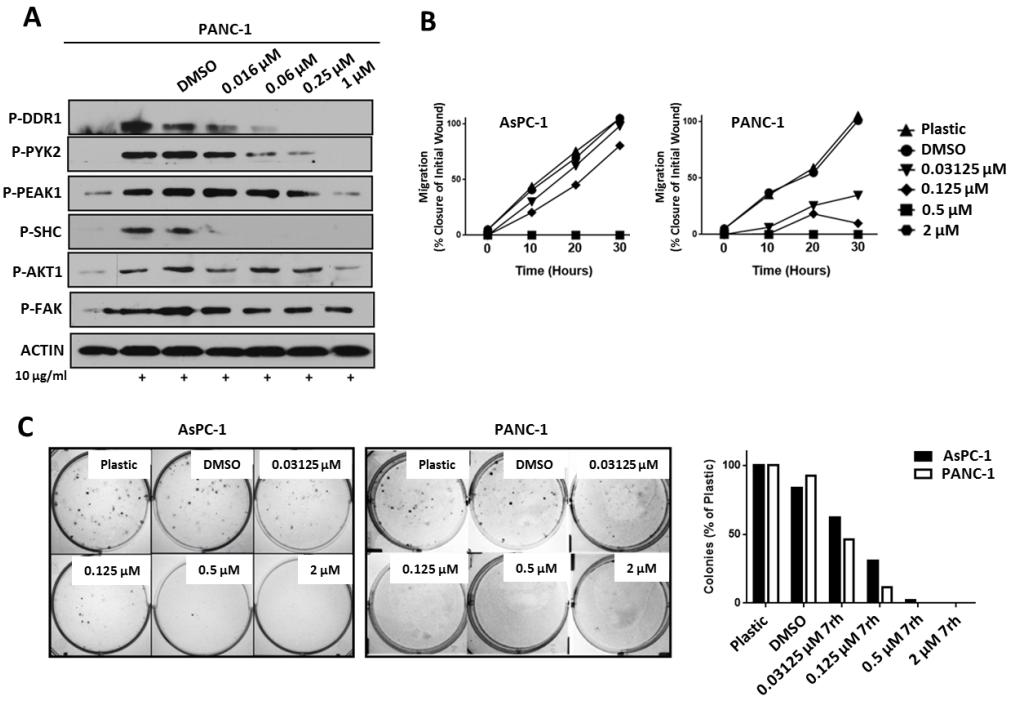

Figure 4.2: Signaling and functional consequences of DDR1 inhibition by 7rh in human PDA cell lines.

(A) 7rh inhibited DDR1-mediated signaling in a concentration dependent manner in human PDA cell line PANC-1. Cells were treated with 7rh for 24 hours. Lysates were probed for the indicated targets by western blot analysis. (B) 7rh inhibited migration of human PDA cell lines in a concentration-dependent manner via scratch migration assay. Cell migration was assessd over a 30 hour period. (C) 7rh inhibited liquid colony formation of human PDA cell lines in a concentration dependent manner. Liquid colony formation was assessed after 2 weeks of 7rh treatment. Concentrations used were 0.03125 µM, 0.125 µM, 0.5 µM, and 2 µM.

A

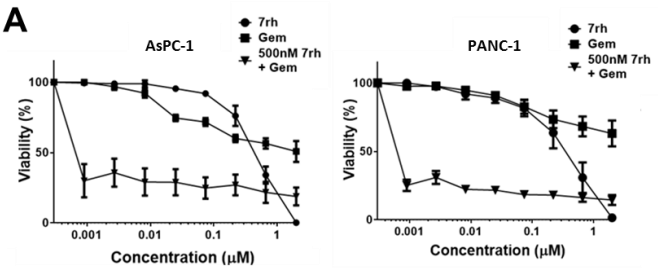

	AsPC-1	PANC-1
7rh (nM) Avg IC_{50}	490 (6)	380 (4)
Gemcitabine (nM) Avg IC_{50}	2000 (3)	2000 (4)
250 nM 7rh + Gem Avg IC_{50}	1725 (3)	16.4 (3)
500 nM 7rh + Gem Avg IC_{50}	2.05 (2)	0.035 (3)

B

	7rh (nM) Avg IC_{50}		Gemcitabine (nM) Avg IC_{50}		250 nM 7rh + Gem Avg IC_{50}		500 nM 7rh + Gem Avg IC_{50}	
Coating	Plastic (#)	Collagen (#)	Plastic (#)	Collagen (#)	Plastic (#)	Collagen (#)	Plastic (#)	Collagen (#)
ASPC-1	490 (6)	550 (6)	2000 (3)	2000 (3)	1725 (3)	2000 (4)	2.05 (2)	2.7 (2)
PANC-1	380 (4)	402 (4)	2000 (4)	2000 (3)	16.4 (3)	25.7 (3)	0.035 (3)	0.035 (3)

C

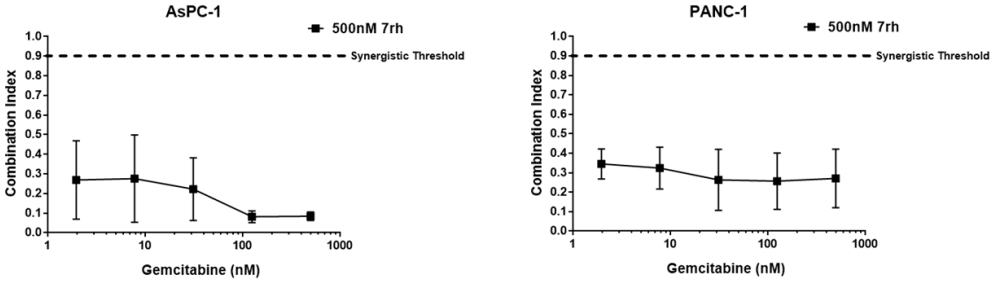

Figure 4.3: 7rh enhanced sensitization of human cell lines to gemcitabine.

(A) Sensitivity of human PDA cell lines (AsPC-1 and PANC-1) to gemcitabine and 7rh mono-treatment assessed by MTS viability assays. Drug sensitivity was assessed in the presence of 4-fold dilutions of each drug. Combination of constant concentrations of 7rh (250 nM or 500 nM) with a titration of gemcitabine enhanced therapeutic response. Drug sensitivity curves and IC_{50}s were calculated with in-house software (Dineen et al., 2010). (B) The IC_{50} of the cell lines for 7rh, gemcitabine, or the combinations, were shifted when plated on collagen I. (C) Synergy was calculated via CompuSyn Synergistical Analysis software (Chou, 2006) which demonstrated the therapeutic potential of this combination. A combination index (CI) less than 0.9 was considered synergistic relationship.

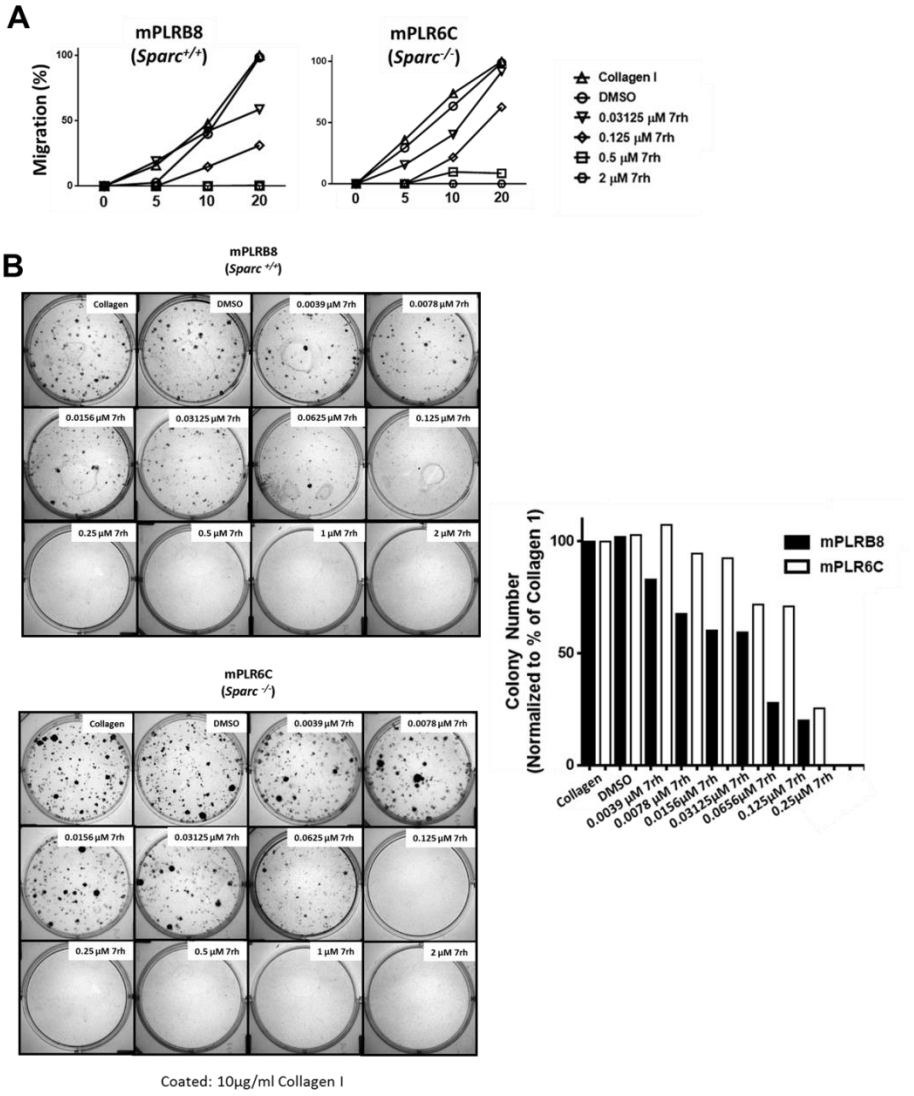

Figure 4.4: Functional consequences of DDR1 inhibition by 7rh in murine PDA cell lines.

(A) 7rh inhibited migration of murine PDA cell lines mPLRB8 (*Sparc*$^{+/+}$) and mPLR6C (*Sparc*$^{-/-}$) in a concentration-dependent manner via scratch migration assay. Cell migration was assessed over a 20 hour time period. Concentrations used were 0.03125 µM, 0.125 µM, 0.5 µM, and 2 µM. (B) 7rh inhibited liquid colony formation of murine PDA cell lines mPLRB8 (*Sparc*$^{+/+}$) and mPLR6C (*Sparc*$^{-/-}$) in a concentration dependent manner. Concentrations used were 0.0039 µM, 0.0078 µM, 0.0156 µM, 0.03125 µM, 0.0656 µM, 0.125 µM, 0. 25 µM, 0.5 µM, 1 µM, and 2 µM.

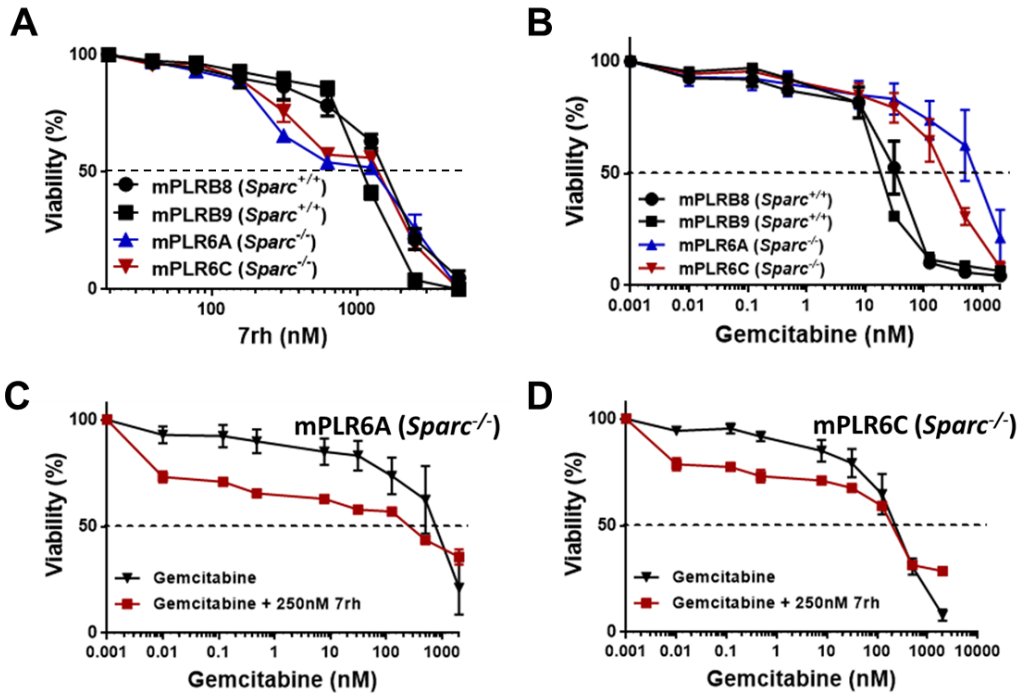

E

	Gemcitabine (nM) Avg IC_{50}	7rh (nM) Avg IC_{50}	250 nM 7rh + Gem Avg IC_{50}
mPLRB8	38.6 (5)	1525 (4)	n/a
mPLRB9	20.3 (4)	1175 (4)	n/a
mPLR6A	754 (5)	947.5 (4)	360 (2)
mPLR6C	285 (5)	1400 (6)	325 (2)

Figure 4.5: 7rh enhanced sensitization of *Sparc*$^{-/-}$ cell lines to gemcitabine.

(A) Sensitivity of murine PDA cell lines mPLRB8 (*Sparc*$^{+/+}$) and mPLR6C (*Sparc*$^{-/-}$) to gemcitabine and 7rh mono-treatment assessed by MTS viability assays. Drug sensitivity was assessed in the presence of 4-fold dilutions of each drug. Combination of constant concentrations of 7rh (250 nM) with a titration of gemcitabine enhanced therapeutic response. Drug sensitivity curves and IC_{50}s were calculated with in-house software (Dineen et al., 2010). Addition of 7rh + gemcitabine to *Sparc*$^{-/-}$ cell lines led to an enhanced therapeutic window compared to their sensitivity to gemcitabine alone.

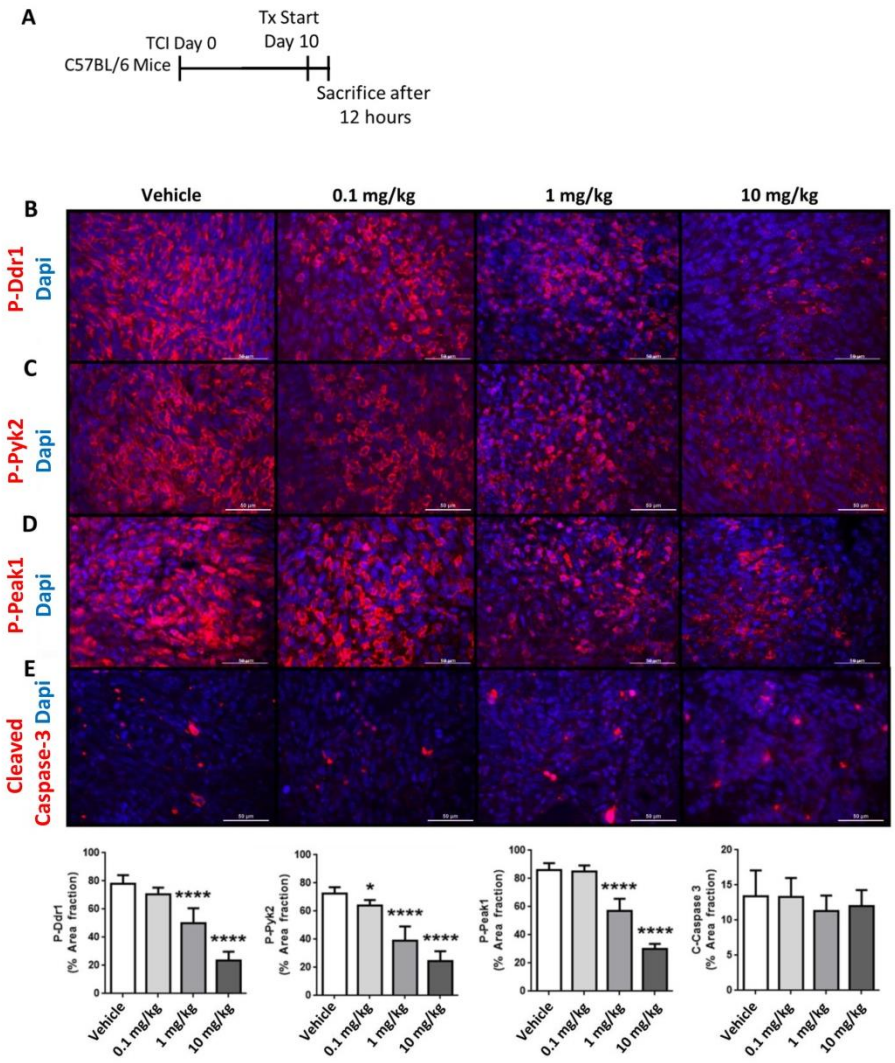

Figure 4.6: 7rh reduced collagen-mediated signaling in a concentration-dependent manner.

(A) Schematic representation of animal experiment. Mouse Pan02 cell line was orthotopically injected into *C57BL/6* mice and a one-time dose of 7rh (0.1, 1, or 10 mg/kg) on day 10 post-TCI. (B-D) Immunohistochemical analysis of tissue from each group depicted a concentration-dependent inhibition of Ddr1 activation and downstream signaling (P-Pyk2 and P-Peak1), as well a significant induction of apoptosis (Cleaved Caspase-3 (E)). Error bars: (*, $p < 0.05$; **, $p < 0.005$; ***, $p < 0.0005$; ****, $p < 0.00005$), one-way ANOVA with Tukey's MCT.

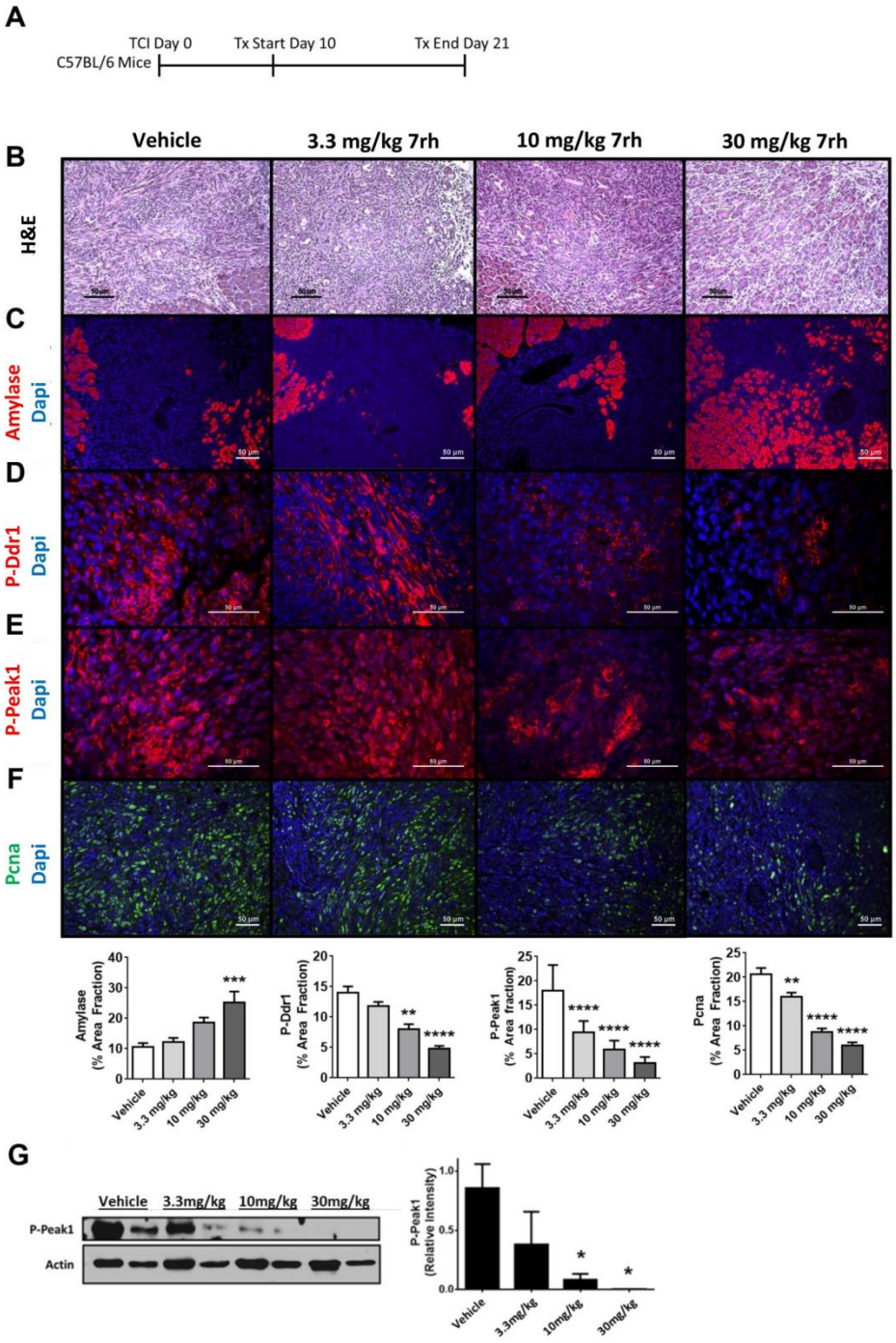

Figure 4.7: 7rh reduced collagen-mediated signaling in a concentration-dependent manner.

Figure 4.7: 7rh reduced collagen-mediated signaling in a concentration-dependent manner.

(A) Schematic representation of animal experiment. Mouse Pan02 cell line was orthotopically injected into *C57BL/6* mice and therapy with a titration of 7rh 3x/week started at day 10 and ended at day 21. (B-C) Histological and immunohistochemical analysis of tissue from each group depicted a concentration-dependent increase in the presence of normal pancreatic tissue (Amylase, C). This was correlated with the inhibition of Ddr1 activation and downstream signaling (P-Peak1) (D-E), as well as a decrease of proliferation (Pcna, F). (G) Protein lysates were generated from PDA tumors from this experiment and analyzed by western blot for the reduction of Ddr1 signaling (Peak1). Error bars: (*, $p < 0.05$; **, $p < 0.005$; ***, $p < 0.0005$; ****, $p < 0.00005$), one-way ANOVA with Tukey's MCT.

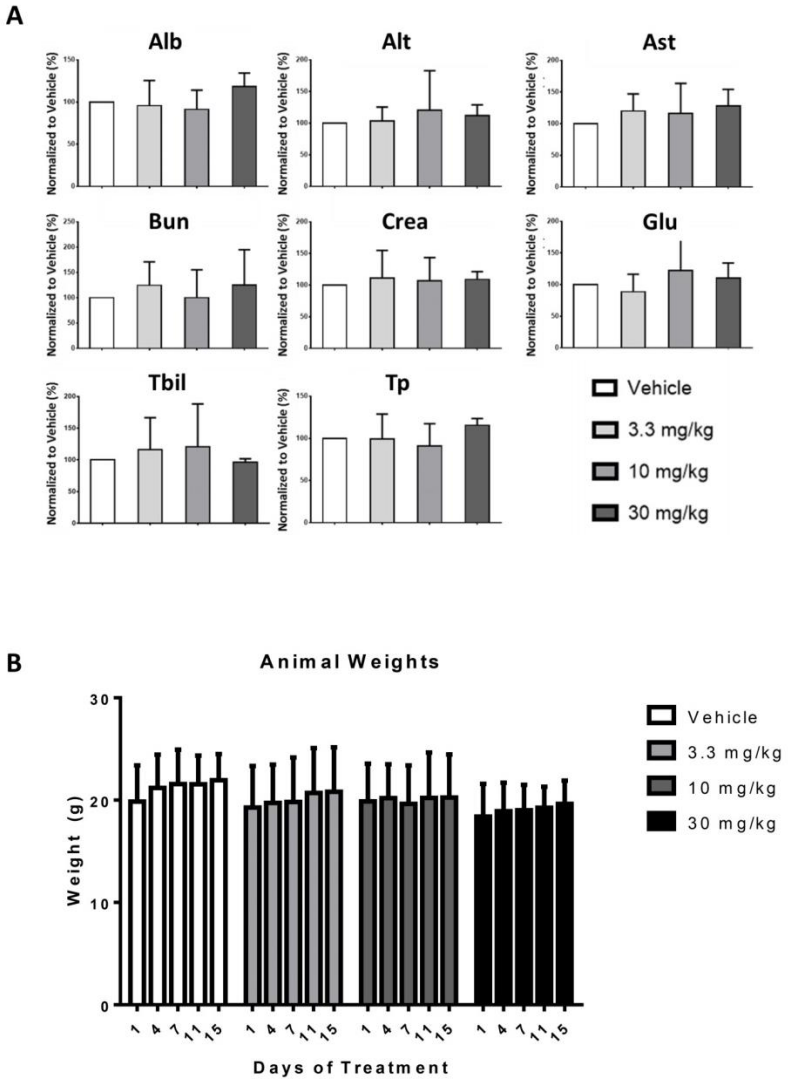

Figure 4.8: Assessment of 7rh tolerability.

Metabolic analysis of metabolites specific for proper liver and kidney function. Metabolites analyzed: Alb (albumin), Alt (liver transaminases), Ast (aspartate transaminase), Bun (blood urea nitrogen), Crea (creatine), Glu (glucose), Tbil (total bilirubin), and Tp (plasma total protein). (B) Animal weights were assessed at the dates indicated. Weights were stable throughout the length of treatment regimen, which indicated that there was no toxicity-related weight loss. Error bars: (*, $p < 0.05$; **, $p < 0.005$; ***, $p < 0.0005$; ****, $p < 0.00005$), one-way ANOVA with Tukey's MCT.

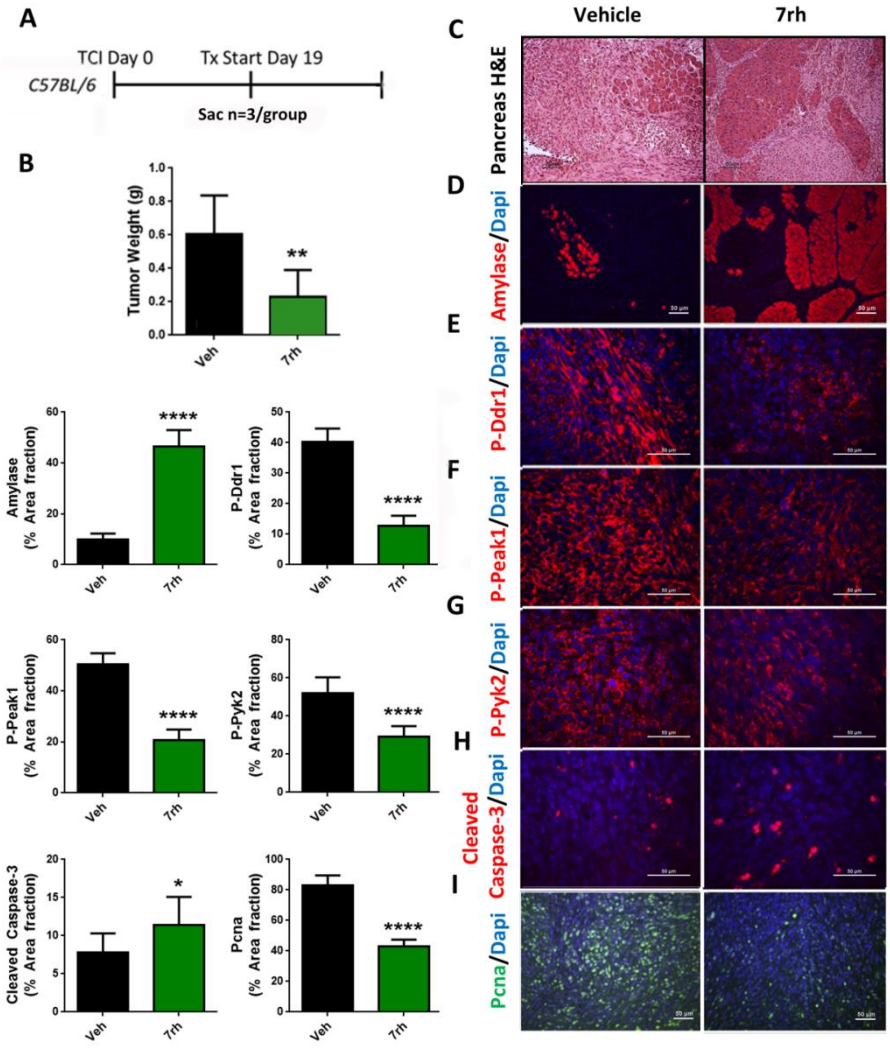

Figure 4.9: 7rh reduced Ddr1-mediated tumorigenicity and signaling.

(A) Schematic representation of animal experiment. Mouse Pan02 cell line was orthotopically injected into *C57BL/6* mice and 7rh therapy of 25 mg/kg 3x/week started at day 19 and ended at day 40. (B) 7rh treatment reduced tumor burden compared to vehicle, led to a greater presence of normal acinar tissue (C, D). (E-G) Immunohistochemical analysis of tissue from each group depicted inhibition of Ddr1 activation and downstream signaling (P-Peak1, P-Pyk2) which was correlated with enhanced apoptosis (Cleaved Caspase-3, H) and reduced proliferation (Pcna, I). Error bars: (*, $p < 0.05$; **, $p < 0.005$; ***, $p < 0.0005$; ****, $p < 0.00005$), one-way ANOVA with Tukey's MCT.

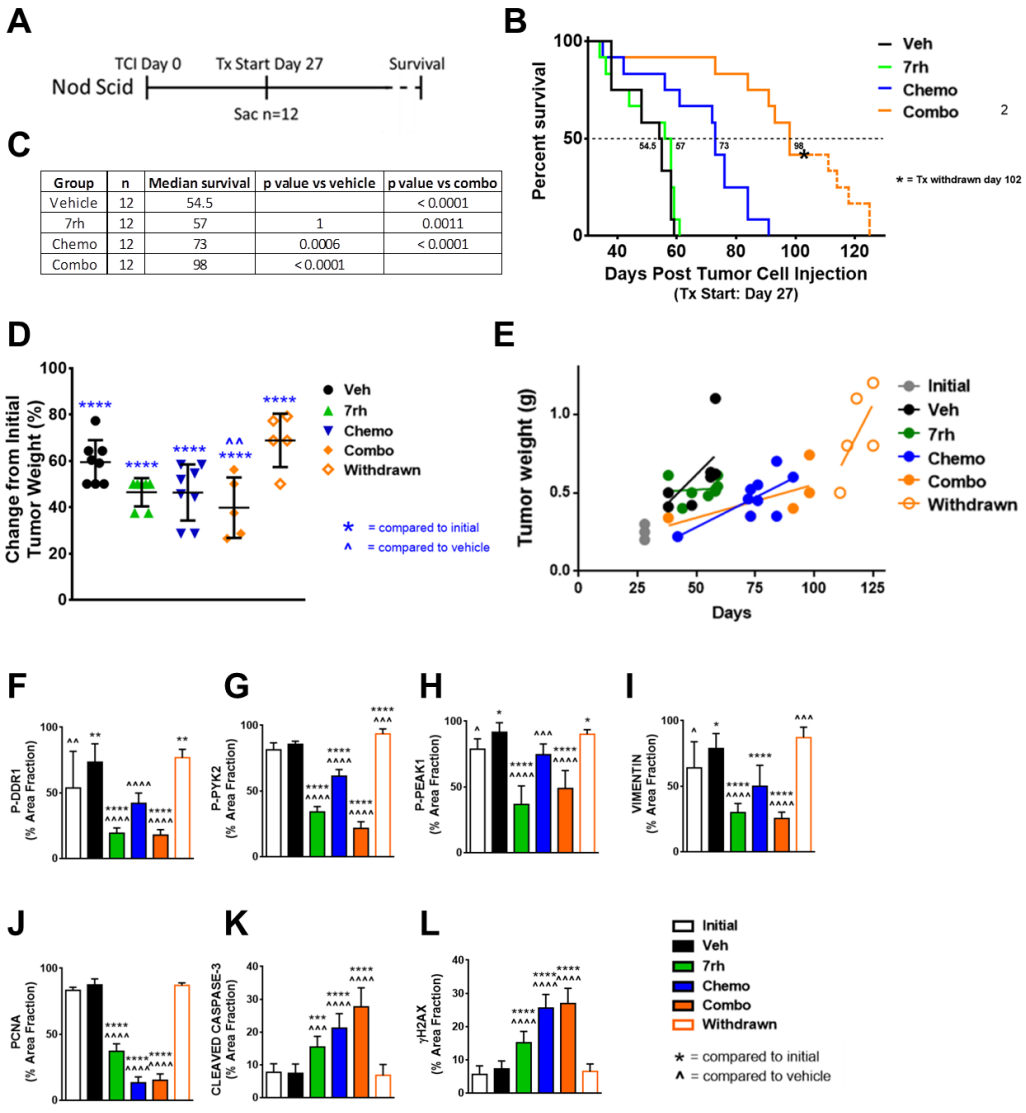

Group	n	Median survival	p value vs vehicle	p value vs combo
Vehicle	12	54.5		< 0.0001
7rh	12	57	1	0.0011
Chemo	12	73	0.0006	< 0.0001
Combo	12	98	< 0.0001	

Figure 4.10: 7rh in combination with chemotherapy reduced DDR1-mediated signaling and tumorigenicity in a PDA xenograft model.

Figure 4.10: 7rh in combination with chemotherapy reduced DDR1-mediated signaling and tumorigenicity in a PDA xenograft model.

(A) Schematic representation of animal experiment. Human AsPC-1 cell line was orthotopically injected into Nod Scid mice, therapy started at day 27 and ended as animals became moribund. Animals were treated with vehicle, 7rh (25 mg/kg, 3x/week), standard of care chemotherapy regimen including gemcitabine (15 mg/kg, 2x/week) plus nab-paclitaxel (5 mg/kg, 2x/week), or the combination of chemotherapy and 7rh. (B-C) The combination of 7rh plus chemotherapy significantly enhanced the overall median of survival compared to the other groups. (D-E) The combination reduced tumor burden. (E) Each animal's tumor weight was documented on the day of its sacrifice. (F-L) Immunohistochemical analysis of tissue from each group depicted that the combination more effectively inhibited DDR1 activation and downstream signaling (P-PYK2 and P-PEAK1) as well as levels of a mesenchymal marker (VIMENTIN, I), proliferation (PCNA, J), and enhanced apoptosis (CLEAVED CASPASE-3, K) and DNA damage (YH2AX, L) levels. Error bars: (*, $p < 0.05$; **, $p < 0.005$; ***, $p < 0.0005$; **** $p < 0.00005$) compared to the initial group; (^, $p < 0.05$; ^^, $p < 0.005$; ^^^, $p < 0.0005$; ^^^^, $p < 0.00005$) compared to the vehicle group, one-way ANOVA with Tukey's MCT.

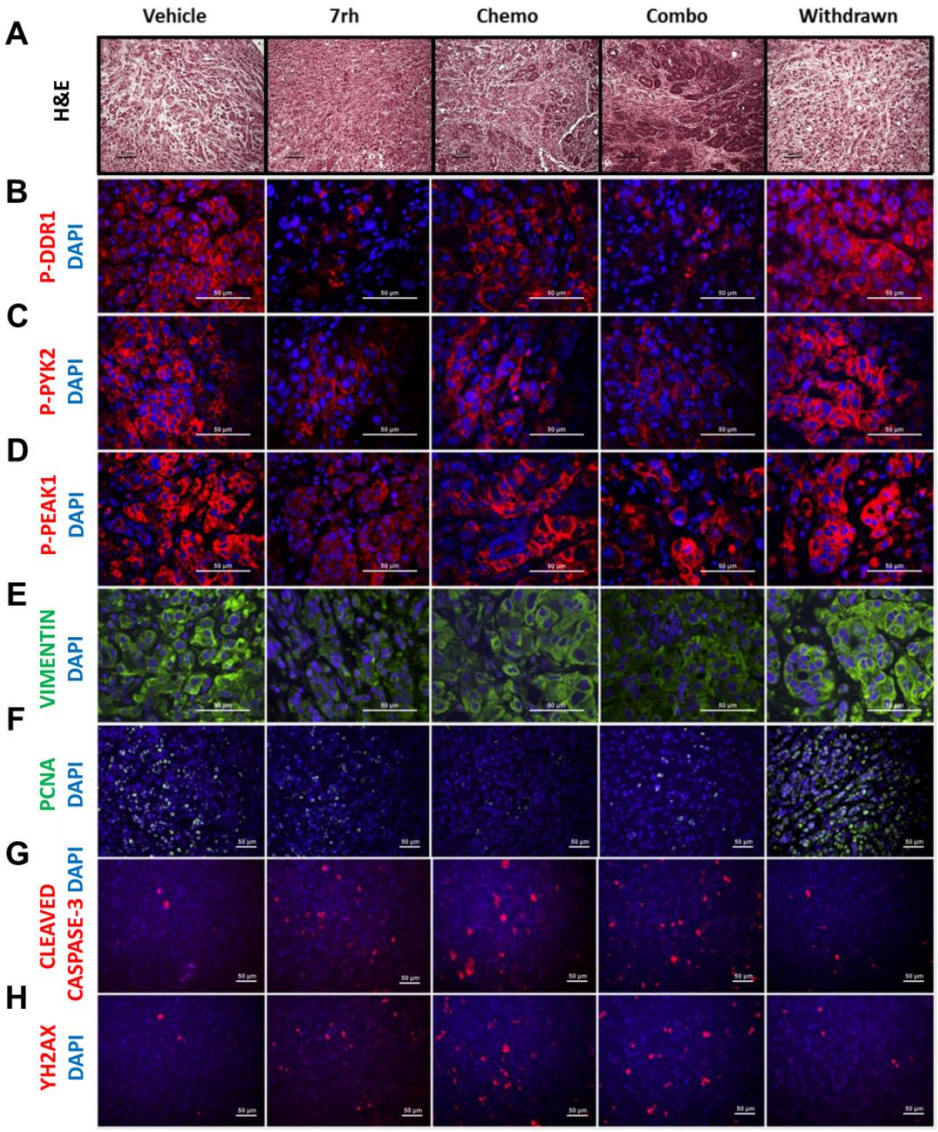

Figure 4.11: 7rh in combination with chemotherapy reduced DDR1-mediated signaling and tumorigenicity in a PDA xenograft model.

(A-H) Qualitative analysis from the xenograft (AsPC-1 cell line) PDA model experiment. Immunohistochemical analysis of tissue from each group depicted that the combination more effectively inhibited DDR1 activation and downstream signaling (P-PYK2 and P-PEAK1) as well as levels of a mesenchymal marker (VIMENTIN, I), proliferation (PCNA, J), and enhanced apoptosis (CLEAVED CASPASE-3, K) and DNA damage (YH2AX) levels.

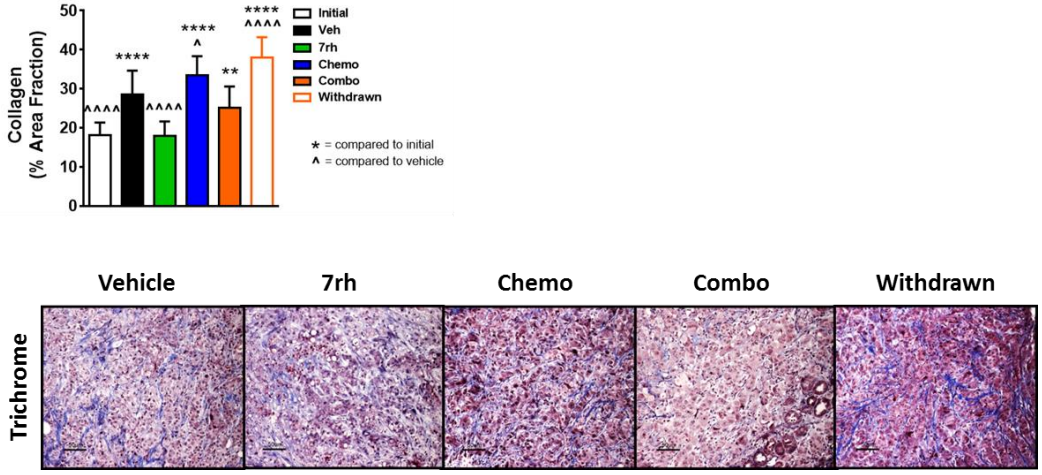

Figure 4.12: Reduction of collagen deposition with 7rh, chemotherapy, and the combination with chemotherapy.

Histological analysis by trichrome stain of tissues from the xenograft model of PDA treated with 7rh, chemotherapy (chemo), or the combination (combo). Reduction of collagen deposition according to the treatment regimen is noted. Error bars: (*, $p < 0.05$; **, $p < 0.005$; ***, $p < 0.0005$; **** $p < 0.00005$) compared to the initial group; (^, $p < 0.05$; ^^, $p < 0.005$; ^^^, $p < 0.0005$; ^^^^, $p < 0.00005$) compared to the vehicle group, one-way ANOVA with Tukey's MCT.

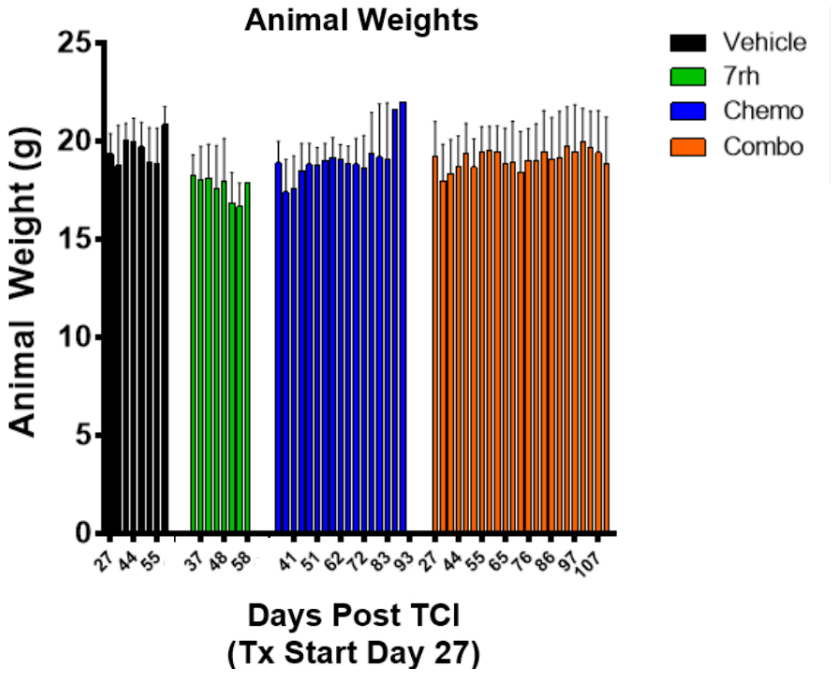

Figure 4.13: Assessment of drug regimen tolerability.

Animal weights were assessed at the dates indicated. Weights were stable throughout the length of the respective treatment regimens, which indicated that there was no toxicity-related weight loss.

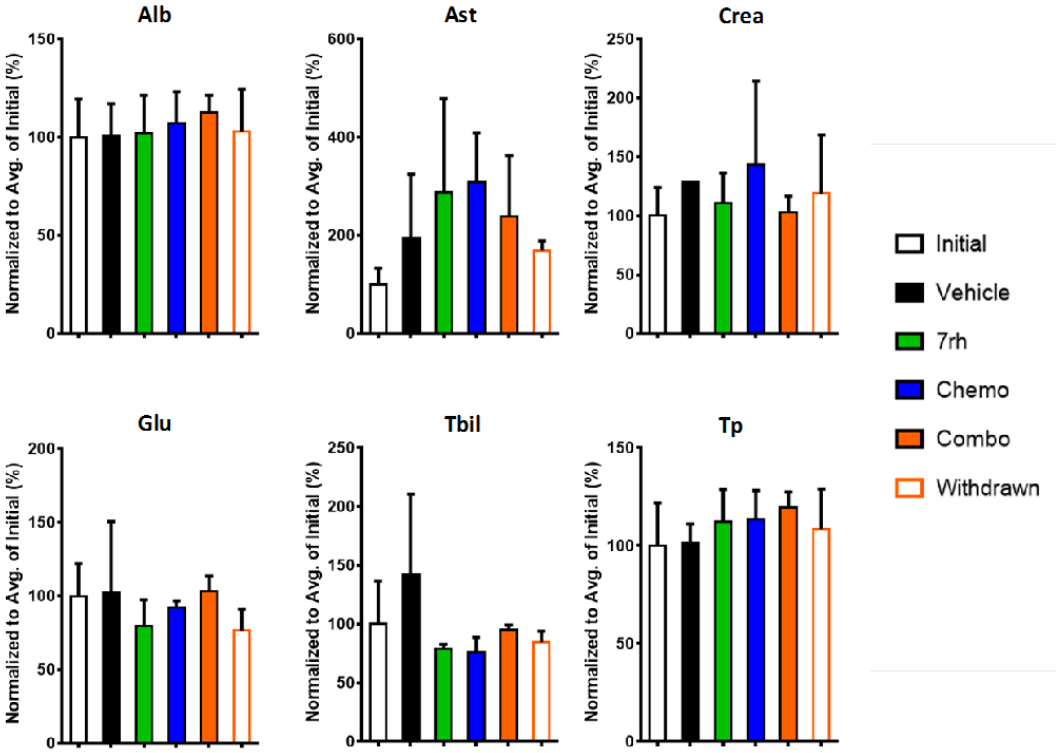

Figure 4.14: Metabolic analysis demonstrated tolerability of 7rh, chemotherapy, and combination regimen.

Metabolic analysis of metabolites specific for proper liver and kidney function. Metabolites analyzed: Alb (albumin), Ast (aspartate transaminase), Crea (creatine), Glu (glucose), Tbil (total bilirubin), and Tp (plasma total protein). Error bars: (*, $p < 0.05$; **, $p < 0.005$; ***, $p < 0.0005$; ****, $p < 0.00005$), one-way ANOVA with Tukey's MCT.

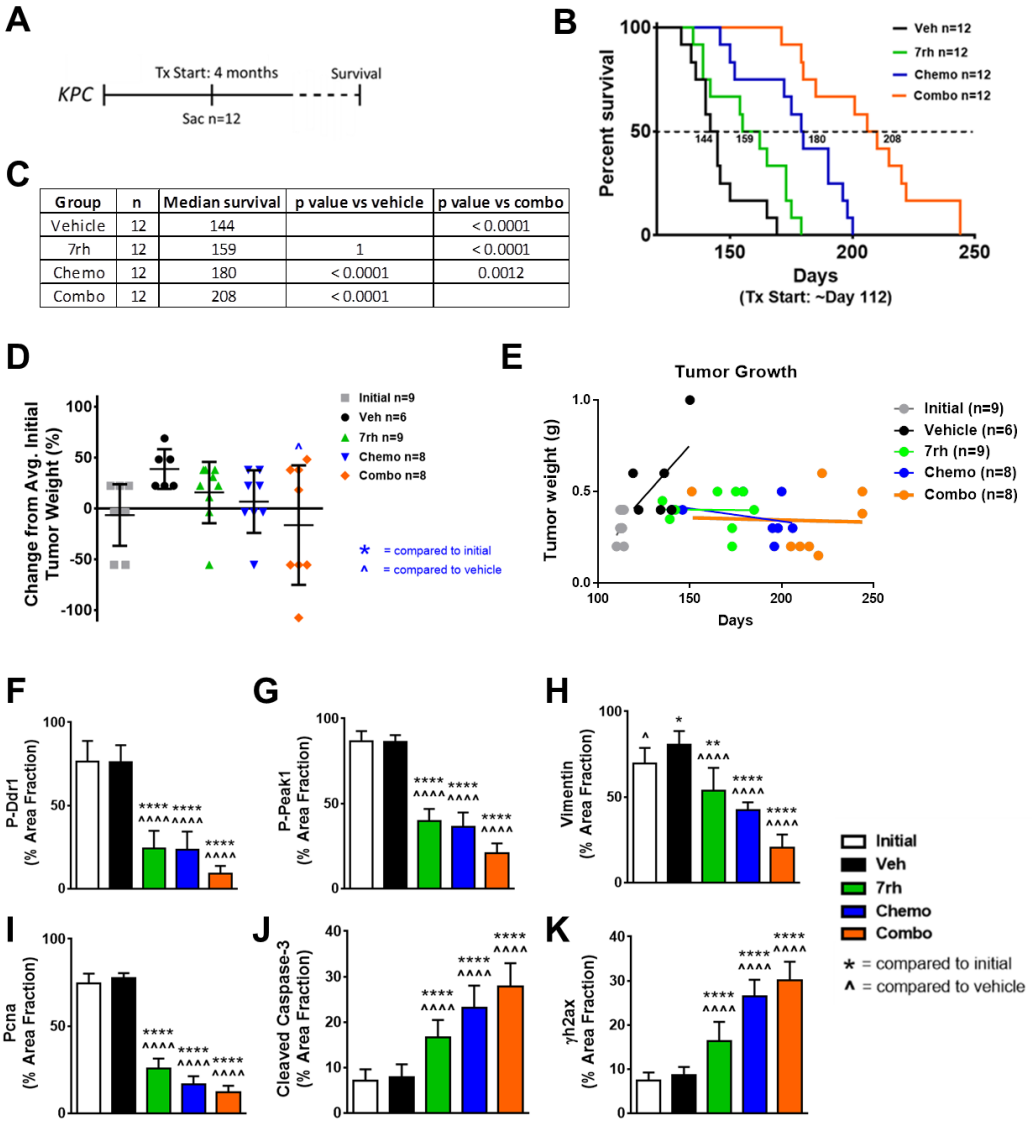

Figure 4.15: 7rh in combination with chemotherapy reduced DDR1-mediated signaling and tumorigenicity in a GEMM of PDA.

Figure 4.15: 7rh in combination with chemotherapy reduced DDR1-mediated signaling and tumorigenicity in a GEMM of PDA.

(A) Schematic representation of animal experiment. *KPC (LSL-Kras$^{G12D/+}$; LSL-Trp53$^{R172H/+}$; P48$^{Cre/+}$)* animal therapy started at 4 months of age and ended as animal became moribund. Animals were treated with vehicle, 7rh (25 mg/kg, 3x/week), standard of care chemotherapy regimen including gemcitabine (15 mg/kg, 2x/week) plus nab-paclitaxel (5 mg/kg, 2x/week), or the combination of chemotherapy and 7rh. (B-C) The combination of 7rh plus chemotherapy significantly enhanced the overall median of survival compared to the other groups. (D-E) The combination reduced tumor burden. (E) Each animal's tumor weight was documented on the day of its sacrifice. (F-K) Immunohistochemical analysis of tissue from each group depicted that the combination more effectively inhibited Ddr1 activation and downstream signaling (P-Peak1) as well as levels of a mesenchymal marker (Vimentin, H), proliferation (Pcna, I), and enhanced apoptosis (Cleaved Caspase-3, J) and DNA damage (yh2ax, K). Error bars: (*, $p < 0.05$; **, $p < 0.005$; ***, $p < 0.0005$; **** $p < 0.00005$) compared to the initial group; (^, $p < 0.05$; ^^, $p < 0.005$; ^^^, $p < 0.0005$; ^^^^, $p < 0.00005$) compared to the vehicle group, one-way ANOVA with Tukey's MCT.

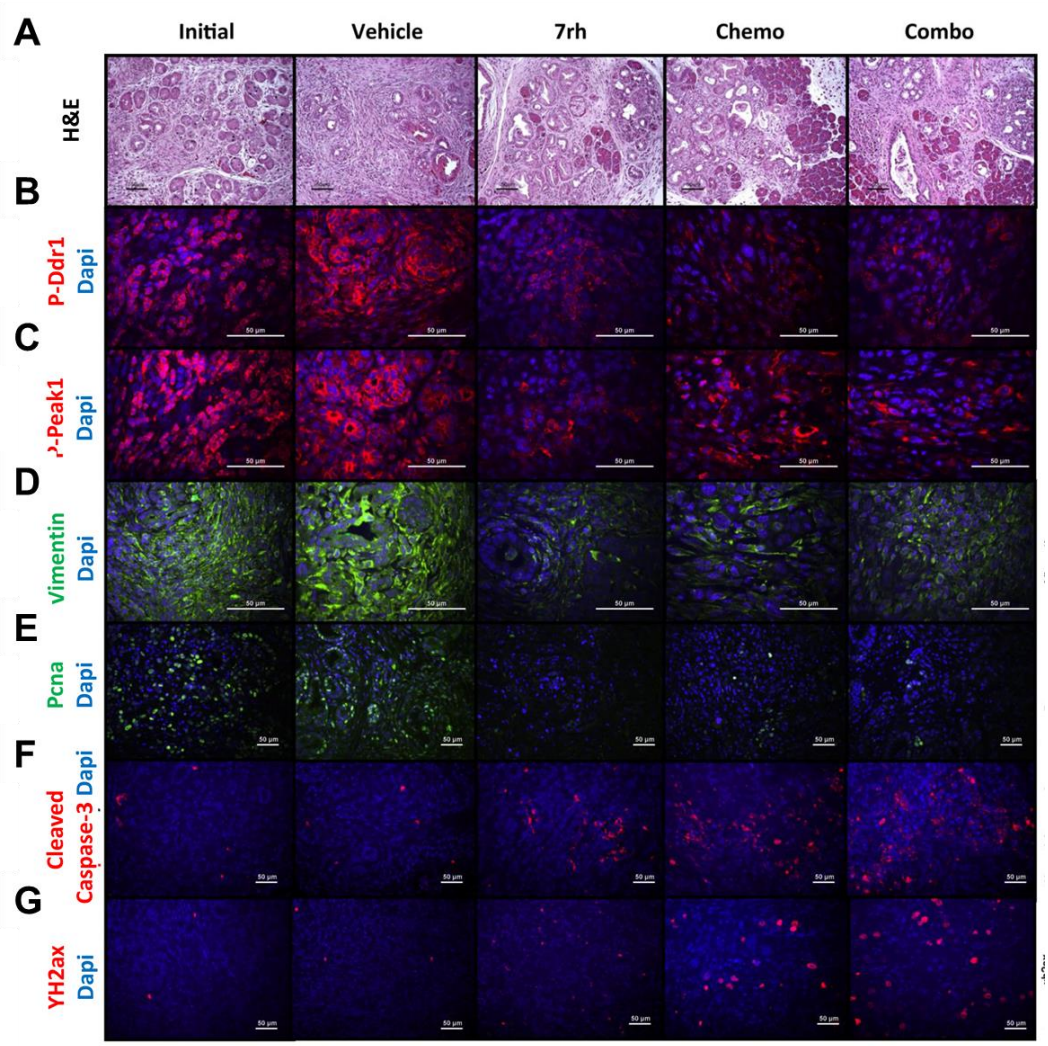

Figure 4.16: 7rh in combination with chemotherapy reduced DDR1-mediated signaling and tumorigenicity in a GEMM of PDA.

(A-G) Qualitative analysis from the *KPC (LSL-Kras$^{G12D/+}$; LSL-Trp53$^{R172H/+}$; P48$^{Cre/+}$)* experiment. Immunohistochemical analysis of tissue from each group depicted that the combination more effectively inhibited Ddr1 activation and downstream signaling (P-Peak1) as well as levels of a mesenchymal marker (Vimentin), proliferation (Pcna), and enhanced apoptosis (Cleaved Caspase-3) and DNA damage (yh2ax) levels.

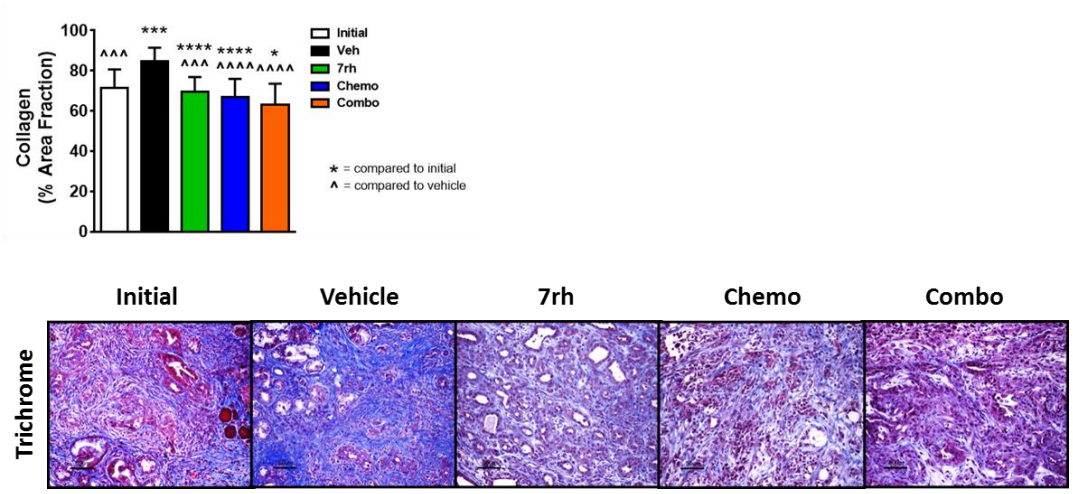

Figure 4.17: Reduction of collagen deposition with 7rh, chemotherapy, and in combination with chemotherapy.

Histological analysis by trichrome stain of tissues from the *KPC* GEMM of PDA treated with 7rh, chemotherapy, or the combination. Reduction of collagen deposition according to the treatment regimen is noted. Error bars: (*, $p < 0.05$; **, $p < 0.005$; ***, $p < 0.0005$; **** $p < 0.00005$) compared to the initial group; (^, $p < 0.05$; ^^, $p < 0.005$; ^^^, $p < 0.0005$; ^^^^, $p < 0.00005$) compared to the vehicle group, one-way ANOVA with Tukey's MCT.

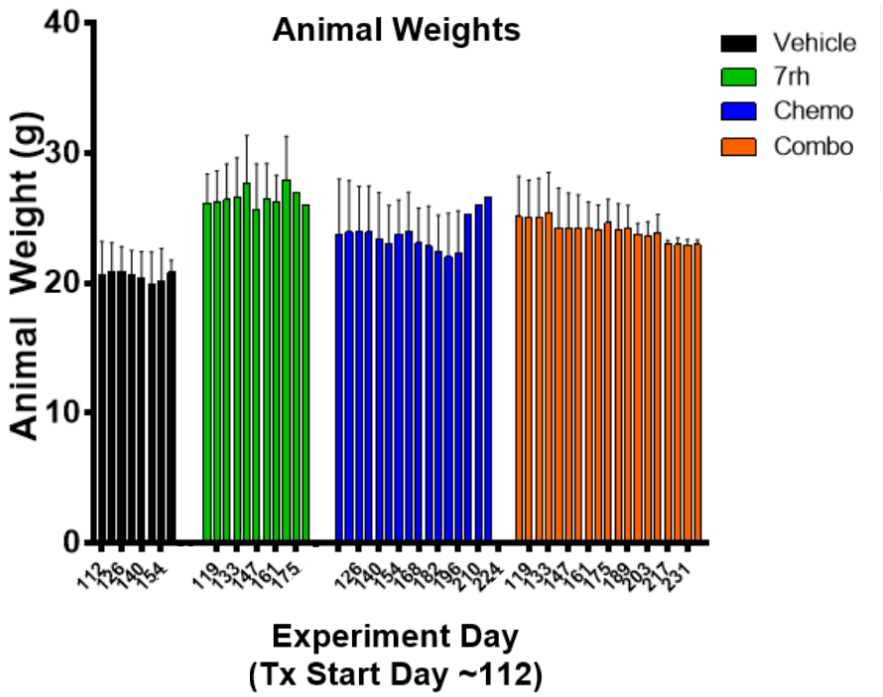

Figure 4.18: Assessment of drug regimen tolerability.

Animal weights were assessed at the dates indicated. Weights were stable throughout the length of the respective treatment regimens, which indicated that there was no toxicity-related weight loss.

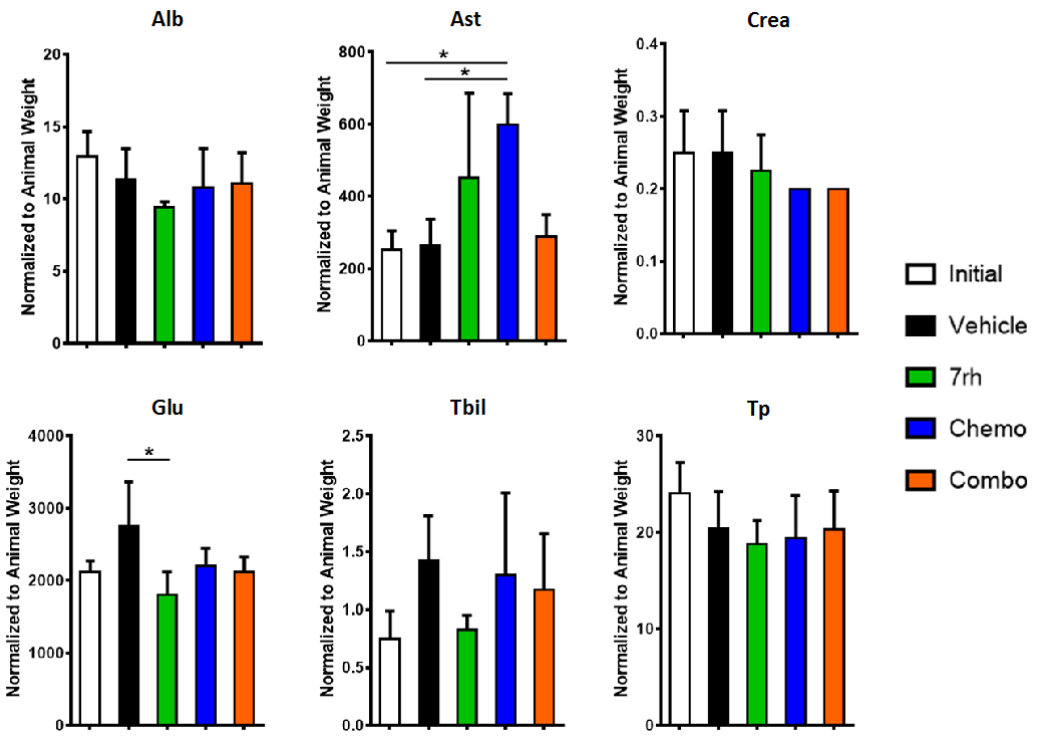

Figure 4.19: Metabolic analysis demonstrated tolerability of 7rh, chemotherapy, and combination regimen.

Metabolic analysis of metabolites specific for proper liver and kidney function. Metabolites analyzed: Alb (albumin), Ast (aspartate transaminase), Crea (creatine), Glu (glucose), Tbil (total bilirubin), and Tp (plasma total protein). Error bars: (*, $p < 0.05$; **, $p < 0.005$; ***, $p < 0.0005$; ****, $p < 0.00005$), one-way ANOVA with Tukey's MCT.

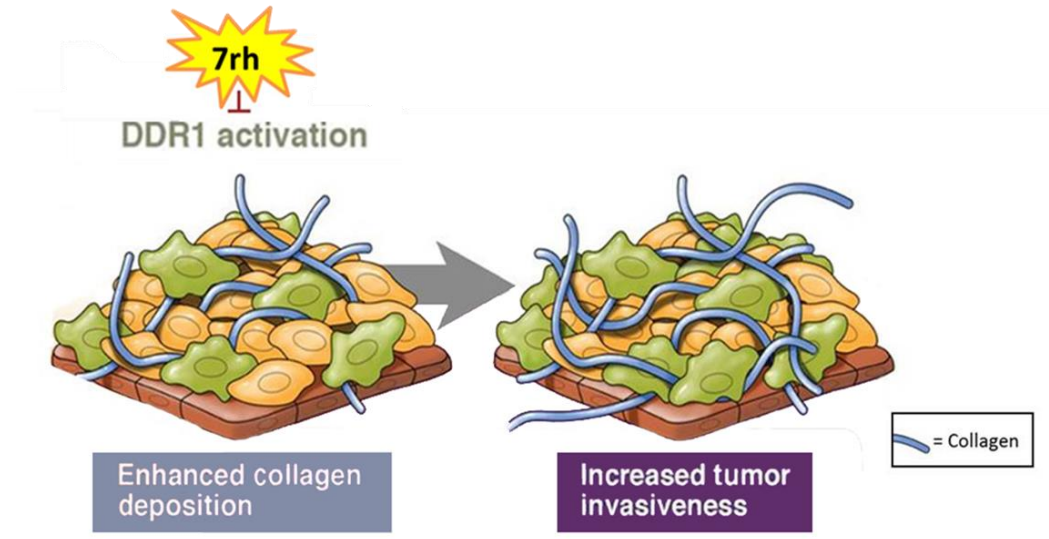

Figure 4.20: Schematic of 7rh-mediated inhibition of DDR1 in PDA.

Schematic representation which depicts the enhanced collagen deposition and increased tumor invasion in PDA and the inhibition of DDR1 by 7rh. Epithelial like tumor cells (gold color) adopt a mesenchymal-like phenotype (olive color), a process that is increased by elevated collagen signaling.

4.4 Discussion

The goal was to assess if changes in collagen deposition and DDR1 activation attenuated tumor response to therapy and contributed to PDA progression. DDR1 and downstream effectors were expressed and activated in human and mouse PDA samples and collagen signaling was important for *in vitro* measures of tumorigenesis. Additionally a novel small molecule inhibitor, 7rh benzamide (M. Gao et al., 2013), effectively abrogated DDR1 signaling and downstream activation, liquid colony tumor cell formation, tumor cell migration, and sensitized human PDA cell lines to chemotherapeutic compounds *in vitro* and *in vivo*. Further 7rh hit its target *in vivo* at doses that were free from observable normal tissue toxicity. Finally, 7rh significantly improved the efficacy of standard of care chemotherapy in robust mouse models of PDA. Moreover the data also highlighted *Sparc* as a biomarker for therapeutic response as the efficacies of 7rh were less effective in $Sparc^{-/-}$*; KIC* cell lines compared to $Sparc^{+/+}$*; KIC* cell lines.

I previously found that the matricellular protein Sparc (secreted protein acidic and rich in cysteine) reduced collagen I signaling through Ddr1 and that loss of *Sparc* accelerated PDA progression with a concordant increase in Ddr1 signaling (Aguilera et al., 2014). Additionally, it was reported that restoration of *SPARC* expression enhanced radiosensitivity and chemosensitivity in pre-clinical models of colon cancer (Tai et al., 2005) and that *SPARC* expression enhanced chemoresponse in cancer patients (Lindner et al., 2015; D. D. Von Hoff et al.,

2011). Thus there was compelling evidence that loss of tumor cell expression of *SPARC* correlated with tumor progression and poor chemoresponse. Moreover, these findings highlighted that collagen signaling through DDR1 is a critical feature in the response of PDA to therapy.

This data has further highlighted the implication of the combination of the 7rh small molecule inhibitor with standard chemotherapeutic regimens *in vivo* as 7rh monotherapy did not elicit a survival advantage (Figure 4.10, Figure 4.15). This may be due in part to the inability of the 7rh dose (25 mg/kg, 3x/week) to elicit a survival advantage. However, Dr. Zhang and colleagues at the Gastric Cancer Center of Sun Yat-sen University in China have collaboratively demonstrated a survival benefit in tumor-bearing mice treated with 7rh monotherapy at 100 mg/kg, 5x/week for 2 weeks. As no toxicities have been previously reported or observed at 25 mg/kg 3x/week over an extended period of time, 100 mg/kg may be tolerable for long-term monotherapy and this merits future exploration. Alternatively, the inability of 7rh monotherapy (25 mg/kg, 3x/week) to elicit a survival advantage may be due to the reduced efficacy of hitting the targets and tumorigenic markers compared to the chemotherapy regimen (gemcitabine plus nab-paclitaxel). Moreover, the inability of 7rh monotherapy to elicit a survival advantage is negligible as the efficacy of the combination regimen in the human xenograft (Figure 4.10) as well as *KPC* GEMM (Figure 4.15) of PDA has exemplified an additive effect of the treatment

regimen. Moreover, this has confirmed that DDR1 blockade in combination with chemotherapeutic agents is promising.

Reports have demonstrated that DDR1 inhibition was linked to reduced tumorigenicity (Kim, Hwang, Aaronson, Mandinova, & Lee, 2011; Y. Li et al., 2015; Sheppard et al., 2012; Shintani et al., 2008; Valencia et al., 2012). Other studies have also demonstrated that high expression levels and/or mutations of DDR1 were frequently detected in multiple cancer cell lines and primary tumor tissues from pancreas (Couvelard et al., 2006), lung (Ding et al., 2008; Miao et al., 2013; Rikova et al., 2007), breast (Barker et al., 1995), and others (Chiaretti et al., 2005; Heinzelmann-Schwarz et al., 2004; Jian et al., 2012; Shimada et al., 2008; Squire et al., 2002; Weiner et al., 1996). Additionally, we have recently reported that DDR1 expression and activity correlated with worse outcome in a large cohort of gastric cancer patients (Hur H, et al submitted). In this study we also found that 7rh-mediated inhibition of DDR1 in gastric cancer cells reduced tumorigenic characteristics *in vitro* and tumor growth *in vivo* (H. Hur et al., 2015, submitted).

Several small molecule inhibitors (imatinib, nilotinib and dasatinib) that were originally developed to target the activity of the Breakpoint Cluster Region-Abelson kinase (Bcr-Abl) also potently inhibited DDR1/DDR2 activity (Day et al., 2008; Rix et al., 2007). Thus, the potential activity of imatinib and vinorelbine in a phase I/II trial in metastatic breast cancer patients (Maass et al., 2014), as

well as dasatinib in numerous clinical trials in solid tumors (Roskoski, 2015), could be due in part to the inhibition of DDRs. Dasatinib in particular demonstrated promising therapeutic efficacy in lung cancer cells which harbored gain-of-function mutations of DDR2 (Ding et al., 2008). Previous studies of two squamous cell carcinoma (SCC) patients with a $DDR2^{S768R}$ mutation were shown to have significant shrinkage of their tumors after dasatinib treatment (Pitini et al., 2013).

While a clinical agent specific for DDR1 is not yet available the data presented here suggested that inhibition of collagen-mediated DDR1 activity can improve the efficacy of standard chemotherapy in pre-clinical models of pancreatic cancer. Critical questions regarding the contribution of DDR1 to tumor progression remain including whether the results will extend to other solid tumors (e.g., lung, breast, gastric), and this will be discussed in the next chapter. Further it is unclear whether responses to DDR1 inhibition will be limited to those tumors that present with extensive stromal deposition, or as suggested by *in vitro* data with AsPC-1 cells, tumor cell production of collagen is critical to DDR1 activation on tumor cells. Addressing these questions is now feasible with the development of highly selective DDR1 inhibitors such as 7rh.

CHAPTER FIVE

Discussion and Future Directions

CHAPTER FIVE

Discussion and Future Directions

5.1 Summary

PDA results in almost a quarter million deaths worldwide every year (Kelber & Klemke, 2010). In the United States, approximately 90% of patients diagnosed with PDA present with metastatic disease and have a median survival of less than one year (Croucher et al., 2013). Moreover, due to the poor prognosis and poor response to therapy, pancreatic cancer is projected to become the second leading cause of cancer-related death in the United States by the year 2030 (Rahib et al., 2014).

Therapy has yet to advance as the patient survival rates and median survival values have not improved over the last decades. Additionally, patients that undergo potentially curative tumor resections succumb to recurring disease and death within the first 2 years; this is due in part to chemoresistance. This has highlighted the pressing need for better therapeutic targets and strategies. Resistance to therapy can arise through a multitude of mechanisms; however, physiological chemoresistance results from the accumulation of ECM proteins in the tumor microenvironment, which is a common characteristic of PDA.

Ultimately I demonstrated the function of a matricellular protein, Sparc, in the regulation of collagen-mediated Ddr1 activation. PDA tumors grown in

Sparc$^{-/-}$ mice exhibited increased collagen signaling and enhanced disease progression, and the loss of *Sparc* expression *in vitro* reduced the sensitivity of PDA cell lines to therapeutic agents. I identified that collagen signaling mediated through Ddr1 stimulated pro-tumorigenic downstream signaling through effectors such as protein tyrosine kinase 2 (Pyk2) and pseudopodium-enriched atypical kinase 1 (Peak1) and this was more pronounced in the absence of *Sparc*. The biology of PEAK1 is not well understood. Other reports suggested that PEAK1 activation led to enhanced tumorigenesis in colon and PDA cancer models and that it may be Src-dependent (Grzesiak et al., 2007; Olive et al., 2009), which fit PEAK1 into the DDR1 signaling cascade. Activation of PEAK1 might be an appropriate marker of collagen-mediated signaling in solid tumors that can be assayed as novel DDR1 inhibitors are tested *in vivo*. My findings ultimately supported that collagen enhanced PDA tumorigenicity through DDR1 and highlighted *SPARC* as a biomarker for patient response.

Reports have demonstrated the difficulty of therapeutically targeting DDR1 either *in vitro* or *in vivo* due to the unspecific nature of currently available inhibitors including imatinib (also known as STI-571 or Gleevec), dasatinib, nilotinib, and bafetinib (also known as INNO-406) (Day et al., 2008; Y. Li et al., 2015; Rix et al., 2007) (Figure 1.5). The utility of these inhibitors has demonstrated potentially therapeutic evidence, though the off-target effects and pharmacokinetics of these compounds deem them unfavorable. Furthermore due

to the evidence that targeting DDR1 presented therapeutic potential I explored the utility of a novel small molecule inhibitor with high specificity towards DDR1, known as 3-(2-(Pyrazolo[1,5-a]pyrimidin-6-yl)-ethynyl) benzamide 7rh (7rh).

7rh benzamide effectively abrogated DDR1 signaling and downstream activation, liquid colony tumor cell formation, tumor cell migration, and sensitized human PDA cell lines to chemotherapeutic compounds *in vitro* and *in vivo*. In summary, my findings demonstrated that collagen signaling enhanced PDA and promoted tumorigenicity of a subset of PDA cells through the promotion of collagen production and stimulation of DDR1. Moreover, collagen signaling through DDR1 is a critical feature in the response of PDA to therapy.

5.2 Future targeting of DDR1

The remarkable efficacy of the 7rh small molecule inhibitor *in vitro* and its sensitization of the standard of care PDA regimens both *in vitro* and *in vivo* highlighted DDR1 as a crucial therapeutic target in the enhancement of overall PDA survival in combination with standard of care chemotherapeutic agents. The future evaluation DDR1 as a therapeutic target includes the continued understanding of DDR1-targeted therapy, the assessment of other novel DDR1 small molecule inhibitors, the efficacy of DDR1 inhibitors in different cancer model systems, and the utility of DDR1 blockade in other diseases.

5.2.1 Assessment of novel DDR1 small molecule inhibitors

Future exploration of DDR1 inhibition on tumor biology includes the development of other novel small molecule inhibitors. Dr. Ke Ding and colleagues have recently generated three novel DDR1 inhibitors, D2202, D2159, and D2197 (unpublished), that I have recently obtained. Inhibitor D2159 is a derivative of 7rh, while D2202 and D2197 harbor a novel scaffold different from 7rh (unpublished). These small molecule inhibitors have displayed similar specificities for DDR1 over other related kinases. The specificity of 7rh and the other three compounds for DDR1 by cell-free kinase assays is 6.8 nM, 19.4 nM, 21.6 nM, and 25.6 nM, respectively (Figure 5.1 A). Preliminary pharmacokinetic studies conducted by Dr. Ke Ding and colleagues (unpublished) for D2159 have suggested its use *in vivo* with a $T_{1/2}$ of 8.2 hours and a bioavailability of 82.3 %, compared to 7rh with a $T_{1/2}$ of 15.53 hours and a bioavailability of 67.4 % (M. Gao et al., 2013).

Through the utilization of the median IC_{50} between DDR1 and DDR2 for D2202 (226 nM), D2159 (172 nM), and D2197 (315 nM), each of these inhibitors reduced the phosphorylation of DDR1 signaling effectors (including DDR1, PYK2, P130CAS, SRC, and PEAK1) (Figure 5.1 B). Importantly, these compounds did not affect the activation of focal adhesion kinase (FAK), an effector that has not been previously associated with DDR1-induced signaling (Shintani et al., 2008).

The sensitivity of human PDA cell lines (AsPC-1 and PANC-1) to 7rh, D2202, D2159, or D2197 treatment was assessed by MTS viability assays in the presence of 4-fold dilutions of each drug (Figure 5.1 C). Drug sensitivity curves and IC_{50}s were calculated with in-house software (Dineen et al., 2010). AsPC-1 was more sensitive to 7rh compared to the other three compounds, while PANC-1 was similarly sensitive to 7rh, D2202, and D2197. The IC_{50} of each compound (D2202= 500 nM, D2159 = 900 nM, and D2197= 530 nM) was combined with a titration of gemcitabine and the combination with D2202 enhanced the sensitivity to gemcitabine compared to the other two compounds (Figure 5.1 D).

Functionally, each of the three compounds comparably reduced migratory function in a human PDA cell line (PANC-1) (Figure 5.2) as well as liquid colony formation (Figure 5.3). Furthermore, 7rh was more efficacious in comparison to the three novel compounds. D2202 merits future exploration compared to D2159 and D2197 as it depicted a more efficacious inhibition DDR1 signaling as well as sensitization of PANC-1 to gemcitabine.

5.2.1.1 Figures

A

Compound ID	Kinase Inhibition (IC_{50}s, nM)			
	DDR1	DDR2	Bcr-Abl	c-Kit
7rh	6.8	101.4	355	>10uM
D2202	19.4	432	7.2uM	>10uM
D2159	21.6	322	5.1uM	>10uM
D2197	25.6	604	>10uM	>10uM

B

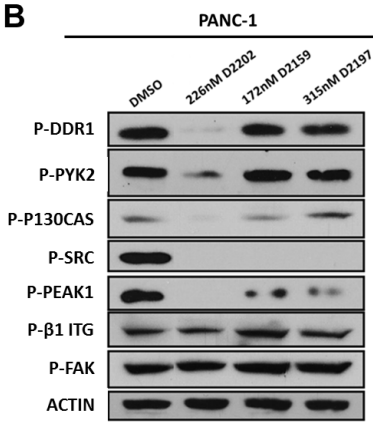

C

	AsPC-1	PANC-1
Gemcitabine (nM) Avg IC_{50}	> 2000 (3)	> 2000 (4)
7rh (nM) Avg IC_{50}	490 (3)	380 (3)
D2202 (nM) Avg IC_{50}	1733 (3)	443 (3)
D2159 (nM) Avg IC_{50}	983 (3)	896 (3)
D2197 (nM) Avg IC_{50}	2767 (3)	533 (3)

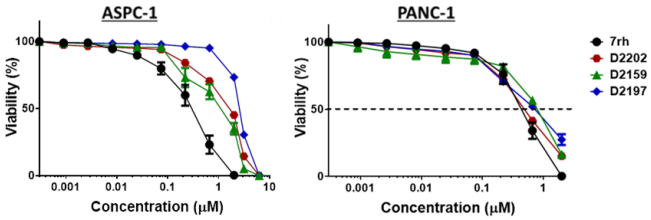

D

	D2202 (nM) Avg IC_{50}	500 nM D2202 + Gem Avg IC_{50}	D2159 (nM) Avg IC_{50}	900 nM D2159 + Gem Avg IC_{50}	D2197 (nM) Avg IC_{50}	530 nM D2197 + Gem Avg IC_{50}
PANC-1	443 (3)	> 2000 (3)	896 (3)	217.5 (2)	533 (3)	> 2000 (3)

Figure 5.1: Evaluation of DDR1-specific small molecule inhibitors: 7rh, D2202, D2159, and D2197.

(A) Cell-free (M. Gao et al., 2013) kinase inhibition assay IC_{50} values for DDR1 inhibitors: 7rh, D2202, D2159, and D2197. (B) DDR1 inhibitors, 7rh, D2202, D2159, and D2197, reduced collagen-mediated signaling in a human PDA cell line (PANC-1). Lysates were probed for the indicated targets by western blot analysis. (C) Sensitivity of human PDA cell lines (AsPC-1 and PANC-1) to 7rh, D2202, D2159, or D2197 treatment assessed by MTS viability assays. Drug sensitivity was assessed in the presence of 4-fold dilutions of each drug. (D) Combination of constant concentrations of D2202 (500 nM), D2159 (900 nM), or D2197 (530 nM) with a titration of gemcitabine enhanced therapeutic response of D2202. Drug sensitivity curves and IC_{50}s were calculated with in-house software (Dineen et al., 2010).

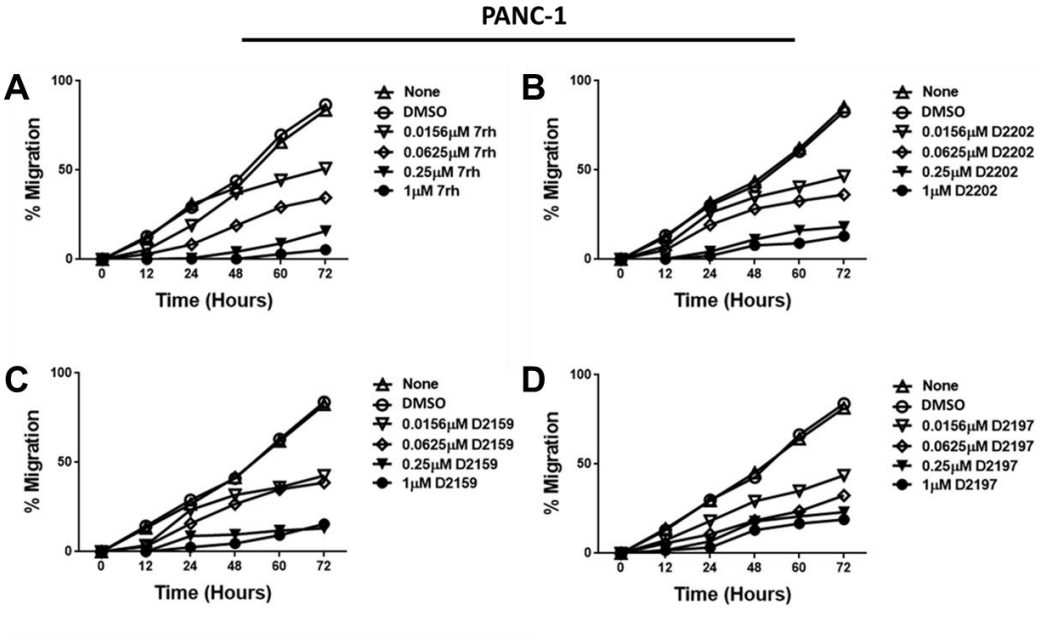

Figure 5.2: Functional utility of DDR1-specific small molecule inhibitors: 7rh, D2202, D2159, and D2197.

Evaluation of DDR1-specific small molecule inhibitors: 7rh, D2202, D2159, and D2197. (A-D) 7rh, D2202, D2159, and D2197 inhibited the migratory ability of a human PDA cell line (PANC-1) through scratch wound-healing analysis. Concentrations used were 0.016 μM, 0.0625 μM, 0.25 μM, and 1 μM.

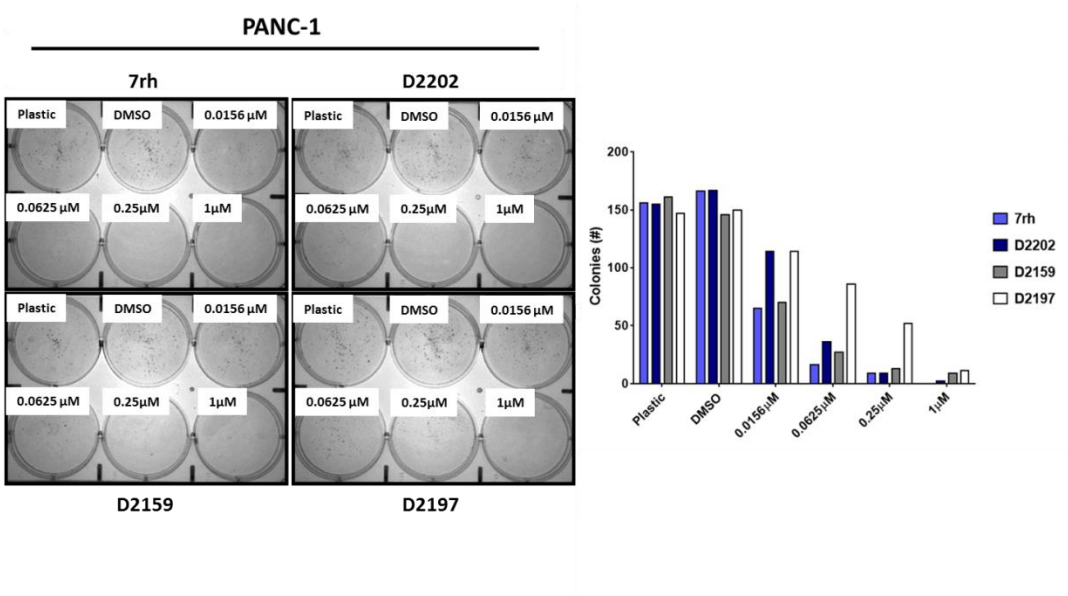

Figure 5.3: DDR1 inhibitors reduced liquid colony formation of a human PDA cell line (PANC-1).

Evaluation of DDR1-specific small molecule inhibitors: 7rh, D2202, D2159, and D2197. (A-D) Titrations of 7rh, D2202, D2159, and D2197 inhibited the liquid colony formation of a human PDA cell line (PANC-1). Concentrations used were 0.016 µM, 0.0625 µM, 0.25 µM, and 1 µM.

5.2.2 DDR1 inhibition in other cancer models

The evaluation of tumorigenic DDR1 signaling in other cancer model systems is relevant as DDR1 is widely and differentially expressed amongst tissue types. DDR1 is expressed at high levels in the pancreas, brain, lung, kidney, spleen, and placenta (Di Marco et al., 1993; Johnson et al., 1993; Laval et al., 1994; Perez et al., 1994), and predominant in epithelial cells (Alves, 2001; Alves et al., 1995). Ultimately, dysregulated and aberrant DDR1 expression was associated with an unfavorable outcome for patients, and altered functions of DDR1 likely contributed to tumorigenesis.

We have recently reported (H. Hur et al, submitted) that DDR1 expression and activity correlated with worse outcome in a large cohort of gastric cancer patients (n=217). Advanced gastric cancer is morphologically classified into four types according to Borrmann's classification. The fourth type of gastric cancer, linitis plastica, is characteristically desmoplastic with profuse stromal involvement (Borchard, 1990). Gastric cancers are also histologically divided into intestinal and diffuse type, based on Lauren's classification (Lauren, 1965). Intestinal type tumors are typically localized while diffuse gastric tumors are invasive with tumor cells interspersed in the stroma. Several reports suggested that stromal rich diffuse gastric tumors have a worse overall prognosis relative to intestinal type cancers (An et al., 2008; Cammerer, Formentini, Karletshofer, Henne-Bruns, & Kornmann, 2012; Otsuji et al., 2004; Stiekema et al., 2013). In

this study collagen deposition, the expression of DDR1, and loss of E-CADHERIN correlated with worse overall prognosis in gastric cancer. Loss of E-CADHERIN in gastric cancer tissue displayed more clinicopathologic significance in tumors that expressed DDR1 and collagen accumulation. DDR1-induced PYK2 phosphorylation and loss of E-CADHERIN was induced by collagen stimulation, and this was reduced by DDR1 inhibition. In xenografts, collagen accumulated as the tumor increased in size. DDR1 inhibition reduced DDR1 activation, EMT and tumor growth. These observations provided strong evidence that collagen signaling participated in the aggressive phenotype of gastric cancer. Further these data indicated that DDR1 is a critical mediator of collagen-induced tumor phenotype and that inhibition of DDR1 is a useful strategy to improve the prognosis of patients with gastric cancer. 7rh-mediated inhibition of DDR1 in gastric cancer cells reduced tumorigenic characteristics *in vitro* and tumor growth *in vivo* (H. Hur et al, submitted). Moreover, in a xenograft model, the effect of 7rh benzamide on the suppression of tumor growth was noted after subcutaneous injection of tumor cells, and treatment was tolerable. These findings were promising and highlight that 7rh benzamide may be a new potential targeting agent for patients with gastric cancer with profuse stromal tissues (H. Hur et al, submitted).

In line with the previous data in pancreatic and gastric cancers, previous clinicopathological parameter analyses in NSCLC patients revealed a significant

correlation between DDR1 overexpression and lymph node metastasis (p= 0.001), which demonstrated the prognostic potential of DDR1 expression (Y. Li et al., 2015; Miao et al., 2013). Additionally, a phosphoproteomic approach demonstrated that DDR1 was among the top 20 RTKs that was highly phosphorylated in a set of 150 NSCLC tumors; specifically, DDR1 was the third-most phosphorylated tyrosine kinase (following Met and Alk) (Rikova et al., 2007; Valiathan et al., 2012).

Other studies have demonstrated that high expression levels and/or mutations of DDR1 were frequently detected in multiple cancer cell lines and primary tumor tissues from pancreas (Couvelard et al., 2006), lung (Ding et al., 2008; Miao et al., 2013; Rikova et al., 2007), breast (Barker et al., 1995), brain (Weiner et al., 1996), ovary (Heinzelmann-Schwarz et al., 2004) head and neck (Squire et al., 2002), liver (Jian et al., 2012), and prostate (Shimada et al., 2008). Silencing DDR1 by siRNA reduced metastatic activity in lung cancer models (Miao et al., 2013; Valencia et al., 2012) and enhanced chemosensitivity to genotoxic drugs in breast cancer cells (Das et al., 2006). Furthermore, DDR1 gain-of-function mutations were identified in various types of cancer cells and primary human NSCLC cancer tissues (Ding et al., 2008). Somatic mutations of DDR1 in lung neoplasms and cancer cells such as G1486T and A496S contributed significantly to the development of lung cancer (Ding et al., 2008).

Some other mutations, including W385C, F866Y, and F824W, for DDR1 have also been reported in various cancer cells (Day et al., 2008; Ford et al., 2007).

Lung cancer is the most prevalent and lethal cancer worldwide (Jemal et al., 2011; Parkin, Pisani, & Ferlay, 1993). Within the United States, there were more than 220,000 new cases of cancers of the lung and bronchus in 2010 and greater than 157,000 deaths, amounting to 15% and 28% of total cancer incidences and deaths, respectively (Jemal, Siegel, Xu, & Ward, 2010). The majority of patients with NSCLC have advanced stage disease at the time of diagnosis (Parkin, Bray, Ferlay, & Pisani, 2005; Webb & Simon, 2010). NSCLC cases are also typically non-responsive to radiation and chemotherapy (Hoffman, Mauer, & Vokes, 2000). Additionally, the highly aggressive and invasive characteristics of NSCLC often lead to metastasis of the tumor within months. The metastatic progression in NSCLC is ultimately the key contributing factor to the severity of this disease (Hoffman et al., 2000) (Feld, Rubinstein, & Weisenberger, 1984; Nguyen, Bos, & Massague, 2009). Because of this, the 5-year survival rate for lung cancer patients remains dismal at approximately 15% in the United States (Parkin et al., 2005; Webb & Simon, 2010). In addition, progress in chemotherapeutic agents over the last decades has not yielded significant improvements in lung cancer patient survival and many lung cancer patients will recur despite multidisciplinary intervention. Therefore, emerging

therapeutic modalities with the potential to improve the prognosis of lung cancer, such as those that inhibit tumor angiogenesis are of special interest.

There has been progress in the comprehension of the biological mechanisms governing the development and progression of lung cancer, which has ultimately led to the discovery of new therapeutic targets. Specifically, the expression of DDR1, collagen I α1, and SPARC was assessed in lung cancer patients (n=1,927) using the Kaplan-Meier Plotter online database (Gyorffy, Surowiak, Budczies, & Lanczky, 2013) which corroborated the PDA gene expression from Figure 3.2 and Figure 3.3. Lung cancer patients with high DDR1 (1,389/1,927) those with high collagen I αI (1,309/1,927), and those with low SPARC (1,410/1,927) levels displayed worse overall prognosis (Figure 5.4). These findings demonstrated the translation of SPARC's regulation of DDR1-mediated tumorigenicity and signaling in PDA as well as NSCLC. The fact that patients with high DDR1 and high collagen I α1 were inversely correlated with the expression of SPARC merits further exploration. Moreover, due to the necessity of better treatment strategies for NSCLC the producers of the 7rh compound, Dr. Ke Ding and collaborators, have recently filed intellectual property patents to assess the pre-clinical efficacy of 7rh in NSCLC patients in China with the long-term goal of utilizing oral 7rh tablets in human patients.

Through collaborations with Dr. Ke Ding at Guangzhou Institutes of Biomedicine and Health and Dr. John Minna at UT Southwestern Medical Center

7rh was evaluated on small set of NSCLC cell lines which differentially express *SPARC* and *DDR1* (HCC4017, H460, and H322) (Figure 5.5). Drug sensitivity was assessed in the presence of 4-fold dilutions of 7rh and demonstrated that the high DDR1 expressing cell line (HCC4017) was the least sensitive to 7rh (Figure 5.5 B-C). Drug sensitivity curves and IC_{50}s were calculated with in-house software (Dineen et al., 2010). These findings corroborated our data from Figure 4.3 in which the high DDR1-expressing cell line (AsPC-1) was less sensitive to 7rh therapy *in vitro*.

The sensitivity of human NSCLC cell lines (HCC4017, H460, and H322) to 7rh, D2202, D2159, or D2197 treatment was assessed by MTS viability assays in the presence of 4-fold dilutions of each drug (Figure 5.6 A-D). Drug sensitivity curves and IC_{50}s were calculated with in-house software (Dineen et al., 2010). The effect of 7rh on these three cell lines was more efficacious compared to the three novel compounds, and the high DDR1 expressing cell line was the least sensitive to each compound. These findings further highlighted DDR1 expression in affecting the sensitivity to therapy as well as the application of DDR1 inhibition in NSCLC. Functionally, all four DDR1 small molecule inhibitors comparably reduced liquid colony formation in two NSCLC cell lines (HCC322 and H1395) (Figure 5.7 A-B) which demonstrated the functional utility of DDR1 inhibition in NSCLC.

5.2.2.2 Figures

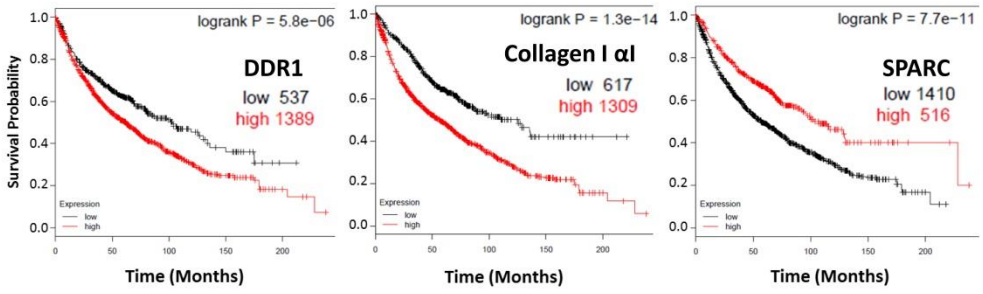

Figure 5.4: Kaplan-Meier analysis of lung cancer patients.

The survival of lung cancer patients with high DDR1 (1,389/1,927) and those with high collagen I α1 (1,309/1,927) expression was inversely correlated with the expression of SPARC (516/1410). Assessed with the Kaplan-Meier plotter: (Gyorffy et al., 2013).

A

Symbol	HCC4017	H460	H322
SPARC	10.53	4.97	4.43
DDR1	12.04	10.51	7.31

B

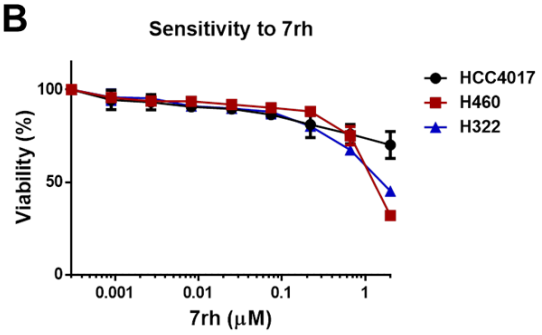

C

	7rh (nM) Avg IC_{50}
HCC4017	> 2000 (2)
H460	1500 (2)
H322	1350 (2)

Figure 5.5: Evaluation of DDR1 inhibition in NSCLC.

(A) Ilumina expression array for SPARC and DDR1 levels in human NSCLC cell lines (HCC4017, H460, and H322). (B) Sensitivity of NSCLC cell lines (HCC4017, H460, and H322) to gemcitabine and 7rh treatment assessed by MTS viability assays. Drug sensitivity was assessed in the presence of 4-fold dilutions of each drug. Drug sensitivity curves and IC_{50}s were calculated with in-house software (Dineen et al., 2010). (C) Table of IC_{50} values.

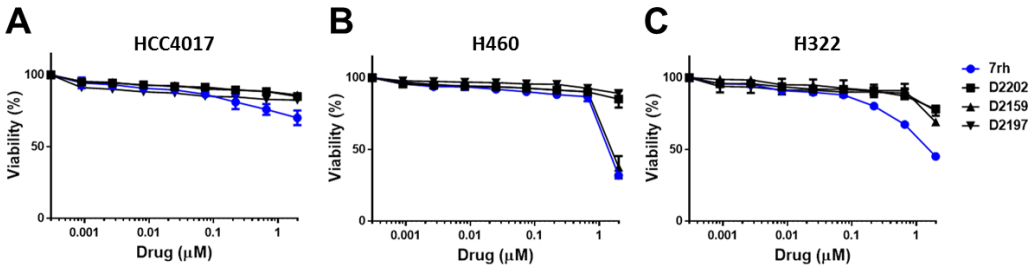

D

	7rh (nM) Avg IC_{50}	D2202 (nM) Avg IC_{50}	D2159 (nM) Avg IC_{50}	D2197 (nM) Avg IC_{50}
HCC4017	> 2000 (2)	> 2000 (2)	> 2000 (2)	> 2000 (2)
H460	1500 (2)	1700 (2)	> 2000 (2)	> 2000 (2)
H322	1350 (2)	1900 (2)	> 2000 (2)	> 2000 (2)

Figure 5.6: Sensitivity of human NSCLC to DDR1 inhibitors.

(A-C) Sensitivity of NSCLC cell lines (HCC4017, H460, and H322) to 7rh, D2202, D2159, or D2197 treatment assessed by MTS viability assays. Drug sensitivity was assessed in the presence of 4-fold dilutions of each drug. Drug sensitivity curves and IC_{50}s were calculated with in-house software (Dineen et al., 2010). (D) Table of IC_{50} values.

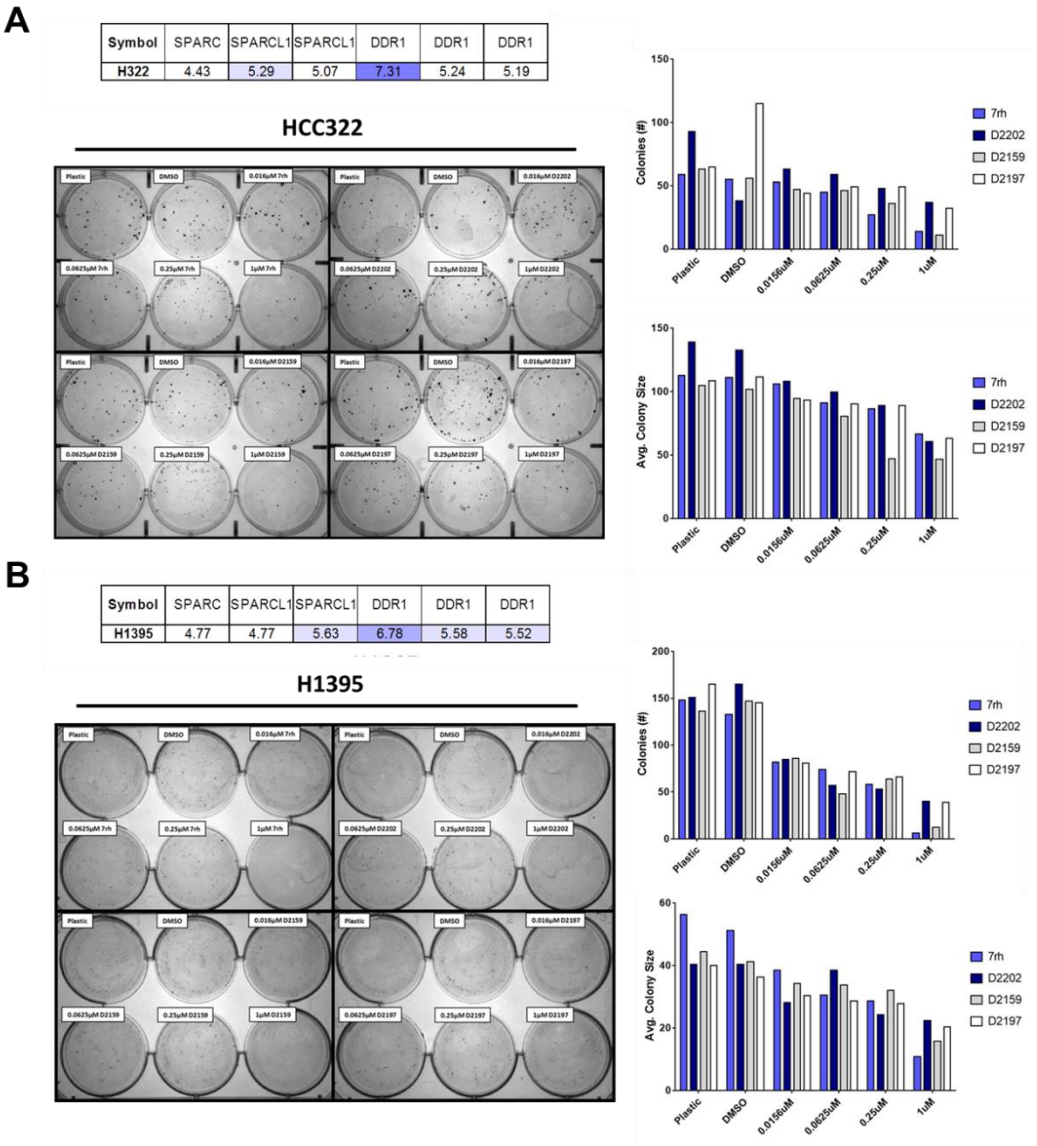

Figure 5.7: Functional utility of DDR1 inhibition in NSCLC.

Evaluation of DDR1-specific small molecule inhibitors: 7rh, D2202, D2159, and D2197. (A-D) 7rh, D2202, D2159, and D2197 inhibited liquid colony formation of two NSCLC cell lines (HCC322 and H1395). Concentrations used were 0.016 µM, 0.0625 µM, 0.25 µM, and 1 µM.

5.3 Targeting ECM components and/or signaling pathways

The dysregulation of ECM-driven signaling programs in cancer and other pathological conditions contribute to the invasive and hostile programs of cells (Valiathan et al., 2012), and contribute to the development of complex microenvironments (H. Liu et al., 2012). However the ECM-mediated signaling pathways that drive these programs are unclear.

5.3.1 Targeting effectors in fibrotic disease

A large number of individuals suffer from the devastating effects of chronic fibrosis, such as pulmonary or cardiac fibrotic diseases. Fibrotic diseases pose serious health problems in current medicine and are an enormous challenge. Approximately 45% of the mortality in the Western developed countries is attributed to fibrotic diseases, and the mortality in underdeveloped or developing countries is higher (Wynn, 2008). In epithelial organs, especially the lung, liver, skin, and kidney, the replacement of normal tissue with collagen-rich tissue is a major factor in progressive loss of organ function and eventual organ failure (Friedman, Sheppard, Duffield, & Violette, 2013). There is currently no effective treatment and the current lack of approved drugs for treatment of these diseases indicates that recent knowledge has not yet been translated into effective therapies (Rosenbloom, Mendoza, & Jimenez, 2013).

In animal models of fibrosis, the disease is provoked by severe initial injury to the epithelium (i.e. bleomycin and fluorescein isothiocyanate treatment or thoracic irradiation in lung, carbon tetrachloride or bile duct ligation in liver, and ureteral obstruction in kidney) (Friedman et al., 2013). Fibrosis often occurs as a result of sustained injury to the epithelium, which causes the overproduction of cytokines and growth factors (Friedman et al., 2013). Tissue fibrosis in virtually every organ is accompanied by accumulation of large numbers of cells that have undergone profound changes in cell function, morphology, and transcriptional regulation. These cells secrete increased amounts and disease-associated forms of collagen (i.e. interstitial collagen types I), as well as other ECM proteins that characterize pathologic fibrosis (Friedman et al., 2013).

DDR1 is upregulated in fibrotic diseases and contributes to the initiation and progression of fibrosis. Recent reports have demonstrated that *Ddr1*$^{-/-}$ mice displayed reduced bleomycin-induced pulmonary injury characterized by reduced collagen (Avivi-Green et al., 2006). DDR1 expression has is elevated in patients with lupus nephritis and Goodpasture's syndrome, both of which are fibrotic diseases, as well as in a mouse model of crescentic glomerulonephritis (Kerroch et al., 2012). Moreover, Alport mice (a model of chronic kidney fibrosis) crossed into the *Ddr1*$^{-/-}$ mice have reduced renal fibrosis and inflammation (Gross et al., 2010).

Imatinib, which inhibits DDR1 (Figure 1.5, Table 1), was shown to abrogate collagen gene expression *in vitro*, and prevent the development of tissue fibrosis *in vivo* (Daniels et al., 2004; Distler et al., 2007). In an *in vivo* model of bleomycin-induced dermal fibrosis, treatment with imatinib at a concentration of 150 mg/kg/day reduced the synthesis of mRNA for *ColI α1*, *ColI α2*, and reduced the accumulation of ECM proteins in a separate model of pulmonary fibrosis (Distler et al., 2007). Imatinib treatment of patients with chronic myelogenous leukemia (CML) displayed regression of concomitant bone marrow fibrosis (Beham-Schmid et al., 2002; Bueso-Ramos et al., 2004). The anti-fibrotic role of imatinib in this context is in part due to the inhibition of Bcr-Abl, recently identified as an important downstream molecule of Tgf-β signaling (a pro-fibrotic factor) (Daniels et al., 2004). However, imatinib inhibition of DDR1-mediated fibrosis should also be explored in this context. This data suggests that DDR1 inhibitors, such as imatinib or 7rh, might usher in a promising new era in the treatment of fibrosis. Moreover, imatinib merits future exploration in the treatment of fibrotic disease due to its favorable pharmacokinetic properties: readily absorbed after oral administration, long half-life (13-16 hours), and taken only once daily (Distler et al., 2007).

A recent report demonstrated the importance of AKT1 in fibrosis, in line with my data which demonstrated that DDR1 blockade inhibited collagen deposition as well as AKT1 phosphorylation. Akt1, the predominant Akt isoform

in tumor cells, endothelial cells, and fibroblasts promoted angiogenesis and vascular protection (J. Chen et al., 2005), wound healing (Somanath, Chen, & Byzova, 2008), inflammation (Di Lorenzo, Fernandez-Hernando, Cirino, & Sessa, 2009), and fibroblast-mediated ECM secretion (Goc, Choudhary, Byzova, & Somanath, 2011) and assembly (Somanath & Byzova, 2009; Somanath, Kandel, Hay, & Byzova, 2007). The PI3K/Akt pathway was hyperactivated during fibrosis (Xia et al., 2010), specifically pulmonary fibrosis (Xia et al., 2008). Moreover, Abdalla and colleagues (Abdalla et al., 2015) demonstrated that *Akt1*$^{-/-}$ mice were protected from hypoxia-induced pulmonary vascular and tissue remodeling, that an Akt1 inhibitor ameliorated progressive chronic hypoxia- and Tgf-β-induced pulmonary fibrosis, and that genetic ablation of Akt1 and pharmacological inhibition of Akt1 (triciribine, TCBN) significantly reduced fibrosis. Currently, TCBN, an Akt inhibitor is in clinical trials for the management of various types of cancers, and initial reports have indicated no serious adverse events (Garrett et al., 2011). Abdalla and colleagues (Abdalla et al., 2015) identified anti-fibrotic and anti-remodeling properties of TCBN as evidenced from the reduced fibrotic lesions, αSMA and matrix deposition, and decreased medial thickening of pulmonary arterioles. These findings highlight that inhibition of DDR1 resulting in AKT1 suppression may further reduce collagen deposition and collagen-mediated tumorigenicity. These findings are also particularly interesting as they have highlighted an avenue of targeting DDR1-AKT1 mediated fibrosis. All

together, the fibrotic actions reported for DDR1 and AKT1 have made it an attractive target in the context of alleviating these inflammatory and fibrotic diseases. Future work on the development of DDR1 and AKT1 inhibitors could benefit the treatment of these diseases.

5.3.2 ECM components and/or signaling in cancer

Prospectively, an assessment of the tumor vasculature could be incorporated into existing standard-of care diagnostic tests, these could include pancreatic computerized axial tomography (CT) (Koay et al., 2014), dynamic contrast enhanced (DCE) MRI (Tofts et al., 1999; Wasser et al., 2003), or perfusion CT (Park et al., 2009). These could derive physiological patient properties from imaging and predict a potential response to cancer therapy, can offer evidence that drug delivery may be limited, and can be used to inform management decisions (Koay et al., 2014). These potential strategies in combination with targeting ECM components and signaling pathways could be therapeutically beneficial.

For example pulmonary fibrosis, also known as fibrosing alveolitis or fibrosing interstitial pneumonia, is a progressive diffuse fibrotic lung disease (Kumar et al., 2003) associated with an increased risk of lung cancer (compared to the general population) (Hubbard, Venn, Lewis, & Britton, 2000; Turner-Warwick, Lebowitz, Burrows, & Johnson, 1980). Lung cancer was the cause of

death in up to 10% of patients with pulmonary fibrosis (Turner-Warwick et al., 1980). However, the operative risks of major pulmonary resection and the long-term survival following resection for NSCLC in patients with pulmonary fibrosis are unknown. Current clinical treatment guidelines recommended for locally advanced NSCLC is the use of radiotherapy (Pfister et al., 2004). Conventionally fractionated radiotherapy for NSCLC consists of 1.8-2.0 Gray fractions given once daily for 5 days each week to a total dose of 60 Gray or more. This treatment strategy was associated with improved regional control and survival ("Clinical practice guidelines for the treatment of unresectable non-small-cell lung cancer. Adopted on May 16, 1997 by the American Society of Clinical Oncology," 1997), but radiation-induced lung toxicity such as pulmonary fibrosis was common. This pathological phenotype highlights that targeting fibrotic signaling networks in NSCLC is a therapeutic avenue to enhance patient outcome in combination with standard therapy. Mammographic densities are also associated with an increased risk of developing histologic changes that are risk factors for breast cancer, and the histologic feature most consistently associated with mammographic densities is stromal fibrosis (Oza & Boyd, 1993). Oza and colleagues (Oza & Boyd, 1993) have suggested that the association between mammographic densities and several other risk factors for breast cancer suggests that these factors may also modulate the activity of growth factors in breast tissue, and that this may be the means by which they influence breast cancer risk.

Studies of targeting ECM components demonstrated that the angiotensin receptor blocker (ARB) losartan reduced collagen I production in cancer associated fibroblasts (CAFs) by inhibition of angiotensin-II-receptor-1 (AT1) (Chauhan et al., 2013), as well as downstream inhibition of transforming growth factor-β1 (Tgf-β1) activation (Diop-Frimpong, Chauhan, Krane, Boucher, & Jain, 2011; J. Liu et al., 2012) through thrombospondin-1 (TSP-1) inhibition (Habashi et al., 2006; Naito et al., 2004; Sweetwyne & Murphy-Ullrich, 2012). These studies suggested that angiotensin blockers led to an enhanced chemotherapeutic delivery by affecting the decompression of vessels in desmoplastic tumors through the reduction of solid stress (Chauhan et al., 2013). Analyses of retrospective clinical data suggested that the use of AT1 blockers (ARBs) to manage hypertension in cancer patients which received standard therapies was correlated with longer survival in pancreatic and other cancers (Keizman et al., 2011; Nakai et al., 2010; Wilop et al., 2009), as well as a reduced risk of recurrence in breast cancer (Chae et al., 2011). However, a causal relationship between the use of ARBs and their clinical benefit has not been revealed (Chauhan et al., 2013). A clinical trial with FOLFIRINOX and losartan in patients with pancreatic cancer is currently ongoing and may demonstrate the utility of stromal depletion and this specific class of drugs (NCT01821729) (Neesse, Algul, Tuveson, & Gress, 2015). However, prior work has suggested that the disruption of the stromal barrier to increase drug delivery was not the only factor that

increased anti-tumor responses (Cook et al., 2012; Neesse et al., 2015). While previous reports have demonstrated the poor prognostic role of stroma-rich PDA (Erkan et al., 2008), recent data has contradicted these findings and has demonstrated that high α-SMA content correlated with increased survival in patients with PDA (Ozdemir et al., 2014; Rhim et al., 2014; W. Q. Wang et al., 2013). Thus, stromal density and proliferation should be carefully considered for both prognostic and therapeutic classifications as the biological behavior, differentiation and tumor vasculature might be profoundly different (Neesse et al., 2015).

Olive et al. (Olive et al., 2009) demonstrated that pharmacological inhibition of the pro-stromal sonic hedgehog (SHH) signaling cascade was therapeutically attractive (Neesse et al., 2015). SHH signaling is involved in the development and maintenance of the stromal compartment (Bailey et al., 2008; Yauch et al., 2008). Recently an inhibitor of the SHH pathway (Smoothened inhibitor IPI-926) was combined with gemcitabine in the *KPC* mouse model which resulted in elevated gemcitabine levels in the tumors and increased cancer cell death (Olive et al., 2009). Through histological analysis, tumors displayed a higher microvessel density (MVD), while collagen I levels were decreased compared to mice treated with vehicle or gemcitabine alone. Additionally, the higher MVD enhanced drug delivery and significantly enhanced overall survival and decreased metastasis to the liver in the IPI-926-plus-gemcitabine treatment

group (Olive et al., 2009). These results highlighted the stromal compartment as a therapeutic target that could improve treatment efficiency though the enhancement of local drug concentrations. In addition to the studies, recent reports have demonstrated that the targeted treatment of stromal cells increased drug delivery as well as drug accumulation in the tumor, with a concurrent increase in therapeutic efficacy (J. M. Lohr & Jesnowski, 2009; Michl & Gress, 2012; Olive et al., 2009). Unfortunately these promising therapeutic effects have not translated into the clinic as PDA patients treated with the combination of IPI-926 and gemcitabine did not display the survival advantage noted from preclinical experiments (Amakye, Jagani, & Dorsch, 2013). Nevertheless, targeting ECM components and signaling pathways offer further insights into the complexity of using pharmacological inhibition to target cells in tumors (Olive et al., 2009). This has been presented as a very promising therapeutic strategy in PDA as this approach may sensitize therapeutic interventions that otherwise fail in patients with PDA (Neesse et al., 2015). Thus finding new pharmacologically relevant targets that block ECM signaling is important.

Recent efforts have focused on exploring the function of an abundant ECM component, hyaluronic acid (HA or hyaluronan), on its role in disease biology and resistance (Provenzano et al., 2012). HA is a glycosaminoglycan (GAG) involved in the structural integrity and flexibility of tissues, particularly in embryogenesis and oncogenesis, though its expression varies widely across

tumors and is generally considered a tumor promoter (Toole, 2004). The median survival (from time of animal enrollment, 12-14 weeks old) of *KPC* mice treated with gemcitabine plus PEGPH20 (HA inhibitor) was enhanced to 91.5 days versus 55.5 days compared to gemcitabine alone (Provenzano et al., 2012). The metastatic tumor burden and interstitial fluid pressure (IFP) were also significantly diminished with the combination therapy (Provenzano et al., 2012). This study demonstrated that the degradation or loss of HA resulted in a reduction of the IFP which permitted chemotherapy to reach the tumor, which resulted in improved survival (Provenzano et al., 2012). This approach is currently in phase II clinical testing to assess PEGPH20 (PEGylated recombinant human hyaluronidase) combined with nab-paclitaxel plus gemcitabine compared to nab-paclitaxel plus gemcitabine in subjects with Stage IV previously untreated pancreatic cancer (WIRB HALO-109-202). Furthermore, SHH merits further study.

Tumor angiogenesis is a hallmark of cancer and has also been a therapeutically attractive avenue for decades as it is required for continued tumor cell growth and metastasis (Hanahan & Weinberg, 2000). A major mediator of angiogenesis in normal physiology and in cancer is vascular endothelial growth factor (VEGF). In many forms of cancer, there was an up-regulation of VEGF family members and the VEGF receptors, which provided a target for cancer therapy (Roskoski, 2007). This target has been utilized, leading to the

development of anti-angiogenic small molecule tyrosine kinase inhibitors such as sorafenib (Nexavar®, BAY 43-9006, Bayer Pharmaceuticals Corp.) and sunitinib (Sutent®, SU11248, Pfizer, Inc.) as well as a number of mAbs against VEGF ligands and receptors (Roskoski, 2007). The clinical use of monoclonal antibodies (mAbs) to treat cancer and other diseases is well established. Evidence that anti-angiogenic therapy in tumors can enhance disease-associated parameters such as local invasion and metastasis is becoming preponderant, as these effects have also been noted with other therapeutic agents. Emerging evidence indicated that *in vivo* blockade of VEGF signaling promoted tumor metastasis (Conley et al., 2012; Ebos et al., 2009; Paez-Ribes et al., 2009) and promoted collagen production (Hwang, Del Priore, Freund, Chang, & Iranmanesh, 2011), and thus remains as a therapeutic avenue in the context of stromal targeting and depletion. Ultimately, the necessity of a multi-pronged approach to target specific tumorigenic effectors (i.e. DDR1) could in fact enhance the efficacy of anti-VEGF therapy to target pancreatic cancer. Further study will enable novel therapeutic options targeting the critical mechanisms that maintain pancreatic cancer.

Numerous cytokines participated in the progression of pancreatic malignancies. Collagen signaling facilitated Tgf-β-mediated changes in tumor cell phenotype and promoted tumor cell survival and chemoresistance. This is particularly relevant to PDA, which is a desmoplastic disease (Grzesiak et al.,

2007; Shields et al., 2012). Mutations in the TGF-β signaling pathway were reported in a large percentage (>50%) of human PDA (Jones et al., 2008). Elevated expression of Tgf-β has promoted tumor development, tumor cell EMT, and tumor cell survival and motility (Friess et al., 1993; Melisi et al., 2008; Nolan-Stevaux et al., 2009; Zhao et al., 2008). Tgf-β has also been shown to induce angiogenesis and collagen deposition (M. Lohr et al., 2001; Truty & Urrutia, 2007). Therefore, specifically targeting the tumorigenic aspects of Tgf-β might provide therapeutic benefit. Pharmacologic strategies that block Tgf-β activity have been explored in preclinical models of pancreatic cancer (reviewed in (Achyut & Yang, 2011)). As discussed by Achyut and Yang (Achyut & Yang, 2011), targeting the Tgf-β pathway altered the tumor microenvironment which ultimately enhanced the outcome of therapy. Previously, 2G8 (also known as MT1), a monoclonal antibody against mouse Tgf-β receptor 2 (Tgf-βr2), reduced primary tumor growth and metastasis in several syngeneic models of breast cancer, primarily through its effects on tumor cells (Zhong et al., 2010). Recent studies from the Brekken laboratory have shown that pharmacologic blockade of stromal Tgf-βr2 inhibited primary tumor growth and metastasis, and promoted epithelial differentiation in mouse models of pancreatic cancer (Ostapoff et al., 2014). The changes in tumor cell phenotype and behavior occurred in the context of microenvironmental changes. These alterations in cellular and extracellular components of the tumor after Tgf-βr2 blockade resulted in a striking reduction in

metastatic spread and help to functionally define the importance of stromal Tgf-βr2 for primary pancreatic tumor growth and metastasis (Ostapoff et al., 2014). Furthermore these combined data suggested another example of targeting tumor-stromal interactions in PDA.

Reports have highlighted the accumulation of ECM proteins which increased pancreatic cancer cell chemoresistance against gemcitabine (Erkan et al., 2007). Previous reports demonstrated stromal targeting through the use of nab-paclitaxel administration. Nab-paclitaxel treatment decreased collagen deposition in resected specimens, which suggested that nab-paclitaxel had an additional effect: tumor-stromal disruption (Alvarez et al., 2013). Additionally, the combination of nab-paclitaxel with gemcitabine increased intra-tumoral gemcitabine concentration, which enhanced antitumor activity (Alvarez et al., 2013; Hamada et al., 2013). The effect of nab-paclitaxel on the depletion of tumor stroma was confirmed in the *KPC* PDA mouse model (Neesse et al., 2014). This new treatment regimen (gemcitabine plus nab-paclitaxel) improved the overall survival and progression-free survival of patients with metastatic pancreatic cancer (Heinemann et al., 2014). Of note, the additional effect of nab-paclitaxel on the tumor stroma, which synergistically potentiated gemcitabine's antitumor effect, suggested the possibility of tumor-stromal interaction-targeting therapy (Hamada et al., 2013; Neesse et al., 2014) in a SPARC independent manner (Neesse et al., 2014). These lines of evidence were an excellent example of the

clinical benefits that can be provided by the evolution of drug delivery methods (Hamada et al., 2013).

5.4 Closing remark

Targeting the signaling pathways influenced by the tumor microenvironment has gained traction and has been validated as a potential approach for the enhancement of chemotherapeutic interventions and the therapeutic outcomes of PDA patients.

APPENDIX A
Human and Mouse Protein Sequence Analysis

Human SPARC:

Query ID:
gi|4507171|ref|NP_003109.1|

Description:
SPARC precursor
[Homo sapiens]

Molecule type:
Amino acid

Query Length:
303

Mouse Sparc:

Subject ID:
gi|6678077|ref|NP_033268.1|

Description:
SPARC precursor
[Mus musculus]

Molecule type:
Amino acid

Subject Length:
302

Range 1: 1 to 302 GenPept Graphics Next Match Previous Match

Score	Expect	Method	Identities	Positives	Gaps
561 bits(1445)	0.0	Compositional matrix adjust.	280/303(92%)	289/303(95%)	1/303(0%)

```
Query  1    MRAWIFFLLCLAGRALAAPQQEALPDETEVVEETVAEVTEVSVGANPVQVEVGEFDDGAE  60
            MRAWIFFLLCLAGRALAAPQQ  +  E  V EETV E T V VGANPVQVE+GEF+DGAE
Sbjct  1    MRAWIFFLLCLAGRALAAPQQTEV-AEEIVEEETVVEETGVPVGANPVQVEMGEFEDGAE  59

Query  61   ETEEEVVAENPCQNHHCKHGKVCELDENNTPMCVCQDPTSCPAPIGEFEKVCSNDNKTFD  120
            ET EEVVA+NPCQNHHCKHGKVCELDE+NTPMCVCQDPTSCPAPIGEFEKVCSNDNKTFD
Sbjct  60   ETVEEVVADNPCQNHHCKHGKVCELDESNTPMCVCQDPTSCPAPIGEFEKVCSNDNKTFD  119

Query  121  SSCHFFATKCTLEGTKKGHKLHLDYIGPCKYIPPCLDSELTEFPLRMRDWLKNVLVTLYE  180
            SSCHFFATKCTLEGTKKGHKLHLDYIGPCKYI PCLDSELTEFPLRMRDWLKNVLVTLYE
Sbjct  120  SSCHFFATKCTLEGTKKGHKLHLDYIGPCKYIAPCLDSELTEFPLRMRDWLKNVLVTLYE  179

Query  181  RDEDNNLLTEKQKLRVKKIHENEKRLEAGDHPVELLARDFEKNYNMYIFPVHWQFGQLDQ  240
            RDE NNLLTEKQKLRVKKIHENEKRLEAGDHPVELLARDFEKNYNMYIFPVHWQFGQLDQ
Sbjct  180  RDEGNNLLTEKQKLRVKKIHENEKRLEAGDHPVELLARDFEKNYNMYIFPVHWQFGQLDQ  239

Query  241  HPIDGYLSHTELAPLRAPLIPMEHCTTRFFETCDLDNDKYIALDEWAGCFGIKQKDIDKD  300
            HPIDGYLSHTELAPLRAPLIPMEHCTTRFFETCDLDNDKYIAL+EWAGCFGIK++DI+KD
Sbjct  240  HPIDGYLSHTELAPLRAPLIPMEHCTTRFFETCDLDNDKYIALEEWAGCFGIKEQDINKD  299

Query  301  LVI  303
            LVI
Sbjct  300  LVI  302
```

Human DDR1:

Query ID:
gi|83977450|ref|NP_054699.2|

Description:
Epithelial discoidin domain-containing receptor 1 isoform 2 precursor [Homo sapiens]

Molecule type:
Amino acid

Query Length:
913

Mouse Ddr1:

Subject ID:
gi|311771514|ref|NP_001185760.1|

Description:
Epithelial discoidin domain-containing receptor 1 isoform 1 precursor [Mus musculus]

Molecule type:
Amino acid

Subject Length:
911

Range 1: 16 to 911 GenPept Graphics ▼ Next Match ▲ Previous Ma

Score	Expect	Method	Identities	Positives	Gaps
1564 bits(4049)	0.0	Compositional matrix adjust.	844/900(94%)	864/900(96%)	5/900(0%)

```
Query  15   VASGDADMKGHFDPAKCRYALGMQDRTIPDSDISASSSWSDSTAARHSRLESSDGDGAWC  74
            V  GDADMKGHFDPAKCRYALGMQDRTIPDSDIS SSSWSDSTAARHSRLESSDGDGAWC
Sbjct  16   VTIGDADMKGHFDPAKCRYALGMQDRTIPDSDISVSSSWSDSTAARHSRLESSDGDGAWC  75

Query  75   PAGSVFPKEEEYLQVDLQRLHLVALVGTQGRHAGGLGKEFSRSYRLRYSRDGRRWMGWKD  134
            PAG VFPKEEEYLQVDL+RLHLVALVGTQGRHAGGLGKEFSRSYRLRYSRDGRRWM WKD
Sbjct  76   PAGPVFPKEEEYLQVDLRRLHLVALVGTQGRHAGGLGKEFSRSYRLRYSRDGRRWMDWKD  135

Query  135  RWGQEVISGNEDPEGVVLKDLGPPMVARLVRFYPRADRVMSVCLRVELYGCLWRDGLLSY  194
            RWGQEVISGNEDP GVVLKDLGPPMVARLVRFYPRADRVMSVCLRVELYGCLWRDGLLSY
Sbjct  136  RWGQEVISGNEDPGGVVLKDLGPPMVARLVRFYPRADRVMSVCLRVELYGCLWRDGLLSY  195

Query  195  TAPVGQTMYLSEA-VYLNDSTYDGHTVGGLQYGGLGQLADGVVGLDDFRKSQELRVWPGY  253
            TAPVGQTM LSE  V+LNDSTYDG+T GGLQYGGLGQLADGVVGLDDFR+SQELRVWPGY
Sbjct  196  TAPVGQTMQLSEVMVHLNDSTYDGYTAGGLQYGGLGQLADGVVGLDDFRQSQELRVWPGY  255

Query  254  DYVGWSNHSFSSGYVEMEFEFDRLRAFQAMQVHCNNMHTLGARLPGGVECRFRRGPAMAW  313
            DYVGWSN SF +GYVEMEFEFDRLR FQ MQVHCNNMHTLGARLPGGVECRF+RGPAMAW
Sbjct  256  DYVGWSNQSFPTGYVEMEFEFDRLRTFQTMQVHCNNMHTLGARLPGGVECRFKRGPAMAW  315

Query  314  EGEPMRHNLGGNLGDPRARAVSVPLGGRVARFLQCRFLFAGPWLLFSEISFISDVVNNSS  373
            EGEP+RH LGG+LGDPRARA+SVPLGG V RFLQCRFLFAGPWLLFSEISFISDVVN+SS
Sbjct  316  EGEPVRHALGGSLGDPRARAISVPLGGHVGRFLQCRFLFAGPWLLFSEISFISDVVNDSS  375

Query  374  PALGGTFPPAPWWPPGPPPTNFSSLELEPRGQQPVAKAEGSPTAILIGCLVAIILLLLLI  433
                 TFPPAPWWPPGPPPTNFSSLELEPRGQQPVAKAEGSPTAILIGCLVAIILLLLLI
Sbjct  376  ----DTFPPAPWWPPGPPPTNFSSLELEPRGQQPVAKAEGSPTAILIGCLVAIILLLLLI  431

Query  434  IALMLWRLHWRRLLSKAERRVLEEELTVHLSVPGDTILINNRPGPREPPPYQEPRPRGNP  493
            IALMLWRLHWRRLLSKAERRVLEEELTVHLSVPGDTILINNRPGPREPPPYQEPRPRG P
Sbjct  432  IALMLWRLHWRRLLSKAERRVLEEELTVHLSVPGDTILINNRPGPREPPPYQEPRPRGTP  491

Query  494  PHSAPCVPNGSALLLSNPAYRLLLATYARPPRGPGPPTPAWAKPTNTQAYSGDYMEPEKP  553
            PHSAPCVPNGSALLLSNPAYRLLLATYARPPRGPGPPTPAWAKPTNTQA SGDYMEPEKP
Sbjct  492  PHSAPCVPNGSALLLSNPAYRLLLATYARPPRGPGPPTPAWAKPTNTQACSGDYMEPEKP  551

Query  554  GAPLLPPPPQNSVPHYAEADIVTLQGVTGGNTYAVPALPPGAVGDGPPRVDFPRSRLRFK  613
            GAPLLPPPPQNSVPHYAEADIVTLQGVTGGNTYAVPALPPGAVGDGPPRVDFPRSRLRFK
Sbjct  552  GAPLLPPPPQNSVPHYAEADIVTLQGVTGGNTYAVPALPPGAVGDGPPRVDFPRSRLRFK  611

Query  614  EKLGEGQFGEVHLCEVDSPQDLVSLDFPLNVRKGHPLLVAVKILRPDATKNARNDFLKEV  673
            EKLGEGQFGEVHLCEV+ PQDLVS DFP++V KGHPLLVAVKILRPDATKNARNDFLKEV
Sbjct  612  EKLGEGQFGEVHLCEVEDPQDLVSSDFPISVHKGHPLLVAVKILRPDATKNARNDFLKEV  671

Query  674  KIMSRLKDPNIIRLLGVCVQDDPLCMITDYMENGDLNQFLSAHQLEDKAAEGAPGDGQAA  733
            KIMSRLKDPNIIRLLGVCVQDDPLCMITDYMENGDLNQFLSA QLE+KA +G  GD ++
Sbjct  672  KIMSRLKDPNIIRLLGVCVQDDPLCMITDYMENGDLNQFLSARQLENKATQGLSGDTESD  731

Query  734  QGPTISYPMLLHVAAQIASGMRYLATLNFVHRDLATRNCLVGENFTIKIADFGMSRNLYA  793
            QGPTISYPMLLHV AQIASGMRYLATLNFVHRDLATRNCLVGENFTIKIADFGMSRNLYA
Sbjct  732  QGPTISYPMLLHVGAQIASGMRYLATLNFVHRDLATRNCLVGENFTIKIADFGMSRNLYA  791

Query  794  GDYYRVQGRAVLPIRWMAWECILMGKFTTASDVWAFGVTLWEVLMLCRAQPFGQLTDEQV  853
            GDYYRVQGRAVLPIRWMAWECILMGKFTTASDVWAFGVTLWEVLMLCR+QPFGQLTDEQV
Sbjct  792  GDYYRVQGRAVLPIRWMAWECILMGKFTTASDVWAFGVTLWEVLMLCRSQPFGQLTDEQV  851

Query  854  IENAGEFFRDQGRQVYLSRPPACPQGLYELMLRCWSRESEQRPPFSQLHRFLAEDALNTV  913
            IENAGEFFRDQGRQVYLSRPPACPQ LYELMLRCWSRE EQRPPF+QLHRFLA+DALNTV
Sbjct  852  IENAGEFFRDQGRQVYLSRPPACPQTLYELMLRCWSREPEQRPPFAQLHRFLADDALNTV  911
```

Human DDR2:

Query ID:
gi|62420886|ref|NP_001014796.1|

Description:
Discoidin domain-containing receptor 2 precursor
[Homo sapiens]

Molecule type:
Amino acid

Query Length
855

Mouse Ddr2:

Subject ID:
gi|158508514|ref|NP_072075.2|

Description:
Discoidin domain-containing receptor 2 precursor
[Mus musculus]

Molecule type:
Amino acid

Subject Length:
854

Range 1: 1 to 854 GenPept Graphics Next Match Previous Match

Score	Expect	Method	Identities	Positives	Gaps
1667 bits(4317)	0.0	Compositional matrix adjust.	820/855(96%)	832/855(97%)	1/855(0%)

```
Query  1    MILIPRMLLVLFLLLPILSSAKAQVNPAICRYPLGMSGGQIPDEDITASSQWSESTAAKY  60
            MI IPRM LVL LLL IL SAKAQVNPAICRYPLGMSGG IPDEDITASSQWSESTAAKY
Sbjct  1    MIPIPRMPLVLLLLLLILGSAKAQVNPAICRYPLGMSGGHIPDEDITASSQWSESTAAKY  60

Query  61   GRLDSEEGDGAWCPEIPVEPDDLKEFLQIDLHTLHFITLVGTQGRHAGGHGIEFAPMYKI  120
            GRLDSEEGDGAWCPEIPV+PDDLKEFLQIDL TLHFITLVGTQGRHAGGHGIEFAPMYKI
Sbjct  61   GRLDSEEGDGAWCPEIPVQPDDLKEFLQIDLRTLHFITLVGTQGRHAGGHGIEFAPMYKI  120

Query  121  NYSRDGTRWISWRNRHGKQVLDGNSNPYDIFLKDLEPPIVARFVRFIPVTDHSMNVCMRV  180
            NYSRDG+RWISWRNRHGKQVLDGNSNPYD+FLKDLEPPIVARFVR IPVTDHSMNVCMRV
Sbjct  121  NYSRDGSRWISWRNRHGKQVLDGNSNPYDVFLKDLEPPIVARFVRLIPVTDHSMNVCMRV  180

Query  181  ELYGCVWLDGLVSYNAPAGQQFVLPGGSIIYLNDSVYDGAVGYSMTEGLGQLTDGVSGLD  240
            ELYGCVWLDGLVSYNAPAGQQFVLPGGSIIYLNDSVYDGAVGYSMTEGLGQLTDGVSGLD
Sbjct  181  ELYGCVWLDGLVSYNAPAGQQFVLPGGSIIYLNDSVYDGAVGYSMTEGLGQLTDGVSGLD  240

Query  241  DFTQTHEYHVWPGYDYVGWRNESATNGYIEIMFEFDRIRNFTTMKVHCNNMFAKGVKIFK  300
            DFTQTHEYHVWPGYDYVGWRNESATNG+IEIMFEFDRIRNFTTMKVHCNNMFAKGVKIFK
Sbjct  241  DFTQTHEYHVWPGYDYVGWRNESATNGFIEIMFEFDRIRNFTTMKVHCNNMFAKGVKIFK  300

Query  301  EVQCYFRSEASEWEPNAISFPLVLDDVNPSARFVTVPLHHRMASAIKCQYHFADTWMMFS  360
            EVQCYFRSEASEWEP A+ FPLVLDDVNPSARFVTVPLHHRMASAIKCQYHFADTWMMFS
Sbjct  301  EVQCYFRSEASEWEPTAVYFPLVLDDVNPSARFVTVPLHHRMASAIKCQYHFADTWMMFS  360

Query  361  EITFQSDAAMYNNSEALPTSPMAPTTYDPMLKVDDSNTRILIGCLVAIIFILLAIIVIIL  420
            EITFQSDAAMYNNS ALPTSPMAPTTYDPMLKVDDSNTRILIGCLVAIIFILLAIIVIIL
Sbjct  361  EITFQSDAAMYNNSGALPTSPMAPTTYDPMLKVDDSNTRILIGCLVAIIFILLAIIVIIL  420

Query  421  WRQFWQKMLEKASRRMLDDEMTVSLSLPSDSSMFNNNRSSSPSEQGSNSTYDRIFPLRPD  480
            WRQFWQKMLEKASRRMLDDEMTVSLSLPS+SSMFNNNRSSSPSEQ SNSTYDRIFPLRPD
Sbjct  421  WRQFWQKMLEKASRRMLDDEMTVSLSLPSESSMFNNNRSSSPSEQESNSTYDRIFPLRPD  480

Query  481  YQEPSRLIRKLPEFAPGEEESGCSGVVKPVQPSGPEGVPHYAEADIVNLQGVTGGNTYSV  540
            YQEPSRLIRKLPEFAPGEEESGCSGVVKP QP+GPEGVPHYAEADIVNLQGVTGGNTY V
Sbjct  481  YQEPSRLIRKLPEFAPGEEESGCSGVVKPAQPNGPEGVPHYAEADIVNLQGVTGGNTYCV  540

Query  541  PAVTMDLLSGKDVAVEEFPRKLLTFKEKLGEGQFGEVHLCEVEGMEKFKDKDFALDVSAN  600
            PAVTMDLLSGKDVAVEEFPRKLL FKEKLGEGQFGEVHLCEVEGMEKFKDKDFALDVSAN
Sbjct  541  PAVTMDLLSGKDVAVEEFPRKLLAFKEKLGEGQFGEVHLCEVEGMEKFKDKDFALDVSAN  600

Query  601  QPVLVAVKMLRADANKNARNDFLKEIKIMSRLKDPNIIHLLAVCITDDPLCMITEYMENG  660
            QPVLVAVKMLRADANKNARNDFLKEIKIMSRLKDPNII LLAVCIT+DPLCMITEYMENG
Sbjct  601  QPVLVAVKMLRADANKNARNDFLKEIKIMSRLKDPNIIRLLAVCITEDPLCMITEYMENG  660

Query  661  DLNQFLSRHEPPNSSSSDVRTVSYTNLKFMATQIASGMKYLSSLNFVHRDLATRNCLVGK  720
            DLNQFLSRHEP +S SSD  TVSY NLKFMATQIASGMKYLSSLNFVHRDLATRNCLVGK
Sbjct  661  DLNQFLSRHEPLSSCSSDA-TVSYANLKFMATQIASGMKYLSSLNFVHRDLATRNCLVGK  719

Query  721  NYTIKIADFGMSRNLYSGDYYRIQGRAVLPIRWMSWESILLGKFTTASDVWAFGVTLWET  780
            NYTIKIADFGMSRNLYSGDYYRIQGRAVLPIRWMSWESILLGKFTTASDVWAFGVTLWET
Sbjct  720  NYTIKIADFGMSRNLYSGDYYRIQGRAVLPIRWMSWESILLGKFTTASDVWAFGVTLWET  779

Query  781  FTFCQEQPYSQLSDEQVIENTGEFFRDQGRQTYLPQPAICPDSVYKLMLSCWRRDTKNRP  840
            FTFCQEQPYSQLSDEQVIENTGEFFRDQGRQ YLPQPA+CPDSVYKLMLSCWRR+TK+RP
Sbjct  780  FTFCQEQPYSQLSDEQVIENTGEFFRDQGRQIYLPQPALCPDSVYKLMLSCWRRETKHRP  839

Query  841  SFQEIHLLLLQQGDE  855
            SFQEIHLLLLQQG E
Sbjct  840  SFQEIHLLLLQQGAE  854
```

REFERENCES

Abbonante, V., Gruppi, C., Rubel, D., Gross, O., Moratti, R., & Balduini, A. (2013). Discoidin domain receptor 1 protein is a novel modulator of megakaryocyte-collagen interactions. *J Biol Chem, 288*(23), 16738-16746. doi: 10.1074/jbc.M112.431528

Abdalla, M., Sabbineni, H., Prakash, R., Ergul, A., Fagan, S. C., & Somanath, P. R. (2015). Akt inhibitor, triciribine, ameliorates chronic hypoxia-induced vascular pruning and TGFbeta-induced pulmonary fibrosis. *Br J Pharmacol*. doi: 10.1111/bph.13203

Achyut, B. R., & Yang, L. (2011). Transforming growth factor-beta in the gastrointestinal and hepatic tumor microenvironment. *Gastroenterology, 141*(4), 1167-1178. doi: 10.1053/j.gastro.2011.07.048

Aguilera, K. Y., Rivera, L. B., Hur, H., Carbon, J. G., Toombs, J. E., Goldstein, C. D., . . . Brekken, R. A. (2014). Collagen signaling enhances tumor progression after anti-VEGF therapy in a murine model of pancreatic ductal adenocarcinoma. *Cancer Res, 74*(4), 1032-1044. doi: 10.1158/0008-5472.CAN-13-2800

Aguirre, A. J., Bardeesy, N., Sinha, M., Lopez, L., Tuveson, D. A., Horner, J., . . . DePinho, R. A. (2003). Activated Kras and Ink4a/Arf deficiency cooperate to produce metastatic pancreatic ductal adenocarcinoma. *Genes Dev, 17*(24), 3112-3126. doi: 10.1101/gad.11587031158703 [pii]

Alberts, S. R., Townley, P. M., Goldberg, R. M., Cha, S. S., Moore, D. F., Jr., Krook, J. E., . . . Sargent, D. J. (2002). Gemcitabine and oxaliplatin for patients with advanced or metastatic pancreatic cancer: a North Central Cancer Treatment Group (NCCTG) phase I study. *Ann Oncol, 13*(4), 553-557.

Alberts, S. R., Townley, P. M., Goldberg, R. M., Cha, S. S., Sargent, D. J., Moore, D. F., . . . Mailliard, J. A. (2003). Gemcitabine and oxaliplatin for metastatic pancreatic adenocarcinoma: a North Central Cancer Treatment Group phase II study. *Ann Oncol, 14*(4), 580-585.

Almoguera, C., Shibata, D., Forrester, K., Martin, J., Arnheim, N., & Perucho, M. (1988). Most human carcinomas of the exocrine pancreas contain mutant c-K-ras genes. *Cell, 53*(4), 549-554. doi: 0092-8674(88)90571-5 [pii]

Alvarez, R., Musteanu, M., Garcia-Garcia, E., Lopez-Casas, P. P., Megias, D., Guerra, C., . . . Hidalgo, M. (2013). Stromal disrupting effects of nab-paclitaxel in pancreatic cancer. *Br J Cancer, 109*(4), 926-933. doi: 10.1038/bjc.2013.415

Alves, F. (2001). Identification of two novel, kinase-deficient variants of discoidin domain receptor 1: differential expression in human colon cancer cell lines. *The FASEB Journal*. doi: 10.1096/fj.00-0626fje

Alves, F., Vogel, W., Mossie, K., Millauer, B., Hofler, H., & Ullrich, A. (1995). Distinct structural characteristics of discoidin I subfamily receptor tyrosine kinases and complementary expression in human cancer. *Oncogene, 10*(3), 609-618.

Amakye, D., Jagani, Z., & Dorsch, M. (2013). Unraveling the therapeutic potential of the Hedgehog pathway in cancer. *Nat Med, 19*(11), 1410-1422. doi: 10.1038/nm.3389

An, J. Y., Kang, T. H., Choi, M. G., Noh, J. H., Sohn, T. S., & Kim, S. (2008). Borrmann type IV: an independent prognostic factor for survival in gastric cancer. *J Gastrointest Surg, 12*(8), 1364-1369. doi: 10.1007/s11605-008-0516-9

Apte, M. V., Park, S., Phillips, P. A., Santucci, N., Goldstein, D., Kumar, R. K., . . . Wilson, J. S. (2004). Desmoplastic reaction in pancreatic cancer: role of pancreatic stellate cells. *Pancreas, 29*(3), 179-187.

Arnold, S. A., & Brekken, R. A. (2009). SPARC: a matricellular regulator of tumorigenesis. *J Cell Commun Signal, 3*(3-4), 255-273. doi: 10.1007/s12079-009-0072-4

Arnold, S. A., Rivera, L. B., Carbon, J. G., Toombs, J. E., Chang, C. L., Bradshaw, A. D., & Brekken, R. A. (2012). Losartan Slows Pancreatic Tumor Progression and Extends Survival of SPARC-Null Mice by Abrogating Aberrant TGFbeta Activation. *PLoS One, 7*(2), e31384. doi: 10.1371/journal.pone.0031384 PONE-D-11-19108 [pii]

Arnold, S. A., Rivera, L. B., Miller, A. F., Carbon, J. G., Dineen, S. P., Xie, Y., . . . Brekken, R. A. (2010). Lack of host SPARC enhances vascular function and tumor spread in an orthotopic murine model of pancreatic carcinoma. *Dis Model Mech, 3*(1-2), 57-72. doi: 10.1242/dmm.003228

Avivi-Green, C., Singal, M., & Vogel, W. F. (2006). Discoidin domain receptor 1-deficient mice are resistant to bleomycin-induced lung fibrosis. *Am J Respir Crit Care Med, 174*(4), 420-427. doi: 10.1164/rccm.200603-333OC

Bailey, J. M., Swanson, B. J., Hamada, T., Eggers, J. P., Singh, P. K., Caffery, T., . . . Hollingsworth, M. A. (2008). Sonic hedgehog promotes desmoplasia in pancreatic cancer. *Clin Cancer Res, 14*(19), 5995-6004. doi: 10.1158/1078-0432.CCR-08-0291

Bantscheff, M., Eberhard, D., Abraham, Y., Bastuck, S., Boesche, M., Hobson, S., . . . Drewes, G. (2007). Quantitative chemical proteomics reveals mechanisms of action of clinical ABL kinase inhibitors. *Nat Biotechnol, 25*(9), 1035-1044. doi: 10.1038/nbt1328

Bardeesy, N., Aguirre, A. J., Chu, G. C., Cheng, K. H., Lopez, L. V., Hezel, A. F., . . . Depinho, R. A. (2006). Both p16(Ink4a) and the p19(Arf)-p53 pathway constrain progression of pancreatic adenocarcinoma in the mouse. *Proc Natl Acad Sci U S A, 103*(15), 5947-5952. doi: 10.1073/pnas.0601273103

Bardeesy, N., & DePinho, R. A. (2002). Pancreatic cancer biology and genetics. *Nat Rev Cancer, 2*(12), 897-909. doi: 10.1038/nrc949

Barker, K. T., Martindale, J. E., Mitchell, P. J., Kamalati, T., Page, M. J., Phippard, D. J., . . . Crompton, M. R. (1995). Expression patterns of the novel receptor-like tyrosine kinase, DDR, in human breast tumours. *Oncogene, 10*(3), 569-575.

Beham-Schmid, C., Apfelbeck, U., Sill, H., Tsybrovsky, O., Hofler, G., Haas, O. A., & Linkesch, W. (2002). Treatment of chronic myelogenous leukemia with the tyrosine kinase inhibitor STI571 results in marked regression of bone marrow fibrosis. *Blood, 99*(1), 381-383.

Berlin, J. D., Catalano, P., Thomas, J. P., Kugler, J. W., Haller, D. G., & Benson, A. B., 3rd. (2002). Phase III study of gemcitabine in combination with fluorouracil versus gemcitabine alone in patients with advanced pancreatic carcinoma: Eastern Cooperative Oncology Group Trial E2297. *J Clin Oncol, 20*(15), 3270-3275.

Borchard, F. (1990). Classification of gastric carcinoma. *Hepatogastroenterology, 37*(2), 223-232.

Bornstein, P., & Sage, E. H. (2002). Matricellular proteins: extracellular modulators of cell function. *Curr Opin Cell Biol, 14*(5), 608-616.

Borza, C. M., & Pozzi, A. (2014). Discoidin domain receptors in disease. *Matrix Biol, 34*, 185-192. doi: 10.1016/j.matbio.2013.12.002

Boschman, C. R., Stryker, S., Reddy, J. K., & Rao, M. S. (1994). Expression of p53 protein in precursor lesions and adenocarcinoma of human pancreas. *Am J Pathol, 145*(6), 1291-1295.

Bradshaw, A. D., & Sage, E. H. (2001). SPARC, a matricellular protein that functions in cellular differentiation and tissue response to injury. *J Clin Invest, 107*(9), 1049-1054. doi: 10.1172/JCI12939

Brekken, R. A., Puolakkainen, P., Graves, D. C., Workman, G., Lubkin, S. R., & Sage, E. H. (2003). Enhanced growth of tumors in SPARC null mice is associated with changes in the ECM. *J Clin Invest, 111*(4), 487-495. doi: 10.1172/JCI16804

Brekken, R. A., & Sage, E. H. (2001). SPARC, a matricellular protein: at the crossroads of cell-matrix communication. *Matrix Biol, 19*(8), 816-827.

Brune, K., Hong, S. M., Li, A., Yachida, S., Abe, T., Griffith, M., . . . Goggins, M. (2008). Genetic and epigenetic alterations of familial pancreatic cancers. *Cancer Epidemiol Biomarkers Prev, 17*(12), 3536-3542. doi: 10.1158/1055-9965.EPI-08-0630

Bueso-Ramos, C. E., Cortes, J., Talpaz, M., O'Brien, S., Giles, F., Rios, M. B., . . . Kantarjian, H. (2004). Imatinib mesylate therapy reduces bone marrow fibrosis in patients with chronic myelogenous leukemia. *Cancer, 101*(2), 332-336. doi: 10.1002/cncr.20380

Burris, H. A., 3rd, Moore, M. J., Andersen, J., Green, M. R., Rothenberg, M. L., Modiano, M. R., . . . Von Hoff, D. D. (1997). Improvements in survival and clinical benefit with gemcitabine as first-line therapy for patients with advanced pancreas cancer: a randomized trial. *J Clin Oncol, 15*(6), 2403-2413.

Cader, F. Z., Vockerodt, M., Bose, S., Nagy, E., Brundler, M. A., Kearns, P., & Murray, P. G. (2013). The EBV oncogene LMP1 protects lymphoma cells from cell death through the collagen-mediated activation of DDR1. *Blood, 122*(26), 4237-4245. doi: 10.1182/blood-2013-04-499004

Cammerer, G., Formentini, A., Karletshofer, M., Henne-Bruns, D., & Kornmann, M. (2012). Evaluation of important prognostic clinical and pathological factors in gastric cancer. *Anticancer Res, 32*(5), 1839-1842.

Capecchi, M. R. (1989). Altering the genome by homologous recombination. *Science, 244*(4910), 1288-1292.

Carafoli, F., Bihan, D., Stathopoulos, S., Konitsiotis, A. D., Kvansakul, M., Farndale, R. W., . . . Hohenester, E. (2009). Crystallographic insight into collagen recognition by discoidin domain receptor 2. *Structure, 17*(12), 1573-1581. doi: 10.1016/j.str.2009.10.012

Carafoli, F., & Hohenester, E. (2012). Collagen recognition and transmembrane signalling by discoidin domain receptors. *Biochim Biophys Acta*. doi: 10.1016/j.bbapap.2012.10.014

Carafoli, F., Mayer, M. C., Shiraishi, K., Pecheva, M. A., Chan, L. Y., Nan, R., . . . Hohenester, E. (2012). Structure of the discoidin domain receptor 1 extracellular region bound to an inhibitory Fab fragment reveals features important for signaling. *Structure, 20*(4), 688-697. doi: 10.1016/j.str.2012.02.011

Carmeliet, P. (2005). VEGF as a key mediator of angiogenesis in cancer. *Oncology, 69 Suppl 3*, 4-10. doi: 88478 [pii] 10.1159/000088478

Carmeliet, P., & Jain, R. K. (2000). Angiogenesis in cancer and other diseases. *Nature, 407*(6801), 249-257. doi: 10.1038/35025220

Castro-Sanchez, L., Soto-Guzman, A., Navarro-Tito, N., Martinez-Orozco, R., & Salazar, E. P. (2010). Native type IV collagen induces cell migration through a CD9 and DDR1-dependent pathway in MDA-MB-231 breast cancer cells. *Eur J Cell Biol, 89*(11), 843-852. doi: 10.1016/j.ejcb.2010.07.004

Cerami, E., Gao, J., Dogrusoz, U., Gross, B. E., Sumer, S. O., Aksoy, B. A., . . . Schultz, N. (2012). The cBio cancer genomics portal: an open platform for

exploring multidimensional cancer genomics data. *Cancer Discov, 2*(5), 401-404. doi: 10.1158/2159-8290.CD-12-0095

Chae, Y. K., Valsecchi, M. E., Kim, J., Bianchi, A. L., Khemasuwan, D., Desai, A., & Tester, W. (2011). Reduced risk of breast cancer recurrence in patients using ACE inhibitors, ARBs, and/or statins. *Cancer Invest, 29*(9), 585-593. doi: 10.3109/07357907.2011.616252

Chauhan, V. P., Martin, J. D., Liu, H., Lacorre, D. A., Jain, S. R., Kozin, S. V., . . . Jain, R. K. (2013). Angiotensin inhibition enhances drug delivery and potentiates chemotherapy by decompressing tumour blood vessels. *Nat Commun, 4*, 2516. doi: 10.1038/ncomms3516

Chauhan, V. P., Stylianopoulos, T., Boucher, Y., & Jain, R. K. (2011). Delivery of molecular and nanoscale medicine to tumors: transport barriers and strategies. *Annu Rev Chem Biomol Eng, 2*, 281-298. doi: 10.1146/annurev-chembioeng-061010-114300

Cheetham, S., Tang, M. J., Mesak, F., Kennecke, H., Owen, D., & Tai, I. T. (2008). SPARC promoter hypermethylation in colorectal cancers can be reversed by 5-Aza-2'deoxycytidine to increase SPARC expression and improve therapy response. *Br J Cancer, 98*(11), 1810-1819. doi: 10.1038/sj.bjc.6604377

Chen, J., Imanaka, N., & Griffin, J. D. (2010). Hypoxia potentiates Notch signaling in breast cancer leading to decreased E-cadherin expression and increased cell migration and invasion. *Br J Cancer, 102*(2), 351-360. doi: 6605486 [pii] 10.1038/sj.bjc.6605486

Chen, J., Somanath, P. R., Razorenova, O., Chen, W. S., Hay, N., Bornstein, P., & Byzova, T. V. (2005). Akt1 regulates pathological angiogenesis, vascular maturation and permeability in vivo. *Nat Med, 11*(11), 1188-1196. doi: 10.1038/nm1307

Chen, Z. Y., Zhang, J. L., Yao, H. X., Wang, P. Y., Zhu, J., Wang, W., . . . Liu, Y. C. (2014). Aberrant methylation of the SPARC gene promoter and its clinical implication in gastric cancer. *Sci Rep, 4*, 7035. doi: 10.1038/srep07035

Chiaretti, S., Li, X., Gentleman, R., Vitale, A., Wang, K. S., Mandelli, F., . . . Ritz, J. (2005). Gene expression profiles of B-lineage adult acute

lymphocytic leukemia reveal genetic patterns that identify lineage derivation and distinct mechanisms of transformation. *Clin Cancer Res, 11*(20), 7209-7219. doi: 10.1158/1078-0432.CCR-04-2165

Chou, T. C. (2006). Theoretical basis, experimental design, and computerized simulation of synergism and antagonism in drug combination studies. *Pharmacol Rev, 58*(3), 621-681. doi: 10.1124/pr.58.3.10

Clinical practice guidelines for the treatment of unresectable non-small-cell lung cancer. Adopted on May 16, 1997 by the American Society of Clinical Oncology. (1997). *J Clin Oncol, 15*(8), 2996-3018.

Collins, M. A., Bednar, F., Zhang, Y., Brisset, J. C., Galban, S., Galban, C. J., . . . Pasca di Magliano, M. (2012). Oncogenic Kras is required for both the initiation and maintenance of pancreatic cancer in mice. *J Clin Invest, 122*(2), 639-653. doi: 10.1172/JCI59227

Conklin, M. W., & Keely, P. J. (2012). Why the stroma matters in breast cancer: insights into breast cancer patient outcomes through the examination of stromal biomarkers. *Cell Adh Migr, 6*(3), 249-260. doi: 10.4161/cam.20567

Conley, S. J., Gheordunescu, E., Kakarala, P., Newman, B., Korkaya, H., Heath, A. N., . . . Wicha, M. S. (2012). Antiangiogenic agents increase breast cancer stem cells via the generation of tumor hypoxia. *Proc Natl Acad Sci U S A, 109*(8), 2784-2789. doi: 10.1073/pnas.1018866109

Conroy, T., Desseigne, F., Ychou, M., Bouche, O., Guimbaud, R., Becouarn, Y., . . . Intergroup, P. (2011). FOLFIRINOX versus gemcitabine for metastatic pancreatic cancer. *N Engl J Med, 364*(19), 1817-1825. doi: 10.1056/NEJMoa1011923

Cook, N., Frese, K. K., Bapiro, T. E., Jacobetz, M. A., Gopinathan, A., Miller, J. L., . . . Tuveson, D. A. (2012). Gamma secretase inhibition promotes hypoxic necrosis in mouse pancreatic ductal adenocarcinoma. *J Exp Med, 209*(3), 437-444. doi: 10.1084/jem.20111923

Couvelard, A., Hu, J., Steers, G., O'Toole, D., Sauvanet, A., Belghiti, J., . . . Pezzella, F. (2006). Identification of potential therapeutic targets by gene-expression profiling in pancreatic endocrine tumors. *Gastroenterology, 131*(5), 1597-1610. doi: 10.1053/j.gastro.2006.09.007

Croucher, D. R., Hochgrafe, F., Zhang, L., Liu, L., Lyons, R. J., Rickwood, D., . . . Daly, R. J. (2013). Involvement of Lyn and the atypical kinase SgK269/PEAK1 in a basal breast cancer signaling pathway. *Cancer Res, 73*(6), 1969-1980. doi: 10.1158/0008-5472.CAN-12-1472

Cullinan, S. A., Moertel, C. G., Fleming, T. R., Rubin, J. R., Krook, J. E., Everson, L. K., . . . et al. (1985). A comparison of three chemotherapeutic regimens in the treatment of advanced pancreatic and gastric carcinoma. Fluorouracil vs fluorouracil and doxorubicin vs fluorouracil, doxorubicin, and mitomycin. *JAMA, 253*(14), 2061-2067.

Daniels, C. E., Wilkes, M. C., Edens, M., Kottom, T. J., Murphy, S. J., Limper, A. H., & Leof, E. B. (2004). Imatinib mesylate inhibits the profibrogenic activity of TGF-beta and prevents bleomycin-mediated lung fibrosis. *J Clin Invest, 114*(9), 1308-1316. doi: 10.1172/JCI19603

Das, S., Ongusaha, P. P., Yang, Y. S., Park, J. M., Aaronson, S. A., & Lee, S. W. (2006). Discoidin domain receptor 1 receptor tyrosine kinase induces cyclooxygenase-2 and promotes chemoresistance through nuclear factor-kappaB pathway activation. *Cancer Res, 66*(16), 8123-8130. doi: 10.1158/0008-5472.CAN-06-1215

Davies, H., Hunter, C., Smith, R., Stephens, P., Greenman, C., Bignell, G., . . . Futreal, P. A. (2005). Somatic mutations of the protein kinase gene family in human lung cancer. *Cancer Res, 65*(17), 7591-7595. doi: 10.1158/0008-5472.CAN-05-1855

Day, E., Waters, B., Spiegel, K., Alnadaf, T., Manley, P. W., Buchdunger, E., . . . Jarai, G. (2008). Inhibition of collagen-induced discoidin domain receptor 1 and 2 activation by imatinib, nilotinib and dasatinib. *Eur J Pharmacol, 599*(1-3), 44-53. doi: 10.1016/j.ejphar.2008.10.014

Dejmek, J., Dib, K., Jonsson, M., & Andersson, T. (2003). Wnt-5a and G-protein signaling are required for collagen-induced DDR1 receptor activation and normal mammary cell adhesion. *Int J Cancer, 103*(3), 344-351. doi: 10.1002/ijc.10752

Desai, N., Trieu, V., Damascelli, B., & Soon-Shiong, P. (2009). SPARC Expression Correlates with Tumor Response to Albumin-Bound Paclitaxel in Head and Neck Cancer Patients. *Translational Oncology, 2*(2), 59-64. doi: 10.1593/tlo.09109

Di Lorenzo, A., Fernandez-Hernando, C., Cirino, G., & Sessa, W. C. (2009). Akt1 is critical for acute inflammation and histamine-mediated vascular leakage. *Proc Natl Acad Sci U S A, 106*(34), 14552-14557. doi: 10.1073/pnas.0904073106

Di Marco, E., Cutuli, N., Guerra, L., Cancedda, R., & De Luca, M. (1993). Molecular cloning of trkE, a novel trk-related putative tyrosine kinase receptor isolated from normal human keratinocytes and widely expressed by normal human tissues. *J Biol Chem, 268*(32), 24290-24295.

DiMartino, J. F., Lacayo, N. J., Varadi, M., Li, L., Saraiya, C., Ravindranath, Y., . . . Dahl, G. V. (2006). Low or absent SPARC expression in acute myeloid leukemia with MLL rearrangements is associated with sensitivity to growth inhibition by exogenous SPARC protein. *Leukemia, 20*(3), 426-432. doi: 10.1038/sj.leu.2404102

Dineen, S. P., Roland, C. L., Greer, R., Carbon, J. G., Toombs, J. E., Gupta, P., . . . Brekken, R. A. (2010). Smac mimetic increases chemotherapy response and improves survival in mice with pancreatic cancer. *Cancer Res, 70*(7), 2852-2861. doi: 0008-5472.CAN-09-3892 [pii] 10.1158/0008-5472.CAN-09-3892

Ding, L., Getz, G., Wheeler, D. A., Mardis, E. R., McLellan, M. D., Cibulskis, K., . . . Wilson, R. K. (2008). Somatic mutations affect key pathways in lung adenocarcinoma. *Nature, 455*(7216), 1069-1075. doi: 10.1038/nature07423

Diop-Frimpong, B., Chauhan, V. P., Krane, S., Boucher, Y., & Jain, R. K. (2011). Losartan inhibits collagen I synthesis and improves the distribution and efficacy of nanotherapeutics in tumors. *Proc Natl Acad Sci U S A, 108*(7), 2909-2914. doi: 10.1073/pnas.1018892108

Distler, J. H., Jungel, A., Huber, L. C., Schulze-Horsel, U., Zwerina, J., Gay, R. E., . . . Distler, O. (2007). Imatinib mesylate reduces production of extracellular matrix and prevents development of experimental dermal fibrosis. *Arthritis Rheum, 56*(1), 311-322. doi: 10.1002/art.22314

Drilon, A., Rekhtman, N., Ladanyi, M., & Paik, P. (2012). Squamous-cell carcinomas of the lung: emerging biology, controversies, and the promise of targeted therapy. *Lancet Oncol, 13*(10), e418-426. doi: 10.1016/S1470-2045(12)70291-7

Ducreux, M., Mitry, E., Ould-Kaci, M., Boige, V., Seitz, J. F., Bugat, R., . . . Rougier, P. (2004). Randomized phase II study evaluating oxaliplatin alone, oxaliplatin combined with infusional 5-FU, and infusional 5-FU alone in advanced pancreatic carcinoma patients. *Ann Oncol, 15*(3), 467-473.

Ebos, J. M., Lee, C. R., Cruz-Munoz, W., Bjarnason, G. A., Christensen, J. G., & Kerbel, R. S. (2009). Accelerated metastasis after short-term treatment with a potent inhibitor of tumor angiogenesis. *Cancer Cell, 15*(3), 232-239. doi: S1535-6108(09)00029-4 [pii] 10.1016/j.ccr.2009.01.021

Edlund, H. (1999). Pancreas: how to get there from the gut? *Curr Opin Cell Biol, 11*(6), 663-668.

Erkan, M., Kleeff, J., Gorbachevski, A., Reiser, C., Mitkus, T., Esposito, I., . . . Friess, H. (2007). Periostin creates a tumor-supportive microenvironment in the pancreas by sustaining fibrogenic stellate cell activity. *Gastroenterology, 132*(4), 1447-1464. doi: 10.1053/j.gastro.2007.01.031

Erkan, M., Michalski, C. W., Rieder, S., Reiser-Erkan, C., Abiatari, I., Kolb, A., . . . Kleeff, J. (2008). The activated stroma index is a novel and independent prognostic marker in pancreatic ductal adenocarcinoma. *Clin Gastroenterol Hepatol, 6*(10), 1155-1161. doi: 10.1016/j.cgh.2008.05.006

Fang, Z., Grutter, C., & Rauh, D. (2013). Strategies for the selective regulation of kinases with allosteric modulators: exploiting exclusive structural features. *ACS Chem Biol, 8*(1), 58-70. doi: 10.1021/cb300663j

Faraci-Orf, E., McFadden, C., & Vogel, W. F. (2006). DDR1 signaling is essential to sustain Stat5 function during lactogenesis. *J Cell Biochem, 97*(1), 109-121. doi: 10.1002/jcb.20618

Farndale, R. W., Lisman, T., Bihan, D., Hamaia, S., Smerling, C. S., Pugh, N., . . . Raynal, N. (2008). Cell-collagen interactions: the use of peptide Toolkits to investigate collagen-receptor interactions. *Biochem Soc Trans, 36*(Pt 2), 241-250. doi: 10.1042/BST0360241

Feld, R., Rubinstein, L. V., & Weisenberger, T. H. (1984). Sites of recurrence in resected stage I non-small-cell lung cancer: a guide for future studies. *J Clin Oncol, 2*(12), 1352-1358.

Ford, C. E., Lau, S. K., Zhu, C. Q., Andersson, T., Tsao, M. S., & Vogel, W. F. (2007). Expression and mutation analysis of the discoidin domain receptors 1 and 2 in non-small cell lung carcinoma. *Br J Cancer, 96*(5), 808-814. doi: 10.1038/sj.bjc.6603614

Francki, A., McClure, T. D., Brekken, R. A., Motamed, K., Murri, C., Wang, T., & Sage, E. H. (2004). SPARC regulates TGF-beta1-dependent signaling in primary glomerular mesangial cells. *J Cell Biochem, 91*(5), 915-925. doi: 10.1002/jcb.20008

Frese, K. K., Neesse, A., Cook, N., Bapiro, T. E., Lolkema, M. P., Jodrell, D. I., & Tuveson, D. A. (2012). nab-Paclitaxel potentiates gemcitabine activity by reducing cytidine deaminase levels in a mouse model of pancreatic cancer. *Cancer Discov, 2*(3), 260-269. doi: 10.1158/2159-8290.CD-11-0242

Friedman, S. L. (2004). Mechanisms of disease: Mechanisms of hepatic fibrosis and therapeutic implications. *Nat Clin Pract Gastroenterol Hepatol, 1*(2), 98-105. doi: 10.1038/ncpgasthep0055

Friedman, S. L., Sheppard, D., Duffield, J. S., & Violette, S. (2013). Therapy for fibrotic diseases: nearing the starting line. *Sci Transl Med, 5*(167), 167sr161. doi: 10.1126/scitranslmed.3004700

Friess, H., Yamanaka, Y., Buchler, M., Ebert, M., Beger, H. G., Gold, L. I., & Korc, M. (1993). Enhanced expression of transforming growth factor beta isoforms in pancreatic cancer correlates with decreased survival. *Gastroenterology, 105*(6), 1846-1856.

Furuse, J., & Nagashima, F. (2013). Current status and future direction of chemotherapy for pancreatic cancer. *Chin Clin Oncol, 2*(1), 6. doi: 10.3978/j.issn.2304-3865.2012.11.04

Furuyama, K., Kawaguchi, Y., Akiyama, H., Horiguchi, M., Kodama, S., Kuhara, T., . . . Uemoto, S. (2011). Continuous cell supply from a Sox9-expressing progenitor zone in adult liver, exocrine pancreas and intestine. *Nat Genet, 43*(1), 34-41. doi: 10.1038/ng.722

Gao, J., Aksoy, B. A., Dogrusoz, U., Dresdner, G., Gross, B., Sumer, S. O., . . . Schultz, N. (2013). Integrative analysis of complex cancer genomics and

clinical profiles using the cBioPortal. *Sci Signal, 6*(269), pl1. doi: 10.1126/scisignal.2004088

Gao, J., Song, J., Huang, H., Li, Z., Du, Y., Cao, J., . . . Gong, Y. (2010). Methylation of the SPARC gene promoter and its clinical implication in pancreatic cancer. *J Exp Clin Cancer Res*, *29*, 28. doi: 1756-9966-29-28 [pii] 10.1186/1756-9966-29-28

Gao, M., Duan, L., Luo, J., Zhang, L., Lu, X., Zhang, Y., . . . Ding, K. (2013). Discovery and optimization of 3-(2-(Pyrazolo[1,5-a]pyrimidin-6-yl)ethynyl)benzamides as novel selective and orally bioavailable discoidin domain receptor 1 (DDR1) inhibitors. *J Med Chem, 56*(8), 3281-3295. doi: 10.1021/jm301824k

Garcia-Trevijano, E. R., Iraburu, M. J., Fontana, L., Dominguez-Rosales, J. A., Auster, A., Covarrubias-Pinedo, A., & Rojkind, M. (1999). Transforming growth factor beta1 induces the expression of alpha1(I) procollagen mRNA by a hydrogen peroxide-C/EBPbeta-dependent mechanism in rat hepatic stellate cells. *Hepatology, 29*(3), 960-970. doi: 10.1002/hep.510290346

Garrett, C. R., Coppola, D., Wenham, R. M., Cubitt, C. L., Neuger, A. M., Frost, T. J., . . . Sebti, S. M. (2011). Phase I pharmacokinetic and pharmacodynamic study of triciribine phosphate monohydrate, a small-molecule inhibitor of AKT phosphorylation, in adult subjects with solid tumors containing activated AKT. *Invest New Drugs*, *29*(6), 1381-1389. doi: 10.1007/s10637-010-9479-2

Ghaneh, P., Costello, E., & Neoptolemos, J. P. (2007). Biology and management of pancreatic cancer. *Gut, 56*(8), 1134-1152. doi: 56/8/1134 [pii] 10.1136/gut.2006.103333

Goc, A., Choudhary, M., Byzova, T. V., & Somanath, P. R. (2011). TGFbeta- and bleomycin-induced extracellular matrix synthesis is mediated through Akt and mammalian target of rapamycin (mTOR). *J Cell Physiol*, *226*(11), 3004-3013. doi: 10.1002/jcp.22648

Greenberg, R. A., Chin, L., Femino, A., Lee, K. H., Gottlieb, G. J., Singer, R. H., . . . DePinho, R. A. (1999). Short dysfunctional telomeres impair tumorigenesis in the INK4a(delta2/3) cancer-prone mouse. *Cell*, *97*(4), 515-525.

Gressner, A. M., & Weiskirchen, R. (2006). Modern pathogenetic concepts of liver fibrosis suggest stellate cells and TGF-beta as major players and therapeutic targets. *J Cell Mol Med, 10*(1), 76-99.

Griffon-Etienne, G., Boucher, Y., Brekken, C., Suit, H. D., & Jain, R. K. (1999). Taxane-induced apoptosis decompresses blood vessels and lowers interstitial fluid pressure in solid tumors: clinical implications. *Cancer Res, 59*(15), 3776-3782.

Gross, O., Girgert, R., Beirowski, B., Kretzler, M., Kang, H. G., Kruegel, J., . . . Weber, M. (2010). Loss of collagen-receptor DDR1 delays renal fibrosis in hereditary type IV collagen disease. *Matrix Biol, 29*(5), 346-356. doi: 10.1016/j.matbio.2010.03.002

Grzesiak, J. J., Ho, J. C., Moossa, A. R., & Bouvet, M. (2007). The integrin-extracellular matrix axis in pancreatic cancer. *Pancreas, 35*(4), 293-301. doi: 10.1097/mpa.0b013e31811f452600006676-200711000-00001 [pii]

Gschwind, A., Fischer, O. M., & Ullrich, A. (2004). The discovery of receptor tyrosine kinases: targets for cancer therapy. *Nat Rev Cancer, 4*(5), 361-370. doi: 10.1038/nrc1360

Gyorffy, B., Surowiak, P., Budczies, J., & Lanczky, A. (2013). Online survival analysis software to assess the prognostic value of biomarkers using transcriptomic data in non-small-cell lung cancer. *PLoS One, 8*(12), e82241. doi: 10.1371/journal.pone.0082241

Habashi, J. P., Judge, D. P., Holm, T. M., Cohn, R. D., Loeys, B. L., Cooper, T. K., . . . Dietz, H. C. (2006). Losartan, an AT1 antagonist, prevents aortic aneurysm in a mouse model of Marfan syndrome. *Science, 312*(5770), 117-121. doi: 10.1126/science.1124287

Hamada, S., Masamune, A., & Shimosegawa, T. (2013). Novel therapeutic strategies targeting tumor-stromal interactions in pancreatic cancer. *Front Physiol, 4*, 331. doi: 10.3389/fphys.2013.00331

Hammerman, P. S., Sos, M. L., Ramos, A. H., Xu, C., Dutt, A., Zhou, W., . . . Meyerson, M. (2011). Mutations in the DDR2 kinase gene identify a novel therapeutic target in squamous cell lung cancer. *Cancer Discov, 1*(1), 78-89. doi: 10.1158/2159-8274.CD-11-0005

Hanahan, D., & Weinberg, R. A. (2000). The hallmarks of cancer. *Cell, 100*(1), 57-70.

Harris, B. S., Zhang, Y., Card, L., Rivera, L. B., Brekken, R. A., & Bradshaw, A. D. (2011). SPARC regulates collagen interaction with cardiac fibroblast cell surfaces. *Am J Physiol Heart Circ Physiol, 301*(3), H841-847. doi: ajpheart.01247.2010 [pii] 10.1152/ajpheart.01247.2010

Hasselaar, P., & Sage, E. H. (1992). SPARC antagonizes the effect of basic fibroblast growth factor on the migration of bovine aortic endothelial cells. *J Cell Biochem, 49*(3), 272-283. doi: 10.1002/jcb.240490310

Heinemann, V., Reni, M., Ychou, M., Richel, D. J., Macarulla, T., & Ducreux, M. (2014). Tumour-stroma interactions in pancreatic ductal adenocarcinoma: rationale and current evidence for new therapeutic strategies. *Cancer Treat Rev, 40*(1), 118-128. doi: 10.1016/j.ctrv.2013.04.004

Heinmoller, E., Dietmaier, W., Zirngibl, H., Heinmoller, P., Scaringe, W., Jauch, K. W., . . . Ruschoff, J. (2000). Molecular analysis of microdissected tumors and preneoplastic intraductal lesions in pancreatic carcinoma. *Am J Pathol, 157*(1), 83-92. doi: 10.1016/S0002-9440(10)64520-8

Heinzelmann-Schwarz, V. A., Gardiner-Garden, M., Henshall, S. M., Scurry, J., Scolyer, R. A., Davies, M. J., . . . O'Brien, P. M. (2004). Overexpression of the cell adhesion molecules DDR1, Claudin 3, and Ep-CAM in metaplastic ovarian epithelium and ovarian cancer. *Clin Cancer Res, 10*(13), 4427-4436. doi: 10.1158/1078-0432.CCR-04-0073

Heller, G., Schmidt, W. M., Ziegler, B., Holzer, S., Mullauer, L., Bilban, M., . . . Zochbauer-Muller, S. (2008). Genome-wide transcriptional response to 5-aza-2'-deoxycytidine and trichostatin a in multiple myeloma cells. *Cancer Res, 68*(1), 44-54. doi: 10.1158/0008-5472.CAN-07-2531

Helmlinger, G., Netti, P. A., Lichtenbeld, H. C., Melder, R. J., & Jain, R. K. (1997). Solid stress inhibits the growth of multicellular tumor spheroids. *Nat Biotechnol, 15*(8), 778-783. doi: 10.1038/nbt0897-778

Hezel, A. F., Deshpande, V., Zimmerman, S. M., Contino, G., Alagesan, B., O'Dell, M. R., . . . Bardeesy, N. (2012). TGF-beta and alphavbeta6 integrin act in a common pathway to suppress pancreatic cancer

progression. *Cancer Res, 72*(18), 4840-4845. doi: 10.1158/0008-5472.CAN-12-0634

Hezel, A. F., Kimmelman, A. C., Stanger, B. Z., Bardeesy, N., & Depinho, R. A. (2006). Genetics and biology of pancreatic ductal adenocarcinoma. *Genes Dev, 20*(10), 1218-1249. doi: 10.1101/gad.1415606

Hingorani, S. R., Petricoin, E. F., Maitra, A., Rajapakse, V., King, C., Jacobetz, M. A., . . . Tuveson, D. A. (2003). Preinvasive and invasive ductal pancreatic cancer and its early detection in the mouse. *Cancer Cell, 4*(6), 437-450.

Hingorani, S. R., Wang, L., Multani, A. S., Combs, C., Deramaudt, T. B., Hruban, R. H., . . . Tuveson, D. A. (2005). Trp53R172H and KrasG12D cooperate to promote chromosomal instability and widely metastatic pancreatic ductal adenocarcinoma in mice. *Cancer Cell, 7*(5), 469-483. doi: 10.1016/j.ccr.2005.04.023

Hoffman, P. C., Mauer, A. M., & Vokes, E. E. (2000). Lung cancer. *Lancet, 355*(9202), 479-485. doi: S0140-6736(00)82038-3 [pii] 10.1016/S0140-6736(00)82038-3

Hruban, R. H., Adsay, N. V., Albores-Saavedra, J., Anver, M. R., Biankin, A. V., Boivin, G. P., . . . Tuveson, D. A. (2006). Pathology of genetically engineered mouse models of pancreatic exocrine cancer: consensus report and recommendations. *Cancer Res, 66*(1), 95-106. doi: 10.1158/0008-5472.CAN-05-2168

Hruban, R. H., Adsay, N. V., Albores-Saavedra, J., Compton, C., Garrett, E. S., Goodman, S. N., . . . Offerhaus, G. J. (2001). Pancreatic intraepithelial neoplasia: a new nomenclature and classification system for pancreatic duct lesions. *Am J Surg Pathol, 25*(5), 579-586.

Hruban, R. H., Iacobuzio-Donahue, C., Wilentz, R. E., Goggins, M., & Kern, S. E. (2001). Molecular pathology of pancreatic cancer. *Cancer J, 7*(4), 251-258.

Hruban, R. H., Wilentz, R. E., Goggins, M., Offerhaus, G. J., Yeo, C. J., & Kern, S. E. (1999). Pathology of incipient pancreatic cancer. *Ann Oncol, 10 Suppl 4*, 9-11.

Hubbard, R., Venn, A., Lewis, S., & Britton, J. (2000). Lung cancer and cryptogenic fibrosing alveolitis. A population-based cohort study. *Am J Respir Crit Care Med, 161*(1), 5-8. doi: 10.1164/ajrccm.161.1.9906062

Hustinx, S. R., Leoni, L. M., Yeo, C. J., Brown, P. N., Goggins, M., Kern, S. E., . . . Maitra, A. (2005). Concordant loss of MTAP and p16/CDKN2A expression in pancreatic intraepithelial neoplasia: evidence of homozygous deletion in a noninvasive precursor lesion. *Mod Pathol, 18*(7), 959-963. doi: 10.1038/modpathol.3800377

Hwang, J. C., Del Priore, L. V., Freund, K. B., Chang, S., & Iranmanesh, R. (2011). Development of subretinal fibrosis after anti-VEGF treatment in neovascular age-related macular degeneration. *Ophthalmic Surg Lasers Imaging, 42*(1), 6-11. doi: 10.3928/15428877-20100924-01

Iacobuzio-Donahue, C. A., Velculescu, V. E., Wolfgang, C. L., & Hruban, R. H. (2012). Genetic basis of pancreas cancer development and progression: insights from whole-exome and whole-genome sequencing. *Clin Cancer Res, 18*(16), 4257-4265. doi: 10.1158/1078-0432.CCR-12-0315

Ikeda, K., Wang, L. H., Torres, R., Zhao, H., Olaso, E., Eng, F. J., . . . Lin, H. C. (2002). Discoidin domain receptor 2 interacts with Src and Shc following its activation by type I collagen. *J Biol Chem, 277*(21), 19206-19212. doi: 10.1074/jbc.M201078200

Iwai, L. K., Chang, F., & Huang, P. H. (2013). Phosphoproteomic analysis identifies insulin enhancement of discoidin domain receptor 2 phosphorylation. *Cell Adh Migr, 7*(2), 161-164. doi: 10.4161/cam.22572

Jacobetz, M. A., Chan, D. S., Neesse, A., Bapiro, T. E., Cook, N., Frese, K. K., . . . Tuveson, D. A. (2013). Hyaluronan impairs vascular function and drug delivery in a mouse model of pancreatic cancer. *Gut, 62*(1), 112-120. doi: 10.1136/gutjnl-2012-302529

Jain, R. K. (2013). Normalizing tumor microenvironment to treat cancer: bench to bedside to biomarkers. *J Clin Oncol, 31*(17), 2205-2218. doi: 10.1200/JCO.2012.46.3653

Jemal, A., Bray, F., Center, M. M., Ferlay, J., Ward, E., & Forman, D. (2011). Global cancer statistics. *CA Cancer J Clin, 61*(2), 69-90. doi: caac.20107 [pii] 10.3322/caac.20107

Jemal, A., Siegel, R., Xu, J., & Ward, E. (2010). Cancer statistics, 2010. *CA Cancer J Clin, 60*(5), 277-300. doi: caac.20073 [pii] 10.3322/caac.20073

Jemal, A., Thun, M. J., Ries, L. A., Howe, H. L., Weir, H. K., Center, M. M., . . . Edwards, B. K. (2008). Annual report to the nation on the status of cancer, 1975-2005, featuring trends in lung cancer, tobacco use, and tobacco control. *J Natl Cancer Inst, 100*(23), 1672-1694. doi: 10.1093/jnci/djn389

Jian, Z. X., Sun, J., Chen, W., Jin, H. S., Zheng, J. H., & Wu, Y. L. (2012). Involvement of discoidin domain 1 receptor in recurrence of hepatocellular carcinoma by genome-wide analysis. *Med Oncol, 29*(5), 3077-3082. doi: 10.1007/s12032-012-0277-x

Johnson, J. D., Edman, J. C., & Rutter, W. J. (1993). A receptor tyrosine kinase found in breast carcinoma cells has an extracellular discoidin I-like domain. *Proc Natl Acad Sci U S A, 90*(12), 5677-5681.

Jones, S., Zhang, X., Parsons, D. W., Lin, J. C., Leary, R. J., Angenendt, P., . . . Kinzler, K. W. (2008). Core signaling pathways in human pancreatic cancers revealed by global genomic analyses. *Science, 321*(5897), 1801-1806. doi: 10.1126/science.1164368

Kadler, K. E., Baldock, C., Bella, J., & Boot-Handford, R. P. (2007). Collagens at a glance. *Journal of Cell Science, 120*(12), 1955-1958. doi: Doi 10.1242/Jcs.03453

Kalluri, R., & Zeisberg, M. (2006). Fibroblasts in cancer. *Nat Rev Cancer, 6*(5), 392-401. doi: 10.1038/nrc1877

Kano, K., Marin de Evsikova, C., Young, J., Wnek, C., Maddatu, T. P., Nishina, P. M., & Naggert, J. K. (2008). A novel dwarfism with gonadal dysfunction due to loss-of-function allele of the collagen receptor gene, Ddr2, in the mouse. *Mol Endocrinol, 22*(8), 1866-1880. doi: 10.1210/me.2007-0310

Karn, T., Holtrich, U., Brauninger, A., Bohme, B., Wolf, G., Rubsamen-Waigmann, H., & Strebhardt, K. (1993). Structure, expression and chromosomal mapping of TKT from man and mouse: a new subclass of receptor tyrosine kinases with a factor VIII-like domain. *Oncogene, 8*(12), 3433-3440.

Keizman, D., Huang, P., Eisenberger, M. A., Pili, R., Kim, J. J., Antonarakis, E. S., . . . Carducci, M. A. (2011). Angiotensin system inhibitors and outcome of sunitinib treatment in patients with metastatic renal cell carcinoma: a retrospective examination. *Eur J Cancer, 47*(13), 1955-1961. doi: 10.1016/j.ejca.2011.04.019

Kelber, J. A., & Klemke, R. L. (2010). PEAK1, a novel kinase target in the fight against cancer. *Oncotarget, 1*(3), 219-223.

Kelber, J. A., Reno, T., Kaushal, S., Metildi, C., Wright, T., Stoletov, K., . . . Klemke, R. L. (2012). KRas induces a Src/PEAK1/ErbB2 kinase amplification loop that drives metastatic growth and therapy resistance in pancreatic cancer. *Cancer Res, 72*(10), 2554-2564. doi: 10.1158/0008-5472.CAN-11-3552

Kerroch, M., Guerrot, D., Vandermeersch, S., Placier, S., Mesnard, L., Jouanneau, C., . . . Dussaule, J. C. (2012). Genetic inhibition of discoidin domain receptor 1 protects mice against crescentic glomerulonephritis. *FASEB J, 26*(10), 4079-4091. doi: 10.1096/fj.11-194902

Keunen, O., Johansson, M., Oudin, A., Sanzey, M., Rahim, S. A., Fack, F., . . . Niclou, S. P. (2011). Anti-VEGF treatment reduces blood supply and increases tumor cell invasion in glioblastoma. *Proc Natl Acad Sci U S A, 108*(9), 3749-3754. doi: 1014480108 [pii] 10.1073/pnas.1014480108

Khosravi, R., Sodek, K. L., Faibish, M., & Trackman, P. C. (2014). Collagen advanced glycation inhibits its Discoidin Domain Receptor 2 (DDR2)-mediated induction of lysyl oxidase in osteoblasts. *Bone, 58*, 33-41. doi: 10.1016/j.bone.2013.10.001

Kim, H. G., Hwang, S. Y., Aaronson, S. A., Mandinova, A., & Lee, S. W. (2011). DDR1 receptor tyrosine kinase promotes prosurvival pathway through Notch1 activation. *J Biol Chem, 286*(20), 17672-17681. doi: 10.1074/jbc.M111.236612

Klimstra, D. S., & Longnecker, D. S. (1994). K-ras mutations in pancreatic ductal proliferative lesions. *Am J Pathol, 145*(6), 1547-1550.

Koay, E. J., Truty, M. J., Cristini, V., Thomas, R. M., Chen, R., Chatterjee, D., . . . Fleming, J. B. (2014). Transport properties of pancreatic cancer describe

gemcitabine delivery and response. *J Clin Invest, 124*(4), 1525-1536. doi: 10.1172/JCI73455

Konitsiotis, A. D., Raynal, N., Bihan, D., Hohenester, E., Farndale, R. W., & Leitinger, B. (2008). Characterization of high affinity binding motifs for the discoidin domain receptor DDR2 in collagen. *J Biol Chem, 283*(11), 6861-6868. doi: 10.1074/jbc.M709290200

Koo, D. H., McFadden, C., Huang, Y., Abdulhussein, R., Friese-Hamim, M., & Vogel, W. F. (2006). Pinpointing phosphotyrosine-dependent interactions downstream of the collagen receptor DDR1. *FEBS Lett, 580*(1), 15-22. doi: 10.1016/j.febslet.2005.11.035

Kotch, F. W., Guzei, I. A., & Raines, R. T. (2008). Stabilization of the collagen triple helix by O-methylation of hydroxyproline residues. *J Am Chem Soc, 130*(10), 2952-2953. doi: 10.1021/ja800225k

Kothiwale, S., Borza, C. M., Lowe, E. W., Jr., Pozzi, A., & Meiler, J. (2014). Discoidin domain receptor 1 (DDR1) kinase as target for structure-based drug discovery. *Drug Discov Today*. doi: 10.1016/j.drudis.2014.09.025

Kumar, P., Goldstraw, P., Yamada, K., Nicholson, A. G., Wells, A. U., Hansell, D. M., . . . Ladas, G. (2003). Pulmonary fibrosis and lung cancer: risk and benefit analysis of pulmonary resection. *J Thorac Cardiovasc Surg, 125*(6), 1321-1327.

Kupprion, C., Motamed, K., & Sage, E. H. (1998). SPARC (BM-40, osteonectin) inhibits the mitogenic effect of vascular endothelial growth factor on microvascular endothelial cells. *J Biol Chem, 273*(45), 29635-29640.

Labrador, J. P., Azcoitia, V., Tuckermann, J., Lin, C., Olaso, E., Manes, S., . . . Klein, R. (2001). The collagen receptor DDR2 regulates proliferation and its elimination leads to dwarfism. *EMBO Rep, 2*(5), 446-452. doi: 10.1093/embo-reports/kve094

Lai, C., & Lemke, G. (1994). Structure and expression of the Tyro 10 receptor tyrosine kinase. *Oncogene, 9*(3), 877-883.

Lane, T. F., Iruela-Arispe, M. L., & Sage, E. H. (1992). Regulation of gene expression by SPARC during angiogenesis in vitro. Changes in

fibronectin, thrombospondin-1, and plasminogen activator inhibitor-1. *J Biol Chem, 267*(23), 16736-16745.

Lauren, P. (1965). The Two Histological Main Types of Gastric Carcinoma: Diffuse and So-Called Intestinal-Type Carcinoma. An Attempt at a Histo-Clinical Classification. *Acta Pathol Microbiol Scand, 64*, 31-49.

Laval, S., Butler, R., Shelling, A. N., Hanby, A. M., Poulsom, R., & Ganesan, T. S. (1994). Isolation and characterization of an epithelial-specific receptor tyrosine kinase from an ovarian cancer cell line. *Cell Growth Differ, 5*(11), 1173-1183.

Leach, S. D. (2004). Mouse models of pancreatic cancer: the fur is finally flying! *Cancer Cell, 5*(1), 7-11.

Lee, S., Hwang, K. S., Lee, H. J., Kim, J. S., & Kang, G. H. (2004). Aberrant CpG island hypermethylation of multiple genes in colorectal neoplasia. *Lab Invest, 84*(7), 884-893. doi: 10.1038/labinvest.3700108

Leitinger, B. (2003). Molecular analysis of collagen binding by the human discoidin domain receptors, DDR1 and DDR2. Identification of collagen binding sites in DDR2. *J Biol Chem, 278*(19), 16761-16769. doi: 10.1074/jbc.M301370200

Leitinger, B. (2014). Discoidin domain receptor functions in physiological and pathological conditions. *Int Rev Cell Mol Biol, 310*, 39-87. doi: 10.1016/B978-0-12-800180-6.00002-5

Leitinger, B., & Kwan, A. P. (2006). The discoidin domain receptor DDR2 is a receptor for type X collagen. *Matrix Biol, 25*(6), 355-364. doi: 10.1016/j.matbio.2006.05.006

Lemeer, S., Bluwstein, A., Wu, Z., Leberfinger, J., Muller, K., Kramer, K., & Kuster, B. (2012). Phosphotyrosine mediated protein interactions of the discoidin domain receptor 1. *J Proteomics, 75*(12), 3465-3477. doi: 10.1016/j.jprot.2011.10.007

Lemmon, M. A., & Schlessinger, J. (2010). Cell signaling by receptor tyrosine kinases. *Cell, 141*(7), 1117-1134. doi: 10.1016/j.cell.2010.06.011

Li, X., Ma, Q., Xu, Q., Duan, W., Lei, J., & Wu, E. (2012). Targeting the cancer-stroma interaction: a potential approach for pancreatic cancer treatment. *Curr Pharm Des*, *18*(17), 2404-2415.

Li, Y., Lu, X., Ren, X., & Ding, K. (2015). Small Molecule Discoidin Domain Receptor Kinase Inhibitors and Potential Medical Applications. *J Med Chem*. doi: 10.1021/jm5012319

Lin, K. L., Chou, C. H., Hsieh, S. C., Hwa, S. Y., Lee, M. T., & Wang, F. F. (2010). Transcriptional upregulation of DDR2 by ATF4 facilitates osteoblastic differentiation through p38 MAPK-mediated Runx2 activation. *J Bone Miner Res*, *25*(11), 2489-2503. doi: 10.1002/jbmr.159

Lindner, J. L., Loibl, S., Denkert, C., Ataseven, B., Fasching, P. A., Pfitzner, B. M., . . . von Minckwitz, G. (2015). Expression of secreted protein acidic and rich in cysteine (SPARC) in breast cancer and response to neoadjuvant chemotherapy. *Ann Oncol*, *26*(1), 95-100. doi: 10.1093/annonc/mdu487

Liu, H., Ma, Q., Xu, Q., Lei, J., Li, X., Wang, Z., & Wu, E. (2012). Therapeutic potential of perineural invasion, hypoxia and desmoplasia in pancreatic cancer. *Curr Pharm Des*, *18*(17), 2395-2403.

Liu, J., Liao, S., Diop-Frimpong, B., Chen, W., Goel, S., Naxerova, K., . . . Xu, L. (2012). TGF-beta blockade improves the distribution and efficacy of therapeutics in breast carcinoma by normalizing the tumor stroma. *Proc Natl Acad Sci U S A*, *109*(41), 16618-16623. doi: 10.1073/pnas.1117610109

Lohr, J. M., & Jesnowski, R. (2009). Pancreatic stellate cells and pancreatic carcinoma: an unholy alliance. *JOP*, *10*(4), 472-473.

Lohr, M., Schmidt, C., Ringel, J., Kluth, M., Muller, P., Nizze, H., & Jesnowski, R. (2001). Transforming growth factor-beta1 induces desmoplasia in an experimental model of human pancreatic carcinoma. *Cancer Res*, *61*(2), 550-555.

Louvet, C., Andre, T., Lledo, G., Hammel, P., Bleiberg, H., Bouleuc, C., . . . de Gramont, A. (2002). Gemcitabine combined with oxaliplatin in advanced pancreatic adenocarcinoma: final results of a GERCOR multicenter phase II study. *J Clin Oncol*, *20*(6), 1512-1518.

Louvet, C., Labianca, R., Hammel, P., Lledo, G., Zampino, M. G., Andre, T., . . . Giscad. (2005). Gemcitabine in combination with oxaliplatin compared with gemcitabine alone in locally advanced or metastatic pancreatic cancer: results of a GERCOR and GISCAD phase III trial. *J Clin Oncol, 23*(15), 3509-3516. doi: 10.1200/JCO.2005.06.023

Lu, K. K., Trcka, D., & Bendeck, M. P. (2011). Collagen stimulates discoidin domain receptor 1-mediated migration of smooth muscle cells through Src. *Cardiovasc Pathol, 20*(2), 71-76. doi: 10.1016/j.carpath.2009.12.006

Luo, Y., He, D. L., Ning, L., Shen, S. L., Li, L., Li, X., . . . Chung, L. W. (2006). Over-expression of hypoxia-inducible factor-1alpha increases the invasive potency of LNCaP cells in vitro. *BJU Int, 98*(6), 1315-1319. doi: BJU6480 [pii] 10.1111/j.1464-410X.2006.06480.x

Ma, W. W., & Hidalgo, M. (2013). The winning formulation: the development of paclitaxel in pancreatic cancer. *Clin Cancer Res, 19*(20), 5572-5579. doi: 10.1158/1078-0432.CCR-13-1356

Maass, N., Schem, C., Bauerschlag, D. O., Tiemann, K., Schaefer, F. W., Hanson, S., . . . Mundhenke, C. (2014). Final safety and efficacy analysis of a phase I/II trial with imatinib and vinorelbine for patients with metastatic breast cancer. *Oncology, 87*(5), 300-310. doi: 10.1159/000365553

Mahadevan, D., & Von Hoff, D. D. (2007). Tumor-stroma interactions in pancreatic ductal adenocarcinoma. *Mol Cancer Ther, 6*(4), 1186-1197. doi: 10.1158/1535-7163.MCT-06-0686

Maitra, A., Adsay, N. V., Argani, P., Iacobuzio-Donahue, C., De Marzo, A., Cameron, J. L., . . . Hruban, R. H. (2003). Multicomponent analysis of the pancreatic adenocarcinoma progression model using a pancreatic intraepithelial neoplasia tissue microarray. *Mod Pathol, 16*(9), 902-912. doi: 10.1097/01.MP.0000086072.56290.FB

Mann, K., Deutzmann, R., Paulsson, M., & Timpl, R. (1987). Solubilization of protein BM-40 from a basement membrane tumor with chelating agents and evidence for its identity with osteonectin and SPARC. *FEBS Lett, 218*(1), 167-172.

Melisi, D., Ishiyama, S., Sclabas, G. M., Fleming, J. B., Xia, Q., Tortora, G., . . . Chiao, P. J. (2008). LY2109761, a novel transforming growth factor beta

receptor type I and type II dual inhibitor, as a therapeutic approach to suppressing pancreatic cancer metastasis. *Mol Cancer Ther, 7*(4), 829-840. doi: 10.1158/1535-7163.MCT-07-0337

Mendis, D. B., Ivy, G. O., & Brown, I. R. (1998). SPARC/osteonectin mRNA is induced in blood vessels following injury to the adult rat cerebral cortex. *Neurochem Res, 23*(8), 1117-1123.

Meyer zum Gottesberge, A. M., Gross, O., Becker-Lendzian, U., Massing, T., & Vogel, W. F. (2008). Inner ear defects and hearing loss in mice lacking the collagen receptor DDR1. *Lab Invest, 88*(1), 27-37. doi: 10.1038/labinvest.3700692

Miao, L., Zhu, S., Wang, Y., Li, Y., Ding, J., Dai, J., . . . Song, Y. (2013). Discoidin domain receptor 1 is associated with poor prognosis of non-small cell lung cancer and promotes cell invasion via epithelial-to-mesenchymal transition. *Med Oncol, 30*(3), 626. doi: 10.1007/s12032-013-0626-4

Michl, P., & Gress, T. M. (2012). Improving drug delivery to pancreatic cancer: breaching the stromal fortress by targeting hyaluronic acid. *Gut, 61*(10), 1377-1379. doi: 10.1136/gutjnl-2012-302604

Mills, C. N., Joshi, S. S., & Niles, R. M. (2009). Expression and function of hypoxia inducible factor-1 alpha in human melanoma under non-hypoxic conditions. *Mol Cancer, 8*, 104. doi: 1476-4598-8-104 [pii] 10.1186/1476-4598-8-104

Mitchell, D. C., & Bryan, B. A. (2010). Anti-angiogenic therapy: adapting strategies to overcome resistant tumors. *J Cell Biochem, 111*(3), 543-553. doi: 10.1002/jcb.22764

Moertel, C. G. (1978). Chemotherapy of gastrointestinal cancer. *N Engl J Med, 299*(19), 1049-1052. doi: 10.1056/NEJM197811092991906

Moore, M. J., Goldstein, D., Hamm, J., Figer, A., Hecht, J. R., Gallinger, S., . . . National Cancer Institute of Canada Clinical Trials, G. (2007). Erlotinib plus gemcitabine compared with gemcitabine alone in patients with advanced pancreatic cancer: a phase III trial of the National Cancer Institute of Canada Clinical Trials Group. *J Clin Oncol, 25*(15), 1960-1966. doi: 10.1200/JCO.2006.07.9525

Naito, T., Masaki, T., Nikolic-Paterson, D. J., Tanji, C., Yorioka, N., & Kohno, N. (2004). Angiotensin II induces thrombospondin-1 production in human mesangial cells via p38 MAPK and JNK: a mechanism for activation of latent TGF-beta1. *Am J Physiol Renal Physiol, 286*(2), F278-287. doi: 10.1152/ajprenal.00139.2003

Nakai, Y., Isayama, H., Ijichi, H., Sasaki, T., Sasahira, N., Hirano, K., . . . Koike, K. (2010). Inhibition of renin-angiotensin system affects prognosis of advanced pancreatic cancer receiving gemcitabine. *Br J Cancer, 103*(11), 1644-1648. doi: 10.1038/sj.bjc.6605955

Neesse, A., Algul, H., Tuveson, D. A., & Gress, T. M. (2015). Stromal biology and therapy in pancreatic cancer: a changing paradigm. *Gut*. doi: 10.1136/gutjnl-2015-309304

Neesse, A., Frese, K. K., Chan, D. S., Bapiro, T. E., Howat, W. J., Richards, F. M., . . . Tuveson, D. A. (2014). SPARC independent drug delivery and antitumour effects of nab-paclitaxel in genetically engineered mice. *Gut, 63*(6), 974-983. doi: 10.1136/gutjnl-2013-305559

Neesse, A., Michl, P., Frese, K. K., Feig, C., Cook, N., Jacobetz, M. A., . . . Tuveson, D. A. (2011). Stromal biology and therapy in pancreatic cancer. *Gut, 60*(6), 861-868. doi: 10.1136/gut.2010.226092

Nguyen, D. X., Bos, P. D., & Massague, J. (2009). Metastasis: from dissemination to organ-specific colonization. *Nat Rev Cancer, 9*(4), 274-284. doi: nrc2622 [pii] 10.1038/nrc2622

Niskakoski, A., Kaur, S., Staff, S., Renkonen-Sinisalo, L., Lassus, H., Jarvinen, H. J., . . . Peltomaki, P. (2014). Epigenetic analysis of sporadic and Lynch-associated ovarian cancers reveals histology-specific patterns of DNA methylation. *Epigenetics, 9*(12), 1577-1587. doi: 10.4161/15592294.2014.983374

Nolan-Stevaux, O., Lau, J., Truitt, M. L., Chu, G. C., Hebrok, M., Fernandez-Zapico, M. E., & Hanahan, D. (2009). GLI1 is regulated through Smoothened-independent mechanisms in neoplastic pancreatic ducts and mediates PDAC cell survival and transformation. *Genes Dev, 23*(1), 24-36. doi: 10.1101/gad.1753809

Okusaka, T., Furuse, J., Funakoshi, A., Ioka, T., Yamao, K., Ohkawa, S., . . . Nakachi, K. (2011). Phase II study of erlotinib plus gemcitabine in Japanese patients with unresectable pancreatic cancer. *Cancer Sci, 102*(2), 425-431. doi: 10.1111/j.1349-7006.2010.01810.x

Olive, K. P., Jacobetz, M. A., Davidson, C. J., Gopinathan, A., McIntyre, D., Honess, D., . . . Tuveson, D. A. (2009). Inhibition of Hedgehog signaling enhances delivery of chemotherapy in a mouse model of pancreatic cancer. *Science, 324*(5933), 1457-1461. doi: 10.1126/science.1171362

Ongusaha, P. P., Kim, J. I., Fang, L., Wong, T. W., Yancopoulos, G. D., Aaronson, S. A., & Lee, S. W. (2003). p53 induction and activation of DDR1 kinase counteract p53-mediated apoptosis and influence p53 regulation through a positive feedback loop. *EMBO J, 22*(6), 1289-1301. doi: 10.1093/emboj/cdg129

Ostapoff, K. T., Awasthi, N., Cenik, B. K., Hinz, S., Dredge, K., Schwarz, R. E., & Brekken, R. A. (2013). PG545, an angiogenesis and heparanase inhibitor, reduces primary tumor growth and metastasis in experimental pancreatic cancer. *Mol Cancer Ther, 12*(7), 1190-1201. doi: 10.1158/1535-7163.MCT-12-1123

Ostapoff, K. T., Cenik, B. K., Wang, M., Ye, R., Xu, X., Nugent, D., . . . Brekken, R. A. (2014). Neutralizing murine TGFbetaR2 promotes a differentiated tumor cell phenotype and inhibits pancreatic cancer metastasis. *Cancer Res, 74*(18), 4996-5007. doi: 10.1158/0008-5472.CAN-13-1807

Otsuji, E., Kuriu, Y., Okamoto, K., Ochiai, T., Ichikawa, D., Hagiwara, A., & Yamagishi, H. (2004). Outcome of surgical treatment for patients with scirrhous carcinoma of the stomach. *Am J Surg, 188*(3), 327-332. doi: 10.1016/j.amjsurg.2004.06.010

Over, B., Wetzel, S., Grutter, C., Nakai, Y., Renner, S., Rauh, D., & Waldmann, H. (2013). Natural-product-derived fragments for fragment-based ligand discovery. *Nat Chem, 5*(1), 21-28. doi: 10.1038/nchem.1506

Oza, A. M., & Boyd, N. F. (1993). Mammographic parenchymal patterns: a marker of breast cancer risk. *Epidemiol Rev, 15*(1), 196-208.

Ozdemir, B. C., Pentcheva-Hoang, T., Carstens, J. L., Zheng, X., Wu, C. C., Simpson, T. R., . . . Kalluri, R. (2014). Depletion of carcinoma-associated

fibroblasts and fibrosis induces immunosuppression and accelerates pancreas cancer with reduced survival. *Cancer Cell, 25*(6), 719-734. doi: 10.1016/j.ccr.2014.04.005

Padera, T. P., Stoll, B. R., Tooredman, J. B., Capen, D., di Tomaso, E., & Jain, R. K. (2004). Pathology: cancer cells compress intratumour vessels. *Nature, 427*(6976), 695. doi: 10.1038/427695a

Paez-Ribes, M., Allen, E., Hudock, J., Takeda, T., Okuyama, H., Vinals, F., . . . Casanovas, O. (2009). Antiangiogenic therapy elicits malignant progression of tumors to increased local invasion and distant metastasis. *Cancer Cell, 15*(3), 220-231. doi: 10.1016/j.ccr.2009.01.027

Paliwal, S., Pande, S., Kovi, R. C., Sharpless, N. E., Bardeesy, N., & Grossman, S. R. (2006). Targeting of C-terminal binding protein (CtBP) by ARF results in p53-independent apoptosis. *Mol Cell Biol, 26*(6), 2360-2372. doi: 10.1128/MCB.26.6.2360-2372.2006

Pancreatric Section, B. S. o. G., Pancreatic Society of Great, B., Ireland, Association of Upper Gastrointestinal Surgeons of Great, B., Ireland, Royal College of, P., & Special Interest Group for Gastro-Intestinal, R. (2005). Guidelines for the management of patients with pancreatic cancer periampullary and ampullary carcinomas. *Gut, 54 Suppl 5*, v1-16. doi: 10.1136/gut.2004.057059

Park, M. S., Klotz, E., Kim, M. J., Song, S. Y., Park, S. W., Cha, S. W., . . . Kim, K. W. (2009). Perfusion CT: noninvasive surrogate marker for stratification of pancreatic cancer response to concurrent chemo- and radiation therapy. *Radiology, 250*(1), 110-117. doi: 10.1148/radiol.2493080226

Parkin, D. M., Bray, F., Ferlay, J., & Pisani, P. (2005). Global cancer statistics, 2002. *CA Cancer J Clin, 55*(2), 74-108. doi: 55/2/74 [pii]

Parkin, D. M., Pisani, P., & Ferlay, J. (1993). Estimates of the worldwide incidence of eighteen major cancers in 1985. *Int J Cancer, 54*(4), 594-606.

Pen, A., Moreno, M. J., Martin, J., & Stanimirovic, D. B. (2007). Molecular markers of extracellular matrix remodeling in glioblastoma vessels: microarray study of laser-captured glioblastoma vessels. *Glia, 55*(6), 559-572. doi: 10.1002/glia.20481

Perez, J. L., Shen, X., Finkernagel, S., Sciorra, L., Jenkins, N. A., Gilbert, D. J., . . . Wong, T. W. (1994). Identification and chromosomal mapping of a receptor tyrosine kinase with a putative phospholipid binding sequence in its ectodomain. *Oncogene, 9*(1), 211-219.

Pfister, D. G., Johnson, D. H., Azzoli, C. G., Sause, W., Smith, T. J., Baker, S., Jr., . . . American Society of Clinical, O. (2004). American Society of Clinical Oncology treatment of unresectable non-small-cell lung cancer guideline: update 2003. *J Clin Oncol, 22*(2), 330-353. doi: 10.1200/JCO.2004.09.053

Pinzani, M., & Rombouts, K. (2004). Liver fibrosis: from the bench to clinical targets. *Dig Liver Dis, 36*(4), 231-242. doi: 10.1016/j.dld.2004.01.003

Pitini, V., Arrigo, C., Di Mirto, C., Mondello, P., & Altavilla, G. (2013). Response to dasatinib in a patient with SQCC of the lung harboring a discoid-receptor-2 and synchronous chronic myelogenous leukemia. *Lung Cancer, 82*(1), 171-172. doi: 10.1016/j.lungcan.2013.07.004

Poplin, E., Feng, Y., Berlin, J., Rothenberg, M. L., Hochster, H., Mitchell, E., . . . Benson, A. B., 3rd. (2009). Phase III, randomized study of gemcitabine and oxaliplatin versus gemcitabine (fixed-dose rate infusion) compared with gemcitabine (30-minute infusion) in patients with pancreatic carcinoma E6201: a trial of the Eastern Cooperative Oncology Group. *J Clin Oncol, 27*(23), 3778-3785. doi: 10.1200/JCO.2008.20.9007

Provenzano, P. P., Cuevas, C., Chang, A. E., Goel, V. K., Von Hoff, D. D., & Hingorani, S. R. (2012). Enzymatic targeting of the stroma ablates physical barriers to treatment of pancreatic ductal adenocarcinoma. *Cancer Cell, 21*(3), 418-429. doi: 10.1016/j.ccr.2012.01.007

Provenzano, P. P., Inman, D. R., Eliceiri, K. W., Knittel, J. G., Yan, L., Rueden, C. T., . . . Keely, P. J. (2008). Collagen density promotes mammary tumor initiation and progression. *BMC Med, 6*, 11. doi: 10.1186/1741-7015-6-11

Puolakkainen, P. A., Brekken, R. A., Muneer, S., & Sage, E. H. (2004). Enhanced growth of pancreatic tumors in SPARC-null mice is associated with decreased deposition of extracellular matrix and reduced tumor cell apoptosis. *Mol Cancer Res, 2*(4), 215-224.

Qi, Y., Gregory, M. A., Li, Z., Brousal, J. P., West, K., & Hann, S. R. (2004). p19ARF directly and differentially controls the functions of c-Myc independently of p53. *Nature, 431*(7009), 712-717. doi: 10.1038/nature02958

Rahib, L., Smith, B. D., Aizenberg, R., Rosenzweig, A. B., Fleshman, J. M., & Matrisian, L. M. (2014). Projecting cancer incidence and deaths to 2030: the unexpected burden of thyroid, liver, and pancreas cancers in the United States. *Cancer Res, 74*(11), 2913-2921. doi: 10.1158/0008-5472.CAN-14-0155

Raines, E. W., Lane, T. F., Iruela-Arispe, M. L., Ross, R., & Sage, E. H. (1992). The extracellular glycoprotein SPARC interacts with platelet-derived growth factor (PDGF)-AB and -BB and inhibits the binding of PDGF to its receptors. *Proc Natl Acad Sci U S A, 89*(4), 1281-1285.

Ram, R., Lorente, G., Nikolich, K., Urfer, R., Foehr, E., & Nagavarapu, U. (2006). Discoidin domain receptor-1a (DDR1a) promotes glioma cell invasion and adhesion in association with matrix metalloproteinase-2. *J Neurooncol, 76*(3), 239-248. doi: 10.1007/s11060-005-6874-1

Reagan-Shaw, S., Nihal, M., & Ahmad, N. (2008). Dose translation from animal to human studies revisited. *FASEB J, 22*(3), 659-661. doi: 10.1096/fj.07-9574LSF

Reed, M. J., Puolakkainen, P., Lane, T. F., Dickerson, D., Bornstein, P., & Sage, E. H. (1993). Differential expression of SPARC and thrombospondin 1 in wound repair: immunolocalization and in situ hybridization. *J Histochem Cytochem, 41*(10), 1467-1477.

Reitherman, R. W., Rosen, S. D., Frasier, W. A., & Barondes, S. H. (1975). Cell surface species-specific high affinity receptors for discoidin: developmental regulation in Dictyostelium discoideum. *Proc Natl Acad Sci U S A, 72*(9), 3541-3545.

Rentz, T. J., Poobalarahi, F., Bornstein, P., Sage, E. H., & Bradshaw, A. D. (2007). SPARC regulates processing of procollagen I and collagen fibrillogenesis in dermal fibroblasts. *J Biol Chem, 282*(30), 22062-22071. doi: 10.1074/jbc.M700167200

Rhim, A. D., Oberstein, P. E., Thomas, D. H., Mirek, E. T., Palermo, C. F., Sastra, S. A., . . . Stanger, B. Z. (2014). Stromal elements act to restrain, rather than support, pancreatic ductal adenocarcinoma. *Cancer Cell, 25*(6), 735-747. doi: 10.1016/j.ccr.2014.04.021

Ricard-Blum, S. (2011). The collagen family. *Cold Spring Harb Perspect Biol, 3*(1), a004978. doi: 10.1101/cshperspect.a004978

Richters, A., Nguyen, H. D., Phan, T., Simard, J. R., Grutter, C., Engel, J., & Rauh, D. (2014). Identification of type II and III DDR2 inhibitors. *J Med Chem, 57*(10), 4252-4262. doi: 10.1021/jm500167q

Rikova, K., Guo, A., Zeng, Q., Possemato, A., Yu, J., Haack, H., . . . Comb, M. J. (2007). Global survey of phosphotyrosine signaling identifies oncogenic kinases in lung cancer. *Cell, 131*(6), 1190-1203. doi: 10.1016/j.cell.2007.11.025

Rix, U., Hantschel, O., Durnberger, G., Remsing Rix, L. L., Planyavsky, M., Fernbach, N. V., . . . Superti-Furga, G. (2007). Chemical proteomic profiles of the BCR-ABL inhibitors imatinib, nilotinib, and dasatinib reveal novel kinase and nonkinase targets. *Blood, 110*(12), 4055-4063. doi: 10.1182/blood-2007-07-102061

Rix, U., Remsing Rix, L. L., Terker, A. S., Fernbach, N. V., Hantschel, O., Planyavsky, M., . . . Superti-Furga, G. (2010). A comprehensive target selectivity survey of the BCR-ABL kinase inhibitor INNO-406 by kinase profiling and chemical proteomics in chronic myeloid leukemia cells. *Leukemia, 24*(1), 44-50. doi: 10.1038/leu.2009.228

Rocha Lima, C. M., Green, M. R., Rotche, R., Miller, W. H., Jr., Jeffrey, G. M., Cisar, L. A., . . . Miller, L. L. (2004). Irinotecan plus gemcitabine results in no survival advantage compared with gemcitabine monotherapy in patients with locally advanced or metastatic pancreatic cancer despite increased tumor response rate. *J Clin Oncol, 22*(18), 3776-3783. doi: 10.1200/JCO.2004.12.082

Rocha Lima, C. M., Savarese, D., Bruckner, H., Dudek, A., Eckardt, J., Hainsworth, J., . . . Green, M. R. (2002). Irinotecan plus gemcitabine induces both radiographic and CA 19-9 tumor marker responses in patients with previously untreated advanced pancreatic cancer. *J Clin Oncol, 20*(5), 1182-1191.

Rocha, S., Campbell, K. J., & Perkins, N. D. (2003). p53- and Mdm2-independent repression of NF-kappa B transactivation by the ARF tumor suppressor. *Mol Cell, 12*(1), 15-25.

Rodrigues, R., Roque, L., Espadinha, C., Pinto, A., Domingues, R., Dinis, J., . . . Leite, V. (2007). Comparative genomic hybridization, BRAF, RAS, RET, and oligo-array analysis in aneuploid papillary thyroid carcinomas. *Oncol Rep, 18*(4), 917-926.

Rosenbloom, J., Mendoza, F. A., & Jimenez, S. A. (2013). Strategies for anti-fibrotic therapies. *Biochim Biophys Acta, 1832*(7), 1088-1103. doi: 10.1016/j.bbadis.2012.12.007

Roskoski, R., Jr. (2007). Vascular endothelial growth factor (VEGF) signaling in tumor progression. *Crit Rev Oncol Hematol, 62*(3), 179-213.

Roskoski, R., Jr. (2015). Src protein-tyrosine kinase structure, mechanism, and small molecule inhibitors. *Pharmacol Res, 94*, 9-25. doi: 10.1016/j.phrs.2015.01.003

Rozenblum, E., Schutte, M., Goggins, M., Hahn, S. A., Panzer, S., Zahurak, M., . . . Kern, S. E. (1997). Tumor-suppressive pathways in pancreatic carcinoma. *Cancer Res, 57*(9), 1731-1734.

Sage, H., Johnson, C., & Bornstein, P. (1984). Characterization of a novel serum albumin-binding glycoprotein secreted by endothelial cells in culture. *J Biol Chem, 259*(6), 3993-4007.

Sage, H., Vernon, R. B., Funk, S. E., Everitt, E. A., & Angello, J. (1989). SPARC, a secreted protein associated with cellular proliferation, inhibits cell spreading in vitro and exhibits Ca+2-dependent binding to the extracellular matrix. *J Cell Biol, 109*(1), 341-356.

Sasaki, T., Hohenester, E., Gohring, W., & Timpl, R. (1998). Crystal structure and mapping by site-directed mutagenesis of the collagen-binding epitope of an activated form of BM-40/SPARC/osteonectin. *EMBO J, 17*(6), 1625-1634. doi: 10.1093/emboj/17.6.1625

Sasaki, T., Miosge, N., & Timpl, R. (1999). Immunochemical and tissue analysis of protease generated neoepitopes of BM-40 (osteonectin, SPARC) which

are correlated to a higher affinity binding to collagens. *Matrix Biol, 18*(5), 499-508.

Sato, N., Fukushima, N., Maehara, N., Matsubayashi, H., Koopmann, J., Su, G. H., . . . Goggins, M. (2003). SPARC/osteonectin is a frequent target for aberrant methylation in pancreatic adenocarcinoma and a mediator of tumor-stromal interactions. *Oncogene, 22*(32), 5021-5030. doi: 10.1038/sj.onc.1206807

Schneider, R., Becker, C., Simard, J. R., Getlik, M., Bohlke, N., Janning, P., & Rauh, D. (2012). Direct binding assay for the detection of type IV allosteric inhibitors of Abl. *J Am Chem Soc, 134*(22), 9138-9141. doi: 10.1021/ja303858w

Schultz, C., Lemke, N., Ge, S., Golembieski, W. A., & Rempel, S. A. (2002). Secreted protein acidic and rich in cysteine promotes glioma invasion and delays tumor growth in vivo. *Cancer Res, 62*(21), 6270-6277.

Seymour, P. A., Freude, K. K., Dubois, C. L., Shih, H. P., Patel, N. A., & Sander, M. (2008). A dosage-dependent requirement for Sox9 in pancreatic endocrine cell formation. *Dev Biol, 323*(1), 19-30. doi: 10.1016/j.ydbio.2008.07.034

Shen, Q., Cicinnati, V. R., Zhang, X., Iacob, S., Weber, F., Sotiropoulos, G. C., . . . Beckebaum, S. (2010). Role of microRNA-199a-5p and discoidin domain receptor 1 in human hepatocellular carcinoma invasion. *Mol Cancer, 9*, 227. doi: 10.1186/1476-4598-9-227

Sheppard, K., Kinross, K. M., Solomon, B., Pearson, R. B., & Phillips, W. A. (2012). Targeting PI3 kinase/AKT/mTOR signaling in cancer. *Crit Rev Oncog, 17*(1), 69-95.

Sherr, C. J. (2001). The INK4a/ARF network in tumour suppression. *Nat Rev Mol Cell Biol, 2*(10), 731-737. doi: 10.1038/35096061

Shields, M. A., Dangi-Garimella, S., Redig, A. J., & Munshi, H. G. (2012). Biochemical role of the collagen-rich tumour microenvironment in pancreatic cancer progression. *Biochem J, 441*(2), 541-552. doi: BJ20111240 [pii] 10.1042/BJ20111240

Shimada, K., Nakamura, M., Ishida, E., Higuchi, T., Yamamoto, H., Tsujikawa, K., & Konishi, N. (2008). Prostate cancer antigen-1 contributes to cell survival and invasion though discoidin receptor 1 in human prostate cancer. *Cancer Sci, 99*(1), 39-45. doi: 10.1111/j.1349-7006.2007.00655.x

Shintani, Y., Fukumoto, Y., Chaika, N., Svoboda, R., Wheelock, M. J., & Johnson, K. R. (2008). Collagen I-mediated up-regulation of N-cadherin requires cooperative signals from integrins and discoidin domain receptor 1. *J Cell Biol, 180*(6), 1277-1289. doi: 10.1083/jcb.200708137

Shrivastava, A., Radziejewski, C., Campbell, E., Kovac, L., McGlynn, M., Ryan, T. E., . . . Yancopoulos, G. D. (1997). An orphan receptor tyrosine kinase family whose members serve as nonintegrin collagen receptors. *Mol Cell, 1*(1), 25-34.

Socha, M. J., Said, N., Dai, Y., Kwong, J., Ramalingam, P., Trieu, V., . . . Motamed, K. (2009). Aberrant promoter methylation of SPARC in ovarian cancer. *Neoplasia, 11*(2), 126-135.

Somanath, P. R., & Byzova, T. V. (2009). 14-3-3beta-Rac1-p21 activated kinase signaling regulates Akt1-mediated cytoskeletal organization, lamellipodia formation and fibronectin matrix assembly. *J Cell Physiol, 218*(2), 394-404. doi: 10.1002/jcp.21612

Somanath, P. R., Chen, J., & Byzova, T. V. (2008). Akt1 is necessary for the vascular maturation and angiogenesis during cutaneous wound healing. *Angiogenesis, 11*(3), 277-288. doi: 10.1007/s10456-008-9111-7

Somanath, P. R., Kandel, E. S., Hay, N., & Byzova, T. V. (2007). Akt1 signaling regulates integrin activation, matrix recognition, and fibronectin assembly. *J Biol Chem, 282*(31), 22964-22976. doi: 10.1074/jbc.M700241200

Sorensen, A. G., Emblem, K. E., Polaskova, P., Jennings, D., Kim, H., Ancukiewicz, M., . . . Jain, R. K. (2012). Increased survival of glioblastoma patients who respond to antiangiogenic therapy with elevated blood perfusion. *Cancer Res, 72*(2), 402-407. doi: 10.1158/0008-5472.CAN-11-2464

Squire, J. A., Bayani, J., Luk, C., Unwin, L., Tokunaga, J., MacMillan, C., . . . Kamel-Reid, S. (2002). Molecular cytogenetic analysis of head and neck squamous cell carcinoma: By comparative genomic hybridization, spectral

karyotyping, and expression array analysis. *Head Neck, 24*(9), 874-887. doi: 10.1002/hed.10122

Stathopoulos, G. P., Syrigos, K., Aravantinos, G., Polyzos, A., Papakotoulas, P., Fountzilas, G., . . . Georgoulias, V. (2006). A multicenter phase III trial comparing irinotecan-gemcitabine (IG) with gemcitabine (G) monotherapy as first-line treatment in patients with locally advanced or metastatic pancreatic cancer. *Br J Cancer, 95*(5), 587-592. doi: 10.1038/sj.bjc.6603301

Stiekema, J., Cats, A., Kuijpers, A., van Coevorden, F., Boot, H., Jansen, E. P., . . . van Sandick, J. W. (2013). Surgical treatment results of intestinal and diffuse type gastric cancer. Implications for a differentiated therapeutic approach? *Eur J Surg Oncol, 39*(7), 686-693. doi: 10.1016/j.ejso.2013.02.026

Stylianopoulos, T., Martin, J. D., Chauhan, V. P., Jain, S. R., Diop-Frimpong, B., Bardeesy, N., . . . Jain, R. K. (2012). Causes, consequences, and remedies for growth-induced solid stress in murine and human tumors. *Proc Natl Acad Sci U S A, 109*(38), 15101-15108. doi: 10.1073/pnas.1213353109

Stylianopoulos, T., Martin, J. D., Snuderl, M., Mpekris, F., Jain, S. R., & Jain, R. K. (2013). Coevolution of solid stress and interstitial fluid pressure in tumors during progression: implications for vascular collapse. *Cancer Res, 73*(13), 3833-3841. doi: 10.1158/0008-5472.CAN-12-4521

Sugimoto, M., Kuo, M. L., Roussel, M. F., & Sherr, C. J. (2003). Nucleolar Arf tumor suppressor inhibits ribosomal RNA processing. *Mol Cell, 11*(2), 415-424.

Suzuki, M., Hao, C., Takahashi, T., Shigematsu, H., Shivapurkar, N., Sathyanarayana, U. G., . . . Gazdar, A. F. (2005). Aberrant methylation of SPARC in human lung cancers. *Br J Cancer, 92*(5), 942-948. doi: 10.1038/sj.bjc.6602376

Sweetwyne, M. T. (2004). Functional Analysis of the Matricellular Protein SPARC with Novel Monoclonal Antibodies. *Journal of Histochemistry and Cytochemistry, 52*(6), 723-733. doi: 10.1369/jhc.3A6153.2004

Sweetwyne, M. T., Brekken, R. A., Workman, G., Bradshaw, A. D., Carbon, J., Siadak, A. W., . . . Sage, E. H. (2004). Functional analysis of the

matricellular protein SPARC with novel monoclonal antibodies. *J Histochem Cytochem, 52*(6), 723-733.

Sweetwyne, M. T., & Murphy-Ullrich, J. E. (2012). Thrombospondin1 in tissue repair and fibrosis: TGF-beta-dependent and independent mechanisms. *Matrix Biol, 31*(3), 178-186. doi: 10.1016/j.matbio.2012.01.006

Tai, I. T., Dai, M., Owen, D. A., & Chen, L. B. (2005). Genome-wide expression analysis of therapy-resistant tumors reveals SPARC as a novel target for cancer therapy. *J Clin Invest, 115*(6), 1492-1502. doi: 10.1172/JCI23002

Tai, I. T., & Tang, M. J. (2008). SPARC in cancer biology: its role in cancer progression and potential for therapy. *Drug Resist Updat, 11*(6), 231-246. doi: 10.1016/j.drup.2008.08.005

Taube, J. H., Herschkowitz, J. I., Komurov, K., Zhou, A. Y., Gupta, S., Yang, J., . . . Mani, S. A. (2010). Core epithelial-to-mesenchymal transition interactome gene-expression signature is associated with claudin-low and metaplastic breast cancer subtypes. *Proc Natl Acad Sci U S A, 107*(35), 15449-15454. doi: 10.1073/pnas.1004900107

Termine, J. D., Kleinman, H. K., Whitson, S. W., Conn, K. M., McGarvey, M. L., & Martin, G. R. (1981). Osteonectin, a bone-specific protein linking mineral to collagen. *Cell, 26*(1 Pt 1), 99-105.

Thomas, S. L., & Rempel, S. A. (2011). SPARC and the Tumor Microenvironment. 301-346. doi: 10.1007/978-94-007-0659-0_17

Tichet, M., Prod'Homme, V., Fenouille, N., Ambrosetti, D., Mallavialle, A., Cerezo, M., . . . Tartare-Deckert, S. (2015). Tumour-derived SPARC drives vascular permeability and extravasation through endothelial VCAM1 signalling to promote metastasis. *Nat Commun, 6*, 6993. doi: 10.1038/ncomms7993

Tofts, P. S., Brix, G., Buckley, D. L., Evelhoch, J. L., Henderson, E., Knopp, M. V., . . . Weisskoff, R. M. (1999). Estimating kinetic parameters from dynamic contrast-enhanced T(1)-weighted MRI of a diffusable tracer: standardized quantities and symbols. *J Magn Reson Imaging, 10*(3), 223-232.

Toole, B. P. (2004). Hyaluronan: from extracellular glue to pericellular cue. *Nat Rev Cancer, 4*(7), 528-539. doi: 10.1038/nrc1391

Toyota, M., Ahuja, N., Ohe-Toyota, M., Herman, J. G., Baylin, S. B., & Issa, J. P. (1999). CpG island methylator phenotype in colorectal cancer. *Proc Natl Acad Sci U S A, 96*(15), 8681-8686.

Tremble, P. M., Lane, T. F., Sage, E. H., & Werb, Z. (1993). SPARC, a secreted protein associated with morphogenesis and tissue remodeling, induces expression of metalloproteinases in fibroblasts through a novel extracellular matrix-dependent pathway. *J Cell Biol, 121*(6), 1433-1444.

Truty, M. J., & Urrutia, R. (2007). Basics of TGF-beta and pancreatic cancer. *Pancreatology, 7*(5-6), 423-435. doi: 10.1159/000108959

Tsai, A. G., Johnson, P. C., & Intaglietta, M. (2003). Oxygen gradients in the microcirculation. *Physiol Rev, 83*(3), 933-963. doi: 10.1152/physrev.00034.2002

Turner-Warwick, M., Lebowitz, M., Burrows, B., & Johnson, A. (1980). Cryptogenic fibrosing alveolitis and lung cancer. *Thorax, 35*(7), 496-499.

Valencia, K., Ormazabal, C., Zandueta, C., Luis-Ravelo, D., Anton, I., Pajares, M. J., . . . Lecanda, F. (2012). Inhibition of collagen receptor discoidin domain receptor-1 (DDR1) reduces cell survival, homing, and colonization in lung cancer bone metastasis. *Clin Cancer Res, 18*(4), 969-980. doi: 10.1158/1078-0432.CCR-11-1686

Valiathan, R. R., Marco, M., Leitinger, B., Kleer, C. G., & Fridman, R. (2012). Discoidin domain receptor tyrosine kinases: new players in cancer progression. *Cancer Metastasis Rev, 31*(1-2), 295-321. doi: 10.1007/s10555-012-9346-z

Van Cutsem, E., Vervenne, W. L., Bennouna, J., Humblet, Y., Gill, S., Van Laethem, J. L., . . . Moore, M. J. (2009). Phase III trial of bevacizumab in combination with gemcitabine and erlotinib in patients with metastatic pancreatic cancer. *J Clin Oncol, 27*(13), 2231-2237. doi: JCO.2008.20.0238 [pii] 10.1200/JCO.2008.20.0238

van Heek, N. T., Meeker, A. K., Kern, S. E., Yeo, C. J., Lillemoe, K. D., Cameron, J. L., . . . Maitra, A. (2002). Telomere shortening is nearly

universal in pancreatic intraepithelial neoplasia. *Am J Pathol, 161*(5), 1541-1547. doi: 10.1016/S0002-9440(10)64432-X

Vogel, S. M., Minshall, R. D., Pilipovic, M., Tiruppathi, C., & Malik, A. B. (2001). Albumin uptake and transcytosis in endothelial cells in vivo induced by albumin-binding protein. *Am J Physiol Lung Cell Mol Physiol, 281*(6), L1512-1522.

Vogel, W., Gish, G. D., Alves, F., & Pawson, T. (1997). The discoidin domain receptor tyrosine kinases are activated by collagen. *Mol Cell, 1*(1), 13-23. doi: S1097-2765(00)80003-9 [pii]

Vogel, W. F., Aszodi, A., Alves, F., & Pawson, T. (2001). Discoidin domain receptor 1 tyrosine kinase has an essential role in mammary gland development. *Mol Cell Biol, 21*(8), 2906-2917. doi: 10.1128/MCB.21.8.2906-2917.2001

Von Hoff, D., Thomas, E., Arena, F. P., Chiorean, E. G., Infante, J. R., & Moore, M. (2012). Randomized phase III study of weekly nab-paclitaxel plus gemcitabine vs. gemcitabine alone in patients with metastatic adenocarcinoma of the pancreas (MPACT). *J Clin Oncol, 30*.

Von Hoff, D. D., Ramanathan, R. K., Borad, M. J., Laheru, D. A., Smith, L. S., Wood, T. E., . . . Hidalgo, M. (2011). Gemcitabine plus nab-paclitaxel is an active regimen in patients with advanced pancreatic cancer: a phase I/II trial. *J Clin Oncol, 29*(34), 4548-4554. doi: JCO.2011.36.5742 [pii] 10.1200/JCO.2011.36.5742

Wagener, D. J., Verdonk, H. E., Dirix, L. Y., Catimel, G., Siegenthaler, P., Buitenhuis, M., . . . Verweij, J. (1995). Phase II trial of CPT-11 in patients with advanced pancreatic cancer, an EORTC early clinical trials group study. *Ann Oncol, 6*(2), 129-132.

Wang, C. Z., Su, H. W., Hsu, Y. C., Shen, M. R., & Tang, M. J. (2006). A discoidin domain receptor 1/SHP-2 signaling complex inhibits alpha2beta1-integrin-mediated signal transducers and activators of transcription 1/3 activation and cell migration. *Mol Biol Cell, 17*(6), 2839-2852. doi: 10.1091/mbc.E05-11-1068

Wang, W. Q., Liu, L., Xu, H. X., Luo, G. P., Chen, T., Wu, C. T., . . . Yu, X. J. (2013). Intratumoral alpha-SMA enhances the prognostic potency of

CD34 associated with maintenance of microvessel integrity in hepatocellular carcinoma and pancreatic cancer. *PLoS One, 8*(8), e71189. doi: 10.1371/journal.pone.0071189

Wasser, K., Klein, S. K., Fink, C., Junkermann, H., Sinn, H. P., Zuna, I., . . . Delorme, S. (2003). Evaluation of neoadjuvant chemotherapeutic response of breast cancer using dynamic MRI with high temporal resolution. *Eur Radiol, 13*(1), 80-87. doi: 10.1007/s00330-002-1654-1

Webb, J. D., & Simon, M. C. (2010). Novel insights into the molecular origins and treatment of lung cancer. *Cell Cycle, 9*(20), 4098-4105. doi: 13588 [pii]

Weiner, H. L., Huang, H., Zagzag, D., Boyce, H., Lichtenbaum, R., & Ziff, E. B. (2000). Consistent and selective expression of the discoidin domain receptor-1 tyrosine kinase in human brain tumors. *Neurosurgery, 47*(6), 1400-1409.

Weiner, H. L., Rothman, M., Miller, D. C., & Ziff, E. B. (1996). Pediatric brain tumors express multiple receptor tyrosine kinases including novel cell adhesion kinases. *Pediatr Neurosurg, 25*(2), 64-71; discussion 71-62.

Wess, T. J. (2005). Collagen fibril form and function. *Adv Protein Chem, 70*, 341-374. doi: 10.1016/S0065-3233(05)70010-3

Wilop, S., von Hobe, S., Crysandt, M., Esser, A., Osieka, R., & Jost, E. (2009). Impact of angiotensin I converting enzyme inhibitors and angiotensin II type 1 receptor blockers on survival in patients with advanced non-small-cell lung cancer undergoing first-line platinum-based chemotherapy. *J Cancer Res Clin Oncol, 135*(10), 1429-1435. doi: 10.1007/s00432-009-0587-3

Wong, H. H., & Lemoine, N. R. (2009). Pancreatic cancer: molecular pathogenesis and new therapeutic targets. *Nat Rev Gastroenterol Hepatol, 6*(7), 412-422. doi: 10.1038/nrgastro.2009.89

Wynn, T. A. (2008). Cellular and molecular mechanisms of fibrosis. *J Pathol, 214*(2), 199-210. doi: 10.1002/path.2277

Xia, H., Diebold, D., Nho, R., Perlman, D., Kleidon, J., Kahm, J., . . . Henke, C. (2008). Pathological integrin signaling enhances proliferation of primary

lung fibroblasts from patients with idiopathic pulmonary fibrosis. *J Exp Med, 205*(7), 1659-1672. doi: 10.1084/jem.20080001

Xia, H., Khalil, W., Kahm, J., Jessurun, J., Kleidon, J., & Henke, C. A. (2010). Pathologic caveolin-1 regulation of PTEN in idiopathic pulmonary fibrosis. *Am J Pathol, 176*(6), 2626-2637. doi: 10.2353/ajpath.2010.091117

Xu, H., Raynal, N., Stathopoulos, S., Myllyharju, J., Farndale, R. W., & Leitinger, B. (2011). Collagen binding specificity of the discoidin domain receptors: binding sites on collagens II and III and molecular determinants for collagen IV recognition by DDR1. *Matrix Biol, 30*(1), 16-26. doi: 10.1016/j.matbio.2010.10.004

Yamanaka, R., Arao, T., Yajima, N., Tsuchiya, N., Homma, J., Tanaka, R., . . . Nishio, K. (2006). Identification of expressed genes characterizing long-term survival in malignant glioma patients. *Oncogene, 25*(44), 5994-6002. doi: 10.1038/sj.onc.1209585

Yang, S. H., Baek, H. A., Lee, H. J., Park, H. S., Jang, K. Y., Kang, M. J., . . . Chung, M. J. (2010). Discoidin domain receptor 1 is associated with poor prognosis of non-small cell lung carcinomas. *Oncol Rep, 24*(2), 311-319.

Yauch, R. L., Gould, S. E., Scales, S. J., Tang, T., Tian, H., Ahn, C. P., . . . de Sauvage, F. J. (2008). A paracrine requirement for hedgehog signalling in cancer. *Nature, 455*(7211), 406-410. doi: 10.1038/nature07275

Yeo, T. P., Hruban, R. H., Leach, S. D., Wilentz, R. E., Sohn, T. A., Kern, S. E., . . . Yeo, C. J. (2002). Pancreatic cancer. *Curr Probl Cancer, 26*(4), 176-275.

Yiu, G. K., Chan, W. Y., Ng, S. W., Chan, P. S., Cheung, K. K., Berkowitz, R. S., & Mok, S. C. (2001). SPARC (secreted protein acidic and rich in cysteine) induces apoptosis in ovarian cancer cells. *Am J Pathol, 159*(2), 609-622. doi: 10.1016/S0002-9440(10)61732-4

Zerlin, M., Julius, M. A., & Goldfarb, M. (1993). NEP: a novel receptor-like tyrosine kinase expressed in proliferating neuroepithelia. *Oncogene, 8*(10), 2731-2739.

Zhang, J., Yang, P. L., & Gray, N. S. (2009). Targeting cancer with small molecule kinase inhibitors. *Nat Rev Cancer, 9*(1), 28-39. doi: 10.1038/nrc2559

Zhang, K., Corsa, C. A., Ponik, S. M., Prior, J. L., Piwnica-Worms, D., Eliceiri, K. W., . . . Longmore, G. D. (2013). The collagen receptor discoidin domain receptor 2 stabilizes SNAIL1 to facilitate breast cancer metastasis. *Nat Cell Biol, 15*(6), 677-687. doi: 10.1038/ncb2743

Zhang, K., Rodriguez-Aznar, E., Yabuta, N., Owen, R. J., Mingot, J. M., Nojima, H., . . . Longmore, G. D. (2012). Lats2 kinase potentiates Snail1 activity by promoting nuclear retention upon phosphorylation. *EMBO J, 31*(1), 29-43. doi: 10.1038/emboj.2011.357

Zhang, S., Bu, X., Zhao, H., Yu, J., Wang, Y., Li, D., . . . Su, J. (2014). A host deficiency of discoidin domain receptor 2 (DDR2) inhibits both tumour angiogenesis and metastasis. *J Pathol, 232*(4), 436-448. doi: 10.1002/path.4311

Zhang, Y., Su, J., Yu, J., Bu, X., Ren, T., Liu, X., & Yao, L. (2011). An essential role of discoidin domain receptor 2 (DDR2) in osteoblast differentiation and chondrocyte maturation via modulation of Runx2 activation. *J Bone Miner Res, 26*(3), 604-617. doi: 10.1002/jbmr.225

Zhao, S., Venkatasubbarao, K., Lazor, J. W., Sperry, J., Jin, C., Cao, L., & Freeman, J. W. (2008). Inhibition of STAT3 Tyr705 phosphorylation by Smad4 suppresses transforming growth factor beta-mediated invasion and metastasis in pancreatic cancer cells. *Cancer Res, 68*(11), 4221-4228. doi: 10.1158/0008-5472.CAN-07-5123

Zhong, Z., Carroll, K. D., Policarpio, D., Osborn, C., Gregory, M., Bassi, R., . . . Wu, Y. (2010). Anti-transforming growth factor beta receptor II antibody has therapeutic efficacy against primary tumor growth and metastasis through multieffects on cancer, stroma, and immune cells. *Clin Cancer Res, 16*(4), 1191-1205. doi: 10.1158/1078-0432.CCR-09-1634